

THE ROLE OF SYN1 IN
EARLY *ARABIDOPSIS* MEIOSIS

by
CHOON LIN TIANG

A thesis submitted to
University of Birmingham
For the degree of
DOCTOR OF PHILOSOPHY

School of Biosciences
University of Birmingham
September 2010

UNIVERSITY OF
BIRMINGHAM

University of Birmingham Research Archive

e-theses repository

This unpublished thesis/dissertation is copyright of the author and/or third parties. The intellectual property rights of the author or third parties in respect of this work are as defined by The Copyright Designs and Patents Act 1988 or as modified by any successor legislation.

Any use made of information contained in this thesis/dissertation must be in accordance with that legislation and must be properly acknowledged. Further distribution or reproduction in any format is prohibited without the permission of the copyright holder.

ABSTRACT

SYN1 is a meiosis-specific *Arabidopsis* homologue of yeast REC8. REC8 is an important component of the meiotic cohesion complex which maintains cohesion between sister chromatids. Cytological analysis of *syn1*^{-/-} has shown chromosome fragmentation at metaphase I. To determine the basis of chromosome fragmentation in the *syn1*^{-/-}, three double mutants were constructed. I have demonstrated that chromosome fragmentation in *syn1* is AtSPO11-1-dependent. Moreover, I have also shown that SYN1 has a role in DSB repair by analysing *Atdmc1*^{-/-}/*syn1*^{-/-} meiocytes. To investigate this further, immunolocalization studies in wild-type and *syn1*^{-/-} were conducted. Distribution of ASY1 and AtZYP1 was affected in *syn1*^{-/-}. Both proteins appeared as aggregates, developing into an abnormal short linear signal in early prophase I, suggesting that both axis formation and synapsis are compromised. Distribution of the recombination proteins AtRAD51 and AtMLH1 was also aberrant. Localization of SYN1 in wild-type nuclei revealed a continuous signal along the chromosome axes. However, careful inspection revealed that this was accompanied by patches of more intense signals, possibly corresponding to DSB regions. To investigate this further I analysed SYN1 distribution in an *Atspo11-1-4*^{-/-} mutant. Whilst faint SYN1 signals were apparent along the axis, no patches of intense signals were visible. Cisplatin-induced DSBs restored AtZYP1 foci in *Atspo11-1-4*^{-/-} and also resulted in restoration of intense patches of the SYN1 signals. This is consistent with the recruitment of SYN1 to DSB sites.

ACKNOWLEDGEMENTS

I would like to thank my supervisors Sue Armstrong and Chris Franklin for providing me with great support and guidance throughout the duration of this project. I would also like to thank Eugenio Sanchez-Moran for helpful discussion and support over the years.

I would like to thank friends from Franklin and Franklin-Tong labs, especially Barend de Graaf and Kim Osman for their help and guidance in molecular biology experiments. I would like to thank Natalie Poulter for showing me the useful software Image J and Excel, and also I would like to thank Sarah Smith for sharing her time and knowledge over the years. I thank Steve Price and Ruth Perry for technical assistance in the lab and to Karen Staples for assistance in the glass house.

Finally, I would like to thank my Mom, Dad and my fiancée Hoi Chin Hew for their love and support.

TABLE OF CONTENTS

CHAPTER 1.....	1
GENERAL INTRODUCTION.....	1
1.1 OVERVIEW OF MITOSIS AND MEIOSIS.....	1
1.2 SISTER CHROMATID COHESION	5
1.2.1 Establishment of sister chromatid cohesion.....	5
1.2.1.1 Cohesins	7
1.2.1.2 Loading of cohesin on sister chromatids	10
1.2.2 Localization of cohesin on the chromosome in meiosis.....	12
1.2.3 Removal of cohesins.....	15
1.2.3.1 Cleavage of cohesin by separase	15
1.2.3.2 Protection of centromeric cohesion	18
1.2.4 <i>Arabidopsis</i> cohesins: SYN1, AtSMC1/AtSMC3 and AtSCC3.....	22
1.2.4.1 SYN1	22
1.2.4.2 AtSMC1 and AtSMC3	23
1.2.4.3 AtSCC3	24
1.3 COHESINS ARE REQUIRED FOR DOUBLE-STRAND BREAK (DSB) REPAIR	25
1.4 HOMOLOGUE PAIRING AND SYNAPSIS.....	26
1.4.1 Homologous chromosome pairing	26
1.4.2 Formation of the synaptonemal complex.....	27
1.5 MEIOTIC RECOMBINATION.....	31
1.5.1 Initial events of meiotic recombination: formation of DSB	31
1.5.2 Processing of meiotic DNA DSB	33
1.5.3 Crossover and non-crossover pathways.....	36
1.6 AIMS OF MY PHD PROJECT	40
CHAPTER 2.....	42
MATERIALS AND METHODS.....	42
2.1 PLANT MATERIALS AND GROWING CONDITIONS.....	42
2.1.1 Plant materials	42
2.1.2 Plant growth media	42
2.1.3 Plant growth conditions	42
2.2 BACTERIAL STRAINS AND CLONING VECTORS.....	43

2.2.1 Bacterial strains	43
2.2.2 Cloning vectors.....	43
2.3 BACTERIA MEDIA, CULTURE AND GROWTH CONDITION	44
2.3.1 Bacterial growth media	44
2.3.1.1 Lysogeny Broth (LB).....	44
2.3.1.2 LB agar.....	44
2.3.2 Bacterial culture	45
2.3.3 Bacterial growth condition.....	45
2.4 ISOLATION OF NUCLEIC ACID FROM PLANT AND BACTERIA	45
2.4.1 Buffer for isolation of nucleic acid.....	45
2.4.2 Isolation of total RNA from plants	46
2.4.2.1 DNase I treatment of plant RNA	46
2.4.3 Isolation of plasmid DNA from bacteria.....	47
2.4.3.1 Boiling Prep method	47
2.4.3.2 Wizard Mini prep method (Promega®)	48
2.4.4 Isolation of DNA from plants for genotyping	48
2.5 POLYMERASE CHAIN REACTION (PCR) TECHNIQUES	48
2.5.1 PCR standard condition	49
2.5.2 Genotyping PCR.....	49
2.5.3 Single colony PCR	49
2.5.4 Reverse Transcriptase-Polymerase Chain Reaction (RT-PCR).....	50
2.5.5 Primer design	58
2.6 NUCLEIC ACID MANIPULATIONS.....	59
2.6.1 Estimation of nucleic acid concentration.....	59
2.6.2 Digestion of DNA with restriction enzymes	59
2.6.3 Agarose gel electrophoresis of DNA and RNA.....	59
2.6.3.1 Solutions for nucleic acid electrophoresis	60
2.6.4 Extraction of DNA from agarose gels	60
2.6.5 Ligation of DNA fragments into vector DNA.....	60
2.6.6 DNA sequencing.....	61
2.7 TRANSFORMATION OF BACTERIAL CELLS.....	61
2.7.1 Transformation of <i>E. coli</i> by heat shock.....	61

2.8 PROTEIN MANIPULATIONS	62
2.8.1 Protein electrophoresis and western blotting solutions	62
2.8.2 Protein test expression, extractions and preparations	64
2.8.2.1 Protein test expression and extractions from bacteria	64
2.8.2.2 Estimating protein concentration.....	71
2.8.2.3 SDS-Polyacrylamide gel electrophoresis (SDS-PAGE)	71
2.8.2.4 Coomassie staining of protein gels	72
2.9 WESTERN BLOTTING.....	73
2.9.1 Protein transfer	73
2.9.2 Antibody probing and protein detection	73
2.10 SLIDE PREPARATION OF MEIOTIC CHROMOSOMES FOR CYTOLOGY	74
2.10.1 Determination of meiotic stage.....	74
2.10.2 Slide preparation for immunolocalization studies	74
2.10.3 Antibody labelling for immunolocalization studies	74
2.10.4 Meiotic time course	75
2.10.5 Slide preparation for cytogenetics studies	76
2.10.6 Fluorescent in situ hybridisation (FISH).....	77
2.11 SLIDE IMAGING.....	78
2.12 CISPLATIN TREATMENT	78
2.12.1 Introduction of cisplatin into meiocytes of <i>Atspo11-1-4^{-/-}</i>	78
2.12.2 Seedling growth on Cisplatin containing MS agar.....	78
CHAPTER 3.....	79
CHARACTERISING A <i>SYN1</i> NULL MUTANT	79
3.1 INTRODUCTION.....	79
3.2 RESULTS	80
3.2.1 Identification of <i>SYN1</i> T-DNA insertion mutant	80
3.2.2 Expression of <i>SYN1</i> gene	84
3.2.3 Cytogenetic analysis of the <i>syn1</i> mutant.....	88
3.2.3.1 Male meiosis in wild-type and <i>syn1</i> mutant.....	88
3.2.3.2 Fluorescence in situ hybridisation (FISH) analysis of chromosome segregation in wild-type and <i>syn1</i> male meiocytes	93
3.2.4 Relationship between SYN1 and other Rec8 homologues.	97

3.3 DISCUSSION	102
3.3.1 T-DNA insertion line (SALK_091193) is a <i>syn1</i> null mutant.....	102
3.3.2 <i>SYN1</i> expression is not specific to meiosis	102
3.3.3 Chromatin is disorganised during early meiosis I in <i>syn1</i> mutants.....	103
3.3.4 <i>SYN1</i> is important for centromeric cohesion at the first meiotic division.	104
CHAPTER 4.....	105
IMMUNOLocalIZATION OF SYN1 PROTEIN.....	105
4.1 INTRODUCTION.....	105
4.2 RESULTS	106
4.2.1 Immunolocalization	106
4.2.1.1 <i>SYN1</i> localizes on meiotic chromosomes	106
4.2.1.2 Immunolocalization of <i>SYN1</i> and <i>AtSMC3/AtSCC3</i> on wildtype (Col 0)	
meiocytes	110
4.2.1.3 Immunolocalization of <i>ASY1</i> and <i>AtSCC3/AtSMC3</i> on <i>syn1</i> meiocytes	117
4.2.1.4 Immunolocalization of <i>SYN1</i> and <i>AtZYP1</i> on wild-type (Col 0) and <i>syn1</i>	
meiocytes.	120
4.2.1.5 Immunolocalization of <i>AtZYP1</i> and <i>ASY1</i> on <i>syn1</i> meiocytes.....	128
4.2.1.6 Immunolocalization of <i>AtRAD51</i> and <i>ASY1</i> on wild-type (Col 0) and <i>syn1</i>	
meiocytes.....	130
4.2.1.7 Immunolocalization of <i>AtMLH1</i> and <i>ASY1</i> on wild-type (Col 0) and <i>syn1</i>	
meiocytes	132
4.3 DISCUSSION	135
4.3.1 Are <i>SYN1</i> patches localized to the sites of DNA double strand break?.....	135
4.3.2 Localization of <i>AtSCC3</i> and <i>AtSMC3</i> along meiotic chromosomes is dependent	
upon <i>SYN1</i>	136
4.3.3 Formation of the synaptonemal complex is disrupted in a <i>syn1</i> mutant	137
4.3.4 <i>SYN1</i> is essential for meiotic recombination progression in <i>Arabidopsis</i>	138
CHAPTER 5.....	140
AN ADDITIONAL ROLE FOR SYN1.....	140
5.1 INTRODUCTION.....	140
5.2 RESULTS	141
5.2.1 Cytogenetic analysis in <i>syn1^{-/-}</i> and <i>Atspo11-1-4^{-/-}</i> double knockout mutant.....	141

5.2.2 Immunolocalization of SYN1 on <i>Atspo11-1-4^{-/-}</i>	146
5.2.3 Immunolocalization of SYN1 on cisplatin-treated <i>Atspo11-1-4^{-/-}</i> meiocytes	150
5.2.4 Cytogenetic analysis in <i>syn1^{-/-}</i> and <i>Atrad51c^{-/-}</i> double knockout mutant	155
5.2.5 Cytogenetic analysis in a <i>syn1^{-/-}/Atdmc1^{-/-}</i> double knockout mutant	159
5.2.6 Seeds of wild-type and <i>SYN1</i> heterozygous plants grew slowly on cisplatin MS medium.	163
5.3 DISCUSSION	168
5.3.1 SYN1 is essential for centromeric cohesion at first meiotic segregation	168
5.3.2 Chromosome fragmentation in <i>syn1</i> is AtSPO11-1-dependent.....	171
5.3.3 SYN1 loading is reduced in <i>Atspo11-1-4^{-/-}</i> meiocytes.....	171
5.3.4 Some SYN1 loading is dependent on DNA double-strand breaks	172
5.3.5 SYN1 has a role in DNA DSB repair.	173
5.3.6 SYN1 and AtRAD51c are essential for DNA double strand break repair.	174
5.3.7 Seeds of wild-type and <i>SYN1</i> heterozygous plants grow slowly in cisplatin MS medium.	175
CHAPTER 6	178
CONCLUSIONS	178
6.1 INTRODUCTION.....	178
6.2. Is SYN1 IMPORTANT IN SISTER CHROMATID COHESION?	178
6.3 SYN1 IS ESSENTIAL FOR MEIOTIC RECOMBINATION PROGRESSION AND SC POLYMERIZATION/ ELONGATION.	180
6.4 SYN1 PLAYS AN IMPORTANT ROLE DURING DNA DOUBLE STRAND BREAK (DSB) REPAIR	181
6.5 FUTURE WORK.....	185
CHAPTER 7	187
REFERENCES	187

LIST OF FIGURES

Figure 1.1	Meiosis and mitosis	2
Figure 1.2	Schematic diagram showing the stages in meiosis I	4
Figure 1.3	The structure of SMC proteins	8
Figure 1.4	A possible model of mitotic and meiotic cohesin complex	9
Figure 1.5	Another two possible models of cohesin complex	11
Figure 1.6	Diagram showing the yeast SCC1 and REC8 during meiosis	13
Figure 1.7	Shugoshin-PP2A protects centromeric cohesin from dissociation during mitotic prophase	19
Figure 1.8	Shugoshin-PP2A protects centromeric cohesin from separase cleavage until metaphase I	21
Figure 1.9	Synaptonemal complex (SC) structure	28
Figure 1.10	Early events of meiotic recombination	34
Figure 1.11	Meiotic crossover and non-crossover pathways following D-loop formation	39
Figure 2.1	The sequence alignment of <i>Arabidopsis</i> SYN1, SYN2, SYN3 and SYN4 proteins	54
Figure 2.2	Alignment of <i>Arabidopsis</i> SYN1 and DNA fragment	56
Figure 2.3	Nucleotide sequence of the SYN1 insert and pET21b vector	57
Figure 2.4	The translation of SYN1 amino acid sequence	57
Figure 2.5	SDS-PAGE analysis of protein test induction	65
Figure 2.6	Western Blot analysis of <i>E.coli</i> BL21(DE3)pLysS/pET21b-SYN1 (C1) and <i>E.coli</i> BL21(DE3)pLysS/pET21b (Control) in protein test expression with and without IPTG	66
Figure 2.7	SDS-PAGE (A) and Western Blot (B) analysis of <i>E.coli</i> BL21(DE3)/pET21b-SYN1 in protein test expression with and without IPTG	69
Figure 2.8	28 days anti-serum was analysed by western blot	70

Figure 3.1	Nucleotide sequence of the plasmid DNA	81
Figure 3.2	Sequence of <i>A. thaliana</i> genomic DNA	82
Figure 3.3	Map of the <i>SYN1</i> locus and exon organisation	83
Figure 3.4	<i>SYN1</i> gene expression in wild-type (Col 0), <i>syn1</i> ^{-/-} and <i>Atspo11-1-4</i> ^{-/-} plants	86
Figure 3.5	Genevestigator expression profile of <i>Arabidopsis SYN1</i> gene	87
Figure 3.6	Meiotic stages in pollen mother cells of wild-type (Col 0) of <i>A. thaliana</i>	91
Figure 3.7	Meiotic stages in pollen mother cells of the SALK line 091193 (<i>syn1</i> mutant) of <i>A. thaliana</i>	92
Figure 3.8	FISH of centromeric probe (pAL38) to pollen mother cells of wild-type <i>A. thaliana</i>	95
Figure 3.9	FISH of centromeric probe (pAL38) to pollen mother cells of the SALK line 091193 (<i>syn1</i> mutant) of <i>A. thaliana</i>	96
Figure 3.10	Alignments of the full length amino acid sequence of the smREC8, ceREC8 and SYN1	100
Figure 3.11	Alignment of the full length amino acid sequence of AFD1, OsRAD21-4 and SYN1	101
Figure 4.1	Immunolocalization of SYN1 protein to nuclei of wild-type (Col 0)	108
Figure 4.2	Immunolocalization of ASY1 and SYN1 proteins to wild-type (Col 0) meiocytes	108
Figure 4.3	Dual immunolocalization of ASY1 (green) and SYN1 (red) to leptotene (A), zygotene (B), early pachytene (C) and late pachytene of wild-type (Col 0)	109
Figure 4.4	Dual immunolocalization of SYN1 (green) and AtSMC3 (red) on meiotic spreads of wild-type <i>Arabidopsis thaliana</i>	112
Figure 4.5	Immunolocalization of SYN1 (green) and AtSMC3 (red) on early pachytene cell (A) of wild-type	113
Figure 4.6	Dual immunolocalization of SYN1 (green) and AtSCC3 (red) on meiocytes of wild-type	114

Figure 4.7	Immunolocalization of SYN1 (green) and AtSCC3 (red) on zygotene cell (A) of wild-type	115
Figure 4.8	Immunolocalization of SYN1 (green) to early pachytene (A) of wild-type	116
Figure 4.9	Immunolocalization of AtSCC3 (red) and ASY1 (green) to meiocytes of <i>syn1</i> mutants	118
Figure 4.10	Immunolocalization of AtSMC3 (red) and ASY1 (green) on meiocytes of <i>syn1</i> mutants	119
Figure 4.11	Immunolocalization of SYN1 (green) and AtZYP1 (red) on meiocytes of wild-type <i>Arabidopsis</i>	122
Figure 4.12	Immunolocalization of SYN1 (green) and AtZYP1 (red) to zygotene (A) of wild-type <i>Arabidopsis</i>	124
Figure 4.13	Immunolocalization of SYN1 (green) and AtZYP1 (red) to pachytene (A) of wild-type <i>Arabidopsis</i>	125
Figure 4.14	A diagram showing the dynamics of SYN1 and AtZYP1 along chromosomes	126
Figure 4.15	Immunolocalization of AtZYP1 (red) and SYN1 (green) on meiocytes of <i>syn1</i> mutants	127
Figure 4.16	Immunolocalization of AtZYP1 (red) and ASY1 (green) to meiocytes of wild-type (A) and <i>syn1</i> mutants (B; C)	129
Figure 4.17	Immunolocalization of AtRAD51 (red) and ASY1 (green) to meiocytes of wild-type (A) and <i>syn1</i> mutant (B; C; D)	131
Figure 4.18	Immunolocalization of AtMLH1 (red) and ASY1 (green) to meiocytes of wild-type (A) and <i>syn1</i> mutant (B; C; D)	133
Figure 5.1	Meiotic stages in pollen mother cells of the <i>Atspo11-1-4</i> mutant of <i>A. thaliana</i>	144
Figure 5.2	Meiotic stages in pollen mother cells of the <i>syn1^{-/-} Atspo11-1-4^{-/-}</i> double knock-out mutant of <i>A. thaliana</i>	145
Figure 5.3	Dual immunolocalization of ASY1 (green) and SYN1 (red) on prophase I nuclei of wild-type (A) and <i>Atspo11-1-4^{-/-}</i> (B) mutant.	148
Figure 5.4	BrdU (green) pulse-labelling combined with immunocytological analysis in wild-type and <i>Atspo11-1-4^{-/-}</i> meiocytes.	149

Figure 5.5	Dual immunolocalization of ASY1 (green) and SYN1 (red) on prophase I nuclei of wild-type (A) and untreated <i>Atspo11-1-4^{-/-}</i> (B) and cisplatin-treated <i>Atspo11-1-4^{-/-}</i> mutant (C).	152
Figure 5.6	Signal intensity analysis of SYN1 on prophase I nuclei of wild-type (Col 0), cisplatin-treated <i>Atspo11-1-4^{-/-}</i> and untreated <i>Atspo11-1-4^{-/-}</i> mutants	153
Figure 5.7	Immunolocalization of AtZYP1 (green) on prophase I nuclei of wild-type (A) and cisplatin-treated <i>Atspo11-1-4^{-/-}</i> mutant (B; C)	154
Figure 5.8	Meiosis stages in pollen mother cells of the <i>Atrad51c^{-/-}</i> mutant of <i>A. thaliana</i>	157
Figure 5.9	Meiotic stages in pollen mother cells of <i>syn1^{-/-}/Atrad51c^{-/-}</i> of <i>A. thaliana</i> .	158
Figure 5.10	Meiotic stages in pollen mother cells of the <i>Atdmc1</i> null mutant of <i>A. thaliana</i> .	161
Figure 5.11	Meiotic stages in pollen mother cells of the <i>syn1^{-/-}/Atdmc1^{-/-}</i> double knock-out mutant of <i>A. thaliana</i> .	162
Figure 5.12	Cisplatin sensitivity phenotype of wild-type and <i>SYN1(Heter)</i> at 14 days after germination	165
Figure 5.13	Cisplatin sensitivity phenotype of wild-type and <i>SYN1(Heter)</i> at 21 days after germination	166
Figure 5.14	Cisplatin sensitivity of wild-type (Col 0) and <i>SYN1(Heter)</i>	167
Figure 6.1	Loading of SYN1 in two different meiotic stages	184

TABLES

Table 1.1	Names of cohesin subunits in various species	6
Table 1.2.	A list of separase cleavage sites in kleisin subunits	17
Table 3.1	Number of chromosome fragments in SALK line 091193 meiocytes	90
Table 3.2	The average number of centromeric FISH signals at different meiotic stages of wild-type and <i>syn1</i> mutant	94
Table 4.1	Immunolocalization of various antibodies in meiocytes of wild-type and <i>syn1</i> mutant	134
Table 5.1	Number of chromosome fragments at metaphase I in wild-type (Col 0), <i>syn1</i> ^{-/-} , <i>Atdmc1</i> ^{-/-} and <i>syn1</i> ^{-/-} / <i>Atdmc1</i> ^{-/-}	160
Table 5.2	Summary of mutant phenotype including chromosome numbers; fragmentation and chromosome segregation	170

APPENDIX

APPENDIX 5.1	Signal intensity analysis of SYN1 on prophase I nuclei of wild-type, cisplatin-treated <i>Atspo11-1-4</i> ^{-/-} and cisplatin free <i>Atspo11-1-4</i> ^{-/-}	177
--------------	---	-----

LIST OF FREQUENT ABBREVIATIONS

ASY1	Asynaptic 1
At	<i>Arabidopsis thaliana</i>
BrdU	Bromodeoxyuridine
Col 0	Columbia ecotype
DAPI	4,6-diaminido-2-phenylindole
DMC1	Disruption of meiotic control 1
DSB	Double strand break
FISH	Fluorescent in situ hybridisation
IPTG	Isopropylthio- β -D-galactosidase
MLH1	MutL homologue 1
PBS	Phosphate buffered saline
PCR	Polymerase chain reaction
PMC	Pollen mother cell
RAD51	RecA protein homologue
REC8	Abnormal recombination 8
RT-PCR	Reverse-transcription polymerase chain reaction
SC	Synaptonemal complex
SCC1	Sister-chromatid cohesion protein 1
SCC3	Sister-chromatid cohesion protein 3
SDW	Sterile distilled water
SDS-PAGE	Sodium-dodecyl-sulfate polyacrylamide gel electrophoresis
SMC1	Structural maintenance of chromosomes 1
SMC3	Structural maintenance of chromosomes 3
SPO11	Sporulation specific protein 11
SYN1	Synaptic 1
T-DNA	Transfer-DNA
WT	Wild-type
ZYP1	Synaptonemal complex protein 1

Chapter 1

General introduction

1.1 Overview of mitosis and meiosis

The process of mitosis involves a single cell division which produces two daughter cells from a single parent cell (Figure 1.1). Each daughter cell is genetically identical to the original parent cell (Zickler and Kleckner, 1998; Cnudde and Gerats, 2005). The mitotic cell division is preceded by the DNA replication which generates one pair of sister chromatids from each original chromosome. Chromosomes are then maintained by sister chromatid cohesion throughout the prophase (Nasmyth, 2001). The kinetochores of chromosomes are attached to spindle fibres that align the chromosomes on the equatorial plate and then separate them to opposite poles. The separated chromatids form into two diploid daughter cells. In contrast, meiosis is a process of two cell divisions, meiosis I and meiosis II, which results in the production of four haploid daughter cells from a single parent cell (Figure 1.1). Each daughter cell carries half the amount of parental genetic material (Zickler and Kleckner, 1998; Cnudde and Gerats, 2005). The first meiotic division (meiosis I) is a reductional division, because the homologous chromosomes segregate into opposite poles. Meiosis I has been divided into a series of stages based on the appearance of chromosomes under a light microscope. These stages are prophase I, metaphase I, anaphase I and telophase I. Meiotic prophase I is further divided into five substages: leptotene, zygotene, pachytene, diplotene and diakinesis (Zickler and Kleckner, 1999; Pawlowski and Cande, 2005). Leptotene is considered as the first meiotic stage that can be distinguished after interphase. Although DNA has been replicated after S phase, the chromosomes are maintained by sister cohesion, which appear as single long thin threads in the nucleus. During early prophase I (Figure 1.2), paternal and maternal

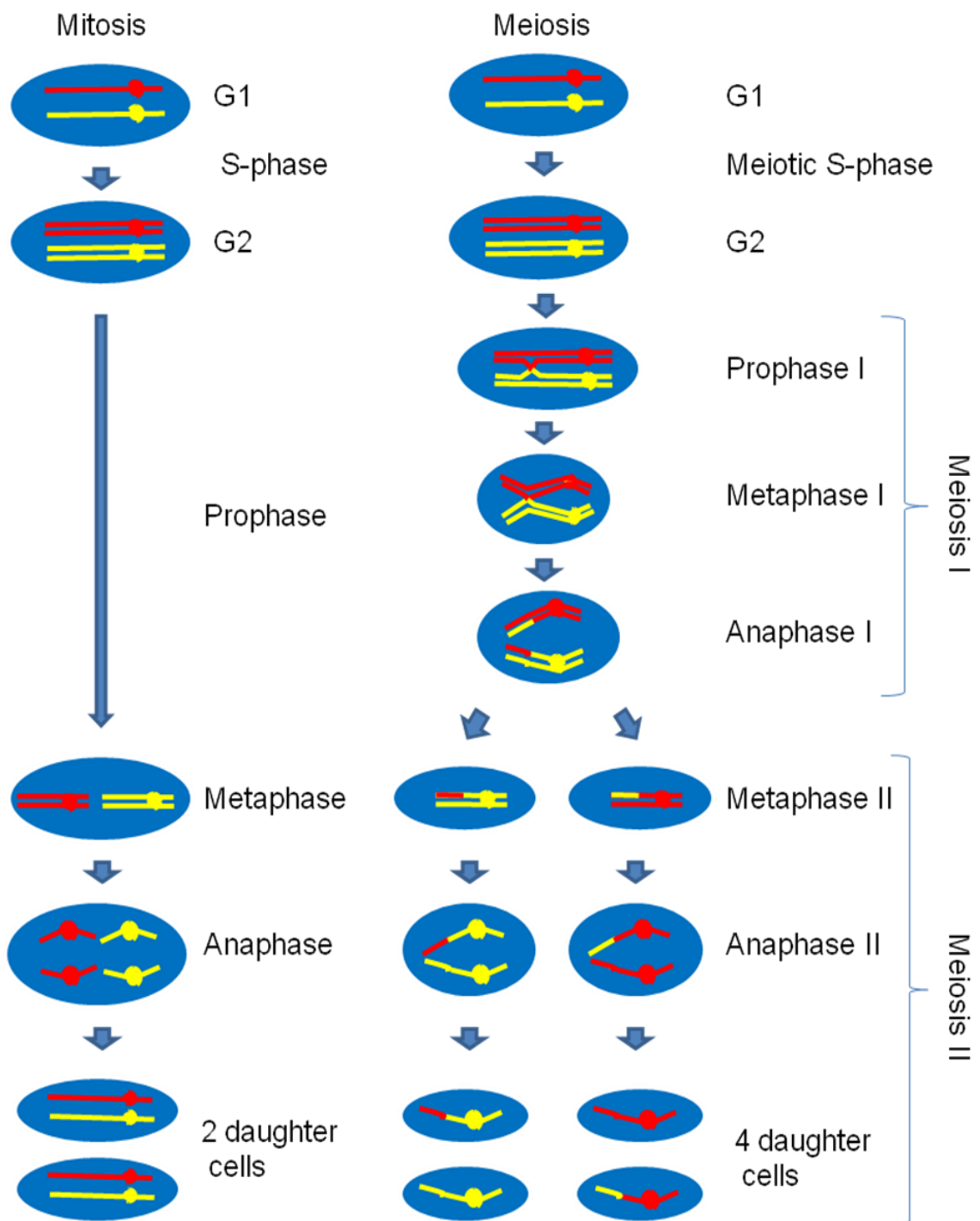


Figure 1.1. Meiosis and mitosis.

A diagram showing how a single cell produces two daughter cells via mitotic cell division and four daughter cells via meiotic cell division. Note: paternal (red) and maternal (yellow) chromosomes are shown in this diagram.

homologous chromosomes search for each other. Once the connection between homologous chromosomes is formed, structural proteins, the synaptonemal complex (SC), are established between chromosomes and the chromosomes are synapsed (Higgins et al., 2005). The synapsis of homologous chromosomes initiates during zygotene and continues through to pachytene when the synapsis of homologous chromosomes is complete. The fully synapsed homologous chromosomes or bivalents appear as thick thread-like structures within the nucleus. At the end of pachytene, the SC proteins begin to disassociate from the chromosomes, which are gradually separated. However, the homologous chromosomes remain tightly associated at chiasmata (singular chiasma), where non-sister chromatids have exchanged genetic material. This stage is defined as diplotene. Further chromosome condensation then occurs to form short bivalents by diakinesis, which marks the end of prophase I. During metaphase I, all the bivalents are aligned on the equatorial plate, due to the pulling forces of the spindle microtubules. The kinetochores of paternal and maternal homologous chromosomes are attached to spindle fibres from different poles. Therefore, paternal and maternal chromosomes are pulled to the opposite poles at anaphase I, forming two sets of chromosomes that remain associated at their centromeres. The second meiotic division (Meiosis II) is similar to mitosis, because the sister chromatids separate to opposite poles; it is also called the equational division (Zickler and Kleckner, 1999; Cnudde and Gerats, 2005; Pawlowski and Cande, 2005).

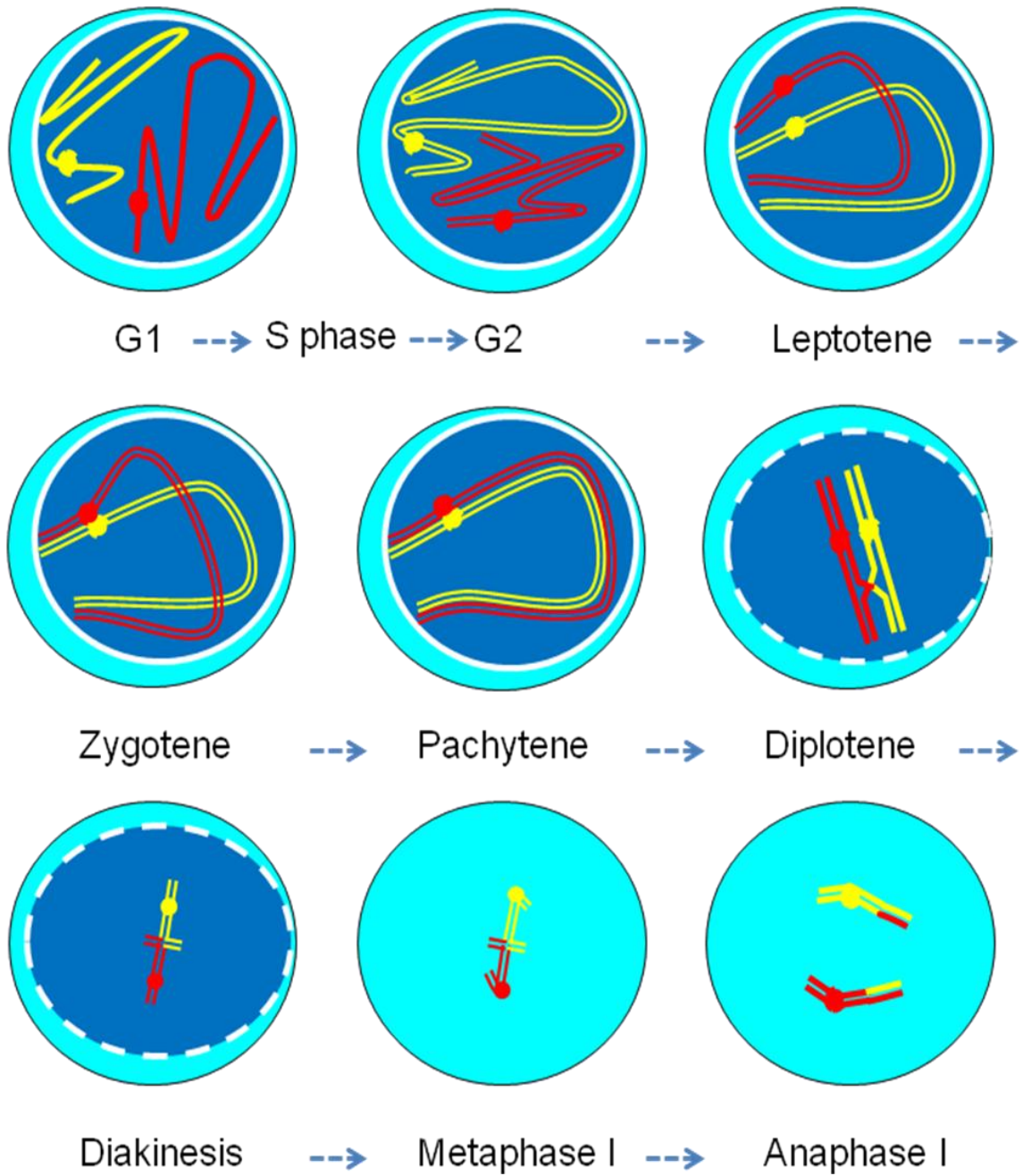


Figure 1.2. Schematic diagram showing the stages in meiosis I.

One pair of homologous chromosomes is shown in this diagram. For more description of stages see text.

Note: paternal (red) and maternal (yellow) chromosomes are duplicated during S-phase.

1.2 Sister chromatid cohesion

Cohesion between sister chromatids is established at the onset of S phase (Guacci et al., 1994). Sister chromatid cohesion is important for the kinetochores of sister chromatids to connect to the microtubules from opposite spindle poles, and also it resists the force of the spindle microtubules while aligned at the equatorial plate. This is essential to accurately segregate chromosomes at anaphase. Therefore, it is crucial to establish and maintain cohesion between sister chromatids until chromosome segregation. In mitosis, cohesion is released completely from chromosome arms and centromeres at the metaphase/anaphase transition stage to allow sister chromatid separation. In contrast, meiotic cohesion is released in two stages. Firstly, cohesion is lost at diakinesis stage from the homologous chromosome arms allowing the chiasmata to be resolved and homologous chromosomes to segregate. Although cohesion is released from chromosome arms, it is still retained at the sister centromeres until metaphase II. During anaphase II, cohesion is lost completely from the sister centromeres, at which point, the sister chromatids separate towards opposite poles (Lee and Orr-Weaver, 2001; Nasmyth, 2001).

1.2.1 Establishment of sister chromatid cohesion

In yeast, sister chromatid cohesion requires two structural maintenance of chromosomes (SMC) proteins, SMC1 and SMC3, and two non-SMC proteins, the mitotic cohesin subunit SCC1 (meiotic cohesin subunit REC8) and SCC3. Together they form a cohesin complex (Guacci et al., 1997; Michaelis et al., 1997). Homologues of these cohesin proteins are also found in other organisms (Table 1.1). Recently, another protein PDS5 was found that is associated with cohesin complex, suggesting that it is essential for maintaining the cohesin on the chromosomes (Panizza et al., 2000).

Table 1.1 Names of cohesin subunits in various species.

species cohesin	<i>S.</i> <i>cerevisiae</i>	<i>S.</i> <i>pombe</i>	<i>C.</i> <i>elegans</i>	<i>D.</i> <i>melangaster</i>	<i>H.</i> <i>sapiens</i>	<i>A.</i> <i>thaliana</i>
SMC1 subunit	SMC1	PSM1	HIM-1	SMC1	SMC1 α (SMC1 β)*	AtSMC1
SMC3 subunit	SMC3	PSM3	SMC-3	SMC3/CAP	SMC3	AtSMC3
Kleisin subunit	MCD1/ SCC1 (REC8)*	RAD21 (REC8)*	SCC-1; COH-1 (REC8; COH-3)*	RAD21 (C(2)M)*	RAD21 (REC8)*	SYN2; SYN4 (SYN1)*
SCC3 subunit	SCC3/ IRR1	PSC3 (REC11)*	SCC-3	SA; SA-2	STAG1; STAG2 (STAG3)*	AtSCC3
PDS5 subunit	PDS5	PDS5	EVL-14	PDS5	PDS5A; PDS5B	N/C

Meiosis specific cohesin subunits are written in a ()* below their mitotic counterparts.

According to WormBase, NCBI database and TAIR, most species contain mitotic and meiotic specific kleisin subunits.

N/C represents that a homologous gene has not been identified.

1.2.1.1 Cohesins

SMC1 and SMC3 are both members of the SMC family which share five conserved domain structures, including amino and carboxyl termini of ATP-binding domains named the Walker A motif and Walker B motif respectively (Figure 1.3A). These two ATP binding domains are connected by two coiled-coil domains separated by a hinge domain (Jones and Sgouros, 2001). Biochemical studies (Haering et al., 2002) revealed that each SMC subunit folds back on itself (Figure 1.3B). As a result the N-terminal domain with Walker A motif and C-terminal domain with Walker B motif come together to form a potentially functional ATP binding cassette (ABC) ATPase (Melby et al., 1998; Hopfner et al., 2000; Lowe et al., 2001; Nasmyth, 2005). Thus, each SMC protein forms intramolecular antiparallel coiled-coils connected one end by the hinge domain and on the other end by an ABC ATPase head domain. Both SMC1 and SMC3 proteins dimerize via interactions between their hinges forming a stable V-shape heterodimer (Figure 1.3C) (Haering et al., 2004). SCC1 is a member of the kleisin (a Greek word meaning “closure”) family of proteins (Haering and Nasmyth, 2003). All kleisin proteins are most conserved at their N and C termini (Schleiffer et al., 2003). Mutation of these conserved termini disrupts the interaction of SCC1 with SMC1/SMC3. Biochemical analyses showed that the N terminal domain of SCC1 binds to the SMC3 head domain while the C terminal domain of SCC1 binds to the SMC1 head domain, forming a ring-like structure that could hold the sister chromatids (Figure 1.4) (Haering et al., 2002; Gruber et al., 2003; Haering et al., 2004). During meiosis, SCC1 is replaced by a meiotic cohesin subunit REC8, another member of the Kleisin family. The similarities between SCC1 and REC8 proteins are restricted to their N and C termini. Biochemical analyses have shown that the C-terminal of REC8 binds to SMC1 and the N-terminal of REC8 binds to SMC3. These results suggest that the N and C termini of SCC1 and REC8 are able to bind with the SMC1 and SMC3 heads to

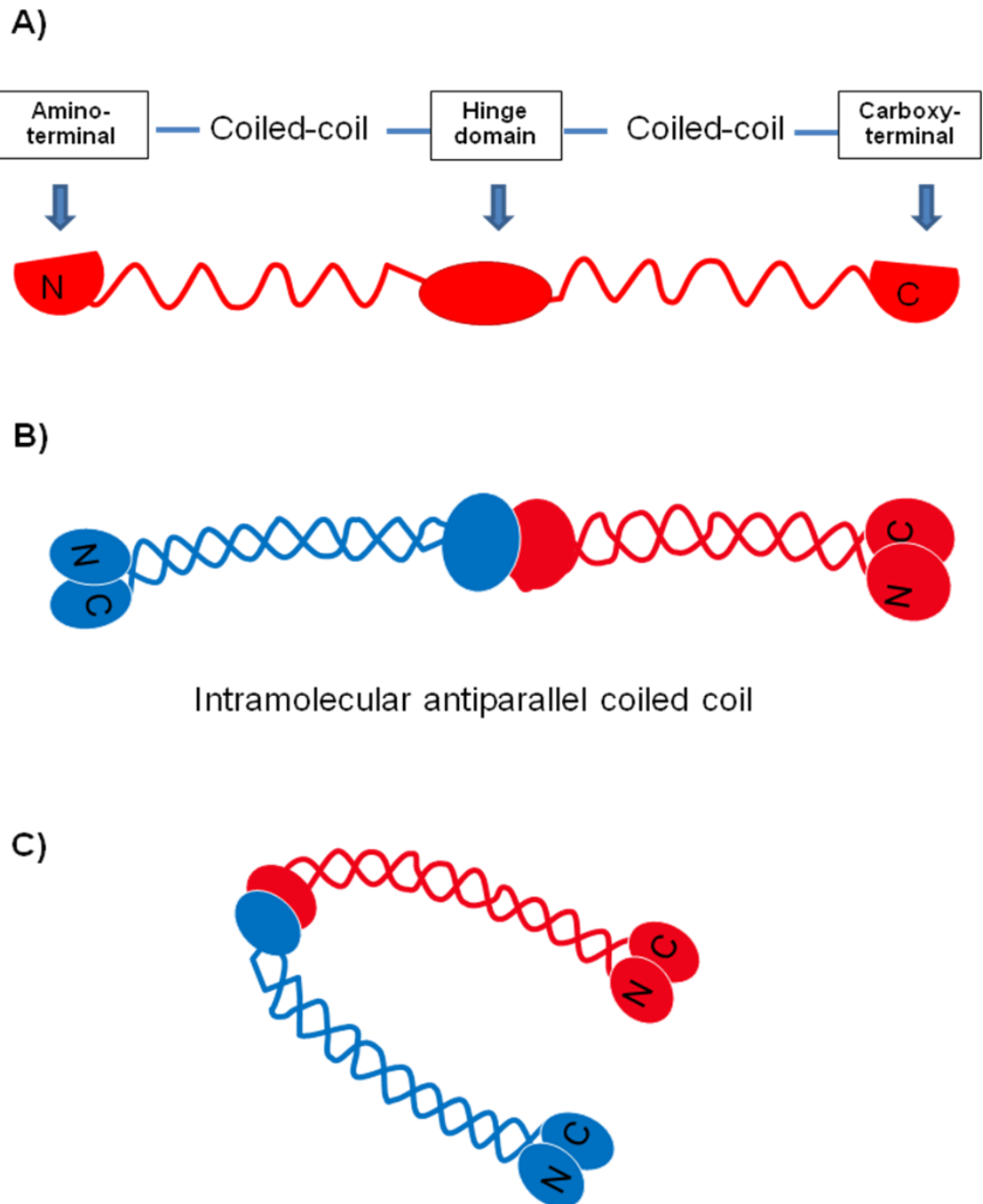


Figure 1.3. The structure of SMC proteins.

(A) SMC contains five domains. There are two coiled coil domains, one hinge domain, N-terminal domain includes a Walker A motif and C-terminal domain includes a Walker B motif. (B) Each SMC protein folds by antiparallel coiled-coil interactions to form a hinge domain at one end and a head domain at the other. (B; C) Hinge-hinge interaction between SMC1 (red) and SMC3 (blue) form a V-shape heterodimer.

Figures, (B) and (C), are modified from Nasmyth (2001).

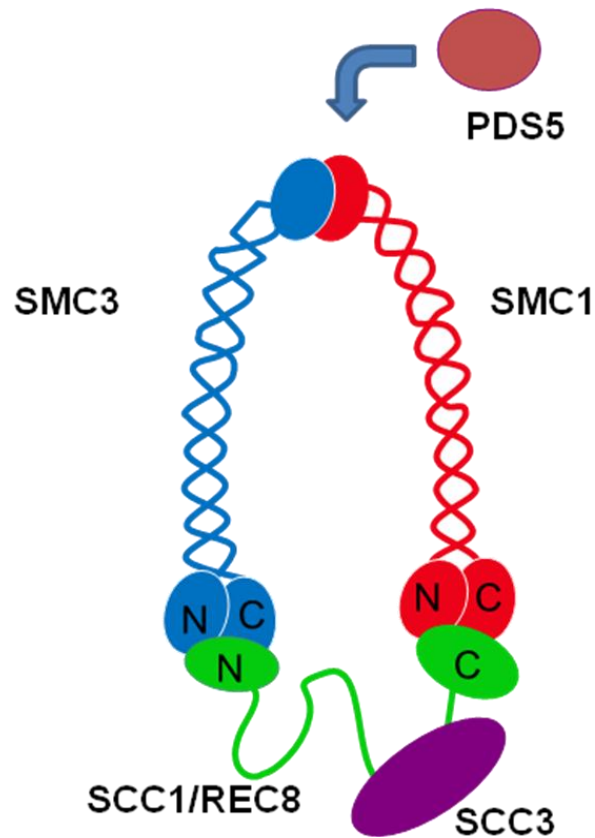


Figure 1.4. A possible model of mitotic and meiotic cohesin complex.

Cohesin complex contains a SMC1-SMC3 heterodimer, kleisin subunit and SCC3 subunit. Biochemical analysis have shown that the N-terminal of kleisin SCC1/REC8 associates with SMC3 head domain and C-terminal of SCC1/REC8 associates with SMC1 head domain forming a cohesin ring-like structure. SCC3 binds directly to C-terminal half of SCC1. Currently, PDS5 has been suggested to associate with the hinge domain. The figure is modified from Nasmyth (2005).

form a ring-like cohesin complex (Gruber et al., 2003). The cohesin complex has also been proposed to form a dimeric ring or a filament structure (Figure 1.5)(Nasmyth, 2005). SCC3 is the fourth cohesin subunit protein, it has been shown that the yeast SCC3 binds directly to the C-terminal half of SCC1 (Nasmyth, 2002). A recent report in vertebrate mitotic cells revealed that SA2 (SCC3-like protein) has a role in cohesin disassociation from chromosome during mitosis (Hauf et al., 2005). Another protein PDS5 is found to associate with the cohesin complex. In vivo analysis showed that weak PDS5 signals are detected on the SMC1/SMC3 hinge domain. However, the physical interaction of PDS5 with hinge domain is still not demonstrated (Mc Intyre et al., 2007).

1.2.1.2 Loading of cohesin on sister chromatids

If cohesin is loaded onto a chromosome during DNA replication, how is the DNA trapped within the cohesin ring-like structure? In yeast, artificial linkage was built between the SMC1 and SMC3 hinge domains. This showed that the establishment of sister chromatid cohesion was inhibited. This observation suggests that a temporary dissociation of SMC1 and SMC3 hinge domains allows DNA to enter the cohesin ring (Gruber et al., 2006). The loading of cohesin onto chromosomes is facilitated by SCC2 together with SCC4. Studies have confirmed that cohesin is not able to associate with the chromosome arms and centromeres in the absence of SCC2 or SCC4 (Ciosk et al., 2000). Another protein Eco1 (also called Ctf7) is also essential for establishing sister chromatid cohesion around S-phase. In yeast, sister chromatid cohesion is affected severely when the activation of Eco1 (Ctf7) is inhibited before entering into S-phase. Interestingly, if inactivation of Eco1 (Ctf7) occurs after S-phase is completed then normal sister chromatid cohesion is observed. This finding indicates that cohesin appears around S-phase to form sister chromatid cohesion, suggesting that Eco1 is

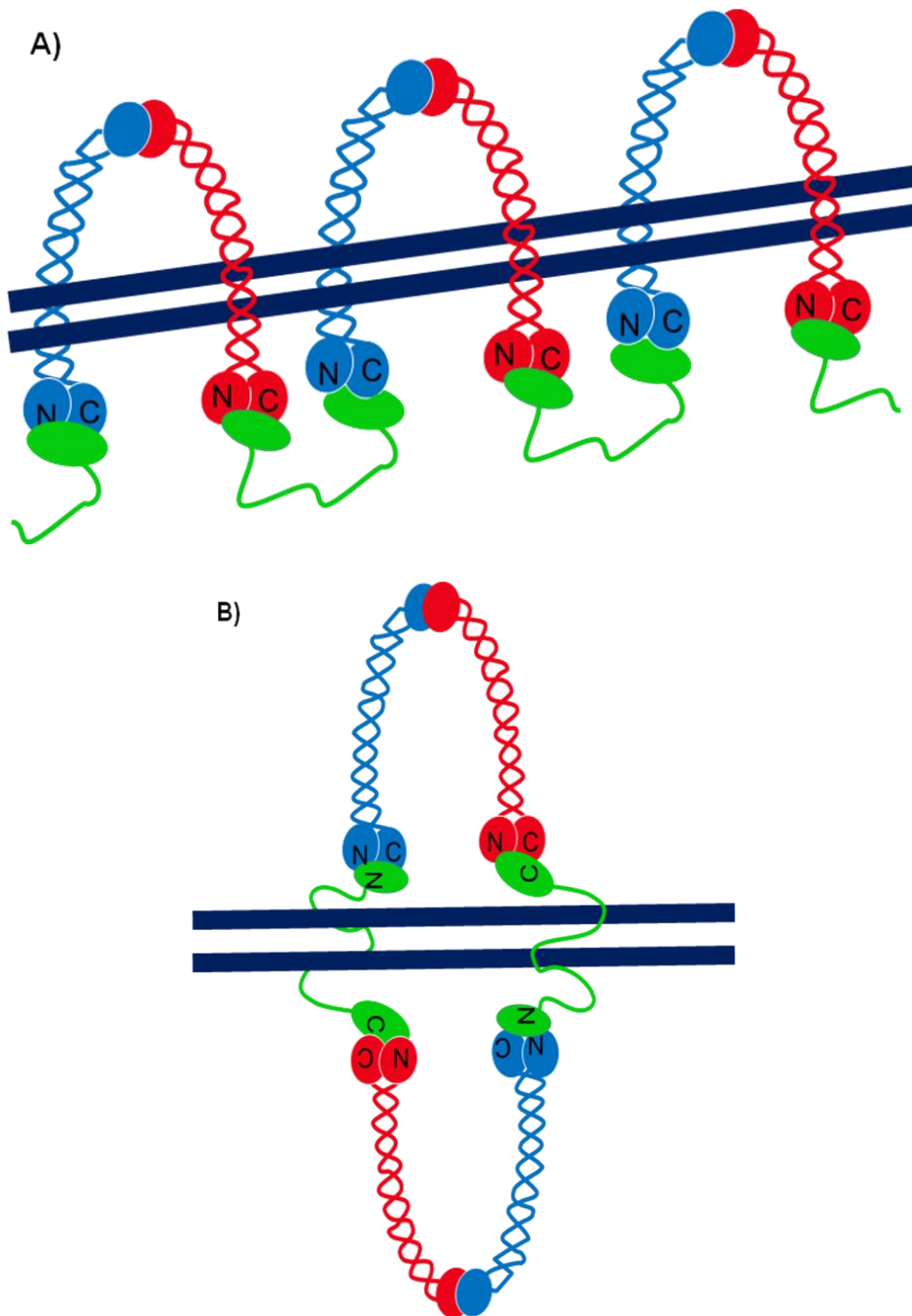


Figure 1.5. Another two possible models of cohesin complex. Kleisin N terminus associates with a SMC1-SMC3 heterodimer and C terminus associates with a different SMC1-SMC3 heterodimer, it can possibly form either a cohesin filament (A) or a dimeric ring (B) structure. Figures are modified from Nasmyth (2005).

required for the formation of cohesive structures between the sister chromatids after cohesin associates with chromosomes (Skibbens et al., 1999; Toth et al., 1999; Noble et al., 2006).

1.2.2 Localization of cohesin on the chromosome in meiosis

Yeast studies showed that the mitotic kleisin subunit SCC1 is replaced by REC8 during early meiosis I (Klein et al., 1999). Complementation studies in *S. pombe* revealed that overexpression of REC8 can rescue the mitotic sister chromatid cohesion in the absence of RAD21/SCC1. However, the meiotic cohesion defect could not be restored in a *rec8* mutant by overexpression of RAD21/SCC1. This indicates that REC8 has a specific role during meiosis that RAD21 cannot support (Watanabe and Nurse, 1999). A yeast antibody to REC8 is observed as a spotty signal on chromosomes at leptotene and zygotene. During pachytene, REC8 is present at the centromere and adjacent chromosome arms (Klein et al., 1999; Watanabe and Nurse, 1999). Although SCC1 is largely replaced by REC8 throughout meiosis I, some SCC1 signals are still detectable on chromosomes (Figure 1.6). Immunolocalization studies confirmed that SCC1 did not colocalize with REC8 from leptotene to pachytene (Klein et al., 1999). The localization of REC8/RAD21 in mammals is different from that of REC8/SCC1 in yeast (*S. pombe* and *S. cerevisiae*). Mammalian REC8 is first observed as foci in premeiotic S phase. During pachytene, both REC8 and RAD21 proteins appear along the entire the length of the chromosomes, indicating that the mitotic cohesin subunit RAD21 has a role in meiosis (Prieto et al., 2004). Mammalian RAD21 is lost from chromosome arms but it is still detectable at the centromeres from metaphase I to metaphase II. During anaphase II, RAD21 signals were no longer observed at the centromeres, indicating that RAD21 is released from the centromeres at metaphase II. These observations suggest that the mitotic cohesin subunit RAD21/SCC1 might have a role in meiotic chromosome cohesion and

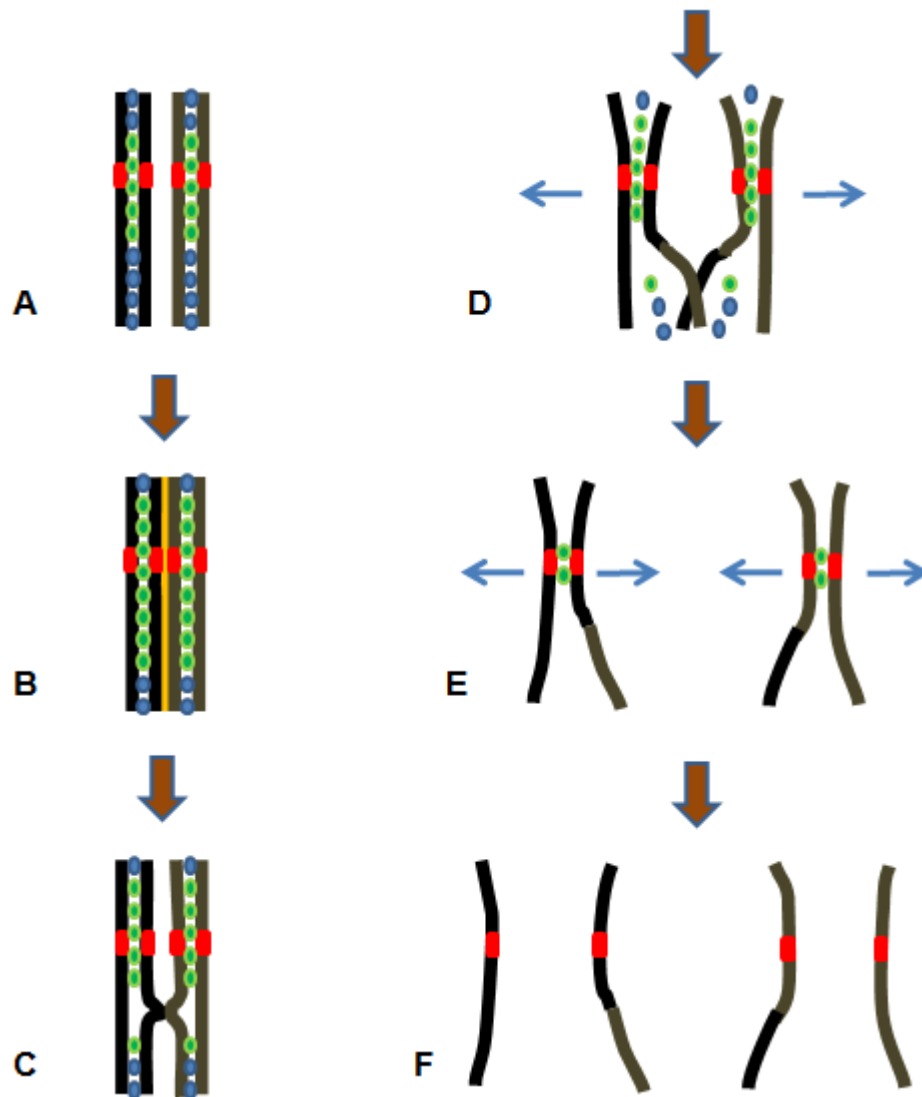


Figure 1.6. Diagram showing the yeast SCC1 (●) and REC8 (●) during meiosis.

In yeast, (A) SCC1 is replaced with the meiotic kleisin subunit REC8 at the onset of meiotic S-phase. (B) During pachytene, SCC1 is largely replaced by REC8 but a little SCC1 is still present at the end of the chromosomes. (C) Cohesin is lost from chromosome arms distal to a chiasma. (D) During the first meiotic division, cohesin is released along the chromosome arm, whereas REC8 is still present at the sister centromere (■) for maintaining the centromeric cohesion until metaphase II (E). (F) During second meiotic division, REC8 is released at centromere allowing sister chromatid separation.

segregation (Xu et al., 2004). Intriguingly, meiotic recombination and homologous chromosome synapsis are still affected when cohesin RAD21 is present in a *rec8* mutant. This suggests that kleisin RAD21 cannot simply replace REC8 in meiotic sister cohesion role (Xu et al., 2005).

In yeast meiocytes, REC8 associates with the V shape SMC1-SMC3 heterodimers forming a meiotic cohesin complex. Immunolocalization studies revealed that the SMC3 colocalizes with REC8 but not with SCC1 on chromosomes during early prophase I (Klein et al., 1999). Substantial signals of SMC3 and REC8 disappear from the chromosome arms after pachytene stage but persist at the centromeric regions until metaphase II, suggesting that SMC3 is required for sister chromatid cohesion in meiosis (Klein et al., 1999). In mammals, SMC1 β , a meiotic variant of SMC1, is found and expressed specifically in the testes. Biochemical analysis showed that SMC1 β co-immunoprecipitated with SMC3 from testis extracts but not in somatic cells. Interestingly mitotic cohesin SMC1 (also called SMC1 α) is still present in meiotic cells, suggesting that SMC1 α is partially replaced by SMC1 β during meiosis (Revenkova et al., 2001). Immunolocalization studies revealed that SMC1 β and SMC3 colocalize with REC8 during early prophase I but disappears from the chromosome arms at metaphase I (Eijpe et al., 2003). SMC1 β but not SMC1 α is present at the centromeres until metaphase II, suggesting that SMC1 β is important for maintaining sister cohesion at centromeric regions during meiotic segregation (Revenkova et al., 2001). Although SMC1 β /SMC3 colocalize with REC8 on chromosomes, the loading of SMC3 protein is not affected in the absence of REC8 meiocytes (Xu et al., 2005), indicating that SMC protein loads on chromosomes before REC8.

In *S. cerevisiae*, SCC3 is the fourth cohesin subunit protein that interacts with both the

mitotic and meiotic cohesin complex (Toth et al., 1999; Nasmyth, 2002). In contrast, *S. pombe* contains two SCC3 homologues, named REC11 and PSC3 respectively. REC11 appears at chromosome arms while PSC3 is present at centromeric region during early meiosis. Immunostaining results showed that both REC11 and PSC3 proteins colocalize with the meiotic kleisin subunit REC8 (Tomonaga et al., 2000; Kitajima et al., 2003). Furthermore, three SCC3 homologues, STAG1, STAG2 and STAG3, were found in mammalian cells but only STAG3 is classified as a meiotic specific cohesin (Pezzi et al., 2000). Co-immunoprecipitation analysis showed that STAG3 interacts with SMC1 and SMC3 in meiocytes but not in somatic cells (Prieto et al., 2002). Immunolocalization studies reveal that this protein colocalizes with REC8 along the chromosome arms in pachytene stage but not at the chromosome ends where only REC8 is detectable (Prieto et al., 2002). STAG3 is released from the chromosome arms and inner part of centromeres during the metaphase-anaphase I transitional stage, indicating that STAG3 is only active in meiosis I (Prieto et al., 2001; Prieto et al., 2002). A previous report showed that the mitotic cohesin subunit RAD21 is still detectable at the centromeres from metaphase I to metaphase II (Xu et al., 2004). It is possible that mitotic cohesin STAG1 or STAG2 might associate with RAD21 to maintain sister centromere cohesion until metaphase II.

1.2.3 Removal of cohesins

1.2.3.1 Cleavage of cohesin by separase

In mitosis, cohesion remains on the chromosomes until the metaphase and anaphase transition stage. At the beginning of anaphase, cohesion is released from chromosomes due to the cleavage of SCC1 (Uhlmann et al., 1999; Uhlmann et al., 2000). Recently, a TEV-cleavable RAD21/SCC1 was created in *D. melanogaster*. Expression of TEV protease

(+TEV) showed that chromosomes fail to gather together on equatorial plate. Thus, the separation of sister chromatids occurred prematurely (Pauli et al., 2008), indicating that the cohesin ring was opened and thereby triggers chromosome separation. In *S. cerevisiae*, two related sequence motifs were identified as SCC1 cleavage sites (Table 1.2). Mutation of both SCC1 cleavage sites prevents the disassociation of SCC1 from sister chromatids (Uhlmann et al., 1999; Uhlmann et al., 2000). These specific cleavage sites of SCC1 are cleaved by an endopeptidase protein called separase (ESP1 in *S. cerevisiae*; Cut1 in *S. pombe*), initiating the separation of the sister chromatids (Uhlmann et al., 1999; Uhlmann et al., 2000). Separase is associated with inhibitory proteins called securin (PDS1 in *S. cerevisiae*; Cut2 in *S. pombe*) and cyclin B at early mitosis (Yanagida, 2000; Gorr et al., 2005). During metaphase and anaphase transition, an ubiquitin protein ligase, the anaphase-promoting complex or cyclosome (APC/C) in conjunction with the Cdc20 protein promotes the ubiquitin-dependent degradation of both securin and cyclin B (Irniger et al., 1995; Cohen-Fix et al., 1996; Funabiki et al., 1996; Yamamoto et al., 1996; Uhlmann, 2003; Nasmyth and Haering, 2005). This process eventually activates the separase allowing this protein to split the kleisin subunit SCC1. Sister chromatids are then separated to their respective poles by the pulling force of the spindle microtubules during anaphase (Ciosk et al., 1998; Uhlmann et al., 1999).

Table 1.2. A list of separate cleavage sites in kleisin subunits.

Species	Kleisin subunit	Cleavage site	Sequence
<i>S. cerevisiae</i>	SCC1	180	174- TSLEV GRRF -182
<i>S. cerevisiae</i>	SCC1	268	262-NSVEQ GRRL -270
<i>S. cerevisiae</i>	REC8	431	425- SSVE RGRKR -433
<i>S. cerevisiae</i>	REC8	453	447-RSHEY GRKS -455
<i>S. pombe</i>	RAD21	179	173-LSIEA GRNA -181
<i>S. pombe</i>	RAD21	231	225-I SIEV GRDA -233
<i>S. pombe</i>	REC8	384	378-SEVE GRDV -386

In yeast meiosis SCC1 is largely replaced by the meiotic kleisin subunit REC8 which also contains two separate cleavage sites. The sequence motifs of REC8 are similar to the two SCC1 cleavage sites (Table 1.2)(Uhlmann et al., 1999). During the first meiotic division, separate is activated to cleave the REC8 and thereby, cohesin is removed from the chromosome arms (Buonomo et al., 2000). Previously, a mutation of separate in mouse oocytes showed that REC8 is not removed from chromosome arms and chiasmata are not resolved during anaphase I, indicating that separate is essential for removing cohesin from bivalents and resolving chiasmata (Kudo et al., 2006). This finding indicates cleavage of the cohesin kleisin by separate triggers both mitotic division and meiotic division in yeast and animals. These observations suggest that the molecular mechanism of chromosome segregation might be universal across different species. However, recent reports in vertebrate mitotic cells revealed that the cleavage of kleisin subunit SCC1 by separate is not required for dissociation of cohesin from chromosome arms during prophase, but is essential for sister

chromatid separation at anaphase (Hauf et al., 2001; Hauf et al., 2005). The cohesin dissociation at prophase depends on two mitotic kinases, Polo-like kinase 1 (Plk1) and Aurora B (Losada et al., 2002; Sumara et al., 2002; Gimenez-Abian et al., 2004). The biochemical analysis of HeLa cell lines in vitro revealed that Plk1 phosphorylates the cohesin subunits SA2 (SCC3-like protein), suggesting that it is essential for cohesin dissociation during prometaphase (Hauf et al., 2005). Phosphorylation of cohesin subunit SA2 by Plk1 is dissociated but not cleaved at prophase, thereby SA2 and other cohesins relocate to the chromosomes in the next cell cycle (Ishiguro and Watanabe, 2007).

1.2.3.2 Protection of centromeric cohesion

In vertebrate mitosis, most cohesin is released from chromosome arms by Aurora B and Plk1 but still small amount of cohesin persists around the centromeric region to hold the sister chromatids. Mitotic cohesin at centromeres is protected from the dissociation of cohesin by Shugoshin (Sgo) protein (Watanabe, 2005). In human, shugoshin, Sgo1, is identified and is expressed in HeLa cells (Watanabe and Kitajima, 2005). Immunostaining of Sgo1 in HeLa cells revealed that this protein appears as a strong signal from prophase until metaphase. By the end of anaphase, Sgo1 is not detectable (Watanabe and Kitajima, 2005). Furthermore, studies in the depletion of human Sgo1 by RNAi revealed that SCC1 is displaced from centromeres before metaphase and separated chromosomes are observed, suggesting that Sgo1 is essential for protection of sister centromere cohesion during prophase (Watanabe and Kitajima, 2005). It is clearly observed that cohesin is not secured from separate cleavage by the Sgo1 but is resistant to the dissociation of cohesin by Aurora B and Plk1 (Hauf et al., 2001; McGuinness et al., 2005). Biochemical analysis revealed that shugoshin interacts with

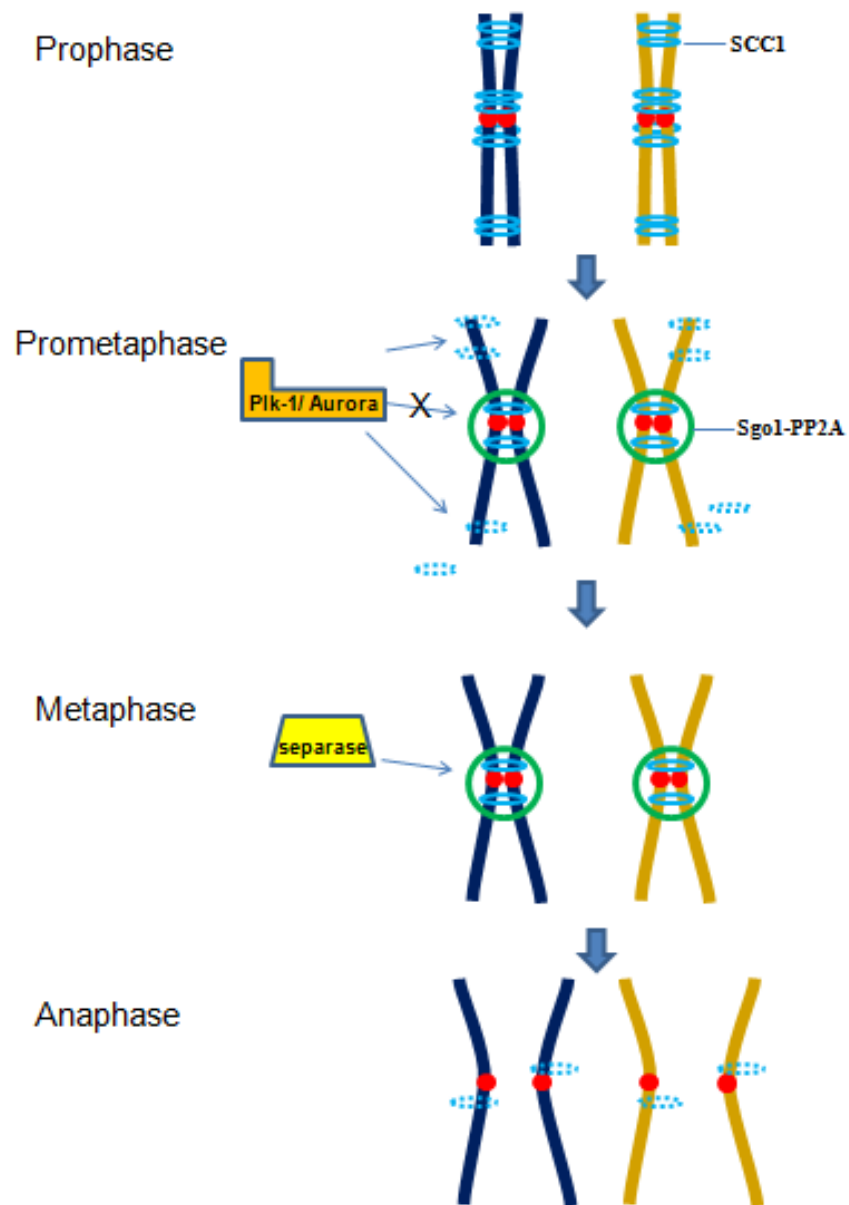


Figure 1.7 Shugoshin-PP2A protects centromeric cohesin from dissociation during mitotic prophase

During prometaphase, Polo-like kinase 1 and Aurora B (orange) disassociate cohesins (blue ring) from chromosome arms but not at centromeric region which is protected by Shugoshin-PP2A complex (green ring). However, this complex does not protect the centromeric cohesin from separase (yellow) cleavage. Therefore, sister chromatids are separated at anaphase.

the protein phosphatase 2A (PP2A) forming a complex (Figure 1.7). This Sgo1-PP2A complex can dephosphorylate cohesin SA2 *in vitro*, suggesting that this Shugoshin-PP2A complex protects centromeric cohesin from dissociation triggered by Plk1 and Aurora B (Kitajima et al., 2006). Meiotic cohesion is released in two steps. During diakinesis, cohesin is released from the chromosome arms but some still remains at the centromeres until metaphase II. During anaphase II, residual cohesin completely disappears from the centromeres allowing separation of sister chromatids. In yeast, mitotic kleisin subunit SCC1 is still present on meiotic chromosomes during prophase I but the sister chromatid cohesin fails to persist at the centromeres in the absence of REC8. Therefore, sister chromatids are separated during early prophase I. A similar result is also observed in a yeast *smc3* mutant (Klein et al., 1999). These observations suggest that SMC3 and REC8 but not SCC1 play a crucial role in sister chromatid cohesion at centromeres during the first meiotic division. This cohesin holds the sister centromeres and, thereby, sister chromatids move to the same pole. What kind of mechanism or protein can retain the cohesin at centromeric region throughout meiosis I until metaphase II? In yeast, it has been discovered that Shugoshin (Sgo1) protects centromeric cohesion during meiosis I (Figure 1.8) (Kitajima et al., 2004). Biochemical analysis also showed that Sgo1 associates with PP2A at the pericentromeric regions during meiosis, as in mitotic mammalian cells (Figure 1.8) (Riedel et al., 2006). Moreover, mutation of PP2A showed premature separation of sister chromatids during anaphase I, which is identical to the *sgo1* mutant phenotype. In addition, the PP2A protein can prevent phosphorylation of REC8 to block the cleavage of REC8 from separase, suggesting that Sgo1-PP2A complex is essential for protection of centromeric cohesion during meiosis (Riedel et al., 2006).

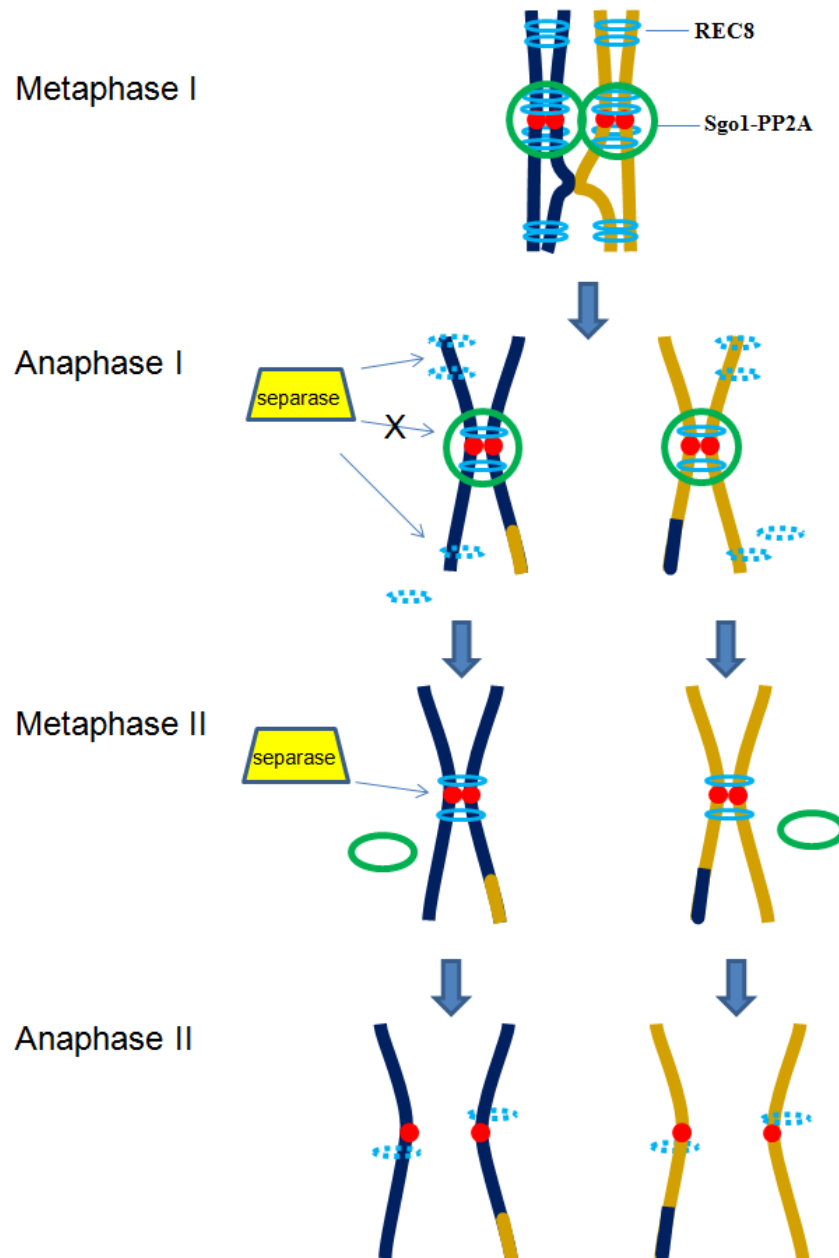


Figure 1.8 Shugoshin-PP2A protects centromeric cohesin from separase cleavage until metaphase I. Separase (yellow box) cleaves cohesins (blue ring) from chromosome arms but not the centromeric cohesin which is protected by Shugoshin-PP2A complex (green ring) during early meiosis. This allows the sister chromatids moving towards the same spindle poles. Before metaphase II, Shugoshin-PP2A disassociates from centromeres. Cohesin without the protection of Shugoshin-PP2A is cleaved by separase during metaphase II. This allows the sister chromatids to separate into opposite poles during anaphase II.

1.2.4 *Arabidopsis* cohesins: SYN1, AtSMC1/AtSMC3 and AtSCC3

1.2.4.1 SYN1

The *Arabidopsis* meiotic kleisin subunit *SYN1* gene has been cloned and encodes a protein with similarity to *S. pombe* RAD21/REC8 and RAD21-like proteins. The N- and C- termini of the SYN1 protein sequence have similarity to other RAD21/REC8 protein in the GenBank database (Bai et al., 1999; Bhatt et al., 1999). Complementation studies in yeast have shown that SYN1 can restore growth in the absence of mitotic kleisin subunit MCD1. This experiment shows that SYN1 performs as a cohesin (Dong et al., 2001). However, SYN1 is not crucial for somatic development in *Arabidopsis*, because vegetative growth appears normal in the *syn1* mutant. This mutant plant is only defective in reproductive growth. Cytological analysis revealed that abnormal chromosomes appear throughout meiosis. In addition, chromosome fragments are observed during metaphase I. Chromosome fragmentation and bridges are seen at anaphase II resulting in the formation of polyads (Bai et al., 1999; Bhatt et al., 1999). Previously, chromosome fragmentation has also been identified in mutants of other REC8 homologues including maize *afd1*, *Sordaria sm-rec8*, mouse *rec8*, worm *rec8* and rice OsRAD21-4 depletion line (Yu and Dawe, 2000; Pasierbek et al., 2001; Xu et al., 2005; Zhang et al., 2006; Storlazzi et al., 2008). Immunolocalization studies using antibodies against SYN1 showed that SYN1 appears on the arms of meiotic chromosome from interphase to anaphase I. Interestingly, SYN1 is not detectable at the centromeres throughout meiosis. Moreover, a substantial amount of the SYN1 protein re-appears in the nucleus of meiocytes during interkinesis (Cai et al., 2003). In contrast to SYN1, yeast REC8 is present at chromosome arms and centromeric regions at the onset of meiotic S phase. During diakinesis, REC8 is released from the chromosome arms but it still retained at the centromeric region until anaphase I (Klein et al., 1999; Watanabe and Nurse, 1999). This

suggested that SYN1 is different from the other REC8 homologues and that other proteins might play a crucial role in centromeric cohesion.

Arabidopsis has another three kleisin genes, *SYN2*, *SYN3* and *SYN4*, which are expressed throughout the plant (Dong et al., 2001; Jiang et al., 2007). A previous report suggests that *SYN2* and *SYN4* may represent mitotic cohesins (da Costa-Nunes et al., 2006) and *SYN3* plays a critical role in the nucleolus of both meiotic and mitotic cells and is also essential for megagametogenesis (Jiang et al., 2007). Although *SYN2* and *SYN3* are related to *SYN1* with greatest similarity at the N- and C- termini, *SYN2* and *SYN3* cannot replace the mitotic kleisin subunit MCD1 in *S. cerevisiae mcd1* mutant line. However, *SYN1* is able to complement in this mutant line, suggesting that *SYN2* and *SYN3* might not be involved in mitotic and meiotic cohesion (Dong et al., 2001).

1.2.4.2 AtSMC1 and AtSMC3

Homologues of *SMC1* and *SMC3* have been identified in *Arabidopsis*, named *AtSMC1* and *AtSMC3* respectively. Both genes are highly expressed in mitotic and meiotic cells. The expression of *AtSMC1* is greatest in floral buds than other tissues (Lam et al., 2005). *AtSMC1* and *AtSMC3* genes encode proteins (approximately 140 kDa) which contain the structures typical of the SMC family of protein, including the N- and C-termini ATP-binding domains and hinge region domain. Mutations of *AtSMC1* and *AtSMC3* showed that embryo and endosperm development are affected, indicating that both proteins are essential for somatic development (Liu Cm et al., 2002). Immunolocalization studies using antibodies against *AtSMC3* showed that the protein appears in cytoplasm and the nucleus (Lam et al., 2005). A signal corresponding to *AtSMC3* is detectable at the onset of interphase. It is distributed along

the entire length of chromosomes during pachytene. A substantial AtSMC3 signal is also observed at the microtubule spindle from metaphase I to telophase I, suggesting that AtSMC3 might play a role in spindle assembly during the first meiotic division (Lam et al., 2005). The AtSMC3 signal is present on meiotic chromosomes in the absence of SYN1, suggesting that AtSMC3 loading on meiotic chromosomes is independent from SYN1 (Lam et al., 2005). Currently, it is not clear whether AtSMC3 colocalizes with other cohesin proteins during meiotic prophase I.

1.2.4.3 AtSCC3

Mammalian cells contain three *SCC3* homologues, called *STAG1*, *STAG2* and *STAG3* respectively. Two of the three *SCC3* homologues, *STAG1* and *STAG2*, are classified as mitotic cohesins but *STAG3* is present on sister chromatids only at early meiosis I (Prieto et al., 2001; Prieto et al., 2002). In contrast to mammals, only one *SCC3* homologue was found in *Arabidopsis*, (*AtSCC3*). According to RT-PCR analysis, this gene is expressed equally in roots, mature leaves and buds. This gene encodes a protein with 21% identity and 40% similarity to *S. cerevisiae* *SCC3* (Chelysheva et al., 2005). Immunolocalization of AtSCC3 revealed that this protein is observed on the chromosome from leptotene to metaphase I (Chelysheva et al., 2005). Mutation of *Atsc3* causes vegetative and reproductive tissues to be smaller than that of wild-type, indicating that it plays an important role in vegetative and reproductive development. Cytological analysis in an *Atsc3* mutant showed low levels of chromosome fragmentation and bridges at metaphase I. However, AtRAD51 foci were distributed normally and some bivalents were found in meiocytes. This suggests that AtSCC3 might not play a crucial role in *Arabidopsis* DNA repair (Chelysheva et al., 2005). Immunolocalization studies revealed that SYN1 appears as a linear signal along the

chromosome in the absence of AtSCC3. An AtSCC3 signal is detectable at interphase in a *syn1* mutant but disassociates from the chromosomes and then disappears at later stages (Chelysheva et al., 2005). It is still unknown whether AtSCC3 physically associates or interacts with SYN1.

1.3 Cohesins are required for double-strand break (DSB) repair

Yeast studies showed that mitotic cohesin mutants, *S. pombe rad21* and *S.cerevisiae rad21*, are sensitive to ionizing irradiation during vegetative growth, suggesting RAD21 plays a role in DNA repair after DSB formation (Birkenbihl and Subramani, 1992; Heo et al., 1998). Two yeast groups have used HO endonuclease to induce a single DSB in mitotic cell (Strom et al., 2004; Unal et al., 2004). These experiments allow observation of protein expression at this specific site. The result showed that cohesin is accumulated around this DSB site. This accumulation around the DNA damage site is not just to maintain sister chromatid cohesion but is also required to stabilize the broken DNA arms to facilitate the DSB repair (Strom et al., 2004; Unal et al., 2004; Lowndes and Toh, 2005). Further support for the role of cohesin in DNA repair comes from studies in mammalian cells which have shown that cohesin is accumulated to the region of DNA damage, created by laser microbeam (Kim et al., 2002). The accumulation of cohesin to the damage site is dependent on the recombination proteins, Mre11 and Rad50. The meiosis kleisin subunit REC8 has also been suggested to have a role in DNA repair. Mutation of REC8 in *S. pombe* shows a decline in meiotic but not mitotic recombination around the centromere region (Parisi et al., 1999). In *S. cerevisiae*, cells lacking REC8 are deficient in double-strand break repair (Klein et al., 1999). These results suggest that yeast REC8 is required for meiotic recombination and DNA repair. Previous complementation studies revealed that *S. cerevisiae* REC8 can rescue the mitotic cohesion in

the absence of MCD1/SCC1, but REC8 is not recruited around the DSB sites. This indicates that REC8 cannot support DNA repair in mitotic cells (Heidinger-Pauli et al., 2008).

1.4 Homologue pairing and synapsis.

1.4.1 Homologous chromosome pairing

During early prophase I, maternal and paternal chromosomes are brought together by a chromosome alignment mechanism that has yet to be fully elucidated. It has been suggested that chromosome morphology, specific DNA sequence or meiotic protein might promote correct recognition and association of homologous chromosomes (Dawe et al., 1994). Previously, Scherthan et al. (1996) demonstrated by using fluorescent *in situ* hybridization (FISH) that homologous chromosomes become paired during telomere clustering. These clustered telomeres attach to the nuclear envelope forming a bouquet arrangement. It is thought that the telomere clustering and bouquet formation might facilitate pairing of homologous chromosomes by bringing them together (Dawe et al., 1994; Scherthan et al., 1996; Trelles-Sticken et al., 1999). In *Arabidopsis*, telomeres associate at the nucleolus rather than on the nuclear envelope during interphase. The clustered telomeres then pair before synapsis. Paired telomeres dissociate from the nucleolus during leptotene without forming a bouquet. This observation suggests that telomere clustering might play an important role in homologous chromosome pairing in *Arabidopsis* (Armstrong et al., 2001). In the maize meiotic mutant *pam1* (*plural abnormalities of meiosis I*), telomeres attach normally to the nuclear envelope forming several small telomere clusters but fail to form a normal bouquet (Golubovskaya et al., 2002). The *pam1* meiocytes exhibit a dramatic reduction in pairing of homologous chromosomes and abnormal synapsis. However, the number of foci of recombination protein RAD51 is normal during zygotene. In addition, some meiocytes of

pam1 are observed to proceed through meiosis I and II in a manner that cannot be distinguished from wild-type (Golubovskaya et al., 2002). Currently, there is no evidence to show that the bouquet is crucial for chromosome pairing, but the clustering of telomeres is probably one of the mechanisms to aid the homology search.

1.4.2 Formation of the synaptonemal complex.

Homologous chromosome pairing appears to be stabilized by a protein structure known as the synaptonemal complex (SC). The SC consists of two lateral elements (LEs) that are derived from the axial elements (AEs). The two LEs sit at the base of the chromatin loops and are connected to each other via transverse filaments (Figure 1.9A). A previous report in yeast suggests that AEs are derived from the cohesin complex (Klein et al., 1999). The immunolocalization of SMC3 and REC8 showed that both proteins colocalize along the axes of the chromosomes during pachytene. Furthermore, an axial element is not established in the absence of REC8, suggesting that cohesin is essential for the formation of SC (Klein et al., 1999). In mammals, it has been suggested that REC8 forms an AE-like structure at the onset of meiotic S-phase allowing the AE formation (Eijpe et al., 2003). In *D. melanogaster*, a distantly related REC8 homologue, C(2)M, is present at the central region of the chromosome (Anderson et al., 2005). Although C(2)M is unlikely to be involved in sister chromatid cohesion, this protein still interacts with cohesin subunit SMC3. Moreover, immunogold labelling studies showed that C(2)M appears at the C-terminal region of transverse filament protein, indicating that C(2)M interacts with both cohesin subunit SMC3 and transverse filament protein (Manheim and McKim, 2003; Heidmann et al., 2004; Anderson et al., 2005). Interestingly, a short SC structure with distinct lateral elements is observed in the *syn1* mutant (Zhao et al., 2006). A similar phenotype is also found in the absence of AFD1, the maize

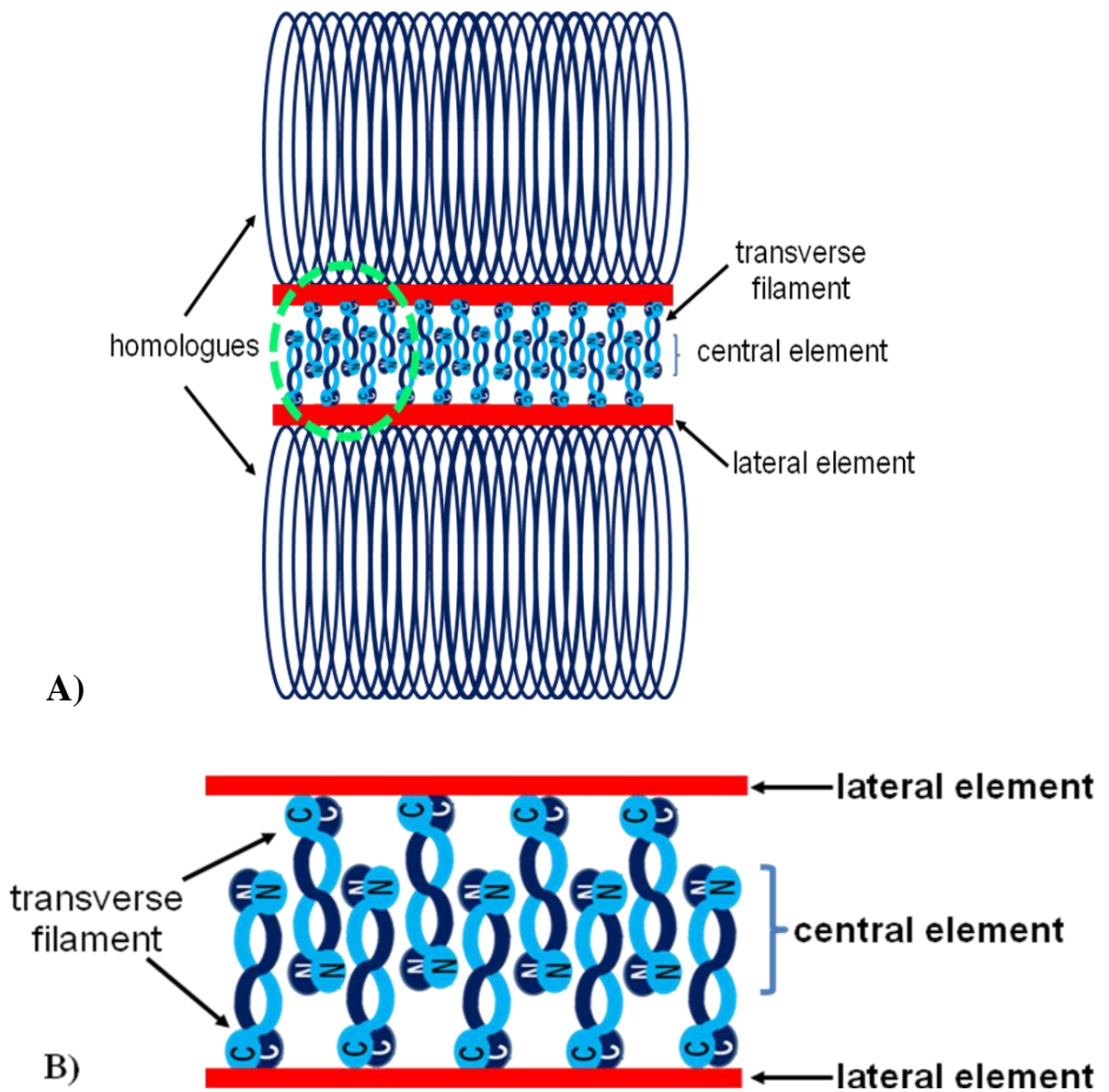


Figure 1.9. Synaptonemal complex (SC) structure

A) Diagram of the SC structure showing that two lateral elements anchor at the base of chromatin loops and are connected via transverse filaments (TFs).

B) is the same SC structure of (A) from the green circle area, showing that C termini of TFs associate with the lateral elements. N termini of TFs overlap in the central region of the SC is called central element.

REC8 homologue. In plants expressing a weak *afd1* allele, it has been shown that longer SC structures are formed in early prophase I. This suggests that the cohesin subunit AFD1 is not required for the establishment of axial element but is essential for the elongation of the axial elements (Golubovskaya et al., 2006).

Synapsis is defined by the formation of SC. In yeast and mammals, synapsis requires DNA double strand break (DSB) formation which is catalysed by the SPO11 protein (Lichten, 2001; Burgess, 2002). As chromosome pairing and synapsis are not found in the *Atspo11-1* mutant, it is apparent that DSBs are essential for synapsis in *Arabidopsis* (Grelon et al., 2001). However, the DSB-dependent synapsis is not universal. In *C. elegans* and *D. melanogaster*, homologous chromosome pairing and synapsis occur normally in the absence of DSB formation. The studies suggest that both species use a different mechanism for synapsis and to establish SC. Studies in *C. elegans* revealed that initial chromosome pairing occurs in the absence of SC. However, crossing over is severely affected in this mutant, suggesting that SC is essential to stabilize the chromosome pairing and promote crossing over (Dernburg et al., 1998; McKim et al., 1998; MacQueen et al., 2002; Vazquez et al., 2002).

In *Arabidopsis*, ASY1 is a protein that is related to the yeast Hop1 protein which contains a HORMA domain (Caryl et al., 2000). In the *asy1* mutant, synapsis of homologous chromosomes is affected during early prophase I. Most chromosomes appear as univalents at metaphase I but a few chiasmata are detected (Ross et al., 1997; Sanchez Moran et al., 2001). ASY1 is observed as punctate foci in meiotic G2 cells. At the leptotene stage, ASY1 appears to develop into a continuous signal along the full length of the chromosome. This signal is maintained until the chromosomes desynapse. Electron microscopy studies in *Brassica*

showed that ASY1 protein is closely localized to the chromosome axes but not on the sister chromatids. This observation suggests that ASY1 protein plays an important role at the interface of the axis-associated chromatin and the SC protein structure (Armstrong et al., 2002). Transverse filament proteins have been identified from yeast (ZIP1) and mammals (SCP1). Both ZIP1 and SCP1 proteins do not share significant primary amino acid sequence identity but do share similarity in secondary structures. The most common characteristic of these proteins is a central region comprising a coiled-coil domain allowing the formation of parallel homodimers with the N-termini from opposing dimers interacting in the central region of the SC and the C-termini associated with the lateral elements (Figure 1.9B) (Meuwissen et al., 1992; Sym et al., 1993; Page and Hawley, 2001; MacQueen et al., 2002). Recently, two transverse filament genes, AtZYP1a and AtZYP1b, in *Arabidopsis* have been identified by using previously known TF proteins in mammals, yeast, *Drosophila* and *C. elegans* to BLAST search against the *Arabidopsis* proteome. Moreover, the BLAST resulting proteins were then compared and screened for number of amino acid residues, mass, pI, coiled coil structure flanked by N- and C-terminal domains and the C-terminal domain (Higgins et al., 2005). Immunolocalization of AtZYP1 revealed that the protein is restricted to meiocytes and is observed as foci at leptotene. These foci appear to lengthen and develop into continuous signals during pachytene. Dual immunolocalization of AtZYP1 and ASY1 showed that AtZYP1 is localized between axis-associated protein ASY1, suggesting that AtZYP1 forms at the central region of SC (Higgins et al., 2005).

1.5 Meiotic recombination

1.5.1 Initial events of meiotic recombination: formation of DSB

In yeast, meiotic recombination is initiated by DNA DSBs. These meiotic DNA cleavage activities are catalysed by a topoisomerase type II like protein called SPO11 (Keeney et al., 1997; Keeney, 2001; Lichten, 2001). SPO11 contains a tyrosine side chain which attacks the phosphodiester backbone, forming a covalent linkage through a 5'-phosphodiester bond to a tyrosine side chain of SPO11 and releasing a free 3' OH-terminus. The SPO11 is released from DNA by either hydrolysis of phosphodiester or a single-strand nucleolytic cleavage, forming a 5' phosphate terminus on the cleaved strand (Keeney et al., 1997). The mechanism of initiation of meiotic recombination is widely conserved in many organisms, including yeast, mouse, human and plants. In the Archaeon *Sulfolobus shibatae*, the DNA topoisomerase VI-A subunit has been identified and shown to be a member of the SPO11 family (Bergerat et al., 1997). This protein is required, together with topoisomerase VI-B subunit, during DNA replication to separate newly formed chromosomes. The topoisomerase VI-A subunit binds and then cleaves to DNA, forming a 5'-phosphotyrosyl linkage (Bergerat et al., 1997).

In contrast to yeast and other eukaryotes, *Arabidopsis* has at least three *SPO11* paralogues, *AtSPO11-1*, *AtSPO11-2* and *AtSPO11-3* (Hartung and Puchta, 2000, 2001). *AtSPO11* was found based on the sequence of *C. elegans SPO11* (Hartung and Puchta, 2000). The *AtSPO11-1* mutant was the first to be identified by using ethyl-methane sulfonate (EMS)-induced mutant lines in the Columbia (Col 0) background as well as T-DNA insertion lines in the ecotype Wassilewskija (WS). These T-DNA and EMS alleles are named *Atspo11-1-1* and *Atspo11-1-2* respectively (Grelon et al., 2001). These two lines show normal vegetative

growth but reduced fertility, where only a few seeds are produced. A cytological analysis revealed that few bivalents at metaphase I are observed in male and female meiocytes, suggesting that either one of the other AtSPO11 homologues could be active in meiocytes to form few bivalents (Grelon et al., 2001). Alternatively, the *Atspo11-1-1* line, where the T-DNA is inserted in exon 1, is able to produce a truncated partially functional protein (Sanchez-Moran et al., 2007). Recently, Sanchez-Moran et al., (2007) report showed that the third mutant allele, *Atspo11-1-3*, did not produce any bivalent meiocytes, indicating that no meiotic recombination in an *AtSPO11-1* mutant.

The *AtSPO11-2* mutant was identified by screening the RIKEN collection and Syngenta collection. Two alleles *Atspo11-2-1* and *Atspo11-2-2* were identified (Stacey et al., 2006). The *Atspo11-2* mutant showed a severely reduced fertility phenotype similar to the *Atspo11-1* mutant. The cytological analysis showed that meiosis is disrupted in the absence of AtSPO11-2. No bivalents are observed at the prophase I, suggesting that AtSPO11-2 is required for meiotic recombination (Stacey et al., 2006). In addition, the cytological analysis in *Atspo11-2xAtrad51* double knock-out mutant showed no chromosome fragmentation in meiosis, indicating that *AtSPO11-2*, like *AtSPO11-1*, is required for DSB induction. It has been suggested that the AtSPO11-1 and AtSPO11-2 proteins might act as a heterodimer to break each DNA strand (Hartung et al., 2007). In contrast to AtSPO11-1 and AtSPO11-2, the AtSPO11-3 protein is one subunit of the topoisomerase VI and is involved in DNA replication in somatic cells. It has been suggested that the AtSPO11-3 is required for plant cell enlargement during normal development (Hartung et al., 2002; Hartung et al., 2007).

After the formation of DSBs in yeast, the ends of the broken DNA are resected from 5' to 3'

by a MRX complex protein which is composed of MRE11, RAD50 and XRS2/NBS1 to generate 3' single-stranded DNA (ssDNA) tails (Figure 1.10) (Smith and Nicolas, 1998; Connelly and Leach, 2002). *RAD50* and *MRE11* homologues have been identified in *Arabidopsis* (Gallego et al., 2001; Bundock and Hooykaas, 2002). Interaction of AtRAD50 and AtMRE11 proteins has been confirmed by using co-immunoprecipitation (Daoudal-Cotterell et al., 2002). In *Atrad50* or *Atmre11* mutants, chromosome fragmentation is observed in meiotic prophase I, suggesting that the DNA DSB repair is defective (Bleuyard et al., 2004b; Puizina et al., 2004). Cytological analysis of meiosis has shown that chromosome fragmentation in the *Atmre11* is rescued by deleting AtSPO11 protein, indicating that chromosome fragmentation in the *Atmre11* is AtSPO11-1 dependent. Recently, an *NBS1* orthologue has been identified in *Arabidopsis* (Akutsu et al., 2007). Studies in AtNBS1 have shown that this protein interacts with the AtMRE11 in the early meiosis (Waterworth et al., 2007). These observations suggest that AtRAD50-AtNBS1-AtMRE11 complex protein acts downstream of AtSPO11-1 in the meiotic recombination pathway.

1.5.2 Processing of meiotic DNA DSB

After single-stranded DNA ends are resected by the MRX/MRN complex a nucleoprotein filament is formed, this nucleofilament invades homologous non-sister chromatid. This process is catalyzed by a recombination complex protein containing RAD51 and DMC1 (Figure 1.10), which are homologues of the RecA recombinase. In yeast, RAD51 is required for both mitotic (intersister) and meiotic (interhomolog) recombination, whereas DMC1 is required for only meiotic recombination and formation of the synaptonemal complex (Masson and West, 2001; Krogh and Symington, 2004). In plants, an *Arabidopsis* homologue of RAD51, AtRAD51, has been identified (Li et al., 2004). According to cytological studies,

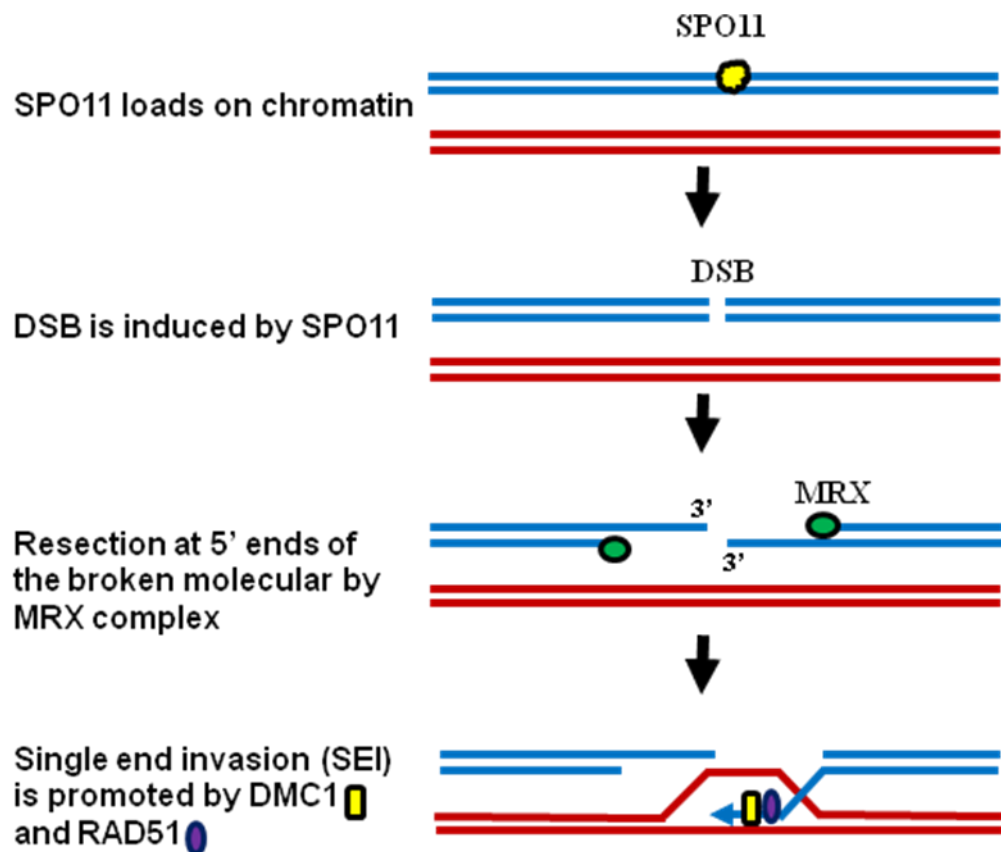


Figure 1.10. Early events of meiotic recombination

SPO11 induces DNA double strand break (DSB) to initiate meiotic recombination. The broken DNA ends are resected by MRX complex forming a single-stranded tails. One of the 3'-OH tails invades its equivalent sequence on the homologous chromosomes to form a displacement loop (D-loop). This process is called single end invasion (SEI) which is promoted by DMC1 and RAD51 recombination proteins.

chromosome pairing and synapsis are affected in the absence of AtRAD51. Furthermore, chromosome fragmentation is observed in meiocytes of *Atrad51* mutant. Cytological studies in *Atspo11-1^{-/-}xAtrad51^{-/-}* showed that chromosome fragmentation is absent throughout meiosis I and II, suggesting that AtRAD51 protein is required for DSB repair. Plants deficient for *AtDMC1*, the *Arabidopsis* homologue of *DMC1*, showed that 10 univalents with no fragmentation observed in the meiocytes, indicating that the DNA DSBs in *Atdmc1* mutant are repaired during early prophase I (Couteau et al., 1999). This observation suggests that the function of AtDMC1 is distinct from AtRAD51 but is still crucial for meiotic recombination and synapsis. Recently, RAD51 paralogs, (RAD51B, RAD51C, RAD51D, XRCC2 and XRCC3) have been identified in birds and mammals (Shinohara et al., 1993; Tebbs et al., 1995; Albala et al., 1997; Dosanjh et al., 1998; Liu et al., 1998; Pittman et al., 1998; Schild et al., 2000). These RAD51 paralogs form two complexes: (1) RAD51B-RAD51C-RAD51D-XRCC2 complex and (2) RAD51C-XRCC3 complex (Masson et al., 2001; Liu et al., 2002). These complexes are thought to play an important role in the assembly of RAD51 during the process of homologous recombination (Sung et al., 2003; Miller et al., 2004). Two *RAD51* paralogues, *AtRAD51C* and *AtXRCC3*, have been identified in *Arabidopsis*. Yeast two hybrids analyses have confirmed that *AtXRCC3* interacts with *AtRAD51C* and also with *AtRAD51* (Osakabe et al., 2002). Moreover, chromosome fragmentation is observed in both *Atrad51c* and *Atxrcc3* mutants. Cytological analyses in *Atspo11-1^{-/-}xAtrad51c^{-/-}* showed that no chromosome fragmentation is found throughout the meiosis (Li et al., 2005), indicating that fragmentation in *Atrad51c* mutant is triggered by AtSPO11-1. In contrast, bridges and fragmented chromosomes are observed during the meiotic division II in *Atspo11-1^{-/-}xAtxrcc3^{-/-}* (Bleuyard et al., 2004a). This observation indicates that chromosome fragmentation in *Atspo11-1xAtxrcc3* double knockout mutant is caused by the absence of AtXRCC3. This

suggests that AtXRCC3 has a role in the post-synapsis and Holliday junction resolution (Bleuyard et al., 2004a).

1.5.3 Crossover and non-crossover pathways

After the MRX complex protein resects the DNA DSBs, single-stranded DNA ends are covered by recombination proteins, DMC1 and RAD51, forming a nucleoprotein filament. This nucleoprotein filament invades one of the non-sister chromatid of the other homologous chromosome in a process called single-end invasion (SEI). Some SEI occurs and then DNA synthesis is initiated. However, the freshly synthesized DNA strand is removed to anneal with the other DSB end. The broken DNA is completely repaired by DNA synthesis, which leads to a non-crossover event. This process is called the synthesis-dependent strand annealing (SDSA) pathway (Allers and Lichten, 2001; Bishop and Zickler, 2004; Borner et al., 2004). Some SEIs form an extensive displacement loop (D-loop). DNA synthesis occurs from the invading strands and then DNA ligation forms the double-Holliday junction (dHJs). This eventually leads to a crossover event (Bishop and Zickler, 2004; Borner et al., 2004). Previous studies in yeast have proposed that at least two separate pathways to yield crossovers (COs) (de los Santos et al., 2003; Argueso et al., 2004). The first pathway, so called class I COs, is associated with a complex of proteins referred to as ZMM protein (Zip1, Zip2, Zip3, Mer3, Msh4 and Msh5) (Borner et al., 2004). Class I COs are subject to crossover interference (Figure 1.11), a mechanism which ensures that two crossovers do not occur in adjacent region on a chromosome. Previous studies have revealed that the MutS homologues MSH4 and MSH5 are to stabilize dHJs (Snowden et al., 2004; Franklin et al., 2006; Higgins et al., 2008b). The MutL homologues MLH1 and MLH3 then maintain the dHJs that ensure CO formation (Franklin et al., 2006; Jackson et al., 2006). The second pathway, so called class II

COs, does not exhibit interference which is dependent on two interacting proteins, Mus81 and Mms4/Eme1 (de los Santos et al., 2003; Berchowitz et al., 2007; Higgins et al., 2008a).

Several studies have shown that *Arabidopsis*, similar to that described in yeast, has two pathways for crossover formation. Copenhaver et al. (2002) was the first to suggest two crossover pathways in *Arabidopsis* by analysing the segregation of molecular markers in the meiotic tetrads produced in quartet mutant. This report estimated that the proportion of crossovers without interference is up to 25% (generally is close to 20%) (Copenhaver et al., 2002). This was experimentally confirmed in a cytological analysis in *Atmsh4* mutant showed that chiasma/crossover frequency is reduced to approximately 15% of wild-type. In addition, these remaining chiasmata/crossovers in the *Atmsh4* mutant are randomly distributed among chromosomes, indicating that these residual chiasmata in *Atmsh4* are interference-insensitive (Higgins et al., 2004). In conclusion, about 85% of COs/chiasmata in *Arabidopsis* arise via the class I interference-dependent pathway and approximately 15% of COs/chiasmata arise via the class II interference-independent pathway. Recently, cytological analysis in *Atmsh4xAtmus81* double mutant revealed a significant decline in the number of chiasmata (0.85 per cell) compare to *Atmsh4* (1.25 per cell). This result indicates that AtMUS81 contributes to around 1/3 of the 15% AtMSH4-independent pathway. This suggests that other proteins might be involved in this interference-independent pathway (Higgins et al., 2008a). A number of proteins have now been described that are essential for class I CO formation. These include the *Arabidopsis* homologue of MER3, AtMER3, which is required for the interference-dependent pathway (Chen et al., 2005; Mercier et al., 2005). The cytological analysis of *Atmer3* mutant shows a reduction in chiasmata and synaptonemal complex formation. These observations suggest that both crossover and SC formation are compromised in the absence of AtMER3 (Chen et al., 2005). Recently, SHOC1, an XPF endonuclease-

related protein, was identified in *Arabidopsis* meiocytes (Macaisne et al., 2008). Cytological analysis in *shoc1* mutant showed that chiasma/crossover frequency is reduced to approximately 15% of wild-type. This result is similar or identical to class I CO mutants, e.g. *Atmsh4^{-/-}* and *Atmsh5^{-/-}*. Furthermore, the number of chiasma/crossover in *shoc1^{-/-}/Atmsh5^{-/-}* double mutant showed no significant difference compared to single knockout gene *shoc1^{-/-}* and *Atmsh5^{-/-}* mutants. This observation suggests that SHOC1 acts in the same pathway as AtMSH5, which is required for class I CO formation in *Arabidopsis* (Macaisne et al., 2008).

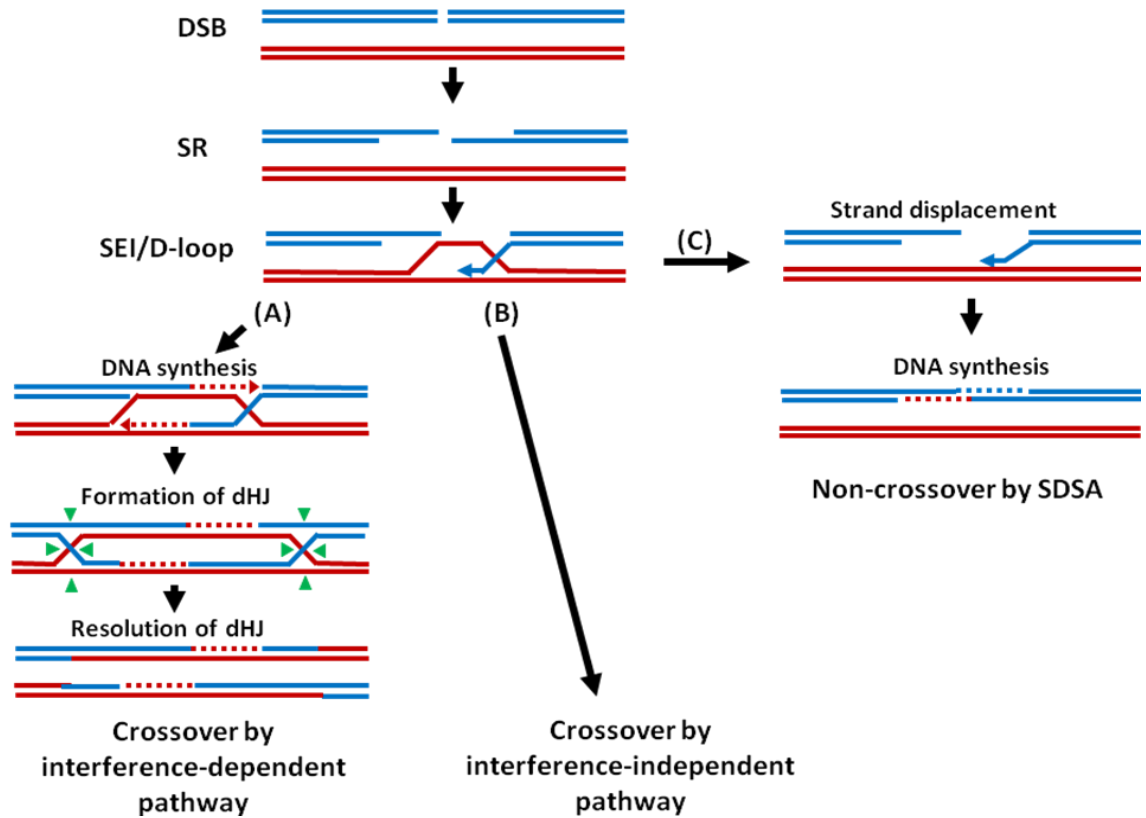


Figure 1.11. Meiotic crossover and non-crossover pathways following D-loop formation. DNA synthesis occurs after single end invasion. It extends the invading strand and enables to anneal to the single stranded tail on the other side of the break, this is called second end capture (SEC). (A) This SEC leads to the formation of the double Holliday junction (dHJ), which can be resolved to crossover. This crossover pathway, interference-dependent pathway, accounts for the majority of meiotic COs (~85%) which are dependent on ZMM protein complex. (B) The remaining COs (~15%) do not show interference and some of these COs arise from MUS81-dependent pathway. (C) The SEI disassociates from the D-loop formation which can generate non-crossover. This mechanism called synthesis-dependent strand annealing (SDSA). Figure is modified from (Osman et al., 2009).

1.6 Aims of my PhD project

The aims of this project are to study, investigate and clarify the possible role for SYN1 in the repair of DSBs. Recent evidence has shown that mitotic cohesin is recruited around DNA DSB sites, suggesting that cohesin has a role in stabilizing broken DNA to facilitate DSB repair (Strom et al., 2004; Unal et al., 2004; Lowndes and Toh, 2005). However, the role of meiotic cohesin in DNA DSB repair remains poorly understood. SYN1 is a meiosis-specific *Arabidopsis* homologue of yeast REC8, an important component of the meiotic cohesin complex which maintains the association of sister chromatids (Bai et al., 1999; Bhatt et al., 1999; Klein et al., 1999). Previous studies of a *syn1* mutant revealed that chromosome fragmentation occurs during metaphase I (Bai et al., 1999; Bhatt et al., 1999). To determine the basis of chromosome fragmentation in *syn1*^{-/-}, a *syn1*^{-/-} and *Atspo11-1-4*^{-/-} double knockout mutant was constructed in our laboratory. In addition, two double knock-out mutants, *syn1*^{-/-} x *Atdmc1*^{-/-} and *syn1*^{-/-} x *Attrad51c*^{-/-}, were constructed, which will be analysed to confirm whether the SYN1 has a role during DNA DSB repair.

To further study the function of SYN1, an antibody against SYN1 was developed, which will be tested for its antibody specificity in chromosome spreads of wild-type (Col 0) and *syn1*^{-/-}. Immunolocalization of various antibodies, ASY1, AtZYP1, AtRAD51 and AtMLH1, in meiocytes of wild-type and *syn1*^{-/-} will also be carried out to investigate the basis of the *syn1* fragmentation phenotype.

To study whether SYN1 is recruited on sister chromatids during DSB formation, *Atspo11-1-4*^{-/-} meiocytes will be treated with cisplatin, a platinum chemical complex which reacts with DNA to create DSBs. Immunolocalization of SYN1 will be examined in meiocytes of cisplatin-treated *Atspo11-1-4*^{-/-} and compared to untreated *Atspo11-1-4*^{-/-} and wild-type (Col 0). By analysing the intensity of SYN1 on each meiocyte, I can therefore uncover the role of

SYN1 during meiotic DNA DSB.

Chapter 2

Materials and methods

2.1 Plant materials and growing conditions

2.1.1 Plant materials

Arabidopsis thaliana ecotype Columbia (0) [Col 0] was chosen in this study for wild-type analysis. The T-DNA insertions in the *SYN1* (SALK_091193, SALK_137095 and SALK_047995), *AtSPO11-1-4* (WiscDsLox_461-464J19), *AtDMC1* (Feldmann line 3668) and *AtRAD51C* (SALK_021960) were obtained from the SALK Institute via NASC for mutant analysis.

2.1.2 Plant growth media

½ Murashige and Skoog (MS) agar (Murashige and Skoog, 1962)

2.2g MS basal salts with Gamborg's vitamins (Sigma)

pH 5.6-5.8 (with KOH)

10g/l agar (Sigma)

Levington M3 compost/ vermiculite mix

Levington M3 plus peat-based compost mix : silver peat = 3: 1 ratio

2.1.3 Plant growth conditions

Seeds were sterilized in 20% Parazone™ bleach on a turning wheel for 15 minutes. The seeds were rinsed three times in SDW before being placed out to air dry in a laminar flow cabinet. Cleaned seeds were placed on an 0.5 MS-agar plate and vernalized 48 hours at 4°C

before moving the MS plate to a growth chamber (at 22 °C with a day length of 16 hours). Alternatively cleaned seeds were vernalized 48 hours at 4°C prior to sowing on Levington M3 compost/vermiculite mix. Plants were grown in a glasshouse at 18-23 °C with a 16 hour light cycle.

2.2 Bacterial strains and cloning vectors

2.2.1 Bacterial strains

Escherichia coli DH5α

SupE44, $\Delta lacU169(\phi 80 lacZ \Delta M15)$, *hsdR17*, *recA1*, *endA1*, *gyrA96*, *thi-1*, *relA1*.

Escherichia coli BL21(DE3)

B, F, *dcm*, *ompT*, *hsdS*($r_B^- m_B^-$), *gal*, λ (DE3)

Escherichia coli BL21(DE3)pLysS

B, F, *dcm*, *ompT*, *hsdS*($r_B^- m_B^-$), *gal*, λ (DE3) [pLysS Cam^r]

2.2.2 Cloning vectors

pDrive (QIAGEN)

pDrive is a 3.85 kb linear form cloning vector with an U overhang at each 3' end which ligates with the A overhang of PCR products. This vector has ampicillin and kanamycin resistance markers and also allows blue / white screening of recombinant colonies in bacteria. This vector has a large number of unique restriction enzyme recognition sites and universal sequencing primer sites to facilitate analysis of cloned PCR products.

pET21b (Novagen)

A 5.4kb vector is designed to produce quickly a large quantity of protein when activated. This vector carries a multiple cloning site downstream of a T7 promoter plus a C-terminal His-Taq sequence. The T7 promoter, which is under the regulation of the IPTG-responsive Lac operator (*lac I*), is specific to only T7 RNA polymerase for the transcription of the desired protein.

2.3 Bacteria media, culture and growth conditions

2.3.1 Bacterial growth media

All media were prepared in distilled water and sterilized by autoclave at 15 psi and 121°C for 20 minutes.

2.3.1.1 Lysogeny Broth (LB)

5.0% (w/v) bacto-yeast extract (Difco)

10.0% (w/v) bacto-tryptone (Difco)

10.0% (w/v) NaCl

2.3.1.2 LB agar

5.0% (w/v) bacto-yeast extract (Difco)

10.0% (w/v) bacto-tryptone (Difco)

10.0% (w/v) NaCl

15.0% (w/v) bacto-agar

2.3.2 Bacterial culture

Antibiotic resistance was selected for by the addition of antibiotics at these respective concentrations: ampicillin-100µg/ml; kanamycin, 50µg/ml (Sigma).

2.3.3 Bacterial growth conditions

E.coli liquid cultures were grown for approximately 16 hours at 37°C on a rotary shaker at 200 rpm. Agar plates were grown inverted for 20 to 24 hours at 37°C. Inoculation of liquid culture and agar plates were carried out under aseptic conditions.

2.4 Isolation of nucleic acid from plant and bacteria

2.4.1 Buffer for isolation of nucleic acid

Plant Extraction Buffer

2.5ml of 2M Tris (pH9.5)

500µl of 1M EDTA

6.25ml of 1M KCl

40.75ml of sterile water (SDW)

Plant Dilution Buffer

3% of BSA in sterile water

2.4.1 Buffer for isolation of nucleic acid

STET Buffer

8% Sucrose

0.5% Triton x-100

50mM NaEOTA (pH8.0)

10 μ M Tris-HCl (pH8.0)

2.4.2 Isolation of total RNA from plants

Total RNA was extracted from *Arabidopsis* plant tissue (less than 100mg per sample) following an RNeasy mini protocol (Qiagen). All equipment was soaked overnight in DEPC treated water and autoclaved prior to use. Plant tissues were frozen in liquid nitrogen and ground-up in a pestle and mortar before vortexing with 450 μ l RLT buffer in a 2ml collection tube. Plant tissues were lysed by RLT buffer which contained guanidine thiocyanate and β -mercaptoethanol to denature proteins and RNase. The tissues were homogenized by centrifugation through a QIAshredder spin column to remove cell debris and reduce viscosity of the lysate. RNA was adsorbed to the silica membrane of an RNeasy mini column. The sample was then washed with ethanol, RW1 and RPE buffers. The silica membrane of column was then dried by centrifugation in an empty collection tube. The RNA was eluted from the column in RNase free water. Eluted RNA was stored at -70°C.

2.4.2.1 DNase I treatment of plant RNA

Plant total RNA extracts were DNase treated prior to RT-PCR analysis using the following:

10X DNase I buffer (Invitrogen)	2 μ l
RNAsin (Promega®)	1 μ l
DNase I (Invitrogen)	1 μ l
Total RNA	10 μ l
<u>RNase Free dH₂O</u>	<u>6μl</u>
<u>Total mix</u>	<u>20μl</u>

DNase I, 10X DNase I buffer, RNase Free dH₂O and RNAsin were added to total RNA samples (total mixture up to 20µl). This mixture was incubated at room temperature for 15 minutes to efficiently degrade genomic DNA in the RNA samples. 2µl of 25mM EDTA was added in the sample and incubated at 65°C for 10 minutes. The EDTA was added to chelate ions in the digestion buffer, therefore to allow the DNase I to be efficiently heat inactivated without loss of RNA. 80µl of RNase-free SDW was added to the sample before RNA phenol-chloroform extraction. 100µl of RNA phenol (Stratagene) with pH 5.3-5.7 was added into the sample, then vortexed and centrifuged 5 minutes in room temperature. The upper aqueous phase of sample was transferred to a fresh tube with the chloroform (200µl) mixture. After centrifugation, the top layer of sample was transferred to another fresh tube. RNA was precipitated in 1µl of glycogen (Roche, 20mg/ml), washed in an ethanol series and eluted in 30µl of RNase-free water. DNase I-treated RNA was stored at -70°C.

2.4.3 Isolation of plasmid DNA from bacteria

Bacterial cultures were grown with shaking at 37°C overnight. Cells were then collected by centrifugation at 13000rpm for 5 minutes. Plasmid DNA was purified from bacteria using the Boiling Prep method and Wizard *Plus* SV miniprep kit (Promega).

2.4.3.1 Boiling Prep method

Cells were harvested by centrifugation and were resuspended in 120µl of STET buffer by vortexing. The cell wall was permeabilised by adding 12µl of lysozyme (10mg/ml), prior to placing the sample in boiling water for 45 seconds. Samples were immediately spun at 13000rpm for 10 minutes. The viscous pellet was removed before adding 10µl of 3M sodium acetate and 500µl of 100% cold ethanol. Sodium acetate allows the nucleic acids to

precipitate. The sample was placed at -20°C for 30 minutes before centrifugation at high speed (13000rpm; 10 minutes). The supernatant was removed. The pellet was washed in 70% ethanol before another spin down at 13000rpm. The DNA pellet was dried under vacuum for 10 minutes before resuspending in 100µl of sterile distilled water.

2.4.3.2 Wizard Mini prep method (Promega®)

The Wizard *Plus* SV Miniprep kit allows isolation of plasmid DNA from bacteria by using a modified alkaline lysis procedure (Birnboim and Doly, 1979). Plasmid DNA was trapped in a membrane column in the presence of high salt, then washed with ethanol twice and eluted in sterile distilled water (40µl). This Wizard *Plus* SV Miniprep DNA purification system (Promega®) was carried out according to the manufacturer's instructions.

2.4.4 Isolation of DNA from plants for genotyping

A fresh leaf disc was taken from the plant and ground with a pipette tip in 40µl of plant extraction buffer in a tube. The sample was incubated at 95°C for 10 minutes, then immediately put on ice to prevent evaporation. The sample was mixed with 40µl of plant dilution buffer and the sample was centrifuged at 13,000rpm for 10 secs. The supernatant containing the genomic DNA was used for plant genotyping by PCR.

2.5 Polymerase chain reaction (PCR) techniques

Polymerase chain reaction (PCR) was carried out with plasmid DNA, genomic DNA or RNA to amplify a PCR product. The PCR reaction including single colony PCR and RT-PCR were carried out using PCR machines manufactured by TECHNE (model: TC-412) and ThermoHybaid. The ThermoPrime *Taq* DNA polymerase from ReddyMix PCR Master Mix

(Thermo Scientific) and RedTaq[®] DNA polymerase from ReadyMix[™] PCR reaction Mix (Sigma) were used for colony PCR and plant genotyping. HotStar Taq DNA polymerase from Qiagen one-step RT-PCR kit (QIAGEN) was routinely used for gene expression and gene cloning. These enzymes produce PCR products with an A overhang which allows direct UA- or TA-cloning. Primers were designed in house and were supplied by MWG Biotech Company.

2.5.1 PCR standard conditions

The initial PCR reaction template melting stage was carried out at 93°C for 30 seconds. The annealing temperature depended on the melting temperature of the primers being used. The temperature was set at 5°C below the melting temperature of the primer pair, this temperature can be estimated by the following equation: $(4XG/C)+(2XA/T)$. The annealing stage was carried out for 1 minute. The extension phase of the amplification was carried out at 72°C. The time for completion of the extension phase was either 30 seconds for ~500bp products or 1 minute for ~1kb products.

2.5.2 Genotyping PCR

1µl sample of genomic DNA was added to a PCR tube containing 12.5µl ReddyMix (Thermo Scientific), 9.5µl SDW, 1µl forward and 1µl of reverse primers. The PCR cycling conditions were carried out as described in the PCR standard conditions (section 2.6.1).

2.5.3 Single colony PCR

A single bacterial colony containing plasmid DNA was picked and added to the ReddyMix PCR Master Mix (Thermo Scientific) with specific reverse and forward primers. The PCR

cycling conditions were carried out as described in PCR standard condition. PCR products were analysed by gel electrophoresis.

2.5.4 Reverse Transcriptase-Polymerase Chain Reaction (RT-PCR)

RT-PCR is a technique to detect expression of mRNA. RNA was first reverse transcribed into complementary DNA (cDNA) using the enzyme reverse transcriptase. The cDNA was used as a template for PCR amplification using specific primers. In this study, RT-PCR was carried out as one-step RT-PCR by using Qiagen one-step RT-PCR kit (QIAGEN) for the gene cloning and gene expression studies. Plant total RNA extracts were treated with DNase I prior to starting the RT-PCR. The DNase I treated RNA was added to a master mix according to the Qiagen one-step RT-PCR protocol (QIAGEN) which is shown below:

<u>Volume</u>	<u>Component</u>
10 μ l	5x QIAGEN OneStep RT-PCR buffer
2 μ l	dNTP Mix (10mM of each dNTP)
2 μ l	QIAGEN OneStep RT-PCR enzyme mix
1 μ l	RNase inhibitor (Promega)
1 μ l	10 μ M Forward Primer
1 μ l	10 μ M Reverse Primer
X μ l	RNase-free water to make up 50.0 μ l total

The RT-PCR thermal cycler conditions were started at 50°C for 30 minutes to allow the reverse transcription of the RNA template. The second step reaction was run at 95°C for 15 minutes to activate the HotStarTaq DNA polymerase and to inactivate the reverse

transcriptases (Omniscript and Sensiscript). The cDNA template was also denatured in this step. For the third cycling step, the annealing temperature was dependent on the melting temperature of the primers being used. The number of cycles in the RT-PCR reaction was set at 30 to avoid saturated PCR products. The final extension reaction was completed at 72°C for 10 minutes. The reactions were held at 10°C until they were removed from the thermal cycler.

RT-PCR was used to investigate the expression pattern of *SYN1* gene. PCR primers (STC and EX8) were designed at the start codon and exon 8 of *SYN1* gene. RT-PCR analysis result showed that *SYN1* transcripts were not detected in all samples. I decided to re-amplify the RT-PCR products. To do that, 1µl of RT-PCR sample was added with Reddy Mix PCR master mix (Therma Scientific). The number of cycles in the PCR was set on 20 to avoid saturating the PCR products.

To produce a specific *SYN1* antibody, *SYN1* cDNA sequence containing amino acids 207 to 384 was selected (Figure 2.1A). The selected region was located at the centre region of the *SYN1* protein and did not contain the N- and C- termini of REC8 domains. If the cDNA includes the N and C termini of the *SYN1*, the antibody will possibly recognize other kleisen subunits e.g. *SYN2*, *SYN3* and *SYN4* (Figure 2.1B and C). It has been reported that both *SYN2* and *SYN4* are required for mitotic sister chromatid cohesion, and *SYN3* is essential for gametogenesis (Dong et al., 2001; Jiang et al., 2007; Schubert et al., 2009). To begin the production of *SYN1* recombination protein, RNA was extracted from wild-type (Col 0) buds using the RNeasy mini protocol (Qiagen) and DNase prior to RT-PCR (QIAGEN) analysis. RNA was converted to cDNA using the enzyme reverse transcriptase. This cDNA was then

used as a template for PCR amplification with S5 forward primer and S6 reverse primer which contain the *NdeI* and *XhoI* restriction sites respectively. These restriction sites allow the cloning of the amplicon in frame into pET21b expression vector. The RT-PCR product was first cloned into the pDrive cloning vector and was then transformed into DH5 α cells. Plasmid DNA was isolated by using Wizard prep kit (Promega) and the DNA insert was confirmed by using nucleotide sequencing reactions. The sequencing showed that three nucleotides were mutated. Two amino acids at position 35 and 161 were mutated from glutamine (Q) to arginine (R) and from glutamic acid (E) to valine (V) (Figure 2.2). To clone into pET21b expression vector, the DNA fragments were released from the pDrive by using the *NdeI* and *XhoI* restriction enzymes. The DNA fragments were gel extracted and cleaned up using the PCR purification kit (QIAGEN). Purified DNA fragments were cloned into the pET21b vector and were then transformed into DH5 α competent cells. The plasmid DNA was again isolated using Wizard prep kit and sequenced to confirm the DNA insert containing the start and stop codons (Figure 2.3). The sequence was also analysed using ExPASy software (<http://us.expasy.org/tools/dna.html>) for translating nucleotide sequence to protein sequence (Figure 2.4). The result showed the expected sequence plus six histidines. The molecular weight of this SYN1 peptide is 22.2kDa.

SYN1	207	MNSNPREGAEIPTTLIPSPPRHHDIPGVNPTSPQRQEQQENRRDGFAEQ	256
DNA fragment	1	MNSNPREGAEIPTTLIPSPPRHHDIPGVNPTSPRQEQQENRRDGFAEQ	50
SYN1	257	MEEQNIIPDKEEHDRPQPAKKRARKTATSAMDYEQTIIAGHVYQSWLQDTS	306
DNA fragment	51	MEEQNIIPDKEEHDRPQPAKKRARKTATSAMDYEQTIIAGHVYQSWLQDTS	100
SYN1	307	DILCRGEKRRKVRGTIRPDMESFKRANMPPTQLFEKDSSYPPLYQLWSKN	356
DNA fragment	101	DILCRGEKRRKVRGTIRPDMESFKRANMPPTQLFEKDSSYPPLYQLWSKN	150
SYN1	357	TQVLQTSSESERHPDLRAEQSPGFVQER	384
DNA fragment	151	TQVLQTSSSVSRHPDLRAEQSPGFVQER	178

Figure 2.2 Alignment of *Arabidopsis SYN1* and DNA fragment.

The amino acid sequences of *Arabidopsis SYN1* and DNA fragment are aligned ClustalW and confirmed in NCBI Blast search (<http://blast.ncbi.nlm.nih.gov/Blast.cgi>).

“|” represents the identities between the two aligned sequences

“.” represents the conservative replacement

The result shows that the amino acid sequence of the DNA fragment has 98.9% sequence identity with *SYN1*. Two conservative substitutions occur at positions 35 and 161, replacing glutamine (Q) with arginine (R) and glutamic acid (E) with valine (V)

Cloning in pET21b

```
CATATGAACTCC AATCC AAGAGAAGGC GCTGAAATACCTACAAC TCTC ATCCC ATCA  
CCACCTCGTCATCATGAC ATTCCC GAAGGAGTCAACCCC ACAAGCCCCGGCGCC  
AGGAGCAAC AGGAGAATC GTAGGGAC GGATTTGCTGAGC AGATGGAGGAACAAA  
ACATACCGGACAAAGAGGAAC ACGATAGACC ACAACC AGC GAAAAAGAGAGCAA  
GAAAGACAGCTACTTCAGCGATGGATTATGAGCAAAC TATTATCGCTGGTC ATGTT  
ACCAGTCATGGCTCC AGGATACTTCTGAC ATTCTC TG TAGGGGGGAAAAGAGAAAG  
GTTGAGGAAC TATCCGGCCAGAC ATGGAAAGTTTCAAACGTGC GAATATGCCACC  
TACACAAC TCTTTGAAAAGGAC AGTTCTTACCCGCCTC AGC TTTACCAGC TTTGGTC  
AAAGAATAC TCAAGTTCTTCAAACCTC ATC ATC TGATCTC GACATCCTGATCTCCGT  
GCGGAACAATC TCCAGGGTTGTT CAGGAGAGACTCTGAGC ACC ACC ACC ACC  
ACTGGAGATCCGGCTGCTAA
```

Figure 2.3 Nucleotide sequence of the *SYN1* insert and pET21b vector.

The sequencing result shows that the *SYN1*-pET21b plasmid contains a start codon in the *NdeI* (CATATG) site and a TAA stop codon downstream of the *Xho I* (CTCGAG) site.

SYN1 peptide

```
MetN SNPREGAEIPTTLIPSPPRHHDIPEGVNP TSPRRQEQQE  
NRRDGF AEQME EQNIPDKEE HDRPQPAKKRARKTATSAMDY  
EQTI IAGHVYQSWLQDTS DILCRGEKRKVRGTIRPDME SFKR  
ANMPPTQLFEKDS SYPPQLYQLWSKNTQVLQTSS SVSRHPD  
LRAEQSPGFVQERLEHHHHHHWRSGC Stop
```

Theoretical pI/Mw: 7.20 / 22216.60

Figure 2.4 The translation of SYN1 amino acid sequence.

The nucleotide sequence (shown in Figure 2.3) was translated into amino acid sequence with ExPASy web software (http://us.expasy.org/tools/pi_tool.html).

The result shows the expected amino acid of SYN1 sequence plus addition of six histidine residues. The molecular weight of the SYN1 peptide is 22.2kDa.

2.5.5 Primer design

Primers were supplied by MWG Biotech Company. A list of primers show below:

S1 forward primer (5'-CTTCTTAAGGATGGCCGCTAC-3')

S2 reverse primer (5'-AGGTTGGAGAGTTCAAGCCAC-3')

DMC1 A primer (5'-CCTGCAATGGTCTCATGATGCATAC-3')

DMC1 B primer (5'-GATGCAATCGATATCAGCCAATTTTAGAC-3')

DMC1 C primer (5'-AGGTACTCTGTCTCTCAATG-3')

DMC1 D primer (5'-ACTAATCCTTCGCGTCAGCAATGC-3')

RAD51C forward primer (5'-TCACAGAGGAGGAAGCATTG-3')

RAD51C reverse primer (5'-TTTTTGGCAAGCTTCATGAAC-3')

LBa1 forward primer (5'-TGGTTCACGTAGTGGGCCATCG-3')

SPO11 forward primer (5'-GAGGAT ATCCAG ATGTCT C-3')

SPO11 reverse primer (5'-AGGAGAGCTTACTTCACGAC-3')

WISC-LB (5'-AACGTCCGCAATGTGTTATTAAGTTGTC-3')

GAPD forward primer (5'-CTTGAAGGGTGGTGCCAAGAAGG-3')

GARD reverse primer (5'-CCTGTTGTGCGCCAACGAAGTCAG-3')

S3 forward primer (5'-GGAGATGATGAAACACAGATGAACTC-3')

S4 reverse primer (5'-CCAAAGCTG GTAAAGCTGAGGC-3')

STC (5'-GTTTTATTCTCACCAGCTTCTAGCTCG-3')

EX8 (5'-GATGGAAGTGTGCTGTTCAAGATCTTC-3')

M13 reverse primer (5'-CAGGAAACAGCTATGAC-3')

T7 promoter (5'-TAATACGACTCACTATAGGG-3')

S5 forward primer 5'-GGCATATGAACTCCAATCCAAGAGAAGG-3'

S6 reverse primer 5'-GCCTCGAGTCTCTCCTGAACAAACCCTGG-3'.

2.6 Nucleic acid manipulations

2.6.1 Estimation of nucleic acid concentration

The concentrations of DNA and RNA were estimated by using spectrophotometer (Jenway 6305) to measure the absorbance of 200 fold diluted samples at 260nm. The absorbance of nucleic acid at 260nm in 1 μ l of sample was converted to the value to a concentration based on an OD_{260nm} reading of 1.0 unit correlating to 50 μ g ml⁻¹ of DNA or 40 μ g ml⁻¹ of RNA.

2.6.2 Digestion of DNA with restriction enzymes

Restriction enzymes were obtained from New England Biolabs and Invitrogen. Plasmid DNA was digested at 37°C between 2 and 16 hours, depending on the amount of DNA and amount of enzyme units that were used. All the digestions were carried out in appropriate buffers supplied with the enzymes. The DNA products were analysed by gel electrophoresis.

2.6.3 Agarose gel electrophoresis of DNA and RNA

Agarose powder was mixed in 0.5x TBS and heated before pouring on the tank of gel electrophoresis apparatus. Ethidium bromide (0.5 μ g ml⁻¹) was added to the molten agarose prior to the gel setting. This allows visualization of both DNA and RNA. The gel images were captured using the FluorS Multi-imager software (BioRad). The concentration of agarose gel employed is dependent on the size of the expected DNA or RNA. A 0.9% (w/v) agarose gel was routinely used to visualize large molecular weight DNA. A 1.5% (w/v) gel was used for DNA with a size less than 300bp. A 1kb DNA ladder marker was used to estimate the size of DNA and RNA.

2.6.3.1 Solutions for nucleic acid electrophoresis

DNA loading buffer:

40% (v/v) glycerol

0.25% bromophenol blue

5x TBE:

0.45 M Tris

0.45 M Orthoboric acid

12.5 mM EDTA

2.6.4 Extraction of DNA from agarose gels

Plasmid DNA was digested and run on an agarose gel. The DNA band was cut from the gel using minimal UV exposure. The gel was transferred to microcentrifuge tubes and weighed. The DNA was extracted from RESolve low melting point agarose (Geneflow) gel using the QIAquick gel extraction kit (QIAGEN). The gel was dissolved in three volumes (w/v) of buffer QG at 50°C for 10 minutes prior to transferring onto a QIAquick spin column. The sample was washed with 750µl buffer PE, and was then centrifuged to dry. DNA was eluted in 30µl nuclease free water. DNA was analysed by gel electrophoresis prior to being used in ligation reactions.

2.6.5 Ligation of DNA fragments into vector DNA

Two major types of ligation were carried out during this study. “A” overhang ended PCR products were generated with using RT-PCR kit (QIAGEN) or ReddyMix PCR Master Mix (Thermo Scientific Reddy Mix). This “A” overhang ended PCR product allows direct

ligation into the pDrive cloning vector with an U overhang at each 3' end. 3µl PCR product was added on a tube to 1µl (50ng µl⁻¹) pDrive cloning vector (QIAGEN) together with 5µl 2X ligation Master Mix and 1µl distilled water to make up total volume 10µl. The ligation-reaction mixture was incubated at 15°C~17°C for 16 hours. Alternatively for expression of *SYN1* a ligation was carried out by adding insert DNA to pET21b (Novagen) with T4 DNA ligase (Invitrogen). The insert DNA and pET21b vector were mixed at a ratio of 3:1 (600ng insert DNA and 200ng vector) in total a 10µl volume, with 0.5µl T4 DNA ligase and 1µl 10X DNA T4 ligase buffer. The reaction was incubated at 15°C~17°C for 16 hours prior to the transformation.

2.6.6 DNA sequencing

DNA sequencing was carried out using the big dye terminator labelling mix method by the Functional Genomics Laboratory at The University of Birmingham. This method relies on fluorescently-labelled di-deoxy-dNTPs that are incorporated during the PCR reaction. Each different di-deoxy-dNTP is labelled with a different fluorescent tag that was read automatically by the capillary sequencer ABI3700 (Applied Biosystems). Wizard plasmid DNA (200-600ng) was added in 4µl of 0.8pmol µl⁻¹ primer (e.g, T7 promoter) and distilled water to make up total volume of 10µl. The sequencing reagents were added robotically by the Roboseq 4204s before undergoing thermal cycling. The reactions were then cleaned up using a silica column method and eluted in diformamide and loaded onto the ABI3700.

2.7 Transformation of Bacterial cells

2.7.1 Transformation of *E.coli* by heat shock

4µl ligation products were added to a pre-thawed 100µl aliquot of competent cells. The

mixture was incubated on ice for 30 minutes before heat-shocked at 42°C for 45 seconds. The tube was placed on ice before adding 500µl LB broth. The mixture was then incubated at 37°C for one hour. The incubated mixture was spread onto LB agar plates with appropriate antibiotics. The LB agar plate was incubated at 37°C for 16 to 18 hours. The plates were stored at 4°C.

2.8 Protein manipulations

2.8.1 Protein electrophoresis and western blotting solutions

5x SDS loading dye:

67.5% (v/v) Tris-HCL (2M, pH6.8)

10% (w/v) SDS

50% (w/v) glycerol

5% beta-mercaptoethanol

0.005% (w/v) bromophenol blue

5x ELFO buffer:

125 mM Tris

950 mM glycine

0.1% (v/v) SDS

pH8.3

Blocking solution:

10% (v/v) 10 xTBS

5% (w/v) milk powder

Protein transfer buffer:

25 mM Tris

190 mM glycine

20% methanol

pH8.0

TBS:

8.8 g/l NaCl

20ml/l 0.5M Tris-HCL (pH8.0)

Coomassie stain

0.1% coomassie blue R-250

45% (v/v) SDW

45% (v/v) methanol

10% glacial acetic acid

Destain solution

30% (v/v) methanol

10% (v/v) acetic acid

2.8.2 Protein test expression, extractions and preparations

2.8.2.1 Protein test expression and extractions from bacteria

The pET21b expression vector contains a short DNA sequence called *lac* operator which is located downstream of the T7 promoter region. Binding of the *lac* repressor at *lac* operator site interferes with the association of T7 RNA polymerase to its promoter. Therefore, the target gene is not expressed. Isopropyl β -D-thiogalactopyranoside (IPTG), an artificial inducer of the *lac* operon, binds to the *lac* repressor protein to remove inhibition of the T7 promoter. This allows the T7 RNA polymerase to increase its ability to transcribe the inserted gene.

The plasmid DNA, pET21b-SYN1, was transformed into *E. coli* BL21(DE3)pLysS competent cells and was then used in induction experiments to test expression of the recombinant protein. Protein expression was induced by addition of IPTG to a final concentration of 1mM; a culture with only pET21b was also set up at the same time as a control. Soluble and insoluble protein fractions from induced (IPTG) and non-induced (no IPTG) culture were resolved by SDS-PAGE (12.5% gel). Coomassie Blue staining showed a faint band in the insoluble protein fraction between 22kDa and 36kDa (arrows, figure 2.5). To confirm whether the SYN1 recombinant protein was present in the soluble protein fraction, samples were analysed using western blotting with an anti-histidine antibody and alkaline phosphatase. The result showed that bands in IPTG-induced soluble and insoluble fractions were visualized by alkaline phosphatase detection solution (1X APDB/NET/BCIP). However, the band in the insoluble protein fraction was stronger than that in the soluble protein fraction, suggesting that the high levels of SYN1 recombinant protein was located in cytoplasmic inclusion bodies (figure 2.6).

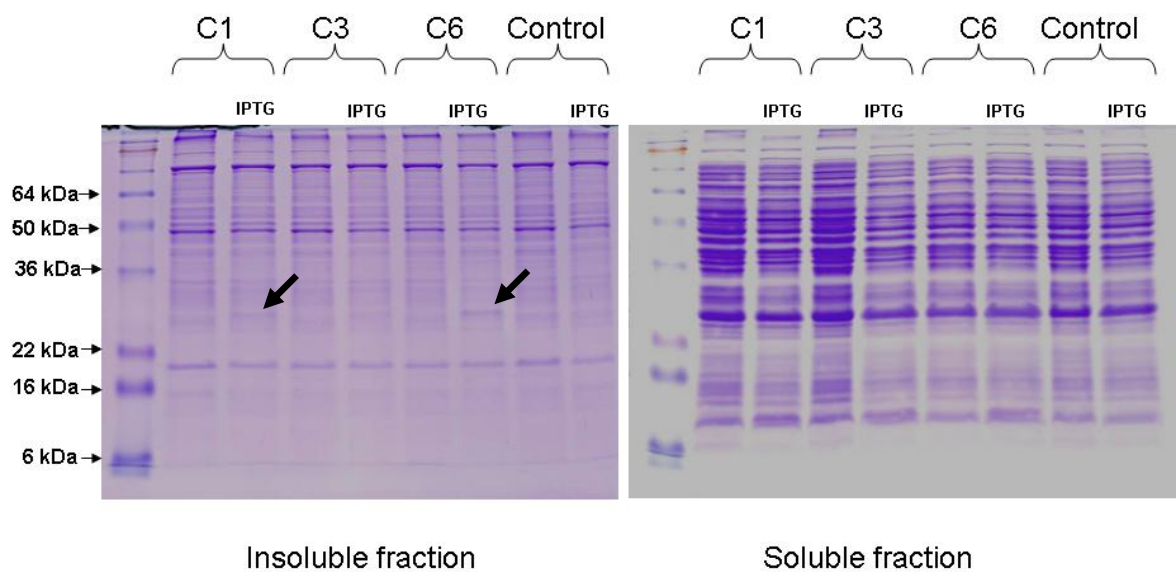


Figure 2.5. SDS-PAGE analysis of protein test induction

Three *E.coli* BL21(DE3)pLysS /pET21b-*SYNI* (C1, C3, C6) and one *E coli* BL21(DE3)pLysS/pET21b (Control) are selected for the protein text induction. Each sample has been treated with and without IPTG. Both insoluble and soluble fractions are resolved on 12.5% SDS-PAGE. Proteins are stained with Coomassie R250. Note: (↘) arrow shows protein expression.

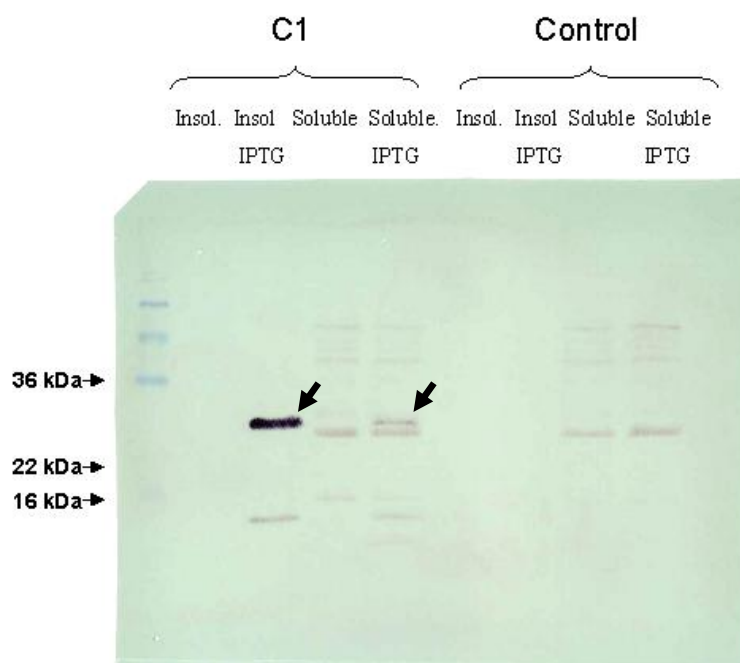


Figure 2.6 Western Blot analysis of *E.coli* BL21(DE3)pLysS/pET21b-*SYN1* (C1) and *E.coli* BL21(DE3)pLysS/pET21b (Control) in protein test expression with and without IPTG.

In the C1 sample, two bands (↙) in between 22 and 36 kDa corresponding to *SYN1* recombinant protein are detected by using anti-his tagged antibody and alkaline phosphatase. Exquivalent bands are not detected in control samples.

As the yield of protein in the test expression was rather low, I decided to transform the pET21b-*SYN1* construct into *E.coli* BL21(DE3) competent cells as an alternative to using BL21(DE3)pLysS. The BL21 (DE3) competent cell is a strain for high-level protein expression, but the leaky expression of T7 polymerase can lead to problems if the recombinant protein is toxic to the *E. coli* cell. The BL21(DE3)pLysS competent cells expresses T7 lysozyme, an inhibitor of T7 RNA polymerase, which prevents any toxicity problem before the induction with IPTG.

Plasmid DNA, pET21b-*SYN1*, was transformed into *E.coli* BL21(DE3) cells and then grown on LB selective agar plates overnight. A single colony of transformed *E. coli* was selected and inoculated into 60ml of LB broth (Ampicillin 100µg/ml) and incubated 16 hours on a rotary shaker (200rpm) in 37°C room. This overnight culture (5ml) was then inoculated into pre-warmed LB broth (50ml). The culture was incubated at 37°C until an OD_{600nm} reached to 0.6. 1mM IPTG was added into the culture and incubated for another 3 hours. A culture without IPTG was used as a control and set up at the same time. The cells were harvested by centrifugation (16,000g, 10 minutes, 4°C) and the pellets were then stored in a freezer. The bacterial pellet was resuspended in 1ml of BugBuster Master Mix (Novagen) containing BugBuster Protein extraction reagent with Benzonase Nuclease and rLysozymetm solution. The suspension was placed on a shaking platform for 20 minutes at room temperature. The mixture was centrifuged (16,000g) at 4°C for 20 minutes prior to collecting the supernatant in a fresh tube. This supernatant containing soluble proteins was resuspended in SDS gel loading buffer. The pellet was resuspended with another 1ml of BugBuster Master Mix to obtain a high purity preparation by solubilising and removing contaminating proteins. 6 volumes of 10X diluted BugBuster Master Mix was then added to the resuspended pellet and vortexed for 1 minute. The suspension was centrifuged at 5,000xg

for 15 minutes at 4°C prior to resuspending the pellet with 0.5 volumes of 10X diluted BugBuster Master Mix. This washing step was repeated two to three times. The suspension was centrifuged at 16,000g for 15 minutes in 4°C. The pellet comprising protein inclusion body was collected and resuspended in PBS and SDS gel loading buffer for SDS-PAGE analysis. Soluble and insoluble protein fractions from induced and non-induced culture were resolved and analysed by SDS-PAGE with Coomassie Blue staining and Western blotting. Coomassie Blue staining and Western blotting analysis showed a high level of SYN1 recombinant protein in the IPTG-induced insoluble protein fraction but a low level in the IPTG-induced soluble protein fraction (Figure 2.7). Compared with protein test expression using BL21(DE3)pLysS, a high yield of SYN1 recombinant protein was obtained by using *E. coli* BL21(DE3). A large scale (110ml) induction was carried out from which a final yield of 2.5µg per µl of SYN1 protein was obtained. In total a yield of 1.3 mg was produced. The purified SYN1 recombinant protein was sent to the BioGene Company (Berlin) to generate anti-SYN1 antibody in rabbit.

2.8.2.1.1 Validation of SYN1 anti-serum

The immune serum was received about 28 days after the first injection. The SYN1 pre-immune and anti-sera were tested for cross-reactivity against the SYN1 recombinant protein in western blotting (Figure 2.8). Western blotting analysis revealed that a band corresponding to the SYN1 recombinant protein with a predicted molecular weight of 22.2kDa was detected with the SYN1 antiserum. The band was not detected with the pre-immune serum. This indicates that the SYN1 anti-serum contains antibodies that recognise the SYN1 recombinant protein. The anti-SYN1 antibody was then further purified by using the Immobilize *E. coli* Lysate Kit (PIERCE).

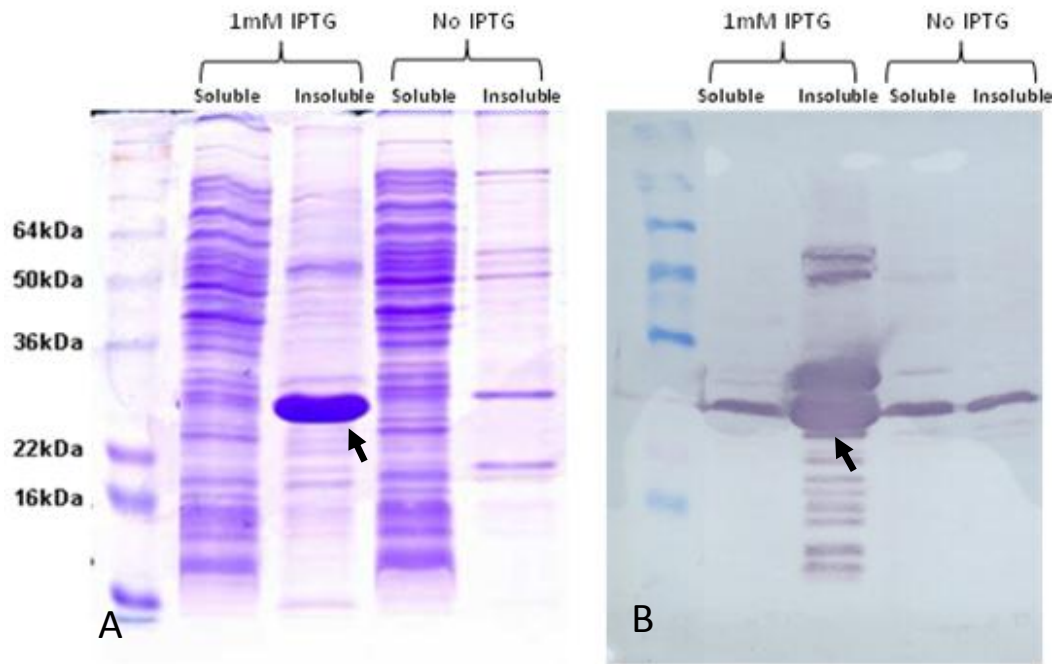


Figure 2.7. SDS-PAGE (A) and Western Blot (B) analysis of *E.coli* BL21(DE3)/pET21b-SYN1 in protein test expression with and without IPTG.

(A) Samples are treated with and without IPTG. Both insoluble and soluble fractions are resolved on 12.5% SDS-PAGE. With the new protein test expression protocol and BL21(DE3) competent cell, high protein expression () is detected in the induced insoluble sample. (B) All samples in between 22 and 36 kDa corresponding to SYN1 recombinant protein are detected by using anti-his tagged antibody and alkaline phosphatase.

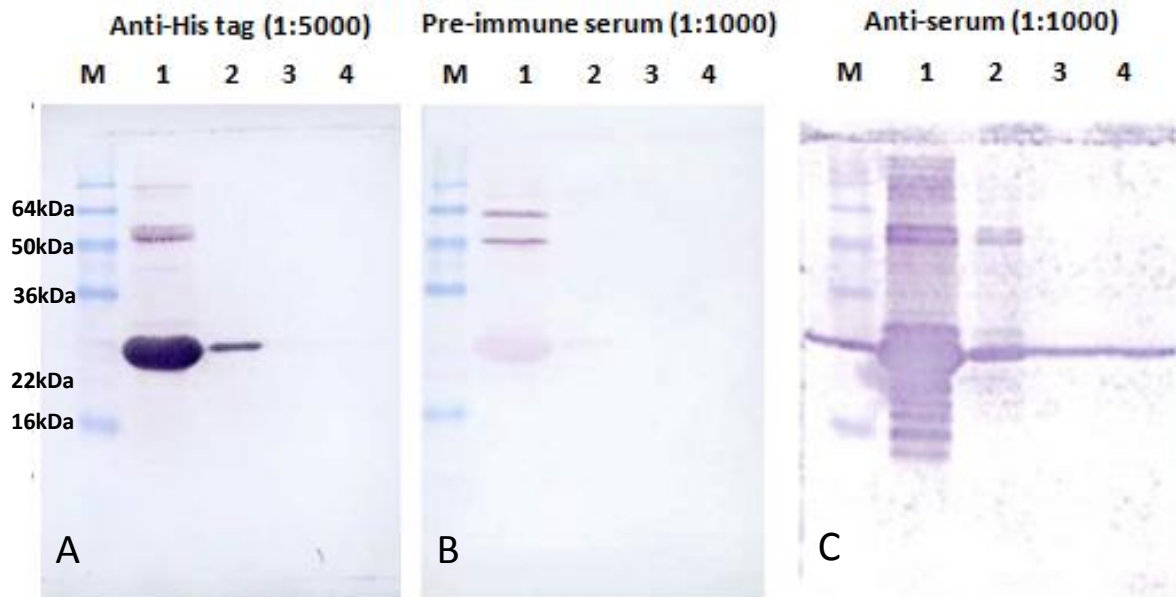


Figure 2.8. 28 days anti-serum was analysed by western blot.

Four different dilutions SYN1 recombinant protein were loaded in each SDS-PAGE. (M: See blue marker; 1: undiluted inclusion body; 2: diluted 10X inclusion body; 3: diluted 100X inclusion body; 4: diluted 1000X inclusion body). (A) Samples (undiluted and 10X diluted inclusion body) in between 22 and 36 kDa corresponding to SYN1 recombinant protein are detected by using anti-his tagged antibody and alkaline phosphatase. (B) All samples in between 22 and 36 kDa are not detected with pre-immune serum. (C) Samples (undiluted and 10X diluted inclusion body) in between 22 and 36 kDa are detected by using anti-serum.

2.8.2.2 Estimating protein concentration

The concentration of protein was estimated using the BioRad assay according to manufacturer's instructions. The protein assay reagent containing Coomassie brilliant blue G-250 was added to diluted protein samples. The mixture was placed at room temperature for 10 minutes prior to measuring protein concentration. The absorbance was measured at 595nm using a spectrophotometer. Estimation of protein concentration was compared with bovine albumin (BSA) as a standard.

2.8.2.3 SDS-Polyacrylamide gel electrophoresis (SDS-PAGE)

Proteins were analysed by SDS-PAGE using a BioRad kit. Different percentages of resolving and stacking gels were cast as follows:

10% Resolving Gel

6.1 ml Sterile distilled water

3.75ml Resolving buffer (1.5M Tris, pH8.8)

150µl 10% Sodium Dodecyl Sulphate (SDS)

5ml Acrylamide (Protogel)

75µl 15% Ammonium per sulphate (APS)

15µl N,N,N,N-tetramethylethylenediamine (TEMED) (Sigma)

12.5% Resolving Gel

4.8 ml Sterile distilled Water

3.75ml Resolving buffer (1.5M Tris, pH8.8)

150µl 10% Sodium Dodecyl Sulphate (SDS)

6.3 ml Acrylamide (Protogel)

75µl 15% Ammonium per sulphate (APS)

15µl N,N,N,N-tetramethylethylenediamine (TEMED) (Sigma)

Stacking Gel

3 ml Sterile Distilled Water

1.25ml Stacking buffer (0.5M Tris, pH6.8)

50µl 10% Sodium Dodecyl Sulphate (SDS)

625µl Acrylamide (Protogel)

25µl 15% Ammonium per sulphate (APS)

5µl N,N,N,N-tetramethylethylenediamine (TEMED) (Sigma)

Proteins were mixed with 5X final protein loading buffer before boiling the sample for 5 minutes. Proteins were loaded on a SDS-PAGE and run in 1x ELFO buffer according to the manufacturer's instructions at 80- 150V for 2 to 3 hours.

2.8.2.4 Coomassie staining of protein gels

Gels were stained at room temperature in fresh Coomassie stain for three hours. Stained gel was destained overnight in destain solution. Gels were washed in SDW and preserved between cellophane sheets after taking or scanning a picture of the gel.

2.9 Western blotting

2.9.1 Protein transfer

Proteins were resolved by SDS-PAGE. The gel was then transferred onto one sheet of Whatman paper soaked in protein transfer buffer. A nylon transfer membrane (Hybond-C extra, Amersham) was cut to size, soaked in protein transfer buffer and then laid over the gel. One more sheet of Whatman paper was soaked in protein transfer buffer and laid on top of the membrane. This arrangement was placed between two electroblotting pads (BioRad) and inserted into an electroblotting tank (BioRad). This tank was filled with protein transfer buffer. A BioRad power pack was used to blot the gel at 400 mA (~1.5 hours, 4°C). Following this, the nylon transfer membrane was removed and placed in blocking solution on rotary shaker at 4°C room.

2.9.2 Antibody probing and protein detection

The blot was incubated with primary antibodies, Anti-Histidine Tagged protein and Anti-SYN1, which was diluted in 1:1000 in milk block solution for 1hr 30 min. After the primary antibody incubation, the blot was washed 3x 10 min in blocking solution and then incubated with anti-rabbit alkaline phosphatase (1:10,000 dilution), for 1 hour. The blot was then washed 3x 10 min in blocking solution. The blot was incubated in the dark with alkaline phosphatase detection solution (1X APDB/NBT/BCIP) until the target protein was detected. The blot was washed with 2x 5min in PBS to stop the detection.

2.10 Slide preparation of meiotic chromosomes for cytology

2.10.1 Determination of meiotic stage

It is necessary to check the meiotic stage of the material to be studied before analysis. To do this material was stained in lacto-propionic orcein (1%(w/v) natural orcein (Sigma), 49.5% (v/v) propionic acid, 49.5% (v/v) lactic acid (LP orcein). Dissected anthers were placed on a microscope slide and covered with a single drop of lacto-propionic orcein. Material was covered with a glass cover slip and the cover slip pressed down to release pollen mother cells (PMCs). Stained preparations were viewed under phase-contrast.

2.10.2 Slide preparation for immunolocalization studies

Arabidopsis buds were dissected from the inflorescence under stereomicroscope. Stems and large (yellow) buds were removed and those of approximately 0.2-0.6 mm were used for the immunolocalisation. To each slide, dissected anthers from approximately 10 buds were placed into 10µl EM digestion medium (0.4% cytohelicase (C8274), 1.5% sucrose, and 1% polyvinylpyrrolidone) and incubated for 10 minutes at 37°C in a moist chamber. Anthers were tapped out in digestion mixture by using a brass rod to release pollen mother cells. Following this, a further 10µl EM digestion mix was added to the tapped solution and placed on a hotplate at 37 °C for 2 minutes. 10µl Lipsol spreading medium (1% (v/v) lipsol detergent to pH9.0 with borate buffer) was added and incubated on a hotplate at 37 °C for 2 minutes. Materials were fixed on the slide by adding 20µl 4% (v/v) paraformaldehyde and dried in a laminar flow cabinet for 2 hours (Armstrong et al., 2009).

2.10.3 Antibody labelling for immunolocalization studies

Dried slides were washed in PBS/0.1% Triton for 3X5 minutes. 100µl primary antibody,

diluted 1:500 in EM blocking solution (PBS+0.1% Triton+ 1% BSA), was added directly to the slide which was covered with parafilm. The slides were incubated overnight at 4 °C in a moist chamber. Following the next day, the slides were washed in PBS/0.1% Triton for 3x5 minutes. 100µl secondary antibody was added and incubated for 1 hour at room temperature. Finally the slides were washed in PBS/0.1% Triton for 3X5 minutes and were counterstained with DAPI in Vectashield antifade mounting medium (Vector Laboratories).

2.10.4 Meiotic time course

Flowering stems were cut under water and transferred to BrdU solution ($1 \times 10^{-2} \text{M}$). The stems were left for 2 hours for uptake of BrdU via the transpiration stream. This allowed BrdU incorporated into those cells in S-phase. After 2 hours the stems were transferred from the BrdU to tap water. Buds were collected at 1hour post-BrdU pulse and 30 hours post-BrdU. Immediately, anthers were dissected out from the buds for making the slide preparations as previously described in section (2.10.1). The primary antibody (100µl of anti-SYN1 raised in rabbit; diluted 1:500 in EM blocking solution) was added to the slides, covered by parafilm, and incubated overnight at 4 °C in a moist chamber. The slides were washed in PBS/0.1% Triton for 3X5 minutes. The secondary antibody (anti-rabbit biotin; diluted 1:50 in EM blocking buffer) was added to the slides and incubated for 30 minutes at 37°C. The slides were washed in PBS/0.1% Triton for 2X5 minutes and once in PBS for 5 minutes. The slides were treated with the anti-BrdU raised in mouse (Roche) for 30 minutes at 37°C. Following this, anti-mouse FITC was added to the slide for 30 minutes at 37°C. Finally, Cy3 avidin (1:200 in EM blocking solution) was used to conjugate to the biotin. The material was incubated for 30 minutes at 37°C before washing for 3x5 minutes in PBS/0.1% Triton. The slides were mounted in 10µl of a solution containing 4, 6-diaminido-2-

phenylinidole (DAPI) at 1 mg/ml in Vectashield antifade mounting medium (Vector laboratories) (Armstrong and Jones, 2003).

2.10.5 Slide preparation for cytogenetic studies

The slides were prepared as previously described by Armstrong et al. (2009). Fixed inflorescences were transferred to a black watch-glass containing 1ml 0.01M citrate buffer. Stems and large buds were removed from the black watch-glass. The remaining buds were washed in 1ml 0.01M citrate buffer (buffer stock 0.1M citric acid: 0.1M sodium citrate, diluted 1:10 for a working solution) for 3X5 minutes. The buds were then incubated at 37°C in a moist chamber with an enzyme mixture (0.3% (w/v) pectolyase, 0.3% (w/v) cytohelicase, 0.3% (w/v) cellulose (all from Sigma, in citrate buffer) for 1 hour and 15 minutes. Replacing the enzyme mixture with fresh citrate buffer stopped the enzyme reaction. A single bud was transferred to slide in a drop of water and tapped out using a needle to produce a cell suspension. One drop of 5µl 60% (v/v) acetic acid was then added to the cell suspension and the slide was placed on the hotplate at 45°C for 1 minute. A further 5µl acetic acid was added on the suspension to avoid drying. Finally, 100µl fixative (Absolute ethanol: Glacial acetic acid in 3:1 ratio) was added as a circle around the suspension on the slide and drained away. The slide was dried with a hair drier.

The slides were washed in 2xSSC at room temperature for 10 minutes. Material on the slide was digested in 0.01% (w/v) pepsin (Sigma) in 0.01M HCl at 37°C for 90 seconds. Slides were washed in 2xSSC at room temperature twice for 5 minutes. Material was fixed on the slide in 4% paraformaldehyde pH8.0 for 10 minutes. Following this, slides were dehydrated by passing through an alcohol series, 70%, 85% and 100%. The slides were ready for

fluorescent in situ hybridisation (FISH) or were counterstained with DAPI in Vectashield antifade mounting medium (Vector Laboratories).

2.10.6 Fluorescent in situ hybridisation (FISH)

The pAL38 containing a pericentromeric 360bp repeat sequence (Fransz et al., 2000) was used in cytological study. The pAL38 probe was produced by PCR amplification using the M13 reverse and forward primers followed by random primer labelling in the presence of biotin-labelled dUTP (Roche).

20µl of the probe mixture was made as follows:

14µl hybridization mix (5ml deionised formamide, 1ml 20xSSC, 1g dextran sulphate, pH7) +2µl labelled probe (The pAL38 probe, centromeric probe, was indirectly labelled with biotin) + SDW made up to 20µl.

20µl of the probe mixture was added on the slide and covered with a coverslip (22x22mm) and sealed by rubber solution. The slide was heated on a hot plate at 75°C for 4 minutes. The heated slide was placed in a moist chamber and incubated at 37°C overnight. After the hybridization, the slide was washed three times, 5 minutes each, in the 50% formamide-2xSSC and then washed in 2xSSC and afterwards washed in 4x SSC/0.05% Tween20. All solutions were heated to 45°C. Finally, the slide was washed in 4x SSC/0.05% Tween20 at room temperature for 5 minutes. 100µl of fluorescent antibodies (Cy3 avidin) was added to the slide and covered with parafilm. The slide was incubated in a moist chamber at 37 °C in a dark environment for 30 minutes. Afterwards, the slide was washed in PBS/ 0.1% Triton for three times, 5 minutes each. The slides were mounted in 10µl of a solution containing 4, 6-

diaminido-2-phenylindole (DAPI) at 1mg/ml in Vectashield antifade mounting medium (Vector laboratories)(Armstrong et al., 2009).

2.11 Slide imaging

Slides were examined by fluorescence microscopy using a Nikon Eclipse T300 microscope. Images were captured and analysed by using Cell Analysis (Olympus) software.

2.12 Cisplatin treatment

2.12.1 Introduction of cisplatin into meiocytes of *Atspo11-1-4^{-/-}*

Bud stems of *Atspo11-1-4^{-/-}* were cut to a length of about 3 to 4cm and immersed into 2.5µM cisplatin solution. After 2 hours, the bud stems were transferred from the cisplatin solution to the tap water. At the same time, bud stems of wild-type and *Atspo11-1-4^{-/-}* without cisplatin treatment were immersed in tap water as positive and negative controls. Immunolocalization studies were carried out on spread preparations with anti-SYN1 (rabbit) and anti-ASY1 (rat) antibodies.

2.12.2 Seedling growth on Cisplatin containing MS agar

One hundred seeds were placed on Murashige and Skoog (MS) agar medium with different concentrations of cisplatin (0 µM; 12.5 µM; 25 µM; 50 µM). These were incubated at 4°C in a chamber for two days prior to transfer to a 22°C growth chamber. After growing for three weeks, seedlings were collected and weighed for statistical analysis.

Chapter 3

Characterising a *syn1* null mutant

3.1 Introduction

Budding yeast (*S. cerevisiae*) REC8, a meiotic kleisin subunit of the cohesin complex, is essential for maintaining sister chromatid cohesion during meiosis (Parisi et al., 1999; Haering and Nasmyth, 2003; Haering et al., 2004). During metaphase I, REC8 is released by separase from the chromosome arms but remains at the centromeres, ensuring the sister chromatids are paired at the centromeric region. This ensures they move towards the same pole during the first meiotic division. When REC8 is released from the centromeric region, sister chromatids are able to segregate towards the opposite poles during the second meiotic division. This indicates that REC8 plays a crucial role in chromosome segregation throughout meiosis. *SYN1* has been reported to be the *Arabidopsis* homologue of *REC8* (Bai et al., 1999; Bhatt et al., 1999). However, the function of *SYN1* in meiosis is not well understood. Several studies have reported chromosome fragmentation in plant *rec8* mutants. These include the rice OsRAD21-4 deficient line, maize *afd1* and *Arabidopsis syn1* (Bai et al., 1999; Bhatt et al., 1999; Yu and Dawe, 2000; Zhang et al., 2006). In the *afd1* mutant, low frequencies of small fragments are observed during meiotic prophase I, whereas severe chromosome fragmentations from the *syn1* mutant and OsRAD21-4 deficient line are detectable throughout the meiosis I and II. However, a detailed analysis of chromosome fragmentation in the absence of cohesin has yet to be conducted. To investigate this chromosome fragmentation phenotype, a *syn1* mutant line was identified. In this chapter, a molecular and cytological analysis to characterise this *syn1* mutant line is described.

3.2 Results

3.2.1 Identification of *SYN1* T-DNA insertion mutant

A T-DNA insertion line (SALK_091193) was obtained from the SALK Institute via NASC that contained an insertion in the *SYN1* gene (*At5g05490*). The seeds were grown together with a wild type (Col 0) in the glasshouse. To identify homozygous knockout lines, genomic DNA was isolated from plant leaves and subjected to PCR genotyping using specific primers. Two primers (S1 and S2) were designed to identify the wild type *SYN1* gene. Another two primers (S2 and LBa1) were designed to check for the presence of an insert. To determine the exact site of the T-DNA insertion, the PCR fragments of a homozygous plant were cloned into pDrive cloning vector (Qiagen) prior to nucleotide sequencing. The sequencing result confirmed that the plasmid contained a DNA fragment comprising a T-DNA sequence and an *Arabidopsis* genomic DNA sequence (Figure 3.1). This genomic DNA was analysed by using NCBI blast search and TAIR SeqViewer (Figure 3.2). The result revealed that the genomic DNA sequence was the gene *At5g05490* on chromosome 5. The T-DNA insertion site is located at exon 6 (nucleotide position 1625566; Figure 3.3) of the *SYN1* gene.

```

CTATAGAATACAGCGGCCGCGAGCTCGGGCCCCACACGTGTGGTCTAGAGC
TAGCCTAGGCTCGAGAAGCTTGTGACGAATTCAGATTGGTTACGTTAGTG
GGCCATCGCCCTGATAGACGGTTTTTCGCCCTTGACGTTGGAGTCCACGTTT
TTAATAGTGGACTCTTGTTCAAACTGGAACAACACTCAACCCTATCTCTGG
CTATTCTTTGATTTATAAGGGATTTGCCGATTTTCGGAACCACCATCAAACAG
GATTTTCGCCTGCTGGGGCAAACCAGCGTGGACCGCTTGCTGCAACTCTCTC
AGGGCCAGGCGGTGAAGGGCAATCAGCTGTTGCCCGTCTCACTGGTGAAAA
GAAAAACCACCCAGTACATTA AAAACGTCCGCAATGTGTTATTAAGTTGTC
CAATTTGTCCGGATCCCACCTTACTACCTAAAGGAAAAACCCATGCCAGGTAA
TGTCACATCTTCTTCCTTGAAGGAGCTTCTCATGCCATTGAAGGATTCTGAAG
GATCAAATCGTAAACATAAGAACATTGTCGTGAAGAATAATAGAAATGATTGG
CGTGTTGGATTTTTTTGTTTGCAGGAAAGAGGCTGTTACATTGCCTGAGAAC
GAAGAAGCTGATTTTGGAGATTTGAACAGACTCGTAATGTTCCATAAATTTGG
CAATTACATGGATTTTCAGCAGACTTTTATTTCCATGGTAATCAACTCAATTCC
CTGTGAATTCTAGATTGAATTGGGTATTTATTTTCTTCTACGTCTCAATATTCA
TCAATTCGTAGAATTGTGGCTTGAACTCTCCAACCTAATCACGAATTCGGAT
CCGATACGTAACGCGTCTGCAGCATGCGTGGTACCGAGCTTTCCTTATAGTGA
GTCGTATTAGAGCTTGGCGTAATCATGGTCATAGCTGTTTCTGTGTGAAATT
GTTATCCGCTCACAATTCACACAACATACGAGCCGGAAGCATAAAGTGTA
AGCCTGGGGTGCCTAATGAGTGAGCTAACTCMCATAATTGCGTTGCSTCM
CTGCCCGCTTTCAGTCGAAACTGTCGTGCAGCTGCATAATGATCGCACGCS
GCGGGGARAGGCGGTTGSGTATGGGGC

```

Figure 3.1 Nucleotide sequence of the plasmid DNA

The sequencing result shows that pDrive cloning vector carried a DNA fragment. This DNA fragment contains *Arabidopsis* T-DNA insertion sequence and *Arabidopsis* genomic DNA sequence (Note that blast result shows at Figure3.2).

The pDrive (green) contains two *EcoRI* sites (yellow boxes). LBa1 primer sequence (GGTTACGTTAGTGGGCCATCG) appears in T-DNA insertion sequence (red). S2 reverse primer (GTGGCTTGAACTCTCCAACCT) appears in *Arabidopsis* genomic DNA (blue).

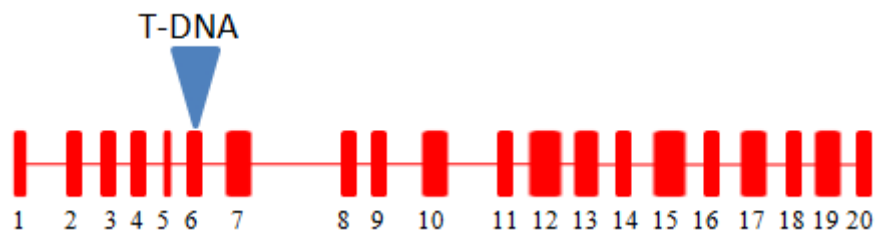


Figure 3.3. Map of the *SYN1* locus and exon organisation.

The 4.4kb open reading frame of *SYN1* located on chromosome 5. The sequence analysis shows the T-DNA insertion in exon 6 of the *SYN1* gene. The position of the T-DNA insertion is represented as an inverted triangle (blue). Exons are represented in red blocks.

3.2.2 Expression of the *SYNI* gene

To investigate the expression pattern of *SYNI* and to determine if its expression was knocked out in SALK_091193, I analysed bud and leaf tissues of wild-type (Col 0), *Atspo11-1-4^{-/-}* and SALK_091193 by using reverse transcription PCR (RT-PCR). The primers (S3 and S4) were designed downstream of the T-DNA insertion and were run by the PCR to show the relative abundance of the *SYNI* transcripts in tissues of wild-type and mutants, using the housekeeping gene *GAPD* as a control. The RT-PCR analysis showed that *SYNI* transcripts were detected in bud and leaf of all samples (data not shown). *SYNI* transcripts were detected in leaf and bud tissues from wild-type (Col 0), *Atspo11-1-4^{-/-}* and SALK_091193, but the *SYNI* level transcripts from the bud samples were higher than that of the leaf. This result suggested that the *SYNI* transcripts in SALK_091193 could be triggered by the activity of a promoter within the T-DNA insertion sequence.

To ensure full length *SYNI* transcripts were not found in the T-DNA insertion line (SALK_091193), two PCR primers (STC and EX8) were designed at the start codon and exon 8 of the *SYNI* gene, which were used to amplify products from wild-type (Col 0), *Atspo11-1-4^{-/-}* and SALK_091193. The amplification analysis showed that *SYNI* transcript was not detectable in all samples. Therefore, second rounds of amplification of *SYNI* were required to detect expression. 1µl of RT-PCR sample was added in Reddy Mix PCR master mix (Therma Scientific). 20 cycles was sufficient for the PCR reaction to avoid saturating the PCR products. The re-amplification analysis revealed that *SYNI* was expressed at the expected size 503bp in bud and leaf samples from the wild-type (Col 0) and *Atspo11-1-4* mutant (Figure 3.4), indicating that *SYNI* is expressed in both reproductive and vegetative tissues. No product was detected in bud and leaf samples from the SALK_091193 line, suggesting that the T-DNA

insertion sequence interrupted expression of the *SYNI* gene. This result implied that SALK_091193 is likely a *synI* null mutant. In addition, the amplification analysis showed that the level of transcription of the *SYNI* gene is relatively low compared with the housekeeping gene *GAPD*.

Data from Genevestigator (<https://www.genevestigator.com/gv/index.jsp>) (Hruz et al., 2008), a microarray database and analysis system which allows average expression levels of given genes across a variety of tissues to be visualized, showed that *SYNI* gene (At5g05490) was expressed in cell culture, flower, stamen, pollen, endosperm, stem, root hair zone and root stele (Figure 3.5), This supports our experimental observation that *SYNI* is expressed in both reproductive and vegetative tissues.

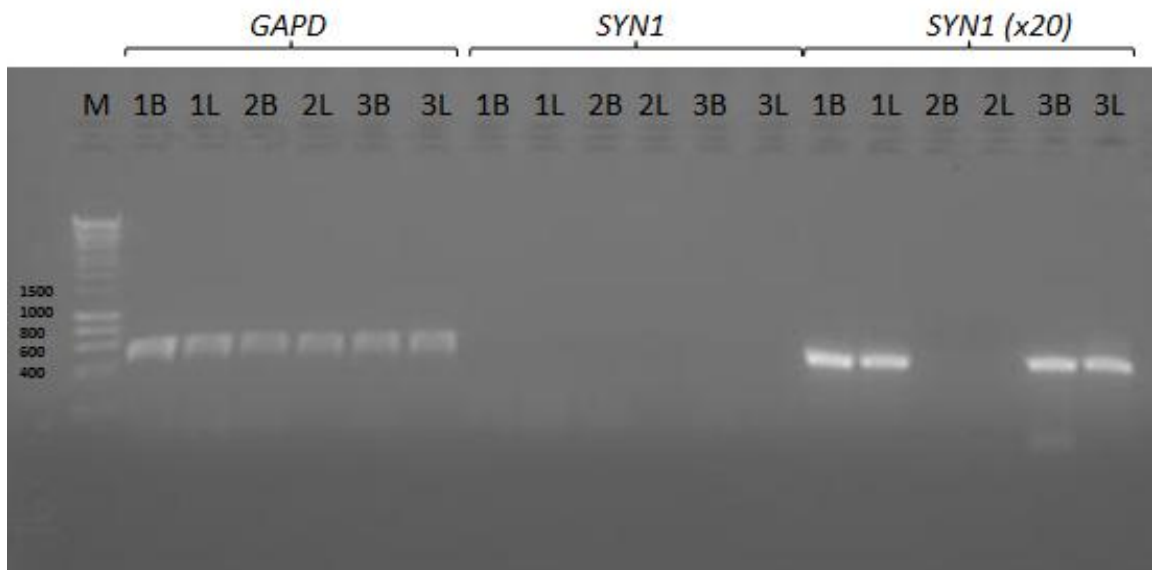


Figure 3.4. *SYNI* gene expression in wild-type (Col 0), *synI*^{-/-} and *Atspo11-1-4*^{-/-} plants.

Two specific primers, STC and EX8, were used to show the relative abundance of the *SYNI* transcripts in wild-type (Col 0), *synI* and *Atspo11-1-4*^{-/-}, using the housekeeping gene *GAPD* as a control. This figure shows that *GAPD* transcripts are equally expressed in all samples, but *SYNI* transcripts were not detected. The re-amplification of *SYNI* with 20 extra cycles (x20) shows that *SYNI* transcripts are only detected in bud and leaves of wild-type and *Atspo11-1-4*^{-/-}.

Note: Wild-type buds (1B) and leaves (1L), *synI*^{-/-} mutant (Salk 091193) buds (2B) and leaves (2L), *Atspo11-1-4*^{-/-} bud (3B) and leaves (3L).

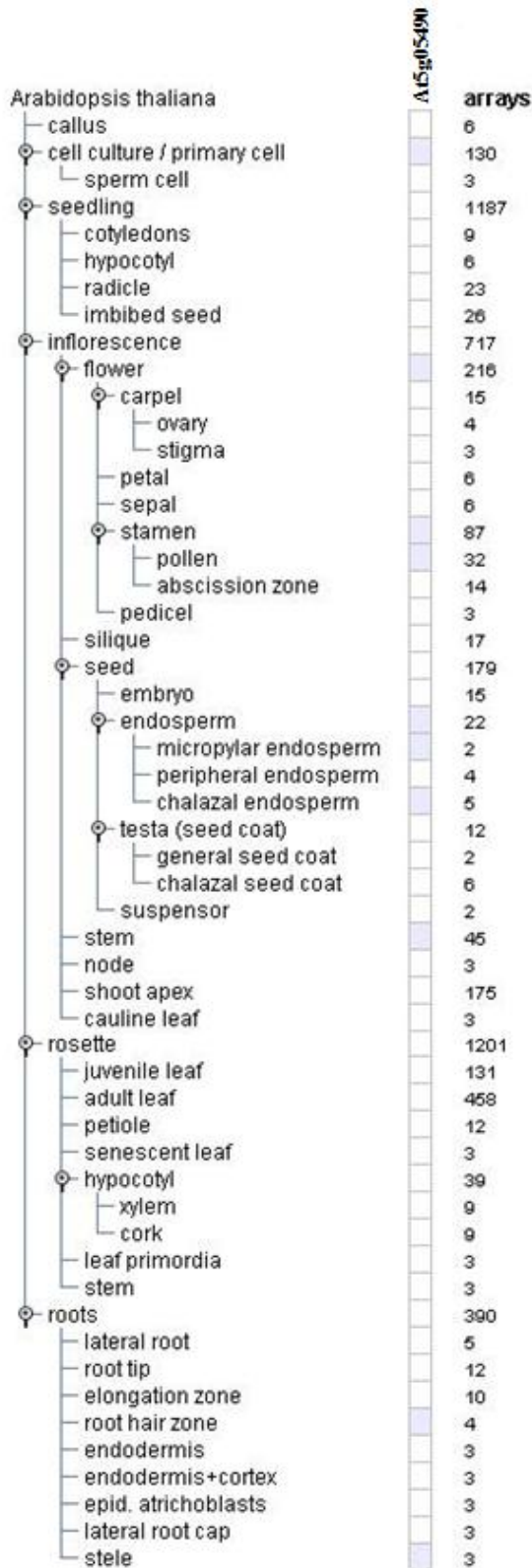


Figure 3.5. Genevestigator expression profile of *Arabidopsis SYN1* gene.

The microarray analysis displays the expression of *SYN1* genes in cell culture, flower, stamen, pollen, endosperm, stem, root hair zone and root stele. For each tissue, we can find out how many arrays are taken into account to calculate the mean value.

3.2.3 Cytogenetic analysis of the *syn1* mutant

3.2.3.1 Male meiosis in wild-type and *syn1* mutant

It was previously reported that chromosome fragmentation is observed in the absence of SYN1 protein (Bai et al., 1999; Bhatt et al., 1999). To confirm the chromosome fragmentation phenotype of *syn1*, I analysed the male meiosis in the wild-type and T-DNA insertion line (SALK_091193) by using chromosome spreads stained with 4, 6-diamidino-2-phenylindole (DAPI).

In wild-type (Col 0) plants, chromosomes stained with DAPI showed chromosomes as normal thin thread structures at leptotene (Figure 3.6A). Synapsed and unsynapsed chromosome regions were observed at the early zygotene (Figure 3.6B). Following further chromosome pairing and synapsis, homologous chromosomes were fully synapsed at the end of pachytene. Therefore, thick and heavily stained homologous chromosomes were observed (Figure 3.6C). As chromosome condensation continued, desynapsis of the homologous chromosome regions increased during diplotene and diakinesis stages. Homologous chromosomes appeared to repel each other slightly thus revealing the chiasmata (Figure 3.6D; E). At metaphase I, five short and thick bivalents were seen to be aligned on the equatorial plate prior to the first meiotic segregation (Figure 3.6F). 10 chromosomes were observed at anaphase I due to the nonsister chromatids of homologous chromosomes moving to opposite poles forming two haploid sets (Figure 3.6G). Two groups of chromosomes were seen to be separated by a band of organelles during prophase II (Figure 3.6H). At the late prophase II, tetrads contained 20 chromosomes arranged in groups of 5 forming four haploid nuclei were observed (Figure 3.6I).

In the T-DNA insertion line (SALK_091193), chromosome abnormalities were found throughout the meiotic program. This made it difficult to identify the early meiotic stages. DAPI showed chromosomes as abnormal thin thread structures (Figure 3.7A; B). Chromosomes were also observed as tangled structures revealing unpaired homologous chromosomes (Figure 3.7C; D). Chromosome fragments were aligned on the equatorial plate (Figure 3.7E). The numbers of chromosome fragments ranged from 7 to 17; Mean=10.17 (Table 3.1; n=53), whereas wild-type meiocytes had the expected five bivalents at metaphase I. During anaphase I, chromosome fragments separated to the opposite poles. Many chromosome fragments remained at centre of cell, the number of chromosome fragments on the equatorial plate ranged from 2 to 22 (Mean=13.1; n=14). The total number of chromosome fragments increased significantly from 10.17 at metaphase I to 32.36 at anaphase I (t-test, $p < 0.001$; Table 3.1) due to the absence of SYN1. The chromosome mis-segregation occurred throughout the meiosis II (Figure 3.7G; H). The number of chromosome fragments showed that there is no significant difference between anaphase I and prophase II (t-test, $p = 0.3756$; Table 3.1), indicating that chromosome fragmentation occurred mainly at meiosis I. This result demonstrated that the chromosome fragmentation likely leads to sterility in *syn1* plants. The cytological analysis also showed that the meiocytes of the T-DNA insertion line (SALK line 091193) is identical to the phenotype of *syn1* (Bai et al., 1999; Bhatt et al., 1999). In the following chapter, the SALK line 091193 will be referred to as *syn1* mutant.

Meiotic stages chromosome fragments	Metaphase I	Anaphase I	Prophase II
Mean (Range)	10.17 (7-17)	32.36 (19-51)	29.68 (17-46)
Number of cells	53	14	16
Standard Deviation	2.465526	7.879936	8.292316
Standard Error	0.337256	2.10637	2.073079

Table 3.1: Number of chromosome fragments in SALK line 091193 meiocytes.

Number of chromosome fragments at metaphase I is significantly lower than that at anaphase I (t-test, $p < 0.001$) and prophase II (t-test, $p < 0.001$). The number of chromosome fragments is not significantly different between anaphase I and prophase II (t-test, $p = 0.3756$).

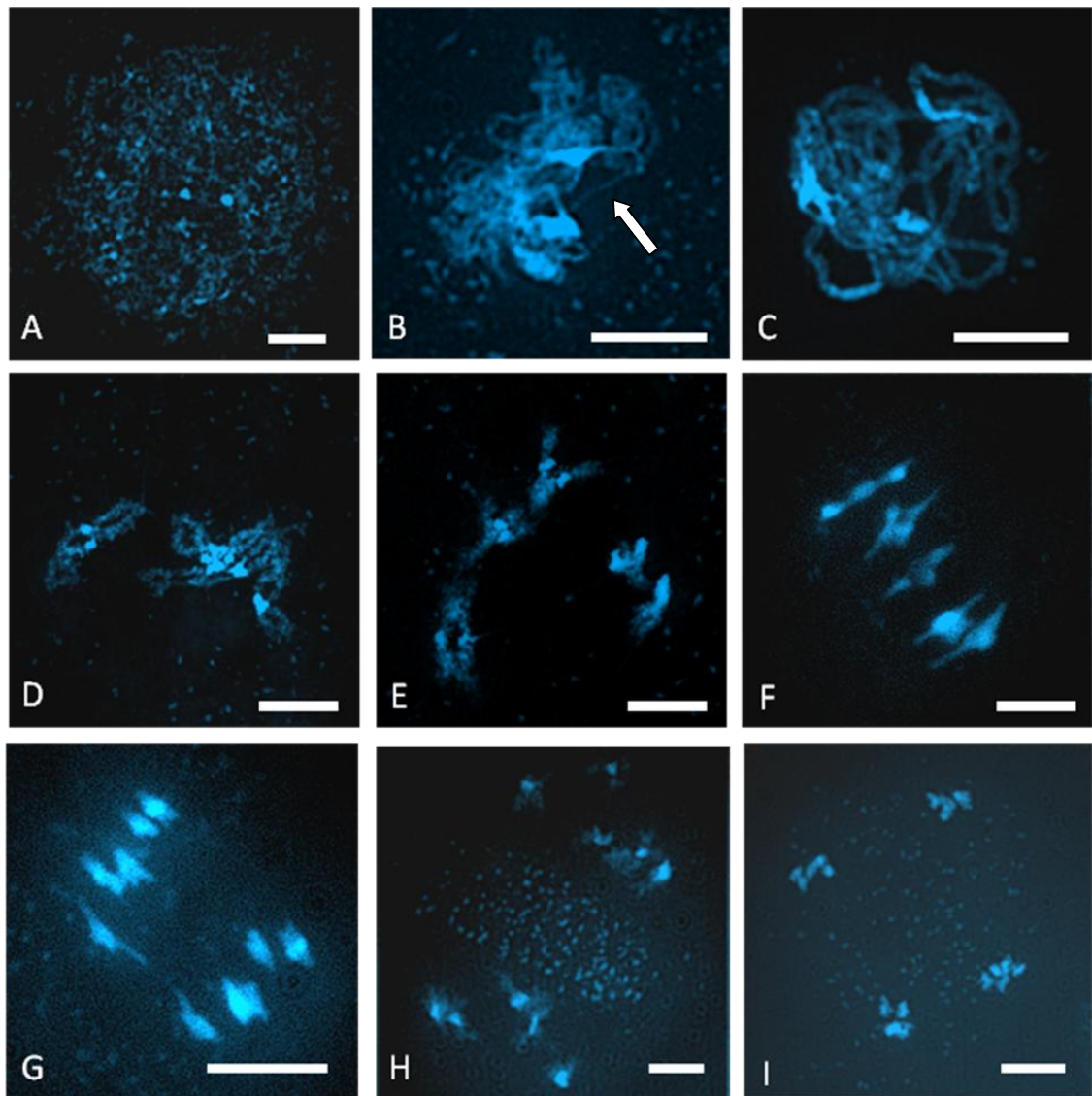


Figure 3.6 Meiotic stages in pollen mother cells of wild-type (Col 0) of *A. thaliana*.

(A) Thin thread chromosomes appear in the early leptotene, (B) Zygotene stage: unsynapsed (arrow) and synapsed homologous chromosomes, (C) Pachytene stage: fully synapsed homologous chromosomes, (D) Diplotene stage: non-sister chromatids of each bivalent repel each other forming chiasmata, (E) Diakinesis stage: paired homologous chromosomes are short and thick, (F) Metaphase I: Five condensed bivalents align on the equatorial plate, (G) Anaphase I: chromosomes migrate towards the same pole. (H) Prometaphase II: two groups of chromosomes are separated from a band of organelle, (I) Telophase I or Tetrad stage: four haploid nuclei. Bars 10 μ m.

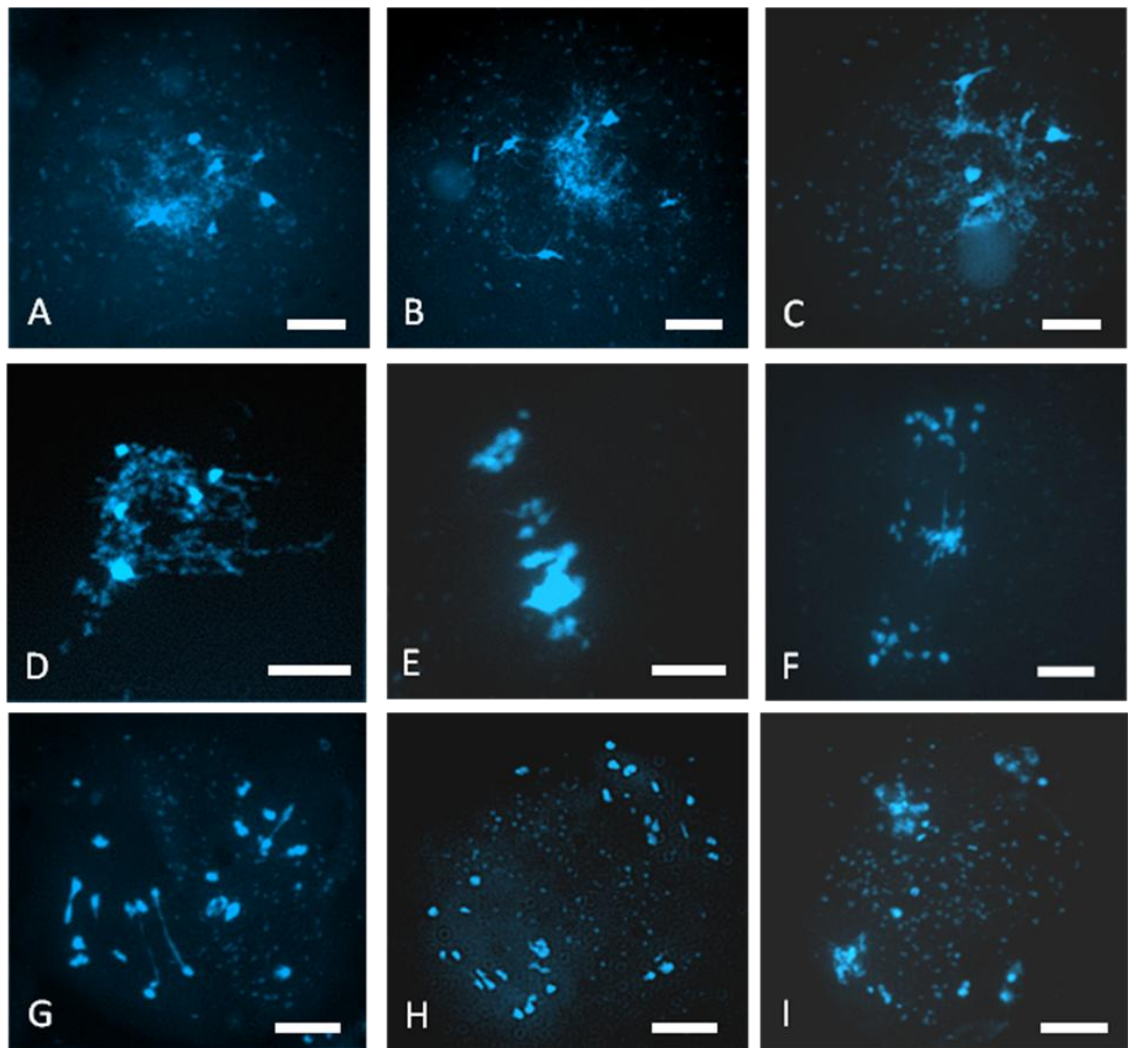


Figure 3.7 Meiotic stages in pollen mother cells of the SALK line 091193 (*syn1* mutant) of *A. thaliana*.

(A) Loose chromatin structures and (B) thin thread chromosomes appear in the early meiotic prophase I, (C, D) tangled chromosomes appear in early prophase I, (E) Metaphase I: chromosome fragments appear on the equatorial plate, (F) Anaphase I: chromosome fragments remain on equatorial plate after chromosomes migrate towards each pole, (G) Early anaphase II: chromosome fragments mis-segregate, (H) Late anaphase II: segregated chromosome fragments are separated from a band of organelles, (I) Tetrad stage: chromosome fragments in four nuclei. Bars 10 μ m.

3.2.3.2 Fluorescence *in situ* hybridisation (FISH) analysis of chromosome segregation in wild-type and *syn1* male meiocytes

To investigate whether SYN1 is essential to maintain cohesion between sister chromatids, I analysed centromere movement in wild-type and *syn1* mutant meiocytes by using the FISH probe, pAL38, a tandemly repeated DNA sequence that localises to the centromeric region of all ten *Arabidopsis* chromosomes. FISH analysis in wild-type meiocytes showed that there are an average of 6.55 (n=20) centromeric signals at early prophase I cell (Table 3.2; Figure 3.8A and B). Ten centromeric FISH signals were detected in diakinesis cells because the non-sister chromatids repelled each other revealing chiasmata (Figure 3.8 B). Following further condensation, five bivalents were aligned on the equatorial plate. Two centromeric signals were detected in each bivalent pointing opposite directions (Table 3.2; Figure 3.8C). After chromosome segregation, non-paired sister chromatids moved towards the opposite poles. There are an average of 10.5 (n=4) and 11.2 (n=5) FISH signals at anaphase I and prometaphase II (Figure 3.8D; E; Table 3.2). Finally, an average of 19 (n=6) FISH signals per cell were detected after sister chromatids segregated to opposite poles (Table 3.2; Figure 3.8F).

In *syn1* meiocytes, an average of 5.65 (n=26) FISH signals were observed on the loose and tangled chromosomes during prophase I (Table 3.2; Figure 3.9 A; B). Following the chromosome condensation, an average of 14.57 (n=7) FISH signals were detected due to the increasing number of chromosome fragments (Table 3.2; Figure 3.9C) during metaphase I. Abnormal centromeric signals were seen distributed on the chromosome fragments. During the first meiotic division, some delay in segregation was apparent (Figure 3.9D). In *syn1* mutant, an average of 19 (n=2) FISH signals were detected at anaphase I whereas in wild-type

(Col 0) an average of 10.5 (n=4) centromeric FISH signals were observed (Table 3.2). The FISH analysis of chromosome segregation in *syn1* meiocytes showed that sister centromeres were not aligned together during anaphase I. Approximately twenty (average=19.14; n=7) centromeric signals were detected at prometaphase II (Figure 3.9E). However, these twenty (average=20.33; n=6) FISH signals were not distributed equally in tetrads due to the chromosome mis-segregation (Figure 3.9F; Table 3.2).

Table 3.2: The average number of centromeric FISH signals at different meiotic stages of wild-type and *syn1* mutant

Meiotic stage	Early prophase I	Metaphase I	Anaphase I	Prometaphase II	Tetrad
Wild-type (Col 0)	6.55 (3-10) *n=20	10 (10) *n=6	10.5 (10-12) *n=4	11.2 (10-14) *n=5	19 (17-20) *n=6
<i>syn1</i> mutant	5.65 (4-8) *n=26	14.57 (13-16) *n=7	19 (18-20) *n=2	19.14 (14-21) *n=7	20.33 (20-21) *n=6

Note: The number of cells examined at each stage is shown next to the *. The range of centromeric FISH signals is shown within brackets

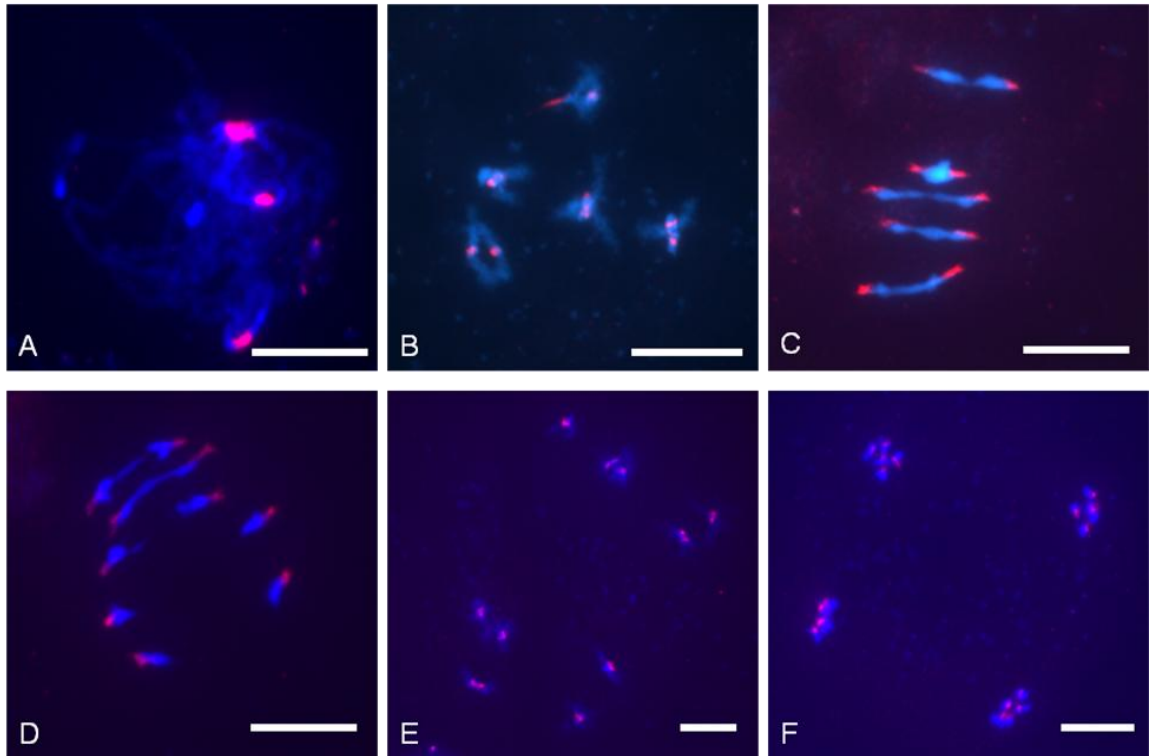


Figure 3.8. FISH of centromeric probe (pAL38) to pollen mother cells of wild-type *A. thaliana*. (A) Five centromeric FISH signals appeared in pachytene stage, (B) Ten centromeric FISH signals were detected in diakinesis, (C) Two centromeric FISH signals were detected in each bivalent during metaphase I, (D) One centromeric FISH signal was detected in sister chromatids during first meiotic segregation, (E) Ten centromeric FISH signals were observed in prometaphase II, (F) After sister chromatids segregation, twenty centromeric FISH signals were detectable in tetrad.

Note: FISH signal is red colour and DAPI is blue colour. Bars 10 μ M.

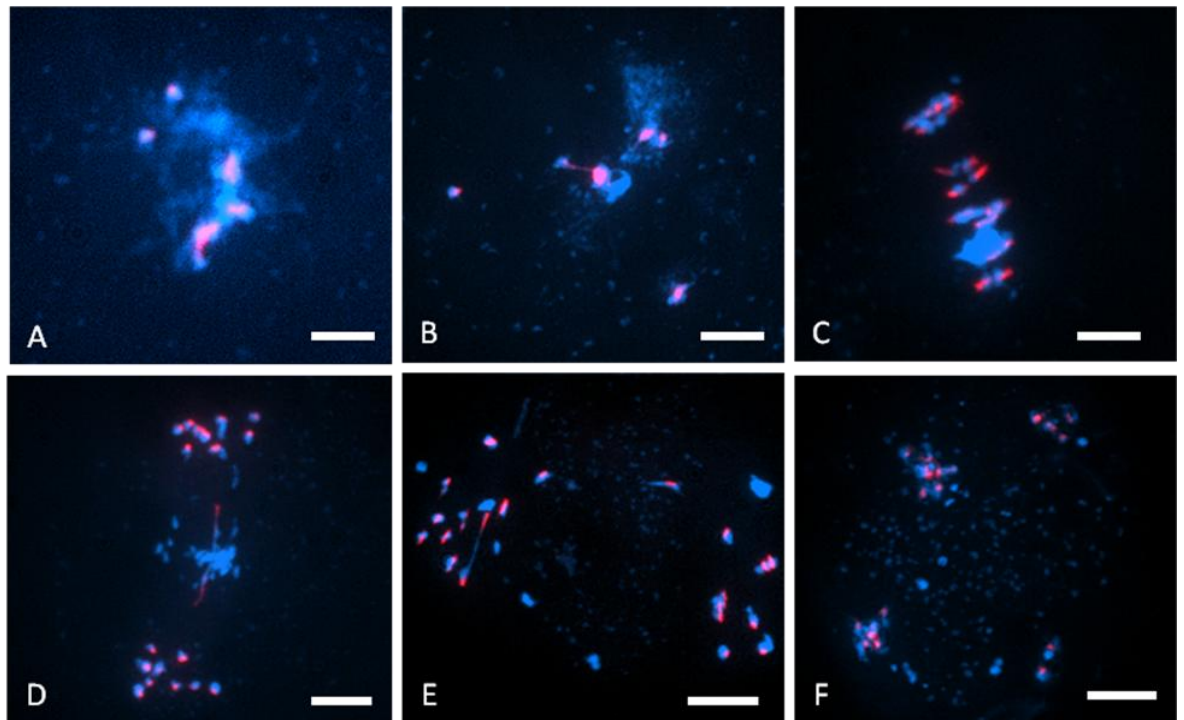


Figure 3.9. FISH of centromeric probe (pAL38) to pollen mother cells of the SALK line 091193 (*syn1* mutant) of *A. thaliana*. (A) and (B) Five centromeric FISH signals were detected in loose chromatin and tangled chromosome during the early prophase I, (C) 16 centromeric FISH signals were detected in metaphase I. (D) 10 centromeric FISH signals were detected in each pole during anaphase I. (E) and (F) 20 centromeric FISH signals were detected at prometaphase II and tetrad. Bars 10 μ m.

3.2.4 Relationship between SYN1 and other Rec8 homologues.

Cytological analysis of *syn1* mutant showed chromosome fragmentation during metaphase I. However, severe fragmentation is rarely detected in non-plant species. It is essential to evaluate the relationship between SYN1 and other REC8 homologues. Six species *Saccharomyces cerevisiae*, *Caenorhabditis elegans*, *Sordaria macrospora*, *Oryza sativa*, *Zea mays* and *Arabidopsis thaliana* were chosen for protein sequence alignment. The amino acid sequences were analysed with ClustalW (<http://www.ebi.ac.uk/Tools/emboss/align/>) using the Blosum62 comparison table (Thompson et al., 1994).

REC8 has been identified in *S. cerevisiae* (Parisi et al., 1999). Currently, chromosome fragmentation has not been found in a yeast *rec8* mutant. The yeast REC8 contains 680 amino acids whereas *A. thaliana* SYN1 has 617 amino acids. REC8 showed only 18% identity to SYN1. Another two REC8 homologues have been identified in *C. elegans*, CeREC8 and *S. macrospora*, SmREC8. It has been reported that chromosome fragments are found in *cerec8* and *smrec8* mutants (Pasierbek et al., 2001; Storlazzi et al., 2008). Both ceREC8 and smREC8 contain 781 and 763 amino acids (Figure 3.10). The analysis showed that the amino acid sequence identity between ceREC8 and SYN1 is lower (18.2% identity) than that between smREC8 and SYN1 proteins (20.7% identity). All REC8 proteins are rather conserved at N- and C- termini. Therefore, this result showed that SYN1 has low identity in full length amino acid sequence with others.

Recently, chromosome fragmentation was identified in other plant REC8 mutants including *Z. mays*, AFD1 (Yu and Dawe, 2000) and *O. sativa*, OsRad21-4 (Zhang et al., 2006). AFD1 and OsRad21-4 contain 602 and 608 amino acids respectively. The levels of amino acid

sequence identity between AFD1 and SYN1 are the same (41% identity) to those between OsRad21-4 and SYN1 protein (41% identity). However, the amino acid sequence identity between AFD1 and OsRad21-4 protein is higher (71% identity; Figure 3.11).

```

SYN1 MFYSHQLLARKAP-LGQIWMATL-----HAKINRKKLDKLDIIQICEEILNPS----- 48
smREC8 MFYSHEILTNQQYGVATVWLVSTFGLRSSNRKISRKAIQGVNVRKACETILQPG----- 54
ceREC8 MVVSAEVIR-KDAVFHVAWILGTG----DSKKLSRREILDQNLPELCHSIEMVPERHRG 55
      * . * : : : . * : . * * : * : : : * . * : :

SYN1 --VPMALRLSGILMGVVIVYERKVKLLFDDVNRFLVEINGAWRTKSVDPDTLLPKGKTH 106
smREC8 --APIALRLQGSLLYGVSRVFSQQCSYVLTDAEKIHMHRFCYFNVLGGSGNALDPQAGKA 112
ceREC8 SATKTGLYLLSLLTYGTVLHQQVDFLKRDRVEKLEKELMKKKSFIILLMAERFDRNQELQR 115
      . * * . * * . : . : . : * : : : . : . :

SYN1 ARKEAVTLPE-----NEEADFG-DFEQTRNVPKFGNYMDFQQTIFISMRLDE 151
smREC8 KRNQLILPDDPDFEVMGLPAFHFDDEGNLATQFQSQASRKTSSQFSPDRFNLTDPDNG 172
ceREC8 KEDKFARLRSKPIMCVEELDRVDLAHLQAI GDELGINGNPGDFIMMDALPNMNQWIDNNS 175
      . : . : . : . : . : . : . :

SYN1 SHVN--NNPEPEDLQQFHQAENITLFEYHG-----SFQTNNETYDRFERF-DIEGD 202
smREC8 SFIIIGLDLPQSSPTNPLYSHSSYSLGPLSQHKPDDMMQFGEPEANAEIFGDW-GIEID 231
ceREC8 ELNAIYGCVEPYLREKEITMHSTFVEGNGSNEHNKERRNDAVIADFSQLLFPEIPEITLG 235
      . . : . : . : . : . * * .

SYN1 DETQMNSNPREGAEIPTTLIPSPRRHHDIPGVNPTSP----- 240
smREC8 ADGNVMATVDE-PELPILRPEEERAYATASGQVHDEPEFHFDQDQLLINGGTAPPEA 290
ceREC8 EKFPIDVDSRKRSAILQEEQEEALQLPKEASEIVQEEP-----TKF 276
      . : : . : . : . *

SYN1 -----QRQEQQENRRDGFQAEQMEEQNIPDKE--EHRP-QPAKKRARKTATSAMDYEQ 290
smREC8 DEVPGLVDPDQVEQAQENQVMAEAEQVIAEEEEPVAEASA-APVRRRQRRRVVLAPD-ED 348
ceREC8 VSIALLPSETVEQPAQEP IQEPIQPI IEEPAQLELPPQELPQLDAIDLVTIPASQQD 336
      : * : : : * : . * : . . . : :

SYN1 TIIAGHVYQSWLQDTS DILCRGEKRKVR-----GTIRPDM 325
smREC8 TKISRHELKSWSN DYLANAERTNNAARRAAATNPAAAKKHAYDLVFGRGVGGVGSFDDGL 408
ceREC8 MVVEYLQLINDLPDDENSRLPPLPKDLELFEDVILPPPAAKSKVEEEDALERARRRPS 396
      : . * . . . .

SYN1 ESFKRANMPPTQLFEKDSSYPQLYLQWSKNTQVLQTSSESERHP-----DLRAEQSPG 379
smREC8 NSGNHRSHPLAALFAG-VDFAAEVLDDIDIDIDEGHEAGRRRGRRRSALEALELEEEEDAER 467
ceREC8 RPVTPINQTDLTLHSTVRPEDPSFAIDSQIHDLVLPQRKKS KRNLP I IHSDDLEIDEA-- 454
      . . . . : : : * . : * . : :

SYN1 FVQERMHNHHQTDHHERSDTSSQNLDSPAELRTRVTRTGKGASVESMMAGSRASPETINRQ 439
smREC8 RVRRLSDENEEHHAQSQQNVAEPQAEAGRLLTGEAEEDAIEGRRDGSALPDPDIPSD 527
ceREC8 -VQKVLQADYSSLVKKEKEDVIAKI PKKTDAAVAVLMNLPEPVFSIGYRLPPEVR--DMFKA 511
      * : . : . : : : : . . . :

SYN1 AADINVTFFYSGDDVRSMPSTPSARGAASINNIEISS--KSRMPNKRPNSS-----P 490
smREC8 APWNRAPSLVPGSSVKGDSHMPGSSRQVSASPLHSRGSHLAHLPPIDRFSDTGSYAPLLH 587
ceREC8 CYNQAVGSPVSDDEEDEDEEEEEYKYAKVCLLSPNRIVEDTLLEEQRPQPEEFPSTDN 571
      . . . . . . . : . : : . : .

SYN1 RRGLEPVAEERPWEHREYEF-----EFSMLPEKRFTADKEILFETASTQTKPVCNQS 543
smREC8 SGGVPDFSSDPVMPGGEDEP-----ELPHLPGGNHGSQLLRRSPSSEAGAATEVMAET 640
ceREC8 INPPRQLQENPVFENLEYEAPPHPI RTARTPTPIKDLKYSVLSLFPTEKRRETSI IAEL 631
      . : : * * . * . : : . : :

SYN1 --DEMITDSIKSHLKH FETPGAPQVESLNKLAVG----- 576
smREC8 --SQVMKDALDRDGRNFLT YVNMVAKTRGETRSLGGGTPS QAVGDGDGNRRRLRQWVAFDE 698
ceREC8 NLDPIPVEEIDP-LTMRTEEELENVRRRQKSSSLGVQFMRTDDLEEDTRRN-----RL 683
      . : : : . : . : *

SYN1 -----MDRNAAKLFFQSCVLATRGVIKVN-----QAEPYGDILI 611
smREC8 LLDEPRDRTRQVATQAFYNVLVLATKNAIKVEQDME-----DFQPFGIEIRV 744
ceREC8 FEDEERTRDAREDELFFYSSGSLLPNNRLNIHKELLNEAEARYPEWVNFNEFTADHRKK 743
      . * : . * . . : : . : . :

SYN1 ARGPNM----- 617
smREC8 GVGVSEAAMLAMMEEDGDA----- 763
ceREC8 AATAFEGLLLSLKNMKVEAKQEDPYFPILVRHISHEEM 781

```

Figure 3.10 Alignments of the full length amino acid sequence of the smREC8, ceREC8 and SYN1.

The SYN1 amino acid sequence is shown aligned with smREC8 (*S. macrospora*) and ceREC8 (*C. elegans*). Sequences are aligned using the ClustalW method with the Blosum62 comparison table. The degree (%) of identity between the amino acid sequence of the smREC8 and SYN1 (20.7%) is very close to those between ceREC8 and SYN1 (18.2%) and between ceREC8 and smREC8 (19.5%).

Note:

“*” marks residues in the column that are identical in all sequences in the alignment

“.” marks conserved substitutions

“.” marks semi-conserved substitutions

“-” marks a gap

3.3 Discussion

3.3.1 T-DNA insertion line (SALK_091193) is a *synI* null mutant

Despite few published studies on *SYN1*, we still do not know very much about the function of this protein. To investigate the role of *SYN1*, I began to search for a *synI* mutant line for my study. A T-DNA insertion line (SALK_091193) was obtained from the SALK institute. I confirmed that the T-DNA sequence was inserted at exon 6 of *SYN1* gene by sequencing selected DNA fragment. Furthermore, *SYN1* transcripts were not detected in this T-DNA insertion line by using RT-PCR analysis, whereas *SYN1* was expressed in wild-type buds and leaves. The cytological analysis showed that abnormal tangled chromosome and chromosome fragmentation appeared during meiotic prophase I. All examination revealed that the T-DNA insertion line (SALK_091193) is a *synI* null mutant.

3.3.2 *SYN1* expression is not specific to meiosis

According to previous reports (Bai et al., 1999; Bhatt et al., 1999), *SYN1* gene transcripts are detected in wild-type floral buds and seedlings. In my work, the RT-PCR analysis confirmed that *SYN1* was expressed in both floral buds and mature leaves at the same levels. In addition, the microarray database and analysis from genevestigator showed that *SYN1* was expressed in cell culture, flower, stamen, pollen, endosperm, stem, root hair zone and root stele. These suggest that *SYN1* expression is not limited in reproductive tissues. In other species, *AFD1* expression is abundant in leaves, tassel and ear of maize (Golubovskaya et al., 2006) but in mouse *REC8* expression appears to be confined to testes and ovary (Lee et al., 2002). Recently, human cancer studies showed that *REC8* is expressed in radiation-induced endopolyploid tumour cells. Furthermore, *REC8* localizes to sister centromeres in these tumour cells (Erenpreisa et al., 2009). It is possible that mitotic cells express *SYN1* but this

protein is not playing a crucial role in vegetative growth. In conclusion, the expression of *SYN1* gene is not meiosis specific, although the defective phenotype of *syn1* mutant is restricted to reproductive organs.

3.3.3 Chromatin is disorganised during early meiosis I in *syn1* mutants.

It has been reported that the chromosome fragmentation is found in the absence of SYN1 in plants (Bai et al., 1999; Bhatt et al., 1999). I have used the T-DNA insertion line (SALK_091193) to investigate this phenotype. Abnormal thin thread-like and tangled chromosomes were detected throughout the early prophase I. It is very difficult to identify individual chromosome and specific meiotic stages until chromosome fragments were aligned on the metaphase plate. These chromosome fragments appeared throughout meiosis I and II and the number of fragments increased from 10.17 (at metaphase I) to 29.68 (at prophase II). Unlike the *syn1* mutant, abnormal loose chromatin and tangled thin thread-like chromosomes were not found in *rec8* mutants of other species (Pasierbek et al., 2001; Xu et al., 2005; Golubovskaya et al., 2006; Zhang et al., 2006). Chromosome fragments are found at much early stages, e.g. pachytene in *O. sativa* OsRad21-4 deficient lines and diakinesis in *C. elegans* REC8 depleted lines (Pasierbek et al., 2001; Zhang et al., 2006). As we know, severe chromosome fragmentation appears in both the *syn1* mutant and OsRad21-4 deficient lines (Zhang et al., 2006). Interestingly, only low frequencies of small fragments are observed in maize *afd1* mutant (Yu and Dawe, 2000). According to sequence analysis the amino acid sequence identity between AFD1 and OsRad21-4 protein is higher (70% identity) than that between OsRad21-4 and SYN1 protein (41% identity). Surprisingly, the cytological outcomes were rather different. Despite the striking differences in the chromosome phenotypes of the three mutants, i.e. *syn1*, *afd1* and OsRad21-4 depletion lines, chromosome segregation is

affected in all of them, regardless of the species. This chromosome mis-segregation is likely to be the basis of plant sterility.

3.3.4 SYN1 is important for centromeric cohesion at the first meiotic division.

In budding yeast, REC8 persists at centromeres to maintain centromeric sister chromatid cohesion throughout meiosis I and disappears at anaphase II. As a result, sister chromatids are separated during the second meiotic division. In the absence of REC8, the cohesion of centromeres is lost during early meiosis I (Klein et al., 1999), whereas in *Arabidopsis syn1*, an average of 5.65 (n=26) FISH centromeric signals was found at prophase I cell, suggesting that centromeric cohesion is still present during early meiosis I. FISH analysis showed that an average of 19 (n=2) centromeric signals was detected at anaphase I whereas in wild-type (Col 0) an average of 10.5 (n=4) centromeric signals was observed, suggesting that loss of cohesion in the centromeric region during anaphase I stage. This phenotype is consistent with fission yeast *rec8* mutant (Watanabe and Nurse, 1999). This result suggests that centromeric cohesion was maintained during early prophase I by other cohesin in the absence of SYN1. However centromeric cohesion was lost during metaphase and anaphase I transition stage, as a result centromeres were not aligned together. This suggests that SYN1 is essential for centromeric sister chromatid cohesion during the first meiotic segregation.

Chapter 4

Immunolocalization of SYN1 protein

4.1 Introduction

Previous reports have indicated that the SYN1 appears along chromosome arms but not at centromeric regions in early meiosis I. The protein is then released from chromosome arms during the first meiotic division. Interestingly, substantial SYN1 signals are detected in the nucleus of prophase II cells (Cai et al., 2003; Chelysheva et al., 2005; Zhao et al., 2006). This observation is inconsistent with the distribution of yeast/mammalian REC8 (Watanabe and Nurse, 1999; Shonn et al., 2002; Lee et al., 2006), where REC8 appears along chromosome arms and centromeric regions in early meiosis I. Centromeric REC8 persists throughout meiosis I and is released by separase at anaphase II. The localization of SYN1 in relation to other cohesin proteins has not been well described in *Arabidopsis*. Therefore, it was decided to raise an anti-SYN1 antibody in order to further investigate the role of SYN1. Recombinant SYN1 protein was expressed in *E. coli* and was then injected into rabbits. The anti-SYN1 antibody was tested by western blotting and examined in spread preparations of pollen mother cells (PMCs) from wild-type (Col 0) and the *syn1* mutant. Meicytes of wild-type (Col 0) and the *syn1* mutant were also examined using antibodies against cohesins, an axis-associated protein and meiotic recombination proteins. The results provide new insights into the roles of SYN1 protein in meiosis.

4.2 Results

4.2.1 Immunolocalization

4.2.1.1 SYN1 localizes on meiotic chromosomes

To investigate the distribution of SYN1 in *Arabidopsis* wild-type (Col 0) meiocytes, chromosome spread preparations of wild-type pollen mother cells (PMCs) were examined by using anti-SYN1 antibody. At the same time, an antibody against the axis-associated protein ASY1 was used on a different slide as a control. Both primary antibodies, anti-SYN1 and anti-ASY1, were raised in rabbit. Anti-rabbit FITC was then used to detect bound antibodies. Immunolocalization studies revealed that the SYN1 appeared as foci in preleptotene meiocytes (Figure 4.1). According to BrdU time course experiment, immunostaining showed that SYN1 signals were detectable in wild-type meiocytes at G2 stage (Figure 5.4A). During leptotene/zygotene stage, a strong punctate signal was present along the chromosomes (Figure 4.2B) but was not detectable in mitotic cells (Figure 4.1), suggesting that anti-SYN1 antibody detects meiosis specific cohesin SYN1. Unlike SYN1, ASY1 appeared as a continuous signal along the chromosome axes during leptotene/zygotene stage (Figure 4.2A).

To further investigate the distribution of SYN1 at early prophase I, chromosome spread preparations of wild-type pollen mother cells (PMCs) were examined by using anti-SYN1 (rabbit) antibody in conjunction with anti-ASY1 (rat) antibody. Immunostaining of SYN1 and ASY1 showed strong signals in the wild-type nuclei at early prophase I. Both proteins were first detectable as foci in the nucleus during early leptotene (Fig 4.3A). As the homologous chromosomes continue to pair and synapse through zygotene, SYN1 appeared as patchy signals running along the chromosome axes. In contrast, ASY1 appeared as rather more defined linear signals along the chromosome axes (Figure 4.3B; C). During early pachytene,

SYN1 was still detectable as a strong patchy signal distributing along the chromosome axes while ASY1 appeared as a thick linear signal. Following further synapsis, SYN1 patchy signals gradually extended to form a continuous signal which colocalized with ASY1 along the chromosome axes during late pachytene stage (Figure 4.3D). Previous reports have only shown SYN1 linear signal running along the chromosome at meiotic prophase I (Cai et al., 2003; Zhao et al., 2006). Therefore, our finding suggested that the distribution of SYN1 along the chromosomes during early meiosis may be slightly different than previously described.

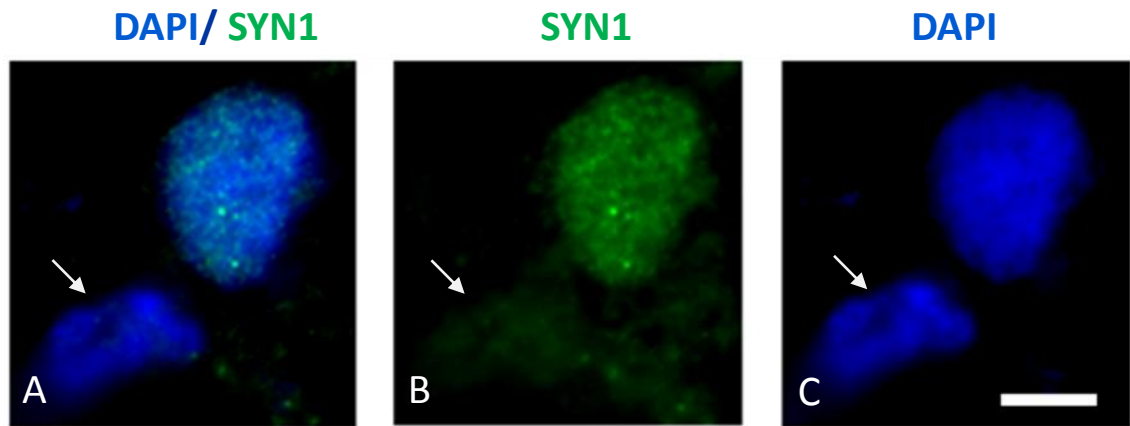


Figure 4.1. Immunolocalization of SYN1 protein to nuclei of wild-type (Col 0). The result shows that the localization of SYN1 (green) appears in meiocyte (Pre-leptotene stage) but not in mitotic cell (white arrow). The chromosomes are counterstained with DAPI (blue). Bar 5 μ m.

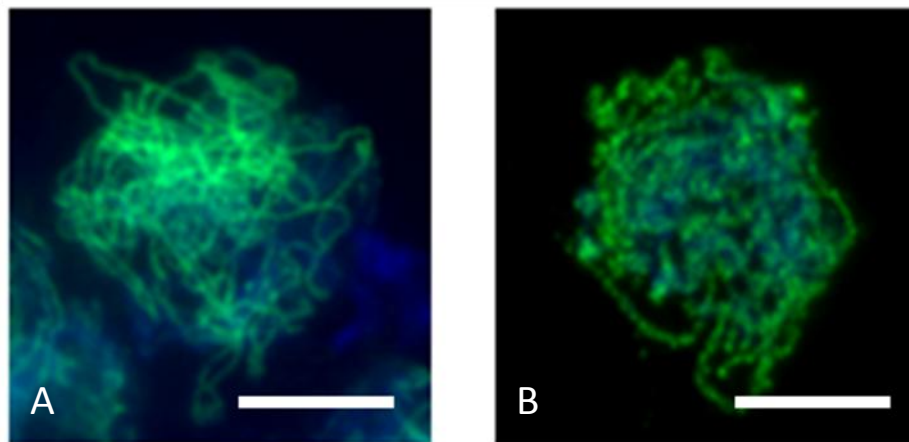


Figure 4.2. Immunolocalization of ASY1 and SYN1 proteins to wild-type (Col 0) meiocytes. The result shows that ASY1 (green) appears as a linear signal (A) and SYN1 (green) appears as numerous punctate foci (B) along the homologous chromosomes in the early prophase I. Bars 5 μ m.

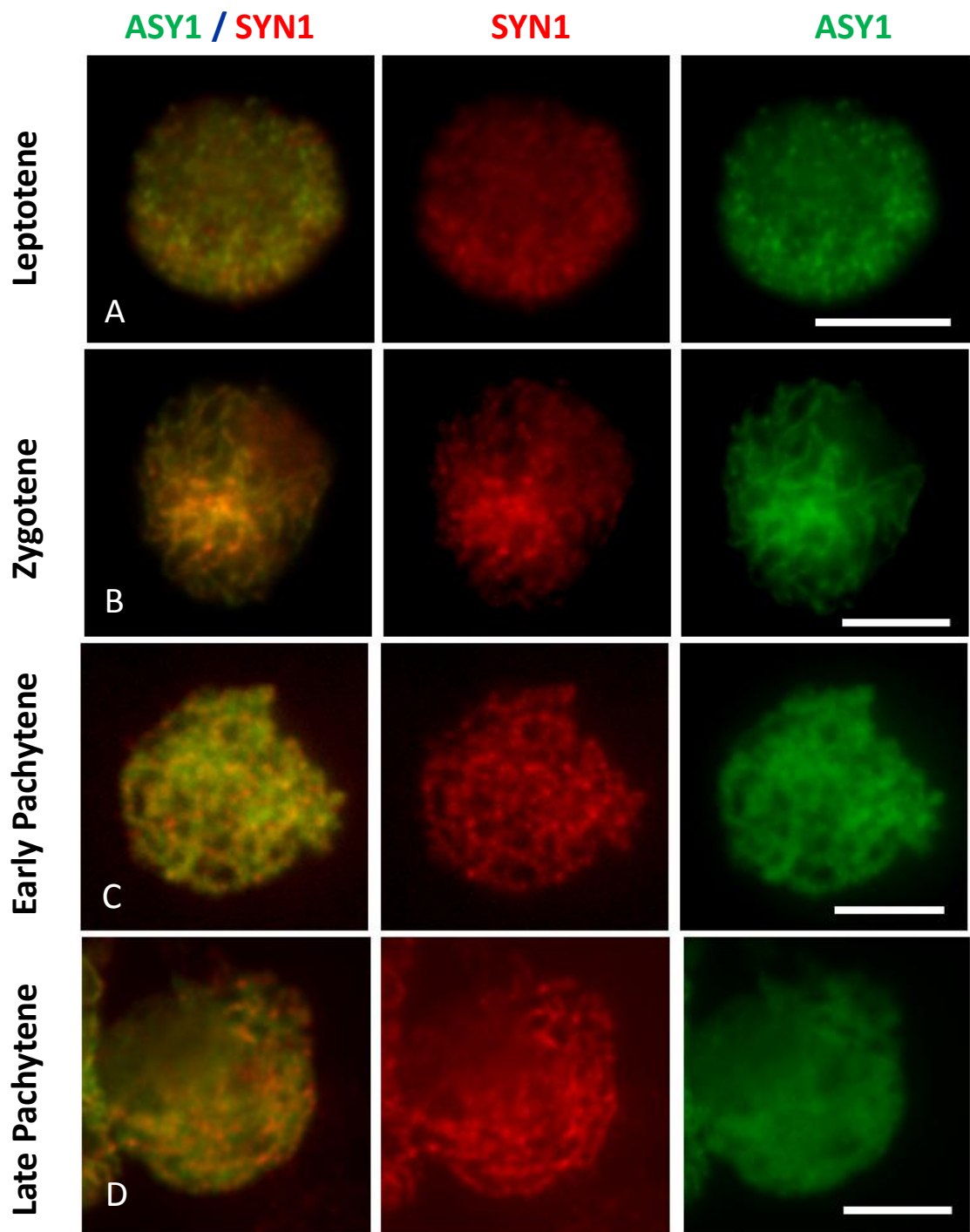


Figure 4.3. Dual immunolocalization of ASY1 (green) and SYN1 (red) to leptotene (A), zygotene (B), early pachytene (C) and late pachytene of wild-type (Col 0). Bars 5 μ m.

4.2.1.2 Immunolocalization of SYN1 and AtSMC3/AtSCC3 on wildtype (Col 0) meiocytes

Studies in yeast have shown that REC8 associates with SMC1 and SMC3 forming a cohesin complex to pair the sister chromatids together (Gruber et al., 2003). However, the association of SYN1 and SMC proteins in *Arabidopsis* is not well understood. To investigate the distribution of SYN1 and AtSMC3, an *Arabidopsis* SMC3 homolog (Lam et al., 2005), chromosome spread preparations of wild-type PMCs were examined by using anti-AtSMC3 (rat) and anti-SYN1 (rabbit). The immunostaining result showed that both SYN1 and AtSMC3 were first detectable as foci at early leptotene (Figure 4.4A). A substantial proportion of the SYN1 signals co-localized with AtSMC3 as the chromosomes continue to pair and synapse during zygotene/pachytene stages (Figure 4.4B). I observed that SYN1 partially co-localized with AtSMC3 at the pre-synaptic chromosome regions (Figure 4.4C; 4.5). By late pachytene, both proteins appeared as linear signals and colocalized along the entire length of chromosomes (Figure 4.4D).

To further investigate the distribution of SYN1 and another cohesin, wild-type (Col 0) meiocytes were examined by using anti-SYN1 and anti-AtSCC3 (rat), an *Arabidopsis* homologue of yeast SCC3. SCC3 is another yeast cohesin subunit that associates with the cohesin complex (Toth et al., 1999; Nasmyth, 2002). Immunostaining showed that both SYN1 and AtSCC3 proteins appeared as foci at early leptotene (Figure 4.6A), developing into a strong patchy signal on chromosomes during zygotene. At this stage, the colocalization of SYN1 and AtSCC3 was detectable on homologous chromosomes but both proteins were less colocalized on non-synaptic regions (Figure 4.6B). I observed that strong AtSCC3 signals appeared at pre-synaptic regions while SYN1 patchy signals were distributed evenly on

chromosomes (Figure 4.7). Importantly, SYN1 patches appeared not to be in register on synapsed homologous chromosomes during early pachytene (Figure 4.6C; 4.8). As the chromosome condensed further, both SYN1 and AtSCC3 appeared as continuous signals along chromosomes at the end of pachytene (Figure 4.6D). The observation revealed that substantial proportion of the SYN1 signal co-localized with AtSMC3 along the chromosomes during zygotene, while colocalization of SYN1 and AtSCC3 increased during pachytene. It is possible that these observations reflect differences in the dynamics of localization of the proteins. However, I cannot exclude the possibility that the availability of the protein epitopes may have influenced these observations.

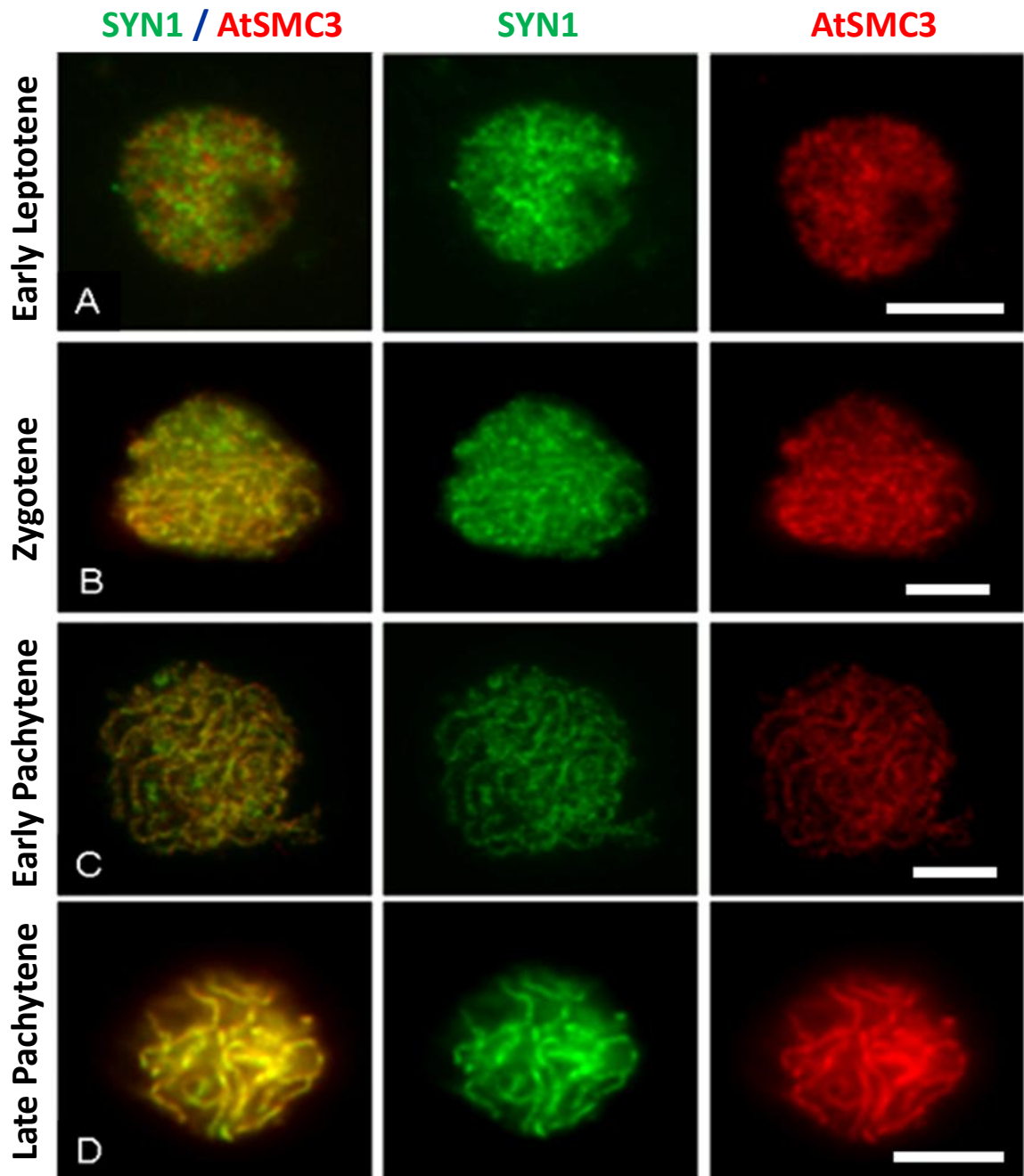


Figure 4.4. Dual immunolocalization of SYN1 (green) and AtSMC3 (red) on meiotic spreads of wild-type *Arabidopsis thaliana*. (A) Leptotene; (B) Zygotene; (C) Early Pachytene; (D) Late Pachytene. Bars 5 μ m.

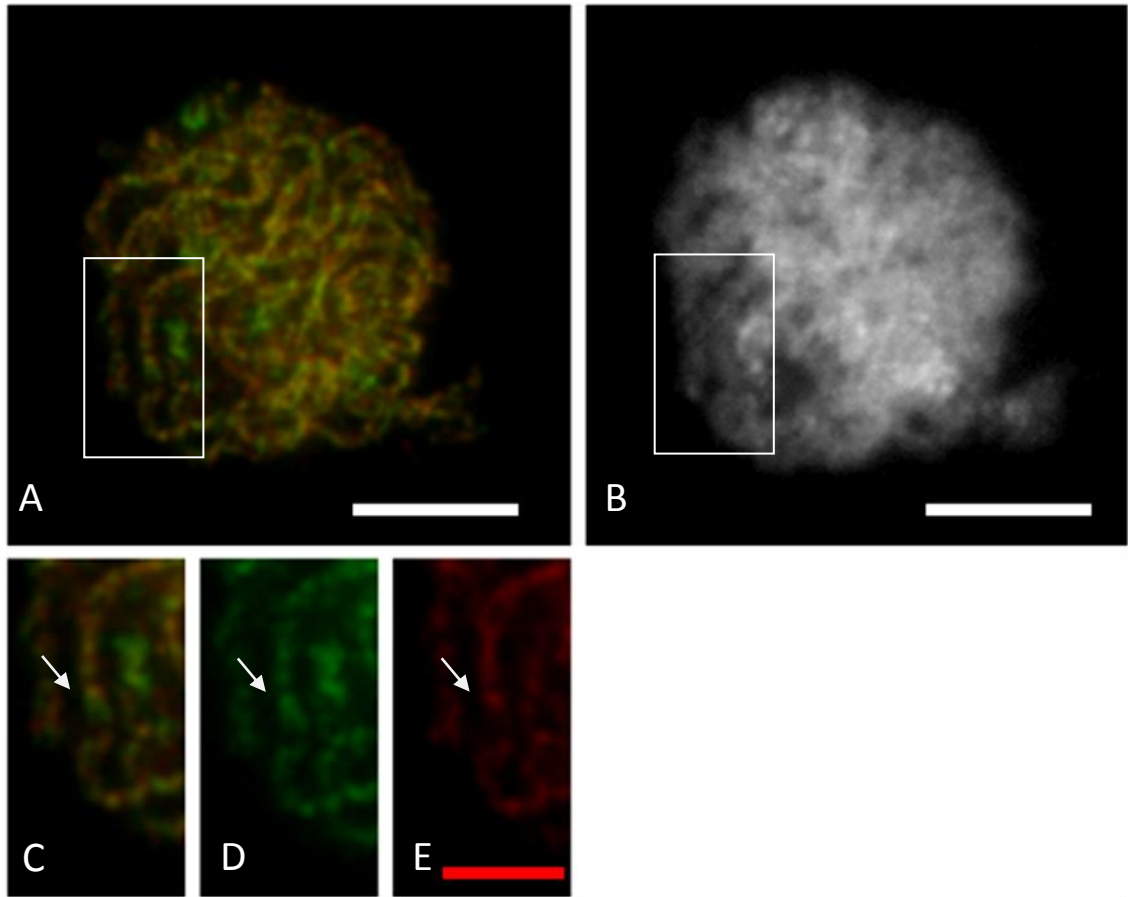


Figure 4.5. Immunolocalization of SYN1 (green) and AtSMC3 (red) on early pachytene cell (A) of wild-type.

(C; D; E) are the same cell of (A) from the boxed area. The results show that a few SYN1 patches do not co-localize with AtSMC3 on the chromosome pre-synaptic region (white arrow). (B) is the same cell as (A) with DAPI staining. White bars 5 μ m; red bar 2.5 μ m.

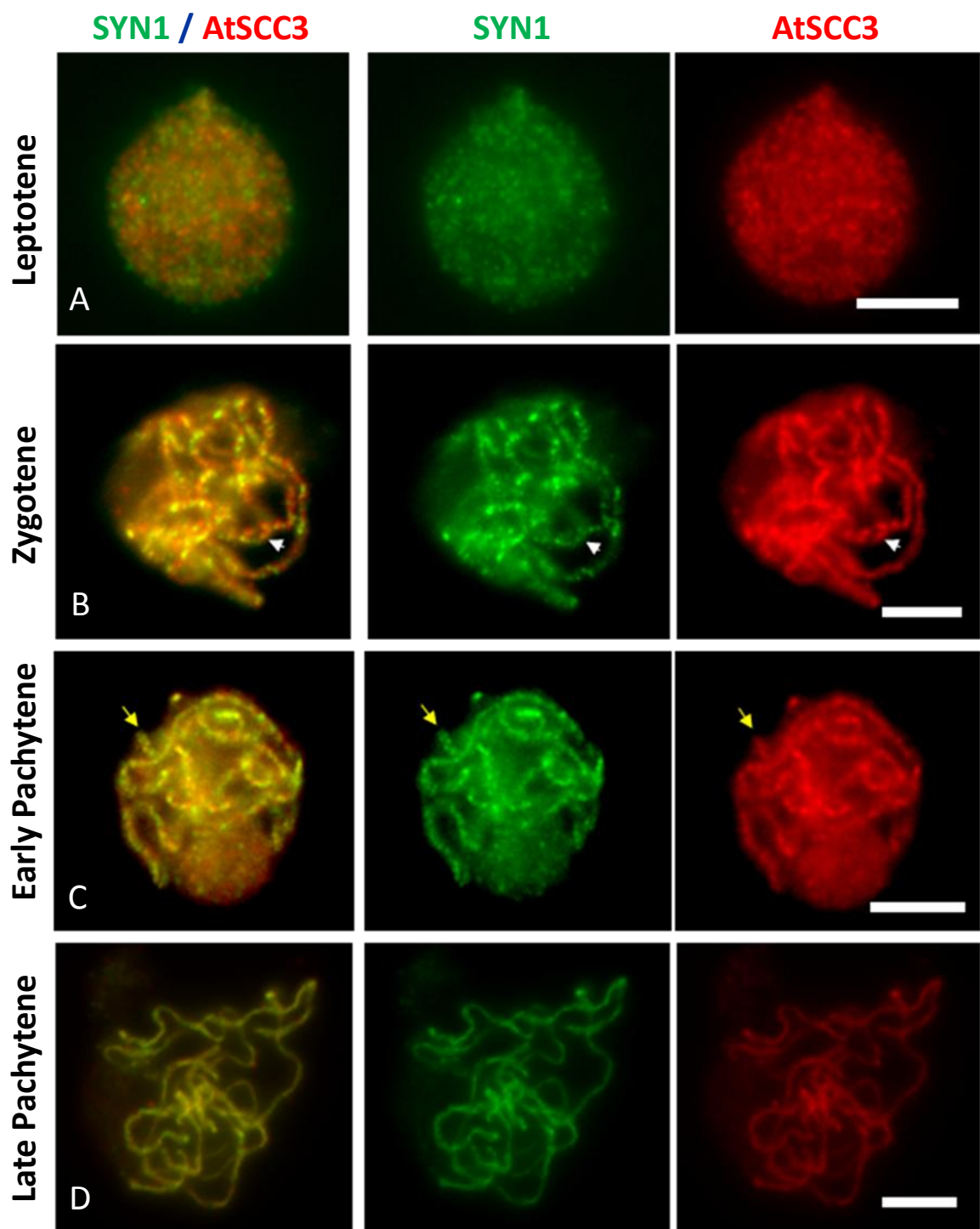


Figure 4.6. Dual immunolocalization of SYN1 (green) and AtSCC3 (red) on meiocytes of wild-type. (A) Leptotene; (B) Zygotene; (C) Early Pachytene; (D) Late Pachytene. Note: Presynaptic region (white arrow) details show in figure 4.7; synapsed homologous chromosome (yellow arrow) details show in figure 4.8. Bars 5 μ m.

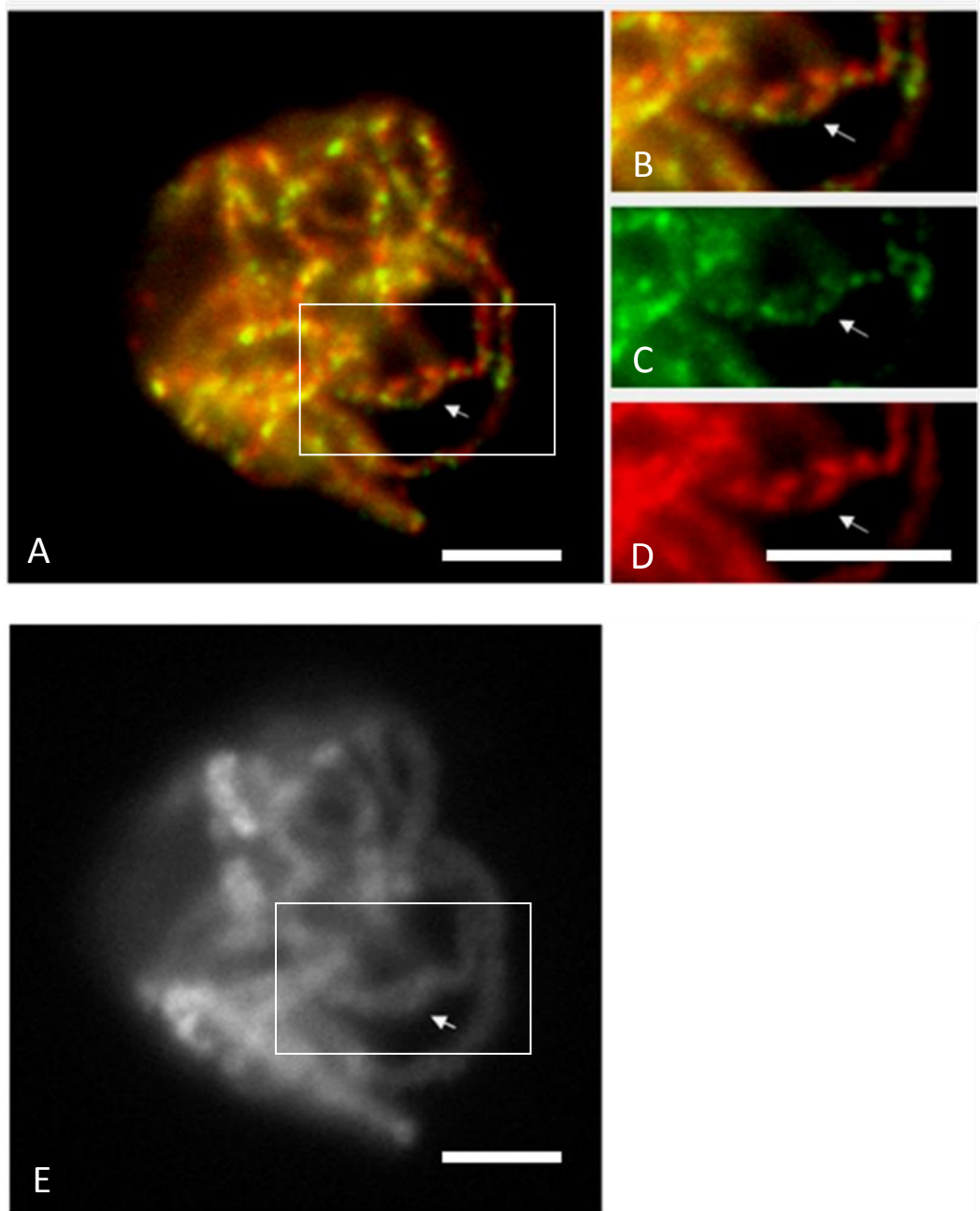


Figure 4.7. Immunolocalization of SYN1 (green) and AtSCC3 (red) on zygote cell (A) of wild-type. (B; C; D) are enlargement of cell (A) from the box area. The results show that the SYN1 and AtSCC3 distribution are not similar in the pre-synaptic region (white arrow). (E) is the same cell of (A) with DAPI staining. Bars 5 μ m.

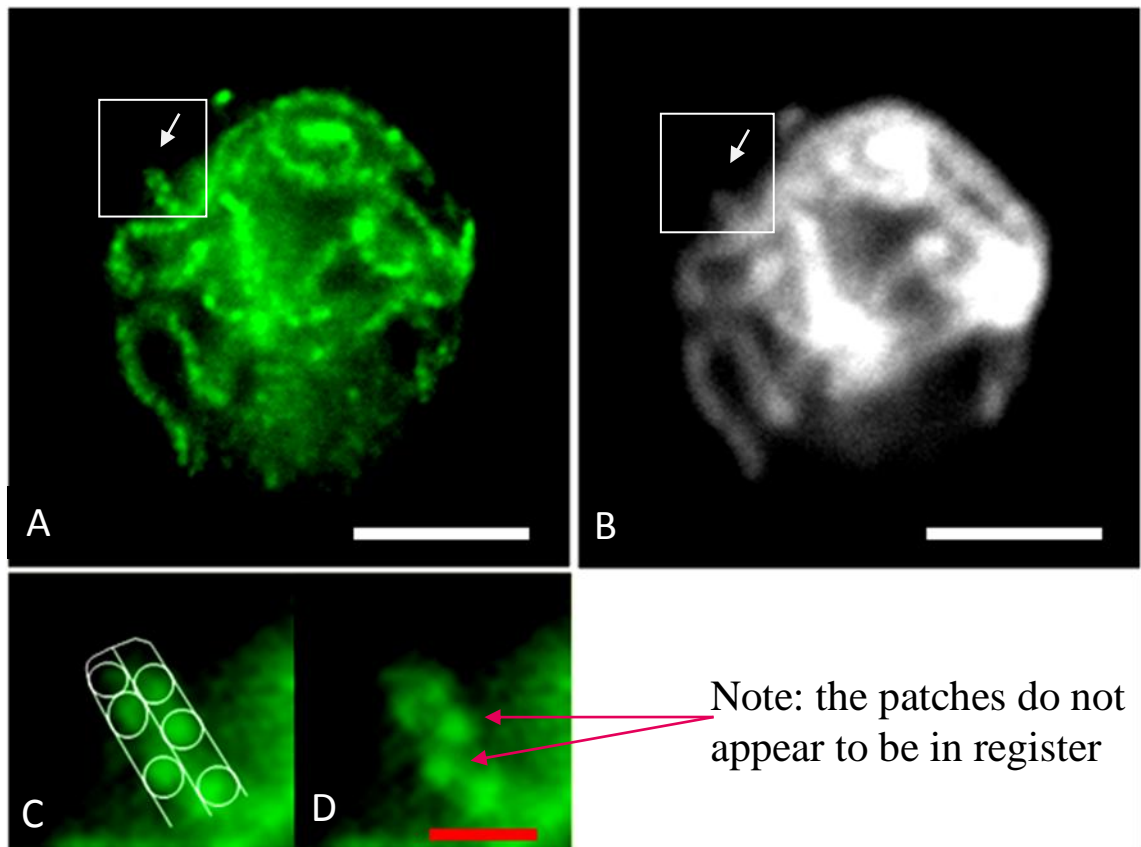


Figure 4.8. Immunolocalization of SYN1 (green) to early pachytene (A) of wild-type. SYN1 patches appear on synapsed homologous chromosome (white arrow). (C; D) are enlargement of cell (A) from the highlighted area, showing that SYN1 patches do not appear to be in register. (B) is the same cell of (A) with DAPI staining. White bars 5 μ m; red bar 1.25 μ m.

4.2.1.3 Immunolocalization of ASY1 and AtSCC3/AtSMC3 on *syn1* meiocytes

I have shown that, in wild-type meiocytes, SYN1 fully colocalized with other cohesins during pachytene. To further investigate the role of SYN1 in the cohesin complex, chromosome spread preparations of *syn1* mutant PMCs were examined by using anti-AtSCC3 (rat) antibody in conjunction with antibody against axis-associated protein, ASY1 (rabbit), to identify the meiotic stages. Immunostaining showed that ASY1 was loaded abnormally throughout meiosis. This protein appeared aggregate in early prophase I (Figure 4.9A), forming into abnormal stretches and short linear signals. By later stages, abnormal thick continuous signals of ASY1 were observed throughout the meiosis of the *syn1* mutant (Figure 4.9B; C). Therefore, it is difficult to identify the early meiotic stages based on the abnormal distribution of ASY1 in *syn1* mutant. Interestingly, cohesin subunit AtSCC3 was not detectable in the *syn1* meiocytes. This result showed that the loading of AtSCC3 on chromosomes was affected severely in the absence of SYN1 protein, suggesting that association of AtSCC3 with the cohesin complex is dependent upon SYN1 during early meiosis I.

To further investigate other cohesins in the *syn1* mutant, meiocytes of *syn1* were examined using antibodies against AtSMC3 (rat) and ASY1 (rabbit). Immunostaining of AtSMC3 revealed that the protein was detectable as foci and fuzzy signals on chromosomes during the early prophase I. This protein appeared to continue developing into fuzzy linear signals which co-localized with ASY1 (Figure 4.10). This observation suggests that the AtSMC3 polymerization was affected by the absence of SYN1. In conclusion, the appearances of AtSCC3 and AtSMC3 were affected severely in the absence of SYN1. This suggests that the meiotic cohesin subunit SYN1 is essential for forming the meiotic cohesin complex.

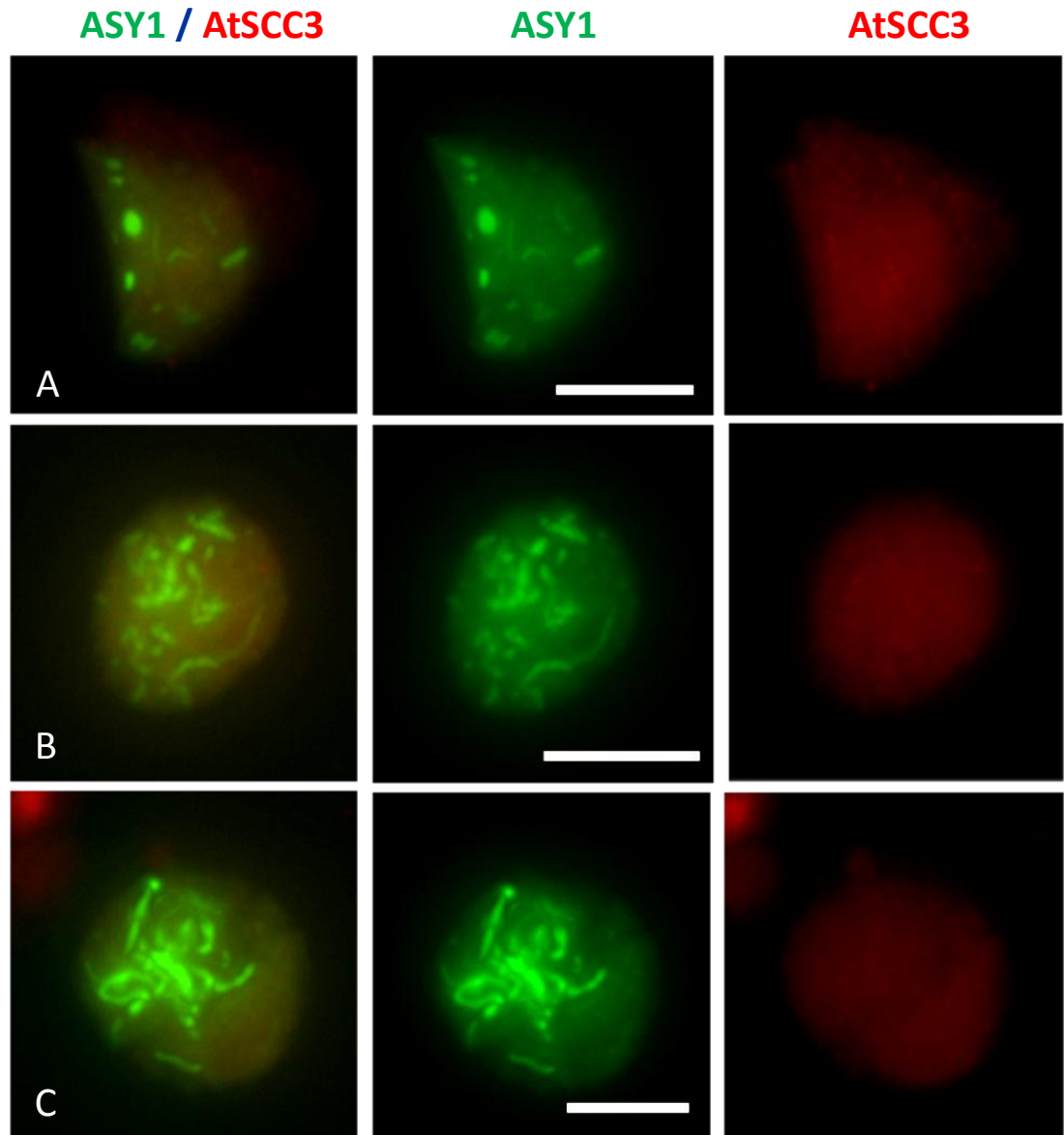


Figure 4.9. Immunolocalization of AtSCC3 (red) and ASY1 (green) to meocytes of *syn1* mutants. ASY1 appears as aggregates in the early meiosis of *syn1* mutant, developing into abnormal linear signals. AtSCC3 is not detectable in meocytes of *syn1* mutant. Bars 5 μ m.

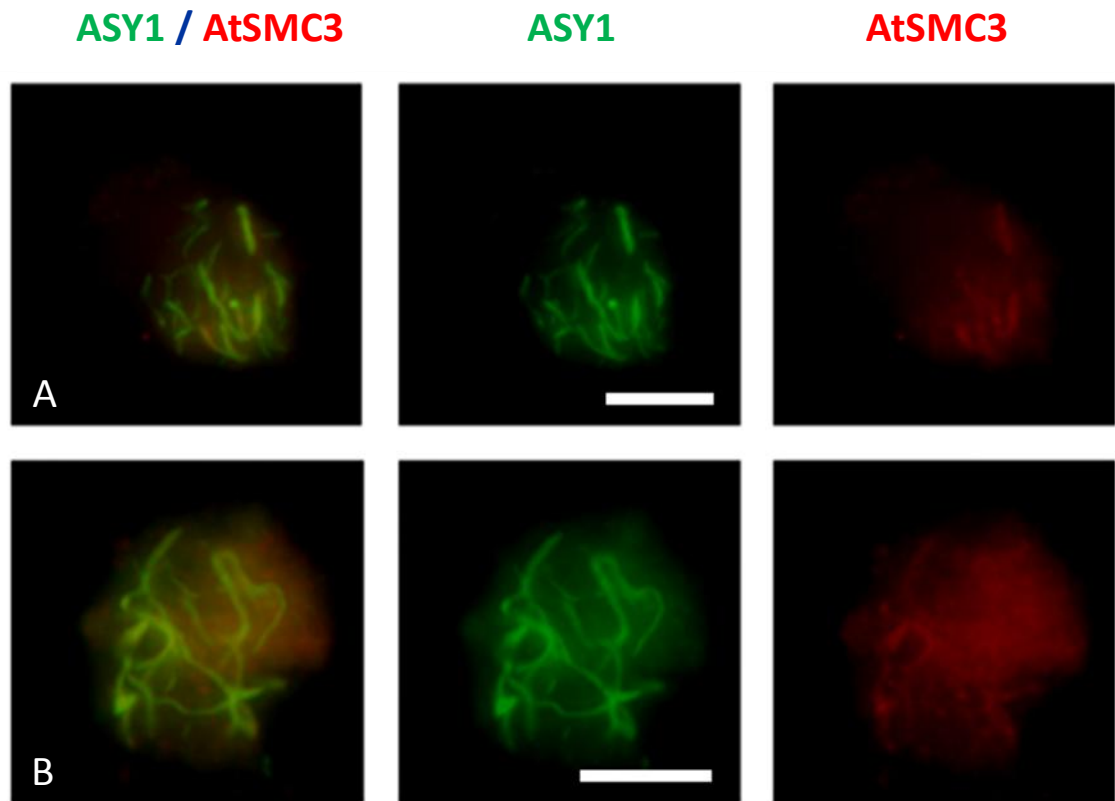


Figure 4.10. Immunolocalization of AtSMC3 (red) and ASY1 (green) on meiocytes of *syn1* mutants. AtSMC3 appears as fuzzy linear signals. These AtSMC3 fuzzy linear signals co-localize with ASY1. Bars 5 μ m.

4.2.1.4 Immunolocalization of SYN1 and AtZYP1 on wild-type (Col 0) and *syn1* meiocytes.

Studies in maize have reported that AFD1/REC8 is a component of the synaptonemal complex (SC) associating with axial and lateral elements at early meiosis I (Golubovskaya et al., 2006). To investigate the distribution of SYN1 and the SC protein AtZYP1, immunolocalization studies were carried out on spread preparations of wild-type pollen mother cells using anti-SYN1 (rabbit) and anti-ZYP1 (rat). Immunostaining revealed that SYN1 was detectable throughout the nucleus at leptotene stage, while AtZYP1 was present at synapsed chromosome regions (Figure 4.11A). During zygotene, AtZYP1 continued to polymerize along the chromosomes to form short linear signals which colocalized only partially with SYN1 patches (Figure 4.11B). I found that two AtZYP1 signals appeared next to a short stretch of AtZYP1 (Figure 4.12; red arrow). This observation suggests that two AtZYP1 signals were first present side by side on the pre-synaptic chromosomal region before forming a strong stretch of AtZYP1 (Figure 4.14; Zone B). During pachytene stage, AtZYP1 appeared as a continuous signal and co-localized with majority of SYN1 running along the chromosome axes (Figure 4.13; curly bracket). I also observed a SYN1-AtZYP1 non-overlapping region, in which two separate SYN1 appeared side by side with AtZYP1 signal (Figure 4.11C and 4.13; white arrow). This observation suggests that a stretch of AtZYP1 forms at the initiating synaptic/premature synaptic region while SYN1 is still not recruited to chromosome core region (Figure 4.14 (Zone C)). AtZYP1 continued to polymerize and colocalized with SYN1 at the mature synapsed region, indicating that the two separate SYN1 signals come together into a single chromosome axis associated signal. This could be a reflection of the formation of synaptonemal complex bringing the homologous chromosomes closer together. Therefore, SYN1 is recruited to the core of chromosomes

(Figure 4.14 (Zone D)).

To further investigate whether SYN1 is a component of the SC, meiocytes of *syn1* were examined using anti-AtZYP1 and anti-SYN1. Immunostaining results showed that AtZYP1 appeared as aggregates in early meiosis I (Figure 4.15A), developing into very short linear signals (Figure 4.15B), while SYN1 signal was not detectable. Continuous signal of AtZYP1 was not seen in the *syn1* meiocytes. The observation revealed that AtZYP1 signal was present at the early meiosis I but the polymerization of SC was affected by the absence of SYN1.

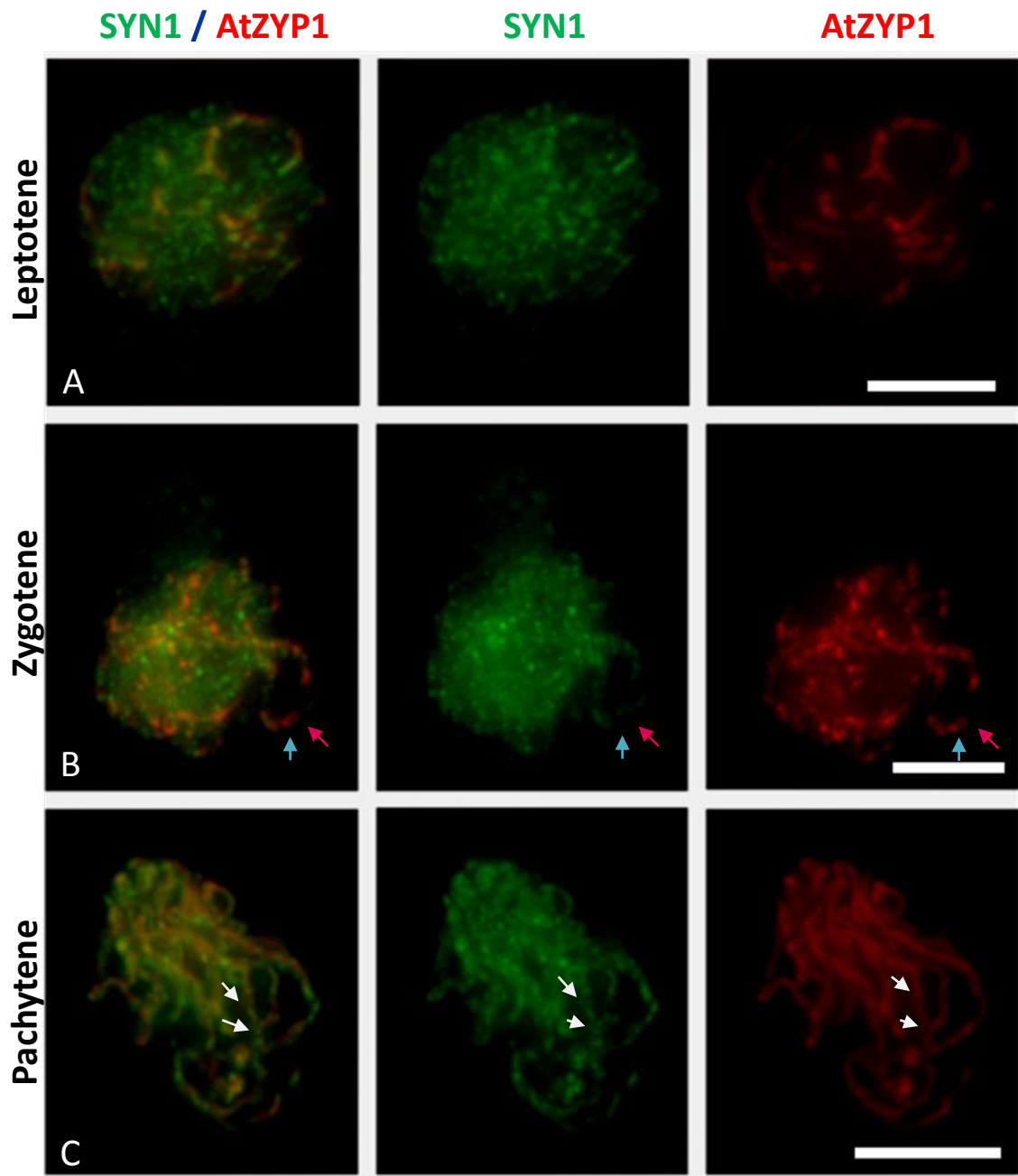


Figure 4.11. Immunolocalization of SYN1 (green) and AtZYP1 (red) on meiocytes of wild-type *Arabidopsis*. (A) AtZYP1 appears at the leptotene stage. (B) Two AtZYP1 foci (red arrow) are detected in the presynaptic region. One strong AtZYP1 signal (blue arrow) is detected in the synaptic region. Detail shown in figure 4.12. (C) At pachytene, AtZYP1 appears as linear signals but two distinct SYN1 signals (white arrow) are detected between AtZYP1. Bars 5 μ m.

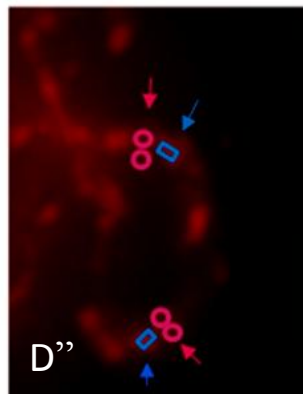
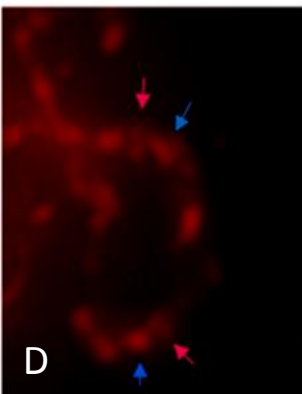
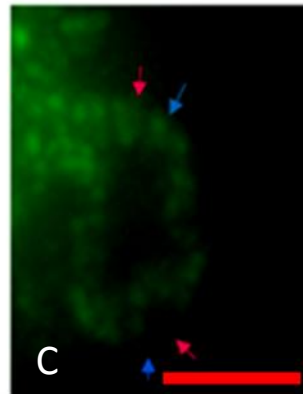
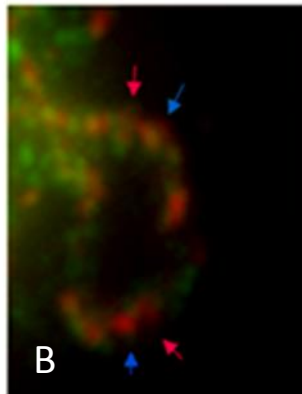
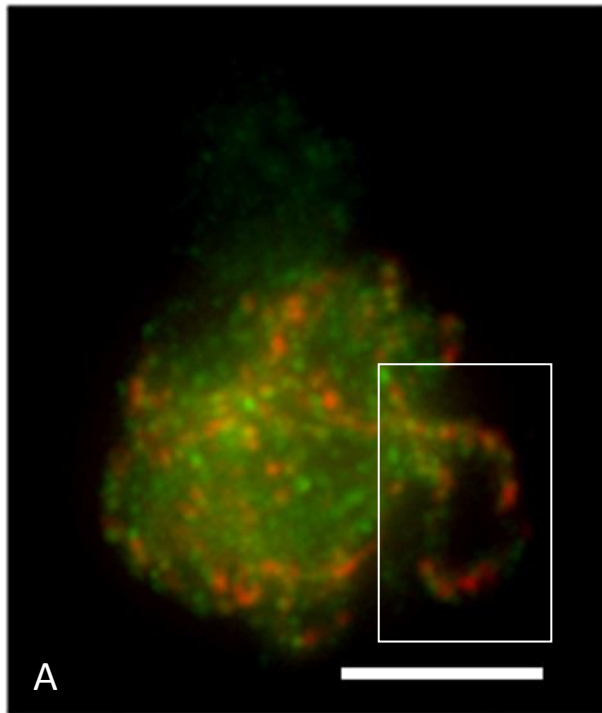


Figure 4.12 Immunolocalization of SYN1 (green) and AtZYP1 (red) to zygotene (A) of wild-type *Arabidopsis*. (B, C, D, D'') are enlargement of (A) from the highlighted area. (B) AtZYP1 signal partially co-localizes with SYN1 some region (blue and red arrows). It shows that AtZYP1 sits in the middle of two SYN1. (C) Two rows of SYN1 are detectable on chromosomes during zygotene, indicating that one row of SYN1 patches appear at one pair of sister chromatids. (D) Two AtZYP1 foci (red arrow) are detected in pre-synaptic region and one strong AtZYP1 signal (blue arrow) is detected in the synapsed region. The AtZYP1 signals (red and blue arrow) partially colocalize with SYN1 (B and C). (D''), an identical picture from (D), is to show that the two AtZYP1 foci (●) appear next to a strong signal or short stretch of AtZYP1 (▣). White bar 5µm; red bar 2.5µm.

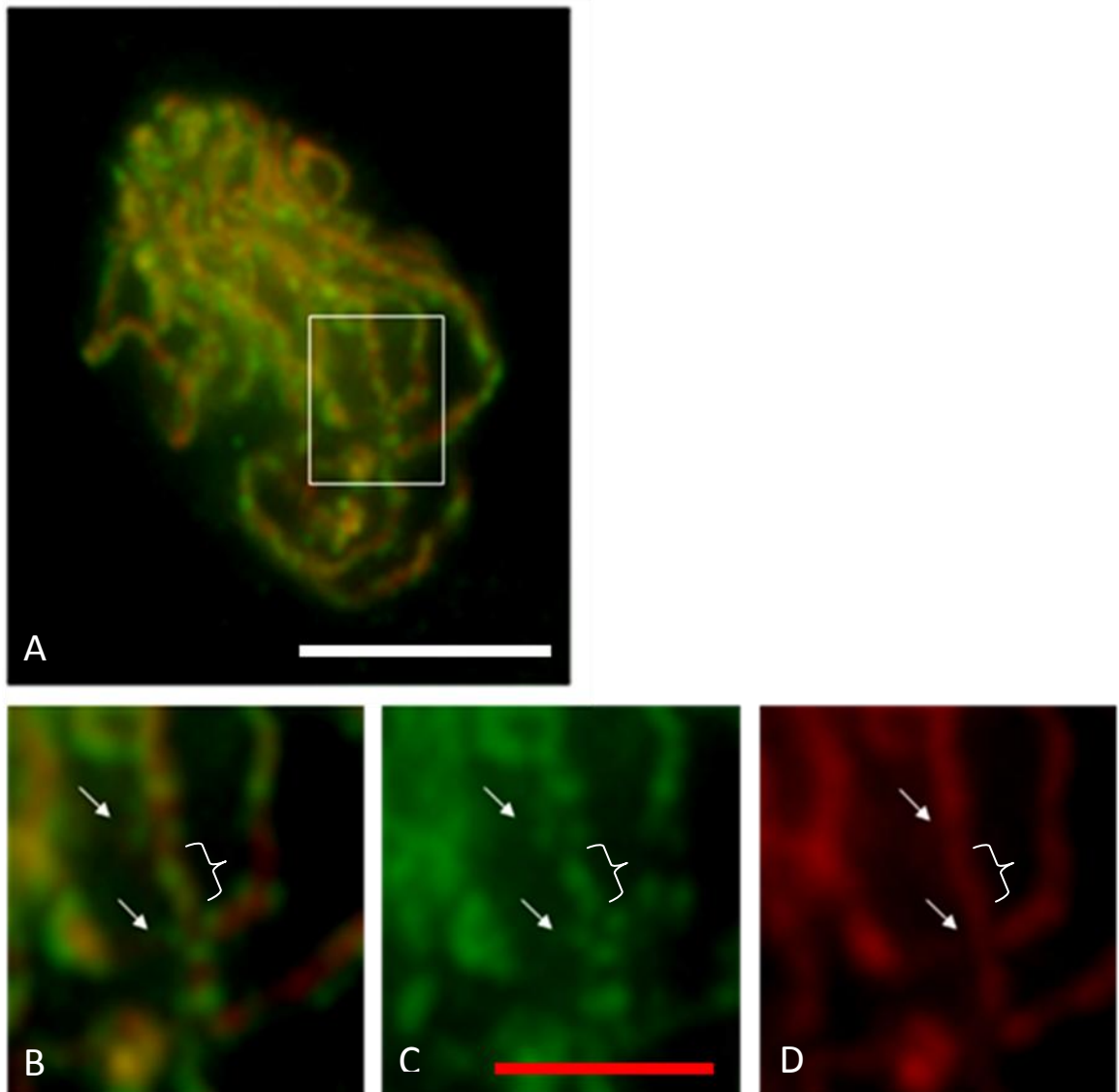


Figure 4.13 Immunolocalization of SYN1 (green) and AtZYP1 (red) to pachytene (A) of wild-type *Arabidopsis*. (B, C, D) are enlargement of (A) from the highlighted area. (B) AtZYP1 signal co-localizes with SYN1 in mature synaptic region (curly brace) but both proteins do not co-localize in initiate/premature synaptic region (arrows). (C, D) show that the AtZYP1 locates in the middle of two SYN1 signals (arrows). White bar 5 μ m; red bar 2.5 μ m.

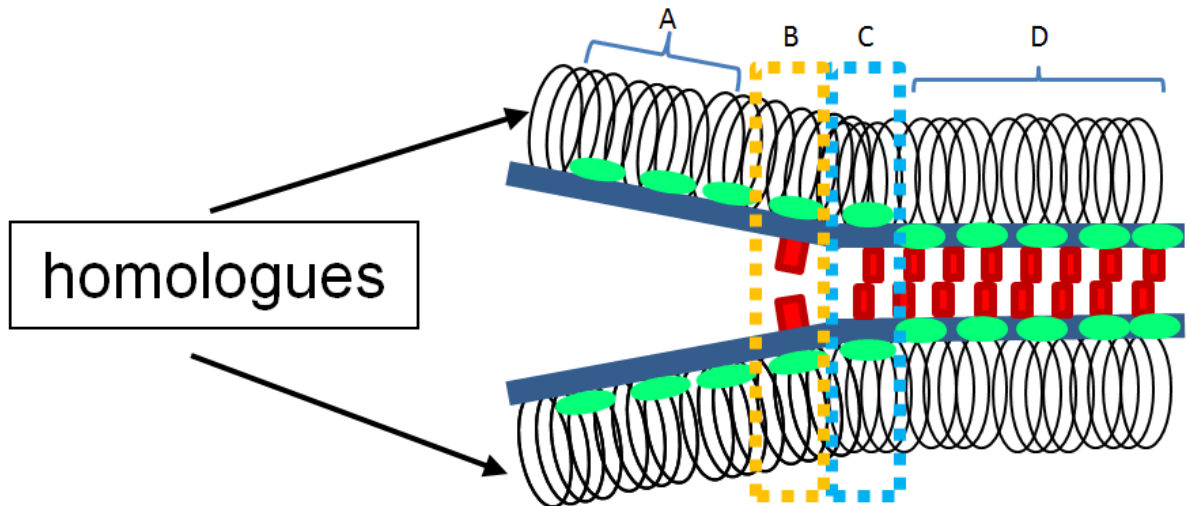


Figure 4.14. A diagram showing the dynamics of SYN1 and AtZYP1 along chromosomes.

Zone A: SYN1 signal (●) is detectable at the non-synaptic chromosomes but not AtZYP1 (■). Note: Chromosome axes (Blue).

Zone B: Two AtZYP1 signals appear at the pre-synaptic chromosome region (detail shown at Figure 4.12; red arrow).

Zone C: Two separate SYN1 appear side by side with an AtZYP1 at initiate synaptic/premature synapsed region (detail shown at Figure 4.11C (white arrow) and 4.12 (blue arrow) and 4.13 (white arrow)).

Zone D (Mature fully synapsed region): AtZYP1 appears as a continuous signal and completely co-localizes with SYN1 running along the chromosome axes.

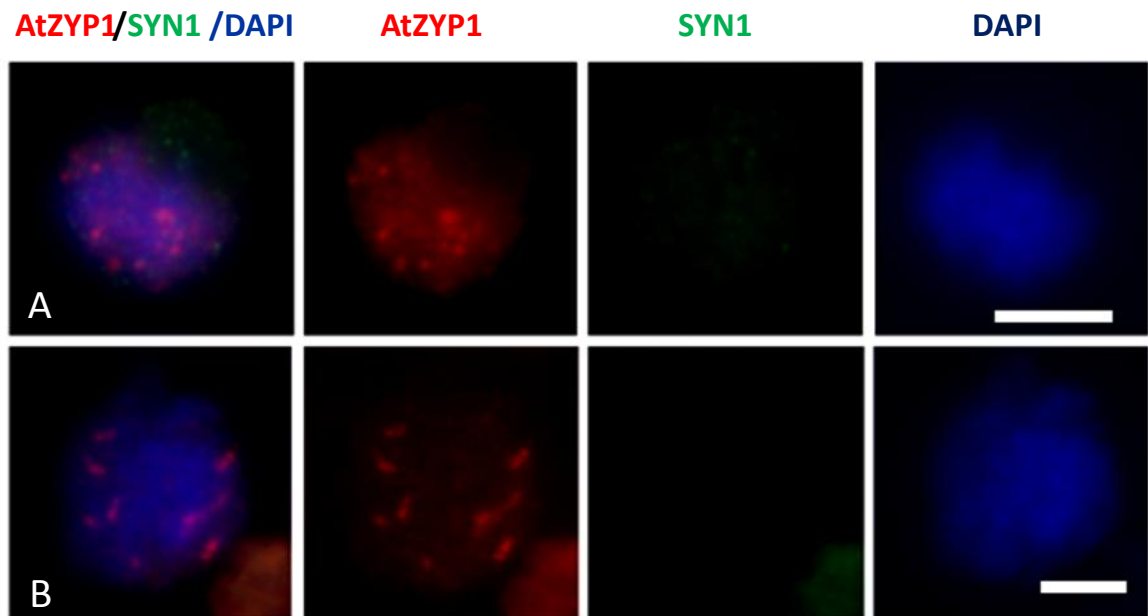


Figure 4.15. Immunolocalization of AtZYP1 (red) and SYN1 (green) on meiocytes of *syn1* mutants. AtZYP1 appears as aggregates (A) at the beginning of SC formation, developing into stretches (B). SYN1 is not detected in meiocytes of the *syn1* mutant. The chromosomes are counterstained with DAPI (blue). Bars 5 μ m.

4.2.1.5 Immunolocalization of AtZYP1 and ASY1 on *syn1* meiocytes.

Immunostaining studies in *syn1* meiocytes revealed that AtZYP1 was present in early prophase I. It is highly possible that the axis-associated protein ASY1 might co-localize with AtZYP1 in the *syn1* mutant. To investigate the distribution of ASY1 and AtZYP1 proteins in more detail, immunolocalization studies were carried out on spread preparations of PMCs from wild-type (Col 0) and the *syn1* mutant. The result, in wild-type (Col 0) as a control, showed that ASY1 and AtZYP1 appeared as a continuous signal running along the chromosome axis during early prophase I (Figure 4.16A). In contrast, the distribution of ASY1 and AtZYP1 along the chromosome was affected in *syn1* meiocytes. Both proteins appeared as aggregates in early prophase I. Interestingly, ASY1 was seen developing into abnormal thick and linear signals, while AtZYP1 appeared as very thick and short linear signals or stretches in the later stages (Figure 4.16B; C). The signals of AtZYP1 either completely or partially co-localized with ASY1 in *syn1* meiocytes. This result showed that both axis formation and synapsis are compromised in the absence of SYN1.

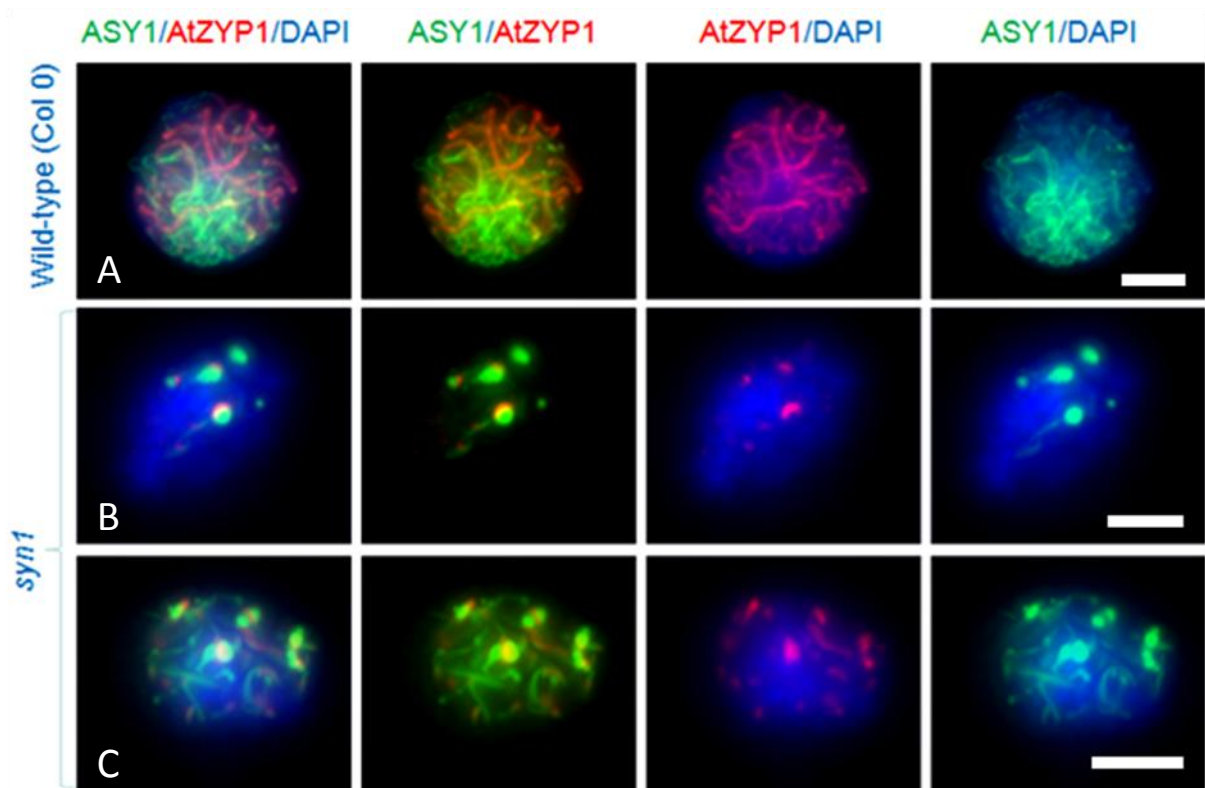


Figure 4.16. Immunolocalization of AtZYP1 (red) and ASY1 (green) to meiocytes of wild-type (A) and *syn1* mutants (B; C). (A) In wild-type, continuous signals of ASY1 and AtZYP1 are detected along homologous chromosome. (B; C) AtZYP1 aggregates co-localize or partially overlap with ASY1 aggregates. Bars 5 μ m.

4.2.1.6 Immunolocalization of AtRAD51 and ASY1 on wild-type (Col 0) and *syn1* meiocytes.

Synapsis is defined by the formation of synaptonemal complex (SC). In yeast and mammals, synapsis requires the formation of DNA double strand breaks (DSBs), which are catalysed by SPO11 protein, to initiate meiotic recombination (Lichten, 2001; Burgess, 2002). The previous immunostaining result showed that the distribution of SC protein, AtZYP1, was abnormal in the *syn1* mutant. This suggests that meiotic recombination might be affected in the absence of SYN1. To investigate how the meiotic recombination proteins behave in *syn1* mutant, antibodies were used against the axis-associated protein ASY1 and recombination protein AtRAD51, an *Arabidopsis* homolog of yeast RAD51 (Doutriaux et al., 1998; Li et al., 2004). AtRAD51 is essential for chromosome pairing, synapsis and the repair of DNA DSBs (Li et al., 2004). Immunostaining in wild-type (Col 0) as a control showed that ASY1 appeared as linear signals along chromosomes while foci of AtRAD51 were widely distributed throughout the nucleus at early prophase I (Figure 4.17A). In contrast, immunolocalization of ASY1 and AtRAD51 showed aberrant distribution in *syn1* meiocytes. Both proteins appeared as aggregates in early prophase I (Figure 4.17B). Interestingly, substantial aggregates of AtRAD51 accumulated around ASY1 (Figure 4.17C). In later stages, ASY1 developed into abnormal linear signals along the chromosomes while AtRAD51 signals reduced significantly (Figure 4.17D). This data showed that AtRAD51 foci were not widely present along the homologous chromosomes of *syn1* mutant, suggesting that the chromosome pairing, synapsis and DSB repair are disturbed by the loss of SYN1.

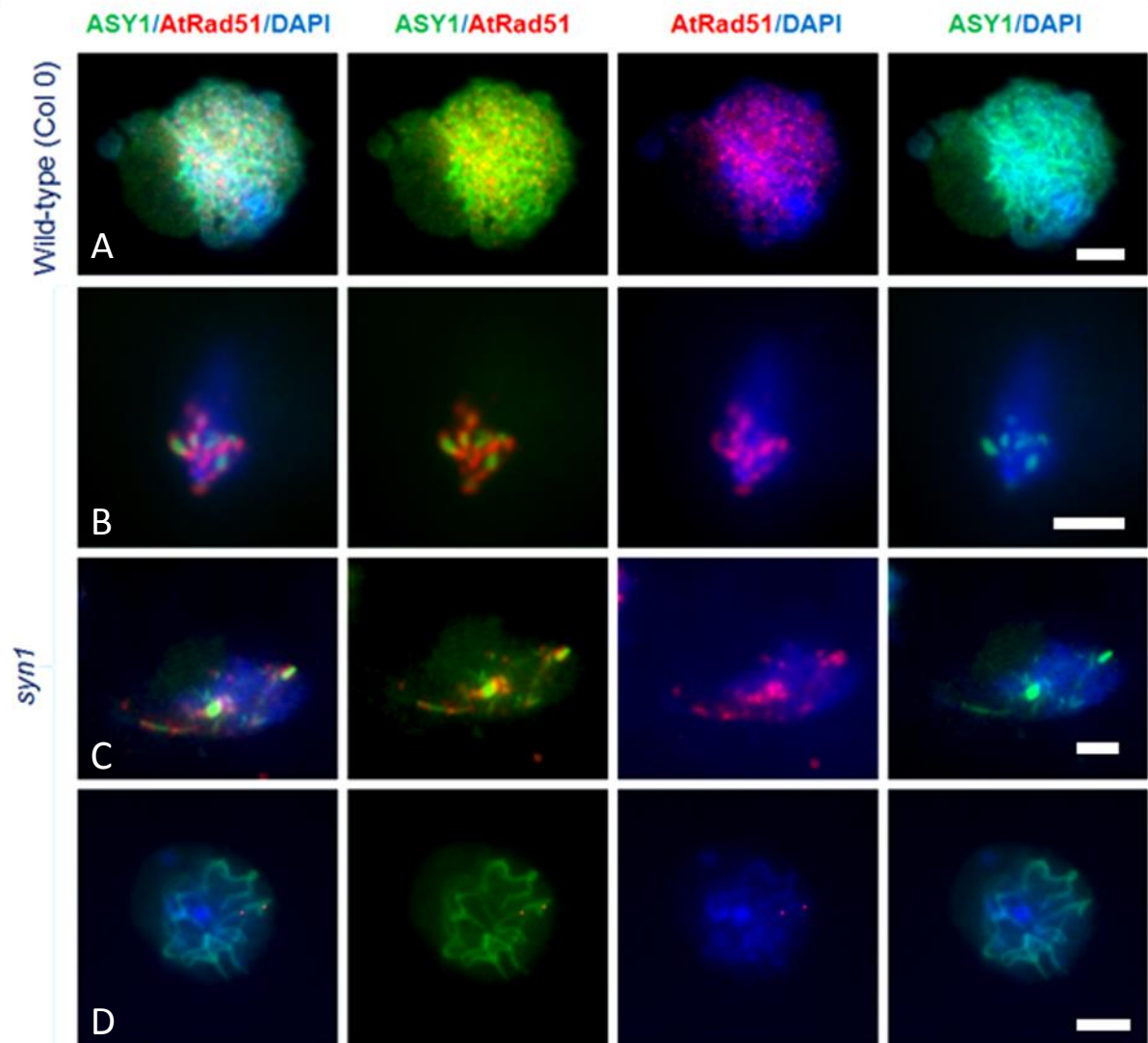


Figure 4.17. Immunolocalization of AtRAD51 (red) and ASY1 (green) to meocytes of wild-type (A) and *syn1* mutant (B; C; D). (A) In wild-type, AtRAD51 foci distribute evenly on linear ASY1 signals. (B; C) In *syn1* mutant, substantial AtRAD51 aggregates are found around ASY1. (D) Few AtRAD51 foci appear on linear ASY1. Bars 5 μ m.

4.2.1.7 Immunolocalization of AtMLH1 and ASY1 on wild-type (Col 0) and *syn1* meiocytes

The immunolocalization result showed that the distribution of AtRAD51 was affected by the absence of SYN1. To investigate the impact of loss of SYN1 on recombination in more detail, immunolocalization was carried out using antibodies against ASY1 and the recombination proteins AtMLH1, an *Arabidopsis* homologue of the *E. coli* MutL (Jean et al., 1999). In yeast, MLH1 acts as a heterodimer with MLH3, which plays an important role in crossovers of meocytes (Wang et al., 1999). In *Arabidopsis*, AtMLH1, in wild-type meocytes, colocalizes with AtMLH3 at pachytene. The number of foci is ~10 which is close to the number of COs. AtMLH1 is found abnormally in the nucleolus of the *Atmlh3* mutant. Analysis of chiasma frequency reveals an approximately 60% reduction in crossovers occurs in the absence of AtMLH3 (Jackson et al., 2006), suggesting that AtMLH1 and AtMLH3 play an important role in meiotic crossing over. Immunostaining studies in wild-type meocytes showed that both ASY1 and AtMLH1 proteins were detectable in early prophase I. ASY1 appeared as linear signals, while AtMLH1 foci were widely distributed in the nucleus of zygotene cell (Figure 4.18A). In contrast to wild-type, immunostaining of AtMLH1 showed abnormal distribution on ASY1 in meocytes of *syn1* mutant. AtMLH1 appeared as aggregates throughout meiosis I. The majority of AtMLH1 signals co-localized with the ASY1 aggregates (Figure 4.18B). After ASY1 elongation, substantial AtMLH1 signal still remained on the ASY1 aggregates (Figure 4.18C; D). This result revealed that the distribution of the recombination protein AtMLH1 was affected in *syn1* mutant.

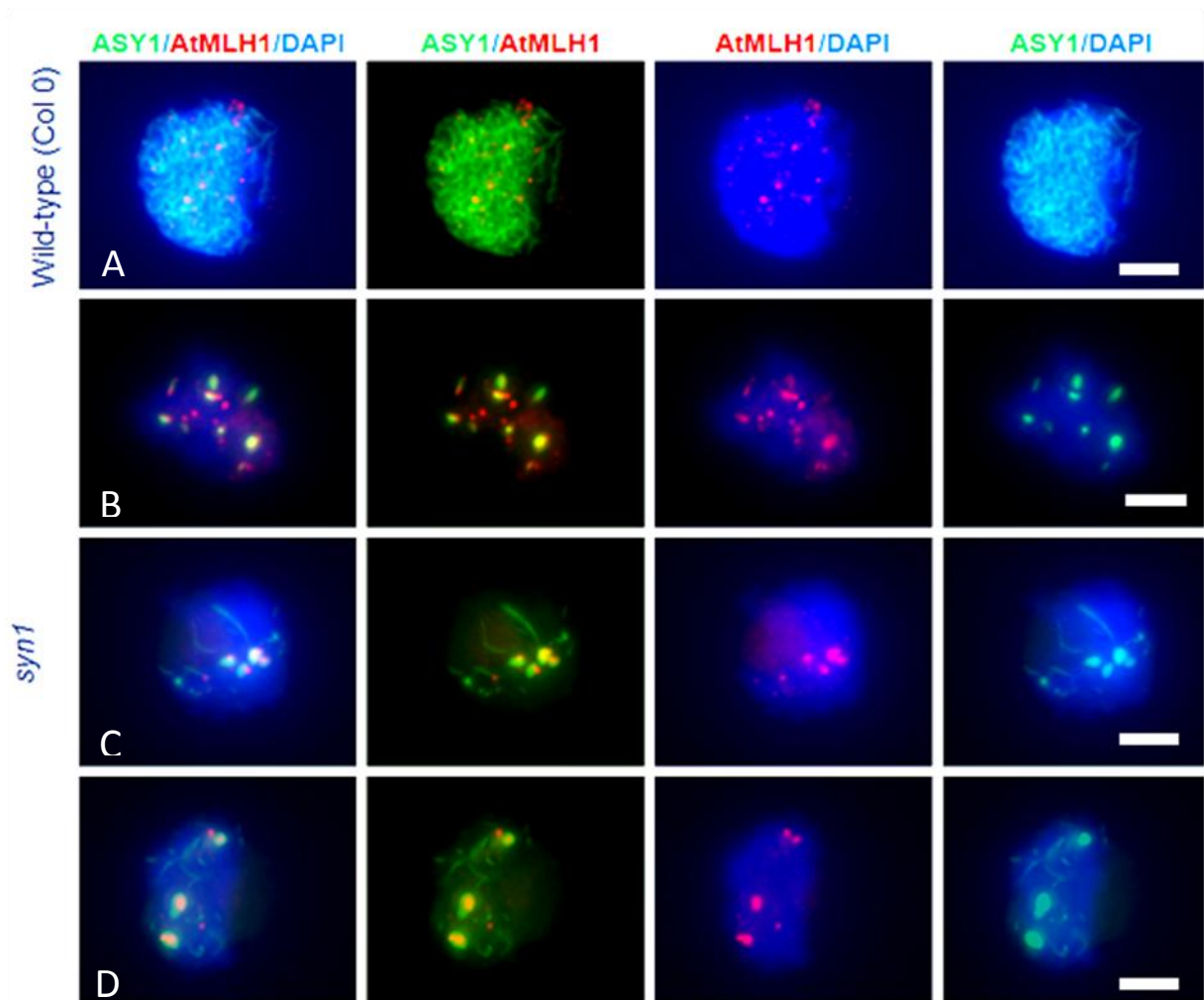


Figure 4.18. Immunolocalization of AtMLH1 (red) and ASY1 (green) to meiocytes of wild-type (A) and *syn1* mutant (B; C; D). (A) In wild-type, AtMLH1 distributes evenly on linear ASY1. (B; C; D) In *syn1* mutant, the majority of AtMLH1 aggregates co-localize with ASY1 aggregates. Bars 5 μ m.

Table 4.1 Immunolocalization of various antibodies in meiocytes of wild-type and *syn1* mutant.

Antibodies Meiocytes	Anti-SYN1	Anti-ASY1	Anti-AtSMC3	Anti-AtSCC3	Anti-AtZYP1	Anti-AtRAD51	Anti-AtMLH1
Wild- type (Col 0)	√	√	√	√	√	√	√
<i>syn1</i> mutant	X	√*	√*	X	√*	√*	√*

Note: √: protein signal appears normal in meiocytes

√*: protein signal appears abnormal in meiocytes

X: protein signal is not detectable in meiocytes

4.3 Discussion

To study the distribution of SYN1 in early meiosis, I raised an anti-SYN1 antibody against the central region of SYN1 (amino acid 207 to 384). This central region was chosen due to lack of similarity to kleisins SYN2, SYN3 and SYN4 which are involved in cohesion during mitosis (Dong et al., 2001; Jiang et al., 2007; Schubert et al., 2009). The immunocytological analysis of SYN1 showed that SYN1 appeared in meiocytes but not in mitotic cells. Furthermore, SYN1 signals were not detected in the *syn1* mutant (Table 4.1). This result indicates that this antibody is specific for the meiotic cohesin SYN1.

4.3.1 Are SYN1 patches localized to the sites of DNA double strand break?

A previous immunolocalization report has suggested that SYN1 appears on chromosome arms but not at the centromere during meiotic prophase I (Cai et al., 2003). Immunostaining of SYN1 revealed that the protein appeared as foci in early meiosis, forming into a more linear, yet patchy pattern during zygotene. Continuous signals of SYN1 were detectable during late pachytene. It is difficult to see any gap in SYN1 linear signals, suggesting that SYN1 could be also located in the centromeres.

A recent report in maize has shown that AFD1/REC8 protein appears as foci in early meiosis, developing into discontinuous short stretches and spots with varying intensities (Wang et al., 2009). A similar result was seen in *Arabidopsis*; SYN1 appeared as foci in early meiosis, forming patches during zygotene stage. These patches did not appear to be in register. Studies in yeast mitotic cells have shown that cohesin is recruited to DNA double-strand break sites (Strom et al., 2004; Lowndes and Toh, 2005). Furthermore, the meiotic kleisin subunit REC8 is expressed in human tumour cells after gamma irradiation (Erenpreisa

et al., 2009). It is possible that SYN1 might have a role during DNA DSB. Therefore, I suggest that SYN1 might accumulate on the site of DNA double-strand break forming a domain or patchy signal.

4.3.2 Localization of AtSCC3 and AtSMC3 along meiotic chromosomes is dependent upon SYN1.

In yeast meiocytes, the cohesion of sister chromatids is essential for chromosome segregation during anaphase I. This cohesion is established by cohesins which include SMC1, SMC3, SCC3 and REC8 proteins (Gruber et al., 2003). In *Arabidopsis*, immunostaining of SYN1 and AtSMC3 revealed that the proteins appeared as foci in early leptotene. SYN1 and AtSMC3 colocalization on meiotic chromosomes increased during zygotene and pachytene. I suggest that SYN1 replaces the mitotic kleisin subunit SYN2 and SYN4 to associate with SMC proteins. Therefore, substantial SYN1 signal is colocalized with SMC3 during zygotene and pachytene. Data from yeast showed that most SCC1/RAD21 is replaced by REC8 during pre-meiotic DNA replication (Klein et al., 1999; Gruber et al., 2003). However, few SCC1 signals are still detectable in pachytene cells (Klein et al., 1999). Currently, we do not have SYN2 and SYN4 antibodies to examine the appearance of mitotic kleisin cohesins in early meiosis.

Few publications are available for cohesin subunit SCC3. It has been reported that yeast SCC3 binds to the COOH-terminal half of SCC1 (Nasmyth, 2002). This binding probably is to stabilize the cohesin complex throughout mitotic cells. In *Arabidopsis*, a recent report showed that AtSCC3 is involved in both mitotic and meiotic divisions (Chelysheva et al., 2005). Unfortunately, the co-localization of AtSCC3 and kleisin subunits, SYN1, SYN2 and

SYN4, is not understood. I have used antibodies against AtSCC3 and SYN1 in chromosome spreads of wild-type meiocytes. The immunostaining result showed that a small amount of SYN1 and AtSCC3 co-localized on the pre-synaptic chromosome region. During pachytene, colocalization of SYN1 and AtSCC3 proteins increased rapidly along the full length of chromosomes. These observations reflect differences in the dynamics of localization of the proteins. However, I showed that AtSCC3 was not observed in *syn1* meiocytes. This result revealed that AtSCC3 loading on chromosomes is dependent upon SYN1. In contrast, fuzzy AtSMC3 signals were found in *syn1* meiocytes. I suggest that AtSMC3 appears on chromosome before SYN1. However, the SMC proteins could not form a stable cohesin complex in the absence of SYN1. As a consequence, abnormal loose chromatin structures appear at early meiosis.

4.3.3 Formation of the synaptonemal complex is disrupted in a *syn1* mutant

A report in rat revealed that REC8 appears on chromosomes and forms axial-element structures (REC8-AEs) during premeiotic S-phase. It has been suggested that REC8 provides a platform for the axial element assembly without requiring SMC1, SMC3, SCP2 and SCP3 (Eijpe et al., 2003). Interestingly, immunostaining of SYN1 and ASY1, an axis-associated protein required for synapsis and crossover formation, in wild-type showed that SYN1 appeared as patches running along ASY1 linear signals at zygotene. By late pachytene, SYN1 co-localized with ASY1 along the chromosomes. This result did not show that SYN1 provides a basis for axis-associated protein assembly. In maize *afd1/rec8* mutant, stretches and short lines of ASY1 are observed during meiosis. It has been suggested that AFD1/REC8 is required for controlling the ASY1 elongation during early meiosis (Golubovskaya et al., 2006). However, ASY1 in the *syn1* mutant appeared as an aggregate in early meiosis,

developing into abnormal linear signals in later stages. This result showed that SYN1 does not affect the localization and normal elongation of ASY1. Therefore, I suggest that SYN1 is required for maintenance of axis-associated protein on chromosomes during axial-element assembly and formation.

Once the axis-associated proteins on chromosomes are stabilized by SYN1, the synaptonemal complex (SC) protein AtZYP1 is loaded on the axial elements of the homologous chromosomes. I have detected two AtZYP1 signals side by side in the pre-synaptic region, developing into one patchy signal which was surrounded by two regions of SYN1. Finally, AtZYP1 co-localized with SYN1 at the synaptic site. It has been suggested that cohesins are essential for the formation of the synaptonemal complex (Klein et al., 1999; Eijpe et al., 2000; Peltari et al., 2001). Interestingly, AtZYP1 appeared as aggregates and short stretches in *syn1* meiocytes. I suggest that SYN1 is not essential for the formation of SC but is required for SC polymerization and elongation. In conclusion, the distribution of both ASY1 and AtZYP1 proteins was abnormal in the *syn1* mutant. This indicates that both axis formation and synapsis are compromised in the absence of SYN1.

4.3.4 SYN1 is essential for meiotic recombination progression in *Arabidopsis*

Our immunostaining of AtZYP1 showed that the protein appeared as aggregates in the *syn1* mutant and co-localized with ASY1 aggregates during early prophase I. Recently, transmission electron microscopy (TEM) analysis showed that abnormal short stretches of SC and polycomplex structures associated with chromatin are detected in *syn1* mutant (Zhao et al., 2006). Clearly, this report is entirely consistent with our finding.

According to a previous report, it was suggested that ASY1 plays an important role in coordinating the activity of the meiotic recombinase, AtDMC1, to promote interhomologue recombination (Sanchez-Moran et al., 2007). I believe that abnormal ASY1 in *syn1* might affect the distribution of recombination proteins. Our data showed aberrant distribution of meiotic recombination proteins, AtRAD51 and AtMLH1, in the *syn1* meiocytes. AtRAD51, an *Arabidopsis* protein that is required for synapsis and DNA DSB repair (Doutriaux et al., 1998; Li et al., 2004), appeared as aggregates and accumulated around ASY1. This indicates that DSB repair was disrupted in the *syn1* mutant. A similar result was seen in maize; RAD51 aggregates were observed in the absence of AFD1/REC8 (Golubovskaya et al., 2006). Another recombination protein, AtMLH1, an *Arabidopsis* protein which localizes to late recombination nodules at late pachytene and marks crossover sites (Franklin et al., 2006; Jackson et al., 2006), appeared as aggregates and co-localized with ASY1 aggregates. This observation suggests that both AtRAD51 and AtMLH1 proteins co-localize as large aggregates together with ASY1, indicating that the processes of meiotic recombination are affected in the absence of SYN1. As a consequence, this can lead to chromosome fragmentation. I suggest that SYN1 is essential for meiotic recombination progression and DSB repair.

Chapter 5

An additional role for SYN1

5.1 Introduction

The initial event of meiotic recombination is triggered by the induction of DSBs by the protein SPO11 (Keeney et al., 1997). The DSBs are resected from the 5' to 3' end by the recombination proteins RAD50 and MRE11 (Smith and Nicolas, 1998). A complex of recombination proteins containing two RecA homologs RAD51 and DMC1 binds to single-stranded DNA ends created by RAD50 and MRE11, forming a nucleoprotein filament (Bishop, 1994). This filament invades homologous chromosome DNA. This process is called single-strand invasion. RAD51 is also required for DNA double strand break repair. Recently, two *Arabidopsis RAD51* paralogous genes, *AtXRCC3* and *AtRAD51C*, have been reported to be involved in meiotic recombination and DSB repair (Bleuyard et al., 2004a; Li et al., 2005). In the absence of several meiotic recombination proteins, DNA DSBs are not repaired. As a result, chromosome fragmentation is observed in *Atxrcc3* and *Atrad51c* mutants. Interestingly, chromosome fragmentation is also found in the absence of cohesin proteins including maize *afd1*, *Sordaria sm-rec8*, mouse *rec8*, *Arabidopsis syn1*, worm *rec8* and rice OsRAD21-4 depletion line (Bai et al., 1999; Bhatt et al., 1999; Yu and Dawe, 2000; Pasierbek et al., 2001; Xu et al., 2005; Zhang et al., 2006; Storlazzi et al., 2008).

Recent studies in yeast cells have shown that mitotic cohesin accumulates at DNA double strand break (DSB) sites where it might facilitate DSB repair (Lowndes and Toh, 2005; Kugou et al., 2009), but the association of SYN1 and DSB site has not been reported. To investigate whether SYN1 plays an important role during DNA double-strand breaks, three

double gene knockout mutants were constructed, *syn1*^{-/-} x *Atspo11-1-4*^{-/-}; *syn1*^{-/-} x *Atdmc1*^{-/-} and *syn1*^{-/-} x *Atrad51c*^{-/-}. The double knockout plants were identified by using PCR to determine the T-DNA insertion sites. Cytological studies conducted on male meiocytes in wild-type (Col 0), mutants and double knockout mutants using chromosome spread preparations stained with 4,6-diamidino-2-phenylindole (DAPI). The cytological analyses of wild-type and *syn1*^{-/-} have been reported in chapter 3. In this chapter, the data from three mutants, *Atspo11-1-4*^{-/-}; *Atdmc1*^{-/-}; *Atrad51c*^{-/-}; and three double gene knockout mutants, *syn1*^{-/-} x *Atspo11-1-4*^{-/-}; *syn1*^{-/-} x *Atdmc1*^{-/-} and *syn1*^{-/-} x *Atrad51c*^{-/-} are presented. To further investigate whether SYN1 is recruited at the DSB sites, I analysed the distribution of SYN1 in *Atspo11-1-4*^{-/-}. In addition, the DSB induction using cisplatin was carried out in meiocytes of *Atspo11-1-4*^{-/-} and *syn1*^{-/-} to examine the role of the SYN1 protein during DNA DSBs.

5.2 Results

5.2.1 Cytogenetic analysis of *syn1*^{-/-} and *Atspo11-1-4*^{-/-} double knockout mutant

To determine the basis of chromosome fragmentation in the *syn1* mutant, I constructed a double knockout mutant of *SYN1* and *AtSPO11-1* genes. AtSPO11-1 is one of the three SPO11 paralogues in *Arabidopsis* that in conjunction with AtSPO11-2 induces DSBs to initiate meiotic recombination (Grelon et al., 2001; Stacey et al., 2006). A previous report (Chelysheva et al., 2005) showed that there is no chromosome fragmentation in the meiocytes of a double gene knockout of *syn1*^{-/-}/*Atspo11-1-1*^{-/-}, but little information was provided regarding early meiotic prophase 1. Recent evidence showed that a few bivalents are found in an *Atspo11-1-1* mutant (Grelon et al., 2001; Chelysheva et al., 2005). This suggested that *Atspo11-1-1* plants are able to produce a truncated SPO11-1 protein which is partly functional (Sanchez-Moran et al., 2007), which led to search for another mutant. A T-DNA insertion line

(WiscDsLox461-464J19) was obtained from the NASC stock. The T-DNA insertion locates in Exon 14 of the *AtSPO11-1* gene (At3g13170). It has been confirmed that the T-DNA insertion line (WiscDsLox461-464J19) is a null mutant (PhD thesis of Nicola Robert at The University of Birmingham UK., 2009). The WiscDsLox461-464J19 line referred to as *Atspo11-1-4^{-/-}*. A *syn1^{-/-}* and *Atspo11-1-4^{-/-}* double knockout mutant was constructed for analysis.

Cytological analysis of *Atspo11-1-4^{-/-}* showed normal thin thread-like chromosomes at early prophase I (Figure 5.1A). Short univalents were observed during chromosome condensation at a diakinesis-like stage (Figure 5.1B). At metaphase I, 10 univalents were aligned at the equatorial plate for the first meiotic division (Figure 5.1C). At anaphase I, the 10 univalents moved randomly to the poles (Figure 5.1D). At anaphase II, the sister chromatids were pulled apart and sister chromosomes moved toward the opposite poles (Figure 5.1E).

In the *syn1^{-/-} / Atspo11-1-4^{-/-}* double knockout mutant, loose and tangled chromosome structures appeared in early prophase I (Figure 5.2A). Upon further condensation, the chromosomes appeared phenotypically similar to that of *Atspo11-1-4^{-/-}* at a diakinesis-like stage (Figure 5.1B; 5.2B). At metaphase I, ten univalents were aligned at the centre of each meiocyte in readiness for the first meiotic division (Figure 5.2C). The sister chromatids of each pair were pulled apart to opposite pole of the cell at anaphase I. A total of 20 separated sister chromatids per meiocyte were observed during the end of first meiotic division (Figure 5.2D; E). There was no evidence of fragmentation and each pole contained 10 sister chromatids. During second meiotic division, the sister chromatids are randomly segregated. This result showed that the *Atspo11-1-4^{-/-}* mutation suppressed the chromosome fragmentation phenotype of *syn1^{-/-}* plants, indicating that the chromosome fragmentation in *syn1^{-/-}* is

AtSPO11-1-dependent.

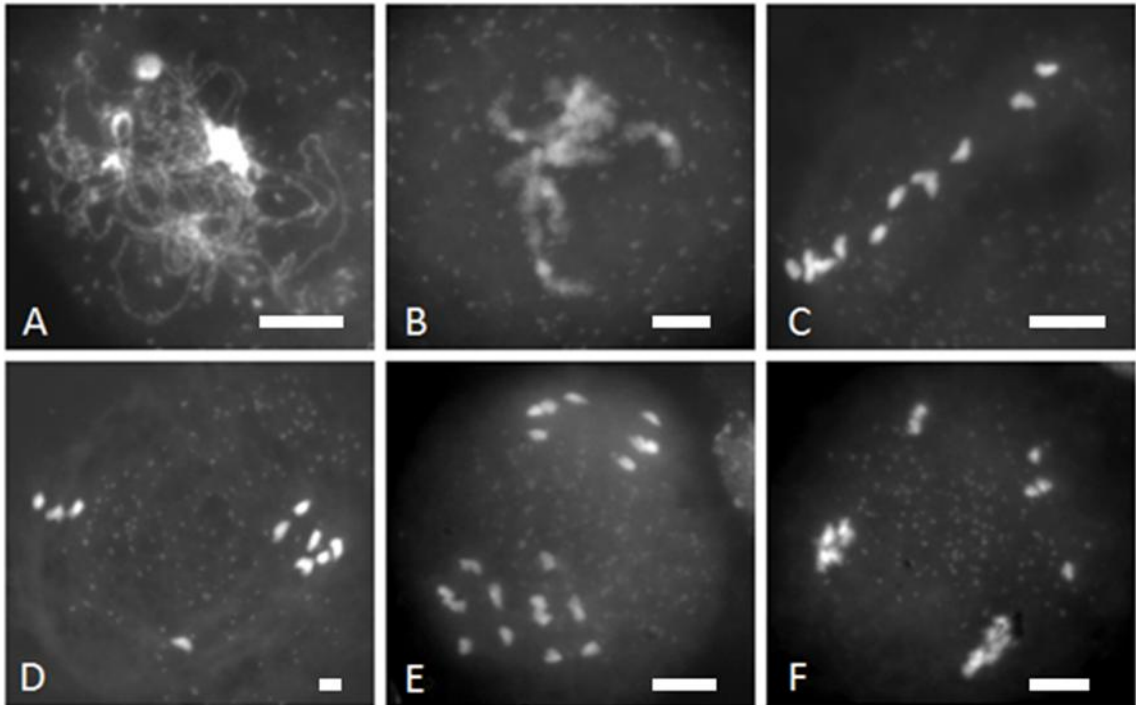


Figure 5.1. Meiotic stages in pollen mother cells of the *Atspo11-1-4* mutant of *A. thaliana*.

(A) Thread-like and unsynapsed chromosomes appear at early meiotic prophase I. (B) condensed univalents at a diakinesis-like stage. (C) Metaphase I showing 10 univalents. (D) 9 univalents move randomly to the poles one univalent is seen lagging on middle of the cell at anaphase I. (E) Sister chromatids are pulled apart during anaphase II (F) Sister chromatids are segregated to produce four sets of chromosome at telophase II. The number of chromosomes in each set is not equal to the haploid set of chromosomes. Bars 10 μ m.

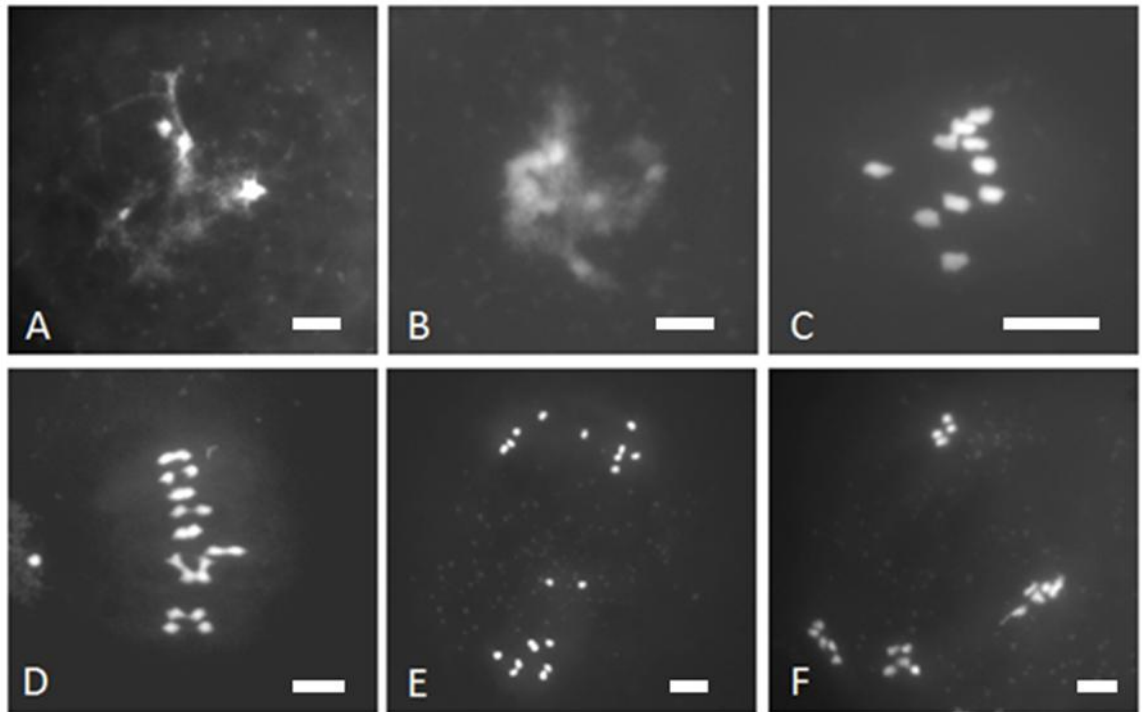


Figure 5.2. Meiotic stages in pollen mother cells of the *synI*^{-/-} / *Atspo11-1-4*^{-/-} double knock-out mutant of *A. thaliana*. (A) Abnormal loose and tangled chromosome structures appear before chromosome condensation. (B) Chromosomes condense at a diakinesis-like stage (C) Ten univalents appear in metaphase I (D) Sister chromatids are pulled apart to opposite pole at early anaphase I (E). Chromosomes are segregated randomly at anaphase II (F). Four sets of chromosome in tetrads. One of the set contains four chromosomes. Bars 10µm.

5.2.2 Immunolocalization of SYN1 on *Atspo11-1-4*^{-/-}.

To investigate SYN1 distribution in the absence of double strand breaks, wild-type (Col 0) and *Atspo11-1-4*^{-/-} meiocytes were examined using antibodies against ASY1 (rat) and SYN1 (rabbit). In order to allow direct comparison between both meiocytes, the image capture conditions were set up with the same exposure time and index of brightness and contrast. Immuno-localization of ASY1 and SYN1 showed that both proteins appeared as strong signals in wild-type meiocytes. Patchy SYN1 signals were distributed on the continuous ASY1 signals in early prophase I (Figure 5.3). In contrast, weak SYN1 foci and strong ASY1 linear signals were detected on *Atspo11-1-4*^{-/-} meiocytes. This observation showed that the SYN1 loading was affected in the *Atspo11-1-4*^{-/-} mutant.

To confirm the decrease of SYN1 signal in *Atspo11-1-4*^{-/-}, wild-type and *Atspo11-1-4*^{-/-} mutant were treated with Bromodeoxyuridine (BrdU). BrdU is a thymidine analogue that can be incorporated into the DNA during the S-phase of the cell cycle. The incorporation of BrdU can be detected immunocytologically by anti-BrdU antibodies. The BrdU labelling method has been described and published as a useful tool for analysing the timing and relationships of meiotic events (Armstrong et al., 2003). Immunolocalization of SYN1 was carried out in chromosome preparations from wild-type and *Atspo11-1-4*^{-/-} meiocytes following BrdU pulse-labelling. The immunostaining result showed that strong SYN1 signals were detectable in wild-type meiocytes at one hour post-S phase (G2 stage). According to a meiotic time-course report, axis-associated protein ASY1 is first detectable at five hour post-S phase (Armstrong et al., 2003), indicating that SYN1 appears before ASY1 in meiocytes of wild-type. Under the same conditions, the SYN1 signals were substantially reduced in *Atspo11-1-4*^{-/-} meiocytes (Figure 5.4 A; B). At 30 hours post-S phase (late pachytene), strong SYN1 signals were still

apparent in the wild-type meiocytes but weak SYN1 signals were detected in *Atspo11-1-4^{-/-}* (Figure 5.4 C; D). These results show that SYN1 loading was reduced at the onset of G2 stage until pachytene in the *Atspo11-1-4^{-/-}* mutant. According a report in yeast mitotic cells, cohesin is recruited to DNA DSB sites where it might facilitate DNA DSB repair (Lowndes and Toh, 2005; Kugou et al., 2009). These suggest that SYN1 loading is affected due to the absence of DNA DSBs.

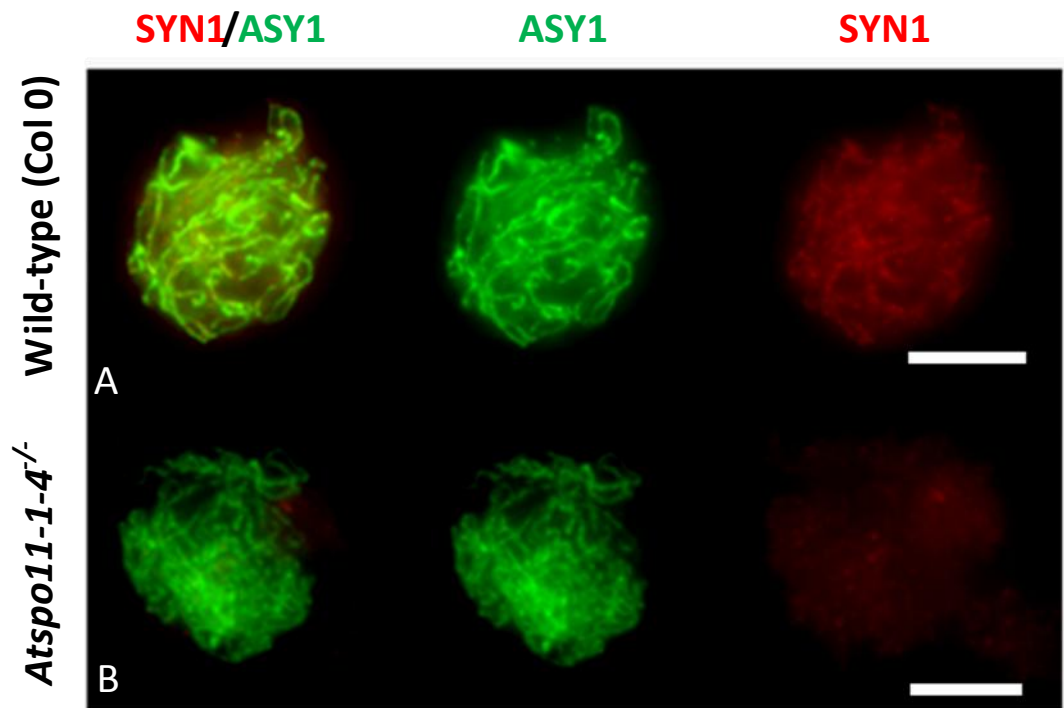


Figure 5.3. Dual immunolocalization of ASY1 (green) and SYN1 (red) on prophase I nuclei of wild-type (A) and *Atspo11-1-4^{-/-}* (B) mutant. Substantial SYN1 foci are localized to chromosomes in wild-type (A) but not in *Atspo11-1-4^{-/-}*. Bars 5 μ m.

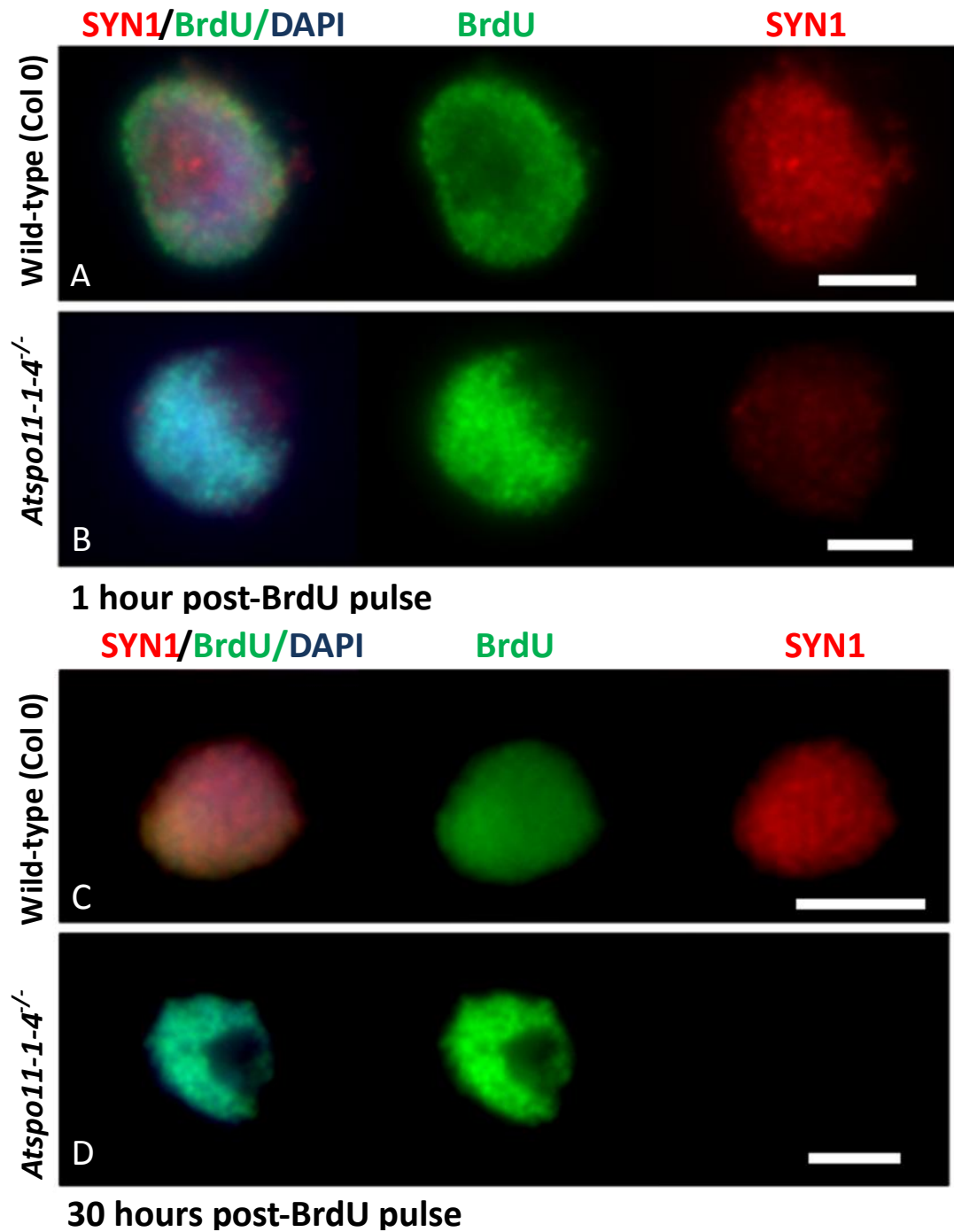


Figure 5.4. BrdU (green) pulse-labelling combined with immunocytological analysis in wild-type and *Atspo11-1-4^{-/-}* meiocytes. Strong SYN1 signal (red) in wild-type meiocytes is shown at 1h (A) and 30 h (C) post-BrdU pulse but weak SYN1 signal is shown in *Atspo11-1-4^{-/-}* at 1h (B) and 30h (D) post-BrdU pulse. The chromosomes are counterstained with DAPI (blue). Bars 5µm.

5.2.3 Immunolocalization of SYN1 on cisplatin-treated *Atspo11-1-4^{-/-}* meiocytes

Previously, I have shown that SYN1 signal was reduced in *Atspo11-1-4^{-/-}* meiocytes by using BrdU pulse-labelling combined with immunocytological analysis. To investigate whether SYN1 loads on sister chromatids during DSB formation, meiocytes of *Atspo11-1-4^{-/-}* were treated with cisplatin. Cisplatin (cis-diaminedichloridoplatinum II) forms platinum chemical complexes which react with DNA to form intrastrand and interstrand crosslinks. The excision of the DNA crosslink creates a DSB (Olive and Banath, 2009). In this study, inflorescences of *Atspo11-1-4^{-/-}* were immersed in cisplatin solution at concentrations of 2.5µM and 5.0µM for a 2 hour pulse. At the same time, inflorescences from wild-type and *Atspo11-1-4^{-/-}* were immersed in tap water as positive and negative controls. Buds were collected and dissected at 28 hour post-cisplatin pulse. Cisplatin-treated buds with high concentration (0.5 µM) were excluded in the following examination because the buds become pale and wilted. Immunolocalization studies were carried out on spread preparations with anti-SYN1 (rabbit) and anti-ASY1 (rat) antibodies. The pixel intensity of meiocytes was analysed by using ImageJ (Appendix 5.1). Immuno-localization analysis showed (Figure 5.5 and 5.6) that the intensity of SYN1 was different between wild-type and untreated *Atspo11-1-4^{-/-}*. The wild-type signal was much stronger than the untreated *Atspo11-1-4^{-/-}*. The statistical analysis showed that there is significant difference between the wild-type and untreated *Atspo11-1-4^{-/-}* (t-test, $p < 0.001$; $n = 50$). Furthermore, the pixel intensity of SYN1 was also significantly different between cisplatin-treated *Atspo11-1-4^{-/-}* and untreated *Atspo11-1-4^{-/-}* (t-test, $p < 0.001$; $n = 50$). The signal in cisplatin-treated *Atspo11-1-4^{-/-}* was stronger than the untreated *Atspo11-1-4^{-/-}*. Although SYN1 signal increased after cisplatin treatment in *Atspo11-1-4^{-/-}*, the wild-type signal was still stronger than the cisplatin-treated *Atspo11-1-4^{-/-}*. The statistical analysis showed that there is significant difference in the intensity between wild-

type and cisplatin-treated *Atspo11-1-4^{-/-}* (t-test, $p=0.0105$; $n=50$). These results show that the SYN1 signal is increased after cisplatin treatment in *Atspo11-1-4^{-/-}*, indicating that SYN1 loading can be restored in the absence of AtSPO11-1 by artificially inducing DSBs with cisplatin. It is also important to investigate whether meiotic recombination can be triggered in the *Atspo11-1-4^{-/-}* mutant by using cisplatin. Therefore, the meiocytes of cisplatin-treated *Atspo11-1-4^{-/-}* were examined by using antibodies against the synaptonemal complex protein AtZYP1. Immunolocalization of AtZYP1 revealed that the protein appeared as strong foci and short linear signals in cisplatin-treated *Atspo11-1-4* meiocytes (Figure 5.7). This result showed that SC formation can be initiated in the absence of AtSPO11-1 protein by using cisplatin.

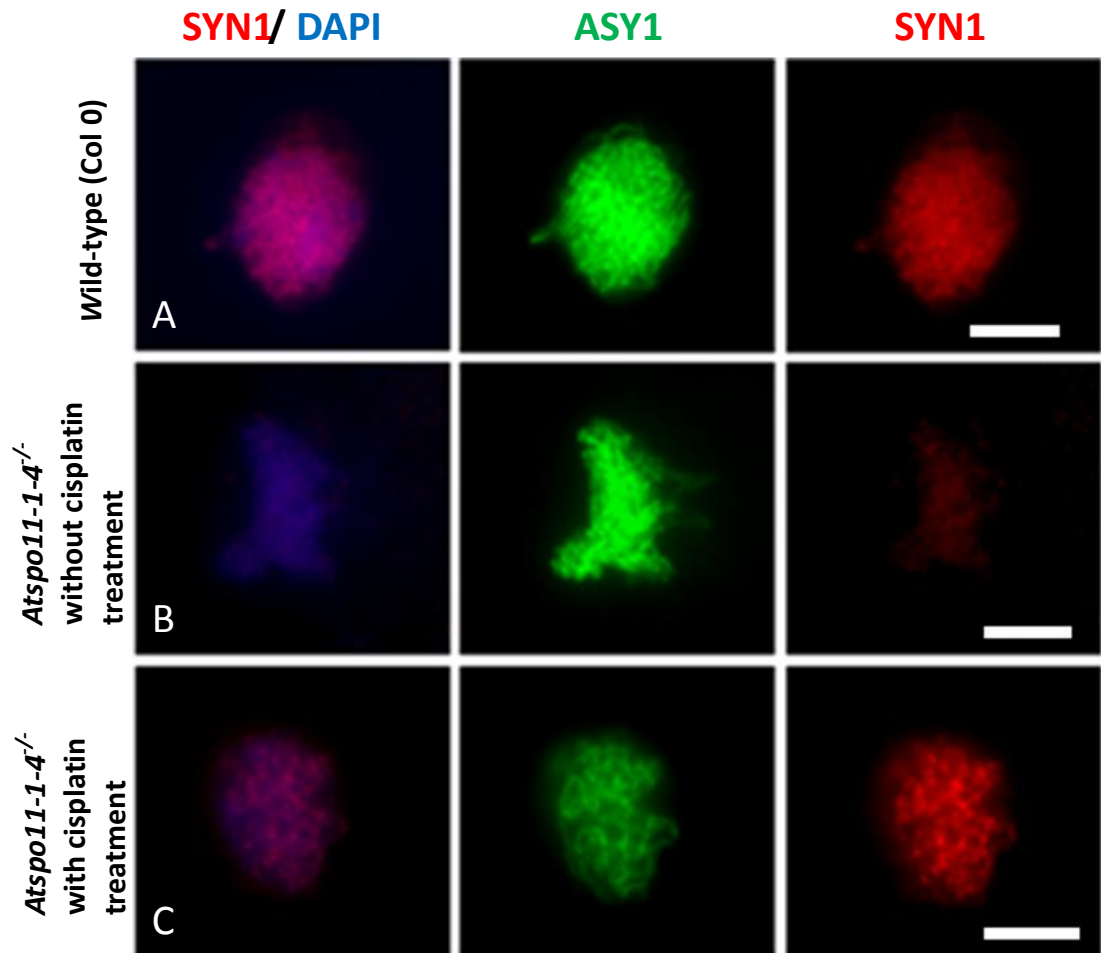
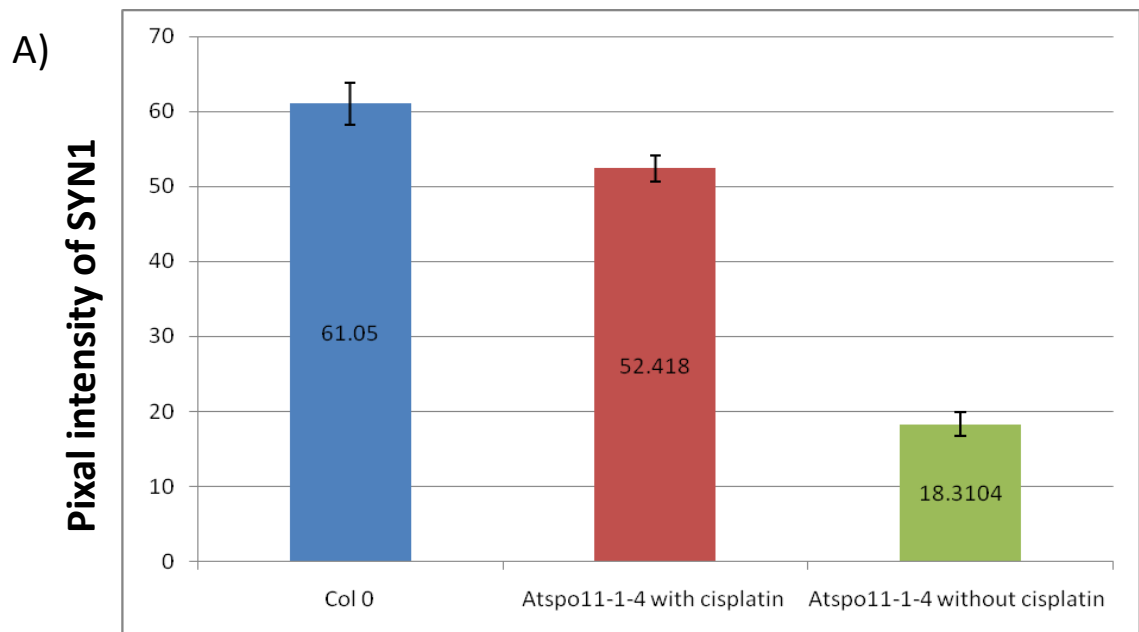


Figure 5.5. Dual immunolocalization of ASY1 (green) and SYN1 (red) on prophase I nuclei of wild-type (A) and untreated *Atspo11-1-4^{-/-}* (B) and cisplatin-treated *Atspo11-1-4^{-/-}* mutant (C). Strong patchy signals of SYN1 appeared on chromosome in wild-type but weak SYN1 signals in *Atspo11-1-4^{-/-}*. After *Atspo11-1-4^{-/-}* treated with cisplatin, strong signals of SYN1 are observed on chromosomes. The chromosomes are counterstained with DAPI (blue). Bars 5 μ m.



B)

	Wild-type (Col 0)	<i>Atspo11-1-4^{-/-}</i> with cisplatin treatment	<i>Atspo11-1-4^{-/-}</i> with cisplatin free
Total (n=50)	3052.509	2620.908	915.52
Mean	61.05018	52.41816	18.3104
Standard Deviation	19.887303	12.37164835	11.70871021
Standard Error	2.81251633	1.749632068	1.655877558

Figure 5.6. Signal intensity analysis of SYN1 on prophase I nuclei of wild-type (Col 0), cisplatin-treated *Atspo11-1-4^{-/-}* and untreated *Atspo11-1-4^{-/-}* mutants.

(A) Signal intensity of *Atspo11-1-4^{-/-}* is significantly lower than that of wild-type ($p < 0.001$; $n = 50$). After cisplatin treatment in *Atspo11-1-4^{-/-}*, the SYN1 signal is significantly higher than that of cisplatin free *Atspo11-1-4^{-/-}* ($p < 0.001$; $n = 50$) but is still lower than that of wild-type ($0.01 < p < 0.05$; $n = 50$). The corresponding p values are calculated in the table (B) and Appendix 5.1.

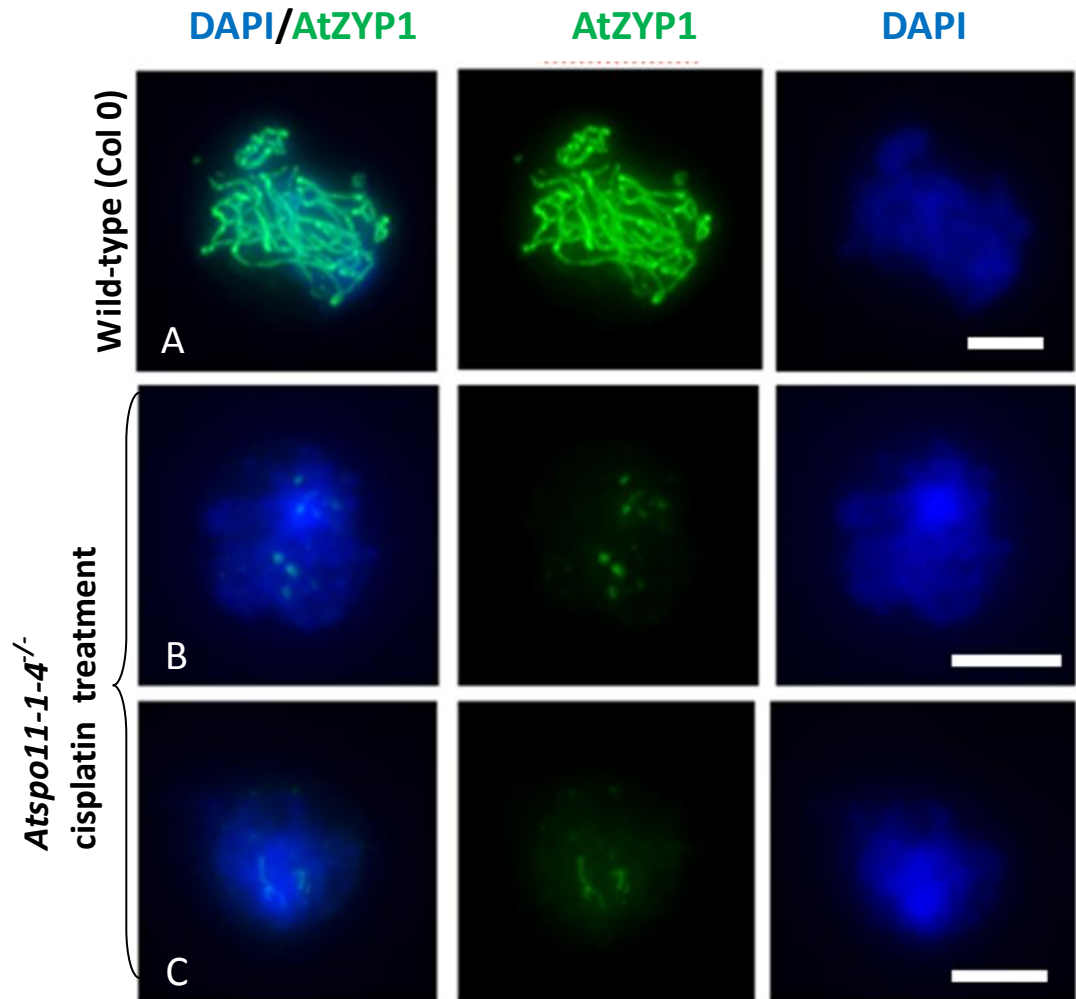


Figure 5.7. Immunolocalization of AtZYP1 (green) on prophase I nuclei of wild-type (A) and cisplatin-treated *Atspo11-1-4^{-/-}* mutant (B; C). The chromosomes are counterstained with DAPI (blue). Continuous signals of AtZYP1 are observed in meocytes of wild-type (A). Few strong patchy (B) and short linear (C) signals are detectable in cisplatin-treated *Atspo11-1-4^{-/-}* meocytes. Bars 5 μ m.

5.2.4 Cytogenetic analysis in *syn1*^{-/-} and *Atrad51c*^{-/-} double knockout mutant

Recently, research in rat showed that RAD51 and DMC1 coimmunoprecipitate with REC8. It has been proposed that the cohesins provide a platform for the assembly of recombination proteins after S phase (Eijpe et al., 2003). To test the relationship between SYN1 and recombination proteins during the formation of DSB, I chose AtRAD51C, an *Arabidopsis* RAD51C ortholog. It has been suggested that AtRAD51C plays an important role in DSB repair (Li et al., 2005). Cytological analysis of *Atrad51c*^{-/-} showed thin threads and unsynapsed chromosomes during the early prophase I (Figure 5.8A). Following the chromosome condensation, the chromosome structure was seriously disrupted. Tangled chromosome fragments were observed, which aligned at the equatorial plate in preparation for the first meiotic segregation (Figure 5.8B). Chromosome bridges and fragments were observed at early anaphase I (Figure 5.8C). A substantial number of chromosome fragments remained in the middle of the meiocyte after five chromosomes migrated toward each pole (Figure 5.8D). Chromosome fragmentation and mis-segregation appeared throughout prophase II (Figure 5.8 E; F).

A *syn1*^{-/-} and *Atrad51c*^{-/-} double knockout mutant was constructed. The cytological analysis showed that chromosome abnormalities were found throughout meiosis. During early prophase I, chromosomes can be seen as loose and tangled structures (Figure 5.9A; B). The tangled chromosomes were aligned at the equatorial plate and segregated towards opposite poles during the first meiotic segregation (Figure 5.9C). Some chromosome fragments remained in the middle of meiocytes and other chromosome fragments moved to the two poles at anaphase I (Figure 5.9D). Chromosome fragmentation and mis-segregation appeared from metaphase I to prophase II, which is very similar to both *Atrad51*^{-/-} and *syn1*^{-/-} mutants.

Cytological analysis showed that chromosome phenotype at early prophase I is significantly different between *syn1^{-/-}/Atrad51c^{-/-}* and *Atrad51c^{-/-}* mutants. Currently, it is impossible to draw a conclusion whether SYN1 and AtRAD51C interact during early meiosis I.

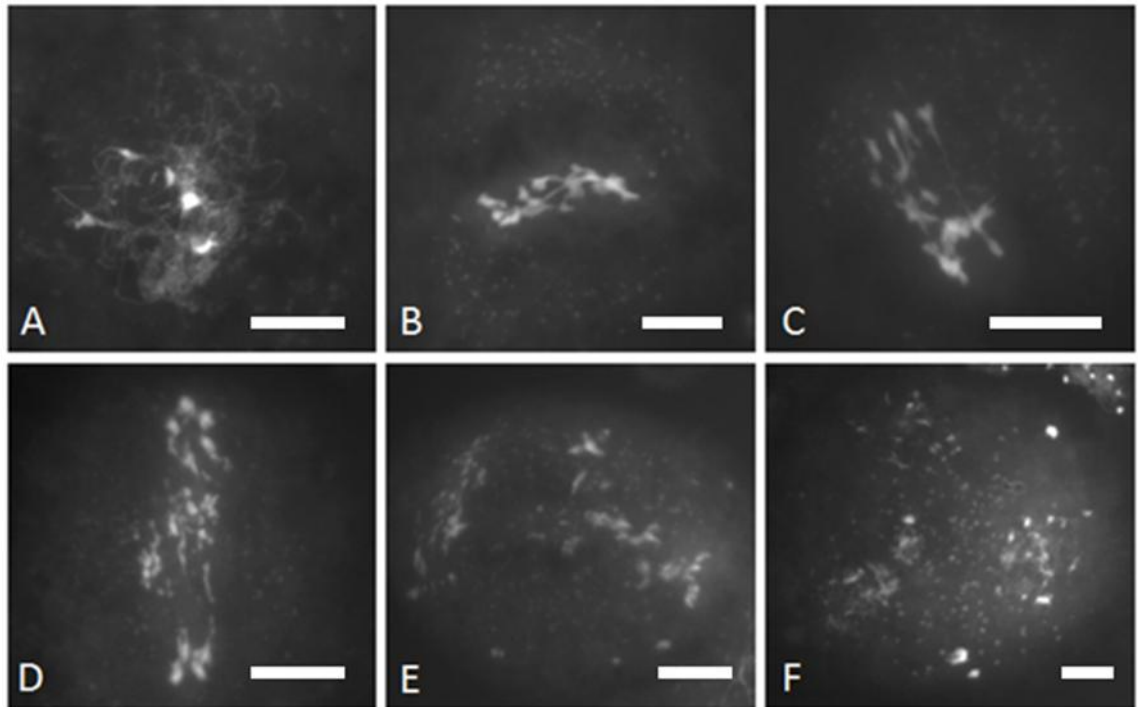


Figure 5.8. Meiosis stages in pollen mother cells of the *Atrad51c*^{-/-} mutant of *A. thaliana*.

(A) Thin and unsynapsed chromosomes appear during early prophase I. (B) Abnormal condensed chromosomes and bridges are seen at metaphase I. (C) Chromosome fragments are randomly segregated at early anaphase I. (D) Each pole of the cell contains 4 or 5 chromosome fragments but a large number of chromosome fragments remain in the middle of the meiocytes during late anaphase I. (E) Chromosomes are randomly segregated at anaphase II (F) Chromosome fragments distribute randomly at telophase II. Bars 10 μ m.

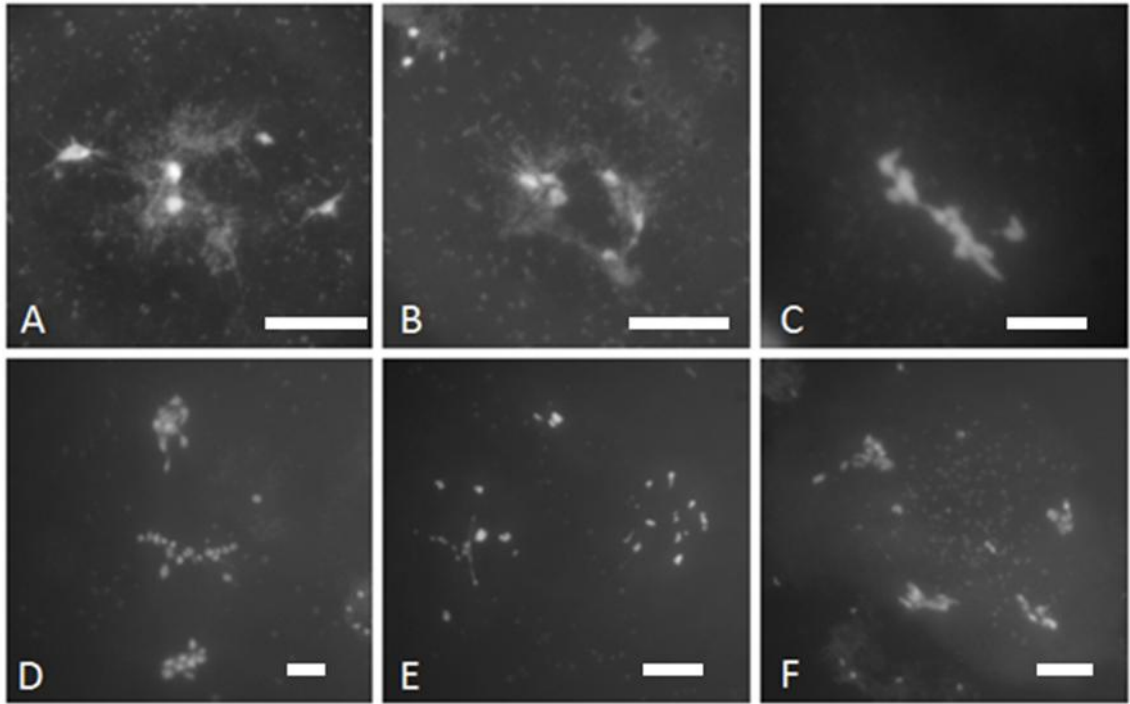


Figure 5.9. Meiotic stages in pollen mother cells of *syn1^{-/-} / Atrad51c^{-/-}* of *A. thaliana*.

(A) Loose and tangled chromosomes appear during early prophase I. (B) Tangled chromosomes appear after chromosome condensation. (C) Bridges and fused chromosomes are aligned on equatorial plate at metaphase I (D) During first meiotic division, 9 or 10 chromosome fragments locate in each pole and many chromosome fragments still remain in the middle of meiocyte. (E) Chromosome fragments are randomly segregated at anaphase II. (F) Chromosome fragments distribute unevenly in four set of haploid products. Bars 10 μ m.

5.2.5 Cytogenetic analysis in a *syn1*^{-/-}/*Atdmc1*^{-/-} double knockout mutant

To find out whether SYN1 has a role in DNA double strand break (DSB) repair, a *syn1*^{-/-} and *Atdmc1*^{-/-} double knockout mutant was constructed. AtDMC1, an *Arabidopsis* homologue of DMC1, promotes interhomologue recombination following AtSPO11-induced DSB formation (Bishop et al., 1992; Couteau et al., 1999; Sanchez-Moran et al., 2007). Cytological analysis of *Atdmc1* showed normal thin thread-like, unsynapsed chromosomes at early prophase I (Figure 5.10A). Condensed univalents were observed at the diakinesis-like stage (Figure 5.10B). 10 univalents were aligned at the equatorial plate at metaphase I (Figure 5.10C; Table 5.1) and each univalent moved to the same pole during the first meiotic segregation. There was no evidence of chromosome fragmentation (Figure 5.10D). The sister chromatids were separated to the opposite pole during the second meiotic division (Figure 5.10E; F). This result showed that despite the lack of CO formation, the DSBs induced by AtSPO11-1 were fully repaired in *Atdmc1*.

In the *syn1* / *Atdmc1* double knockout mutant, abnormal chromosomes appeared throughout the process of meiosis. Diffuse and tangled chromosomes were observed at early meiotic prophase I (Figure 5.11A). This phenotype resembles the meiocytes of the *syn1* single mutant. Condensed and fused chromosome fragments with bridges were observed to align on the equatorial plate (Figure 5.11C). The number of chromosome fragments at metaphase I ranged from 6 to 13 (mean=8.59; n=32; Table 5.1). Chromosome fragments persisted throughout meiotic prophase I and II (Figure 5.11D; E). In conclusion, analysis of *syn1*^{-/-}/*Atdmc1*^{-/-} demonstrated that SYN1 is essential for DSB repair during meiosis.

Table 5.1: Number of chromosome fragments at metaphase I in wild-type (Col 0), *synI*^{-/-}, *AtdmcI*^{-/-} and *synI*^{-/-}/*AtdmcI*^{-/-}

Col 0 & mutants	Metaphase I (Mean)	Number of fragments	Number of cells
Wild-type (Col 0)	5 bivalents	-	n=25
<i>synI</i> ^{-/-}	10.17 fragments;	range from 7 to 17	n=53
<i>AtdmcI</i> ^{-/-}	10 univalents	-	n=22
<i>synI</i> ^{-/-} / <i>AtdmcI</i> ^{-/-}	8.59 fragments	range from 6 to 13	n=32

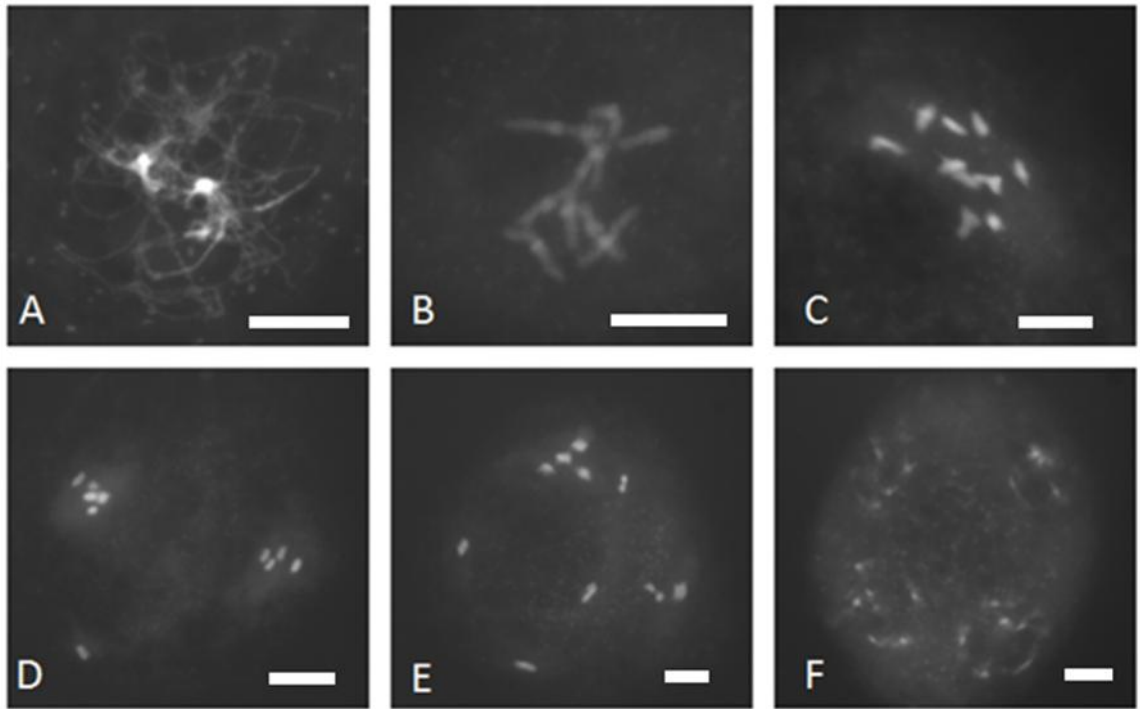


Figure 5.10. Meiotic stages in pollen mother cells of the *Atdmc1* null mutant of *A. thaliana*.

(A) Thin thread-like and unsynapsed chromosomes appear at early prophase I. (B) 10 condensed chromosomes in diakinesis-like stage. (C) 10 univalents at metaphase I. (D) 9 univalents move randomly to the poles at anaphase I, one univalent is seen lagging on middle of the cell. (E) Separated sister chromatids move randomly to opposite pole but some sister chromatids delay separation during anaphase II. (F) Sister chromatids are separated to produce four sets of chromosomes in tetrads. Bars 10 μ m.

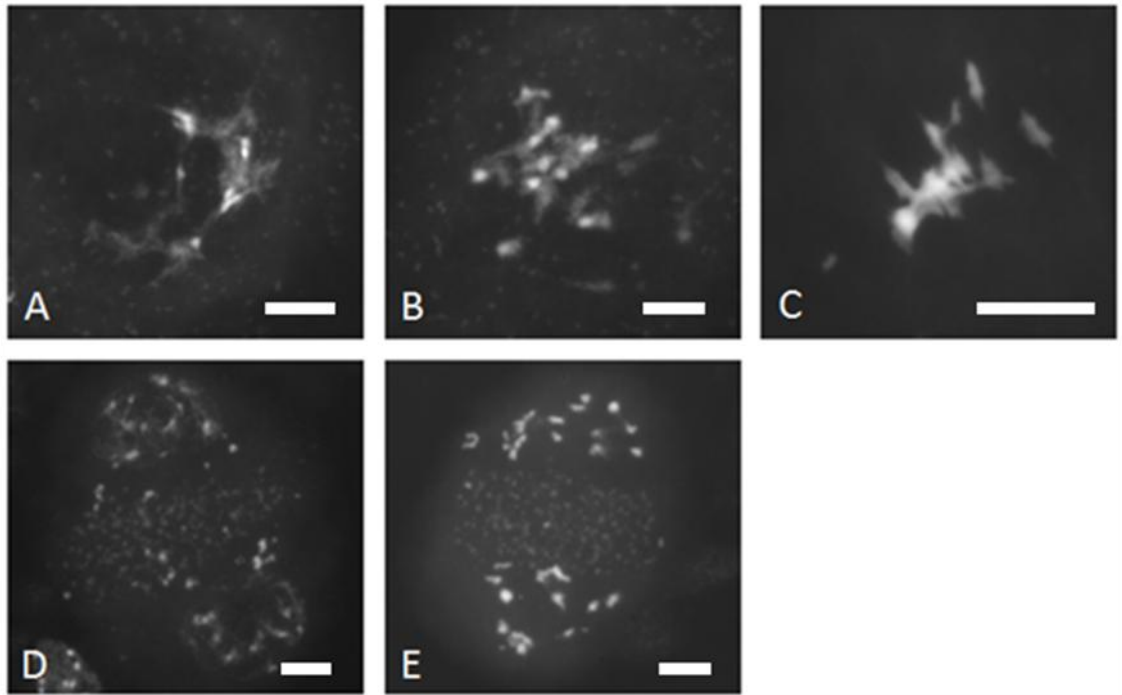


Figure 5.11. Meiotic stages in pollen mother cells of the *synI*^{-/-}/*Atdmc1*^{-/-} double knock-out mutant of *A. thaliana*.

(A) Loose chromatin and tangled structures appear at early prophase I. This phenotype resembles the meiocytes of the *synI* mutant. (B) Abnormal condensed chromosome fragment and univalent at prophase I. (C) Chromosome fragments and bridges appear at metaphase I. (D) chromosome fragments distribute around meiocytes at prophase II. (E) Sister chromatids and chromosome fragments are randomly separated in anaphase II. Bars 10µm.

5.2.6 Seeds of wild-type and *SYNI* heterozygous plants grew slowly on cisplatin MS medium.

Previous studies reported that an *Atrad51c*^{-/-} mutant has a normal vegetative phenotype. Seedlings of the *Atrad51c*^{-/-} are highly sensitive to cisplatin, suggesting that homologous recombination plays a role in mitotic cells during the repair of DNA lesions arising from DNA cross-linking. A similar experiment was also carried out in a mammalian *xrcc3*^{-/-} mutant (De Silva et al., 2002; Abe et al., 2005). Therefore, it is of interest to examine the role of *SYN1* in mitotic cells by using cisplatin. In the experiment, cisplatin sensitivity was measured based on the weight of three week old seedlings grown on Murashige and Skoog (MS) agar medium with different concentrations of cisplatin (0 μ M; 12.5 μ M; 25 μ M; 50 μ M). One hundred seeds from a *SYNI* heterozygote, *SYNI*^{+/-}, plant were placed on one MS agar plate and then incubated in a 22°C growth chamber, while seeds of wild-type (Col 0) plant were grown in parallel as a control. The result showed that all the seedlings of wild-type and *SYNI*^{+/-} grew rapidly producing true leaves at 14 days on cisplatin-free MS medium (Figure 5.12). However, only 50% of wild-type and 30% of *SYNI*^{+/-} seedlings produced true leaves on 12.5 μ M cisplatin medium. Furthermore, at high concentrations of cisplatin (25 μ M and 50 μ M), both the wild-type and *SYNI*^{+/-} seedlings grew slowly producing only primary leaves. After 21 days (Figure 5.13), all the wild-type and *SYNI*^{+/-} seedlings in cisplatin-free MS medium grew rapidly and developed normal size leaves. In contrast, only 81% of wild-type and 53% of *SYNI*^{+/-} seedlings produced true leaves which varied in size on 12.5 μ M cisplatin medium. Only 11% of wild-type and 4% of *SYNI*^{+/-} seedlings produced true leaves on 25 μ M cisplatin medium, while all the seedlings of wild-type and *SYNI*^{+/-} on 50 μ M cisplatin medium failed to grow beyond cotyledon stage, many of which turned brown. This observation revealed that the growth of both wild-type and *SYNI*^{+/-} seedlings were affected by cisplatin.

All the three-week old seedlings were collected and weighed for statistical analysis. This analysis showed that there is no significant difference between the wild-type and *SYNI*^{+/-} seedlings on cisplatin free MS medium (t-test, p=0.8286; n=3; figure 5.14). Moreover, there is no significant difference between the wild-type and *SYNI*^{+/-} seedlings on 12.5µM cisplatin MS medium (t-test, p=0.0837; n=3); 25µM cisplatin MS medium (t-test, p=0.4175; n=3) and 50µM cisplatin MS medium (t-test, p=0.5636; n=3). This indicates that seedlings from *SYNI*^{+/-} plants were not more sensitive to cisplatin than wild-type.

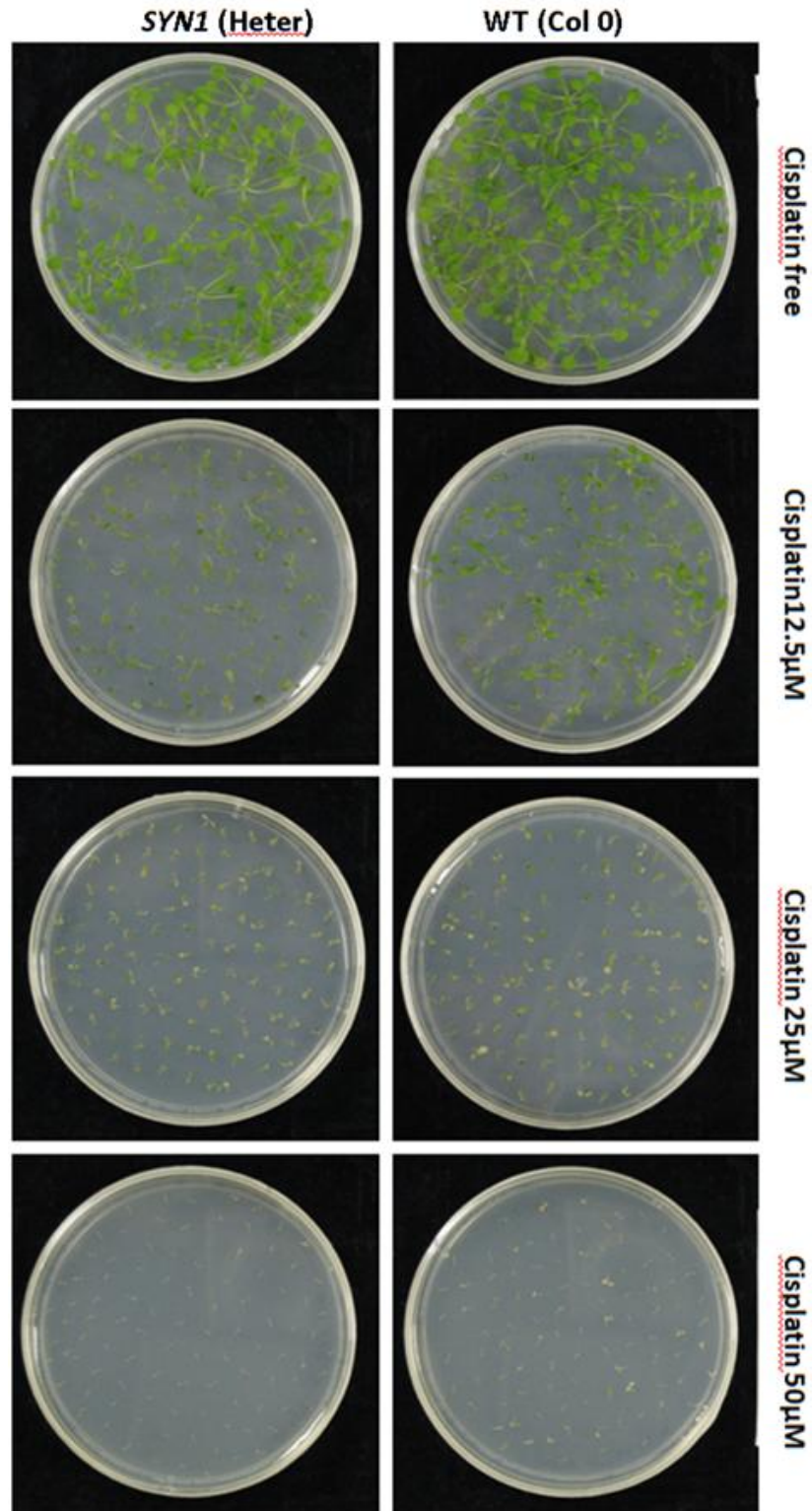


Figure 5.12 Cisplatin sensitivity phenotype of wild-type and *SYN1*(Heter) at 14 days after germination. Seeds of wild-type (Col 0) and *SYN1* heterozygous plants were grown on plates containing cisplatin (0 μM; 12.5 μM; 25 μM; 50 μM). Note: 1) *SYN1*(Heter): seeds from *SYN1* heterozygous plants contain three genotypes *SYN1*^{+/-}, *SYN1*^{-/-}, *SYN1*^{+/+}; 2) Each plate contains 100 seeds.

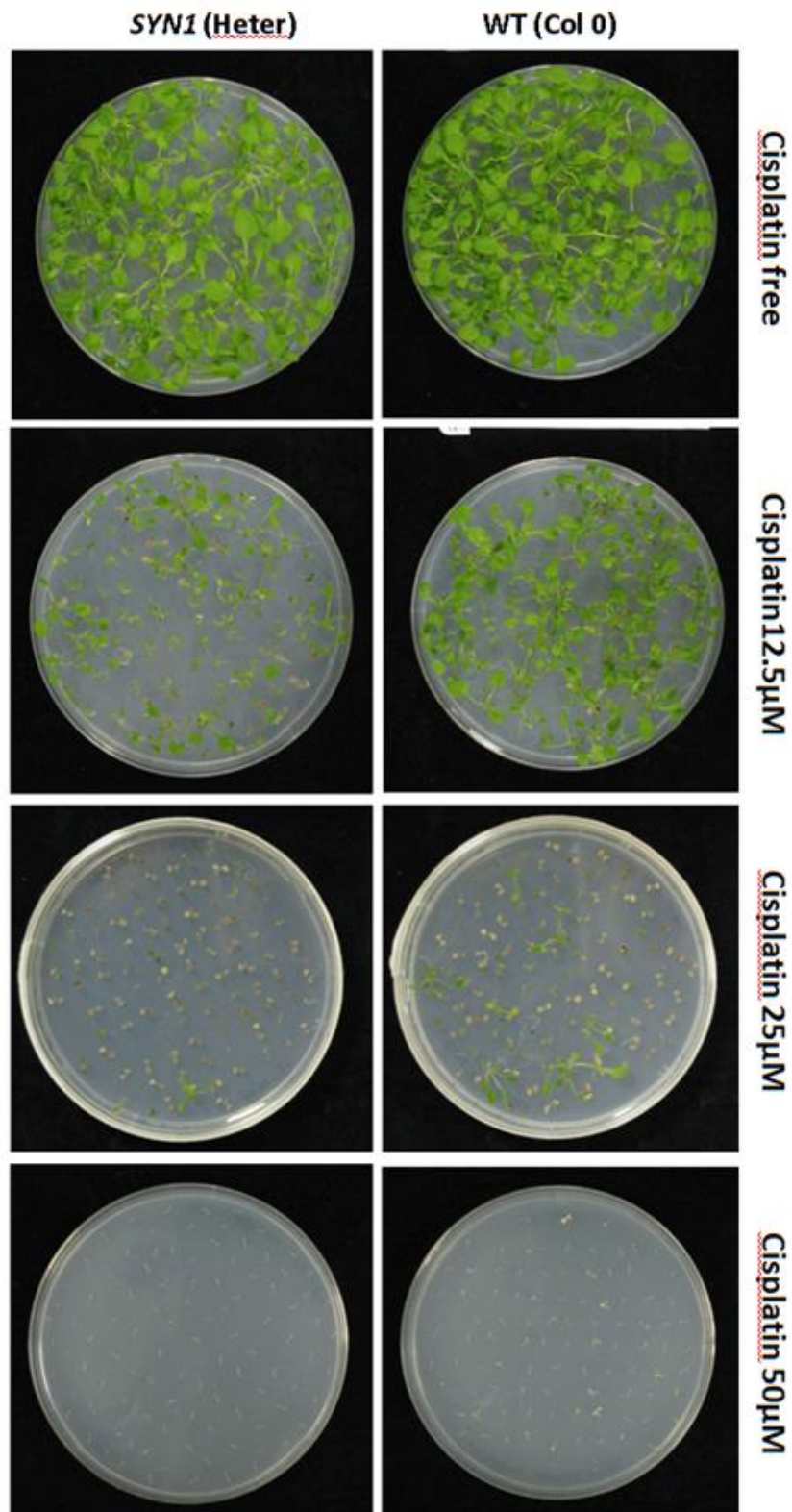


Figure 5.13. Cisplatin sensitivity phenotype of wild-type and *SYN1*(Heter) at 21 days after germination. Seeds of wild-type (Col 0) and *SYN1* heterozygous plants were grown on plates containing cisplatin (0 μM; 12.5 μM; 25 μM; 50 μM). (Note: *SYN1*(Heter): seeds from *SYN1* heterozygous plants contain three genotypes *SYN1*^{+/+}, *SYN1*^{+/-}, *SYN1*^{-/-}).

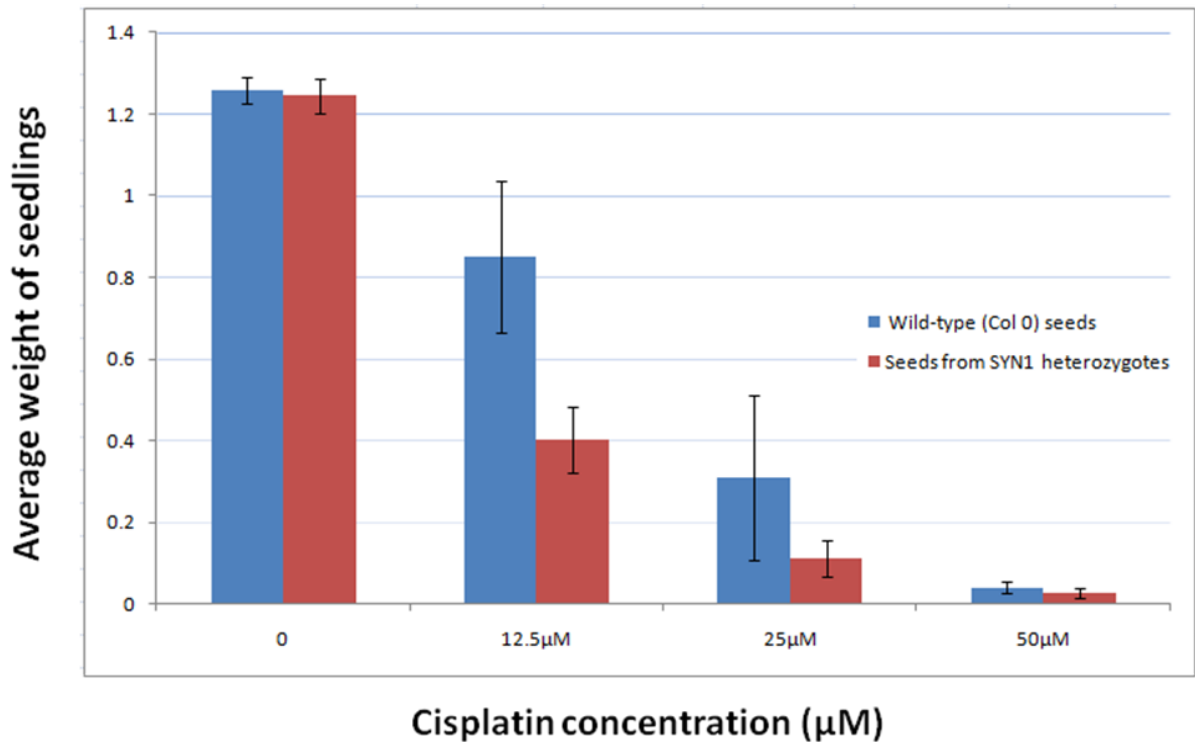


Figure 5.14. Cisplatin sensitivity of wild-type (Col 0) and *SYN1*(Heter).

Seeds of wild-type and *SYN1* heterozygous plants were grown for 21 days on cisplatin (0μM; 12.5μM; 25μM; 50μM) treated MS medium. Weight of wild-type seedlings is compared to *SYN1*(Heter) seedlings for each cisplatin concentration. Statistical analysis shows that weight of wild-type is not significantly different to that of *SYN1*(Heter) in the same cisplatin condition (0μM; 12.5μM; 25μM; 50μM).

Note: *SYN1*(Heter): seeds from *SYN1* heterozygous plants contain three genotypes *SYN1*^{+/-}, *SYN1*^{-/-}, *SYN*^{+/+}.

5.3 Discussion

5.3.1 SYN1 is essential for centromeric cohesion at first meiotic segregation

We obtained a T-DNA insertion line (WiscDsLox461-464J19) which we referred to as *Atspo11-1-4^{-/-}*. Cytological analysis of *Atspo11-1-4* mutant showed 10 univalents during diakinesis-like and metaphase I stages. Bridges between chromosomes were not observed during first meiotic division. Other mutant alleles such as *Atspo11-1-1^{-/-}*, produce a few bivalents in meiocytes (Grelon et al., 2001; Chelysheva et al., 2005). The reports have also shown that these bivalents are pulled apart forming bridges between chromosomes during first meiotic division (Grelon et al., 2001; Chelysheva et al., 2005), indicating that the *Atspo11-1-1^{-/-}* line produces a truncated partially functional protein. Thus, in contrast to *Atspo11-1-1^{-/-}* our data showed that *Atspo11-1-4^{-/-}* is a null mutant.

A *syn1^{-/-}/Atspo11-1-4^{-/-}* double knockout mutant was constructed. The cytological analysis of *syn1^{-/-}/Atspo11-1-4^{-/-}* showed that loose and tangled chromosomes appeared at early prophase I as seen in *syn1*. Furthermore chromosome condensation, 10 univalents were observed to align at the equatorial plate in the meiocytes, showing that sister chromatids were aligned during meiotic prophase I. A similar result has been observed in *Sordaria sm-rec8^{-/-}/spo11^{-/-}*, this double knockout mutant contains 14 univalents, indistinguishable from the phenotype as *spo11* mutant (Storlazzi et al., 2008). In contrast to the phenotype of *Arabidopsis* and *Sordaria*, the *C.elegans* sister chromatids are separated at early prophase I after REC8 depletion in a *spo11* mutant. This observation clearly suggests that cohesion is lost when REC8 is depleted in *C. elegans* (Pasierbek et al., 2001). Currently, we do not know what maintains the sister chromatid cohesion in *syn1^{-/-}/Atspo11-1-4^{-/-}* and *spo11^{-/-}/sm-rec8^{-/-}*. According to a report in yeast, a large quantity of the mitotic kleisin subunit SCC1 is replaced

by REC8 when the cells enter meiotic S phase. Interestingly, SCC1 does not disappear entirely before the first meiotic division (Klein et al., 1999). In mammals, REC8 and RAD21 proteins appear along the chromosomes during pachytene stage (Prieto et al., 2004), suggesting that mitotic kleisin subunit RAD21/SCC1 might have a role in meiosis. It seems likely that this also applies to *Arabidopsis*. Therefore, I suggest that the cohesion of sister chromatids in *syn1^{-/-}/Atspo11-1-4^{-/-}* is maintained by the mitotic kleisin subunits SYN2 and/or SYN4 during early prophase I.

Cytological analysis of *Atspo11-1-4^{-/-}* showed 10 univalents at metaphase I. Each univalent moved to the same pole at anaphase I. In *syn1^{-/-}/Atspo11-1-4^{-/-}*, 10 univalents were located at the equatorial plate during metaphase I and the sister chromatids were then pulled apart during anaphase I (Table 5.2). This result indicated that the centromeric cohesion was lost during meiotic first division. Although I suggest that the mitotic kleisin subunits SYN2 and/or SYN4 maintain the sister chromatid cohesion at early meiosis I, these proteins must be released from sister chromatid arms and centromeres by separase during metaphase I. As a result, the sister chromatids are separated in the absence of both mitotic and meiotic kleisin proteins. This indicates that SYN1 plays a crucial role in centromeric cohesion during first meiotic segregation.

Table 5.2 Summary of mutants phenotype including chromosome numbers; fragmentation and chromosome segregation.

Meiosis I Mutant	Metaphase I			Anaphase I
	5 bivalents	10 univalents	Chromosome fragmentation	Reductional/Equational segregation
Wild-type (Col 0)	√	X	X	Reductional segregation
<i>syn1^{-/-}</i>	X	X	√	NC
<i>Atspo11-1-4^{-/-}</i>	X	√	X	Reductional segregation
<i>Atspo11-1-4^{-/-}/syn1^{-/-}</i>	X	√	X	Equational segregation
<i>Atdmc1^{-/-}</i>	X	√	X	Reductional segregation
<i>Atdmc1^{-/-}/syn1^{-/-}</i>	X	√	√	NC
<i>Atrad51c^{-/-}</i>	X	X	√	NC
<i>Atrad51c^{-/-}/syn1^{-/-}</i>	X	X	√	NC

Note: NC represents not classified.

5.3.2 Chromosome fragmentation in *syn1* is AtSPO11-1-dependent

In the absence of SYN1, chromosome fragmentation was observed at metaphase I. The number of chromosome fragments increased from 10.17 to 32.70 during the first meiotic division (Table 3.1). When *AtSPO11-1* was deleted in a *syn1* mutant, background chromosome fragments were not seen at any stage of the meiotic program, indicating that the chromosome fragmentation was rescued by the *Atspo11-1-4* mutant. Chromosome fragmentation is also observed in *C. elegans rec8* and *S. macrospora sm-rec8* mutants. The cytological evidence showed that *spo11* mutation suppresses the chromosome fragmentation of REC8 depletion line/*sm-rec8* mutant (Pasierbek et al., 2001; Storlazzi et al., 2008). In conclusion, this observation suggests that chromosome fragmentation in *syn1* mutant is triggered by AtSPO11-1.

5.3.3 SYN1 loading is reduced in *Atspo11-1-4^{-/-}* meiocytes.

I have studied the cytology of the *syn1^{-/-}/Atspo11-1-4^{-/-}* double knock-out mutant, showing that the chromosome fragmentation in the *syn1^{-/-}* mutant is AtSPO11-1-dependent. To further investigate the interaction of AtSPO11-1 and SYN1 in early meiosis, I discovered that the SYN1 signal was reduced in the meiocytes of the *Atspo11-1-4^{-/-}* mutant. Statistical analysis confirmed that the signal of SYN1 in wild-type was stronger than that observed in *Atspo11-1-4^{-/-}* meiocytes ($p < 0.001$; $n = 50$). In addition, the BrdU pulse-labelling combined with immunocytological analysis in *Atspo11-1-4^{-/-}* meiocytes revealed that the SYN1 signal was reduced at G2. These results showed that SYN1 loading was affected severely before leptotene in *Atspo11-1-4^{-/-}* meiocytes, suggesting that SYN1 might interact with AtSPO11-1 during S phase. A similar reduction of REC8 is observed in the yeast *spo11^{-/-}* meiocytes (Beth Weiner, Personal communication). According to yeast studies, the mitotic cohesin subunit

SCC1 is replaced by REC8, which is expressed around the time of meiotic S phase (Klein et al., 1999). During this stage, a large amount of SPO11 associates at the REC8 binding sites (Kugou et al., 2009). Therefore, it is highly possible that the AtSPO11-1 protein associates with some of the SYN1 binding sites at the time of DNA replication. This association might be the reason that a large number of SYN1 protein persists on chromosomes throughout meiosis I. I suggest that some SYN1 loading on the chromosomes is regulated by AtSPO11-1.

5.3.4 Some SYN1 loading is dependent on DNA double-strand breaks

In yeast, SPO11 protein specifically regulates the length of S phase (Cha et al., 2000). It has been reported that this protein firstly binds to centromeric regions and then relocates to the chromosome arms during premeiotic DNA replication and persists throughout meiotic prophase I. Interestingly, the initially accumulation of SPO11 around centromeric regions depends on REC8 protein (Kugou et al., 2009). If SPO11 loading depends on REC8 during meiotic S phase, then why is REC8/SYN1 loading on the chromosome affected in the absence of SPO11/AtSPO11-1? To investigate this, I introduced artificial DNA DSBs with cisplatin in the *Atspo11-1-4^{-/-}* mutant. I observed that SYN1 patchy signals reappeared in cisplatin-treated *Atspo11-1-4^{-/-}*. Furthermore, the statistical analysis confirmed that the signal of SYN1 in cisplatin-treated *Atspo11-1-4^{-/-}* was stronger than that observed in untreated *Atspo11-1-4^{-/-}* ($p < 0.001$; $n = 50$). This result showed that loading of SYN1 can be restored in the absence of AtSPO11-1 by artificially inducing DSB formation with cisplatin. I suggest that some SYN1 loading is dependent on DNA DSB induced by AtSPO11-1. Recent studies in yeast revealed that mitotic cohesin is recruited to the DNA DSB sites (Strom et al., 2004; Lowndes and Toh, 2005). Therefore, I hypothesize that the SYN1 associates with chromosomes at the early S phase and thereafter some SYN1 protein re-localizes to the DNA DSB sites to form

domains/patches (Figure 4.16) along the chromosomes during the initial event of meiotic recombination.

5.3.5 SYN1 has a role in DNA DSB repair.

The induction of DNA DSB is triggered by AtSPO11-1 (Grelon et al., 2001; Stacey et al., 2006). These DSBs are not completely repaired in the absence of SYN1. Therefore, chromosome fragments were found at metaphase I. Previous studies have focussed on the role of SYN1 in sister chromatid cohesion. To investigate this other aspect of SYN1, I studied the role it plays in an *AtDMC1* mutant. *AtDMC1* is an *Arabidopsis* orthologue of yeast *DMC1*. DMC1 promotes interhomologue recombination which is an essential process for the formation of the synaptonemal complex during early prophase I (Bishop et al., 1992; Couteau et al., 1999; Sanchez-Moran et al., 2007). In an *Atdmc1* mutant, chromosome fragmentation was not seen throughout the meiosis program. It has been suggested that either DSBs are not formed in the absence of AtDMC1, or AtSPO11-1 induced DSBs are fully repaired in the *Atdmc1* mutant (Couteau et al., 1999). The cytological analysis of *syn1^{-/-}/Atdmc1^{-/-}* showed that chromosome fragments were found during early prophase I. This indicates that the DSBs are formed in the *Atdmc1* mutant. These DSBs are then repaired early in the meiotic recombination in the presence of SYN1, resulting in 10 univalents aligned on metaphase plate without chromosome fragments. Thus, I suggest that SYN1 plays an important role in DSB repair. Immunolocalization of SYN1 has shown that loading of SYN1 can be restored in cisplatin treated *Atspo11-1-4^{-/-}*, suggesting that some SYN1 loading is dependent on DNA DSBs induced by AtSPO11-1. I hypothesize that the meiotic cohesin subunit SYN1 accumulates on the DSB site to stabilize the broken DNA. This stabilization allows the DNA repair proteins to load correctly on the DSB sites.

5.3.6 SYN1 and AtRAD51c are essential for DNA double strand break repair.

I propose that SYN1 is essential for DNA DSB repair, but we still have no idea whether SYN1 associates with recombination proteins during the initial event of meiotic recombination. To investigate the interaction between SYN1 and recombination protein, I selected AtRAD51C, an *Arabidopsis* RAD51C orthologue. Cytological analysis of *Atrad51c*^{-/-} showed thin threads and unsynapsed chromosomes during early prophase I. In contrast, tangled and less condensed chromatin structure was observed in *Atrad51c*^{-/-}/*syn1*^{-/-}, which resembles to the meiocytes of *syn1*^{-/-}, indicating that chromatin structure is affected during early prophase I when SYN1 is deleted from *Atrad51c*^{-/-} mutant. Furthermore, fused and fragmented chromosomes in *Atrad51c*^{-/-} were found during the first meiotic division. A previous report (Li et al., 2005) has shown that the chromosome fragmentation of *Atrad51c* is rescued in the *Atspo11-1* mutant. It has been suggested that AtRAD51C plays an important role in DNA DSB repair (Bleuyard and White, 2004; Li et al., 2004; Bleuyard et al., 2005). In *syn1*^{-/-}/*Atrad51c*^{-/-}, tangled and fragmented chromosomes were also found during metaphase I and anaphase I. This phenotype resembles the meiocytes of *Atrad51c*^{-/-} or *syn1*^{-/-}. Currently, I could not draw a conclusion based on this cytological analysis. Biochemical methods such as chromatin immunoprecipitation (ChIP) and yeast two hybrid (Y2H) could be used to investigate the interaction of SYN1 and AtRAD51C during DNA DSB repair.

5.3.7 Seeds of wild-type and *SYN1* heterozygous plants grow slowly in cisplatin MS medium.

I have shown that the *SYN1* gene transcript was detected in both flower buds and mature leaves. According to previous reports (Bai et al., 1999; Bhatt et al., 1999), *SYN1* is also expressed in seedlings of wild-type. This indicates that the *SYN1* expression is in both reproductive and vegetative tissues. It is important to examine whether SYN1 protein has a role in mitotic cells during DNA double strand breaks. To do so, seeds of *SYN1* heterozygous, *SYN1*^{+/-}, plants were grown on different concentrations of cisplatin (0μM; 12.5μM; 25μM; 50μM) while seeds of wild-type (Col 0) plants were grown in parallel as a control. The three week old seedlings were collected and weighed for statistical analysis. The analysis showed no significant difference between the wild-type and *SYN1*^{+/-} growing in the same concentration of cisplatin. This indicates that the seedlings from the *SYN1*^{+/-} plants were not affected dramatically in cisplatin/MS medium compared to the seedlings of wild-type. However, I cannot conclude that SYN1 is not required in mitotic cells during DNA DSB repair because the results from this experiment are inconclusive. This is due to 75% of the seeds from *SYN1*^{+/-} plant carrying at least a single copy of a functional *SYN1* gene which is enough for them to function as wild-type. For example, 50% wild-type seedlings produced true leaves at 14 day after germination on 12.5μM cisplatin MS medium. In the same condition, 30% of *SYN1*^{+/-} seedlings produced true leaves, which is very close to half of the 75% seedlings from *SYN1*^{+/-} plant (75% seeds from *SYN1*^{+/-} are divided by 2=37.5%). Therefore, it is biased to make a conclusion in this experiment. Recently, a report showed that the meiotic cohesin REC8 is expressed in human tumour cells after gamma irradiation (Erenpreisa et al., 2009). It is necessary to re-investigate the role of SYN1 in mitotic cells. Future studies will examine cisplatin sensitivity in cultured cells derived from wild-type and

syn1^{-/-}. Indeed, this experimental design will provide more convincing data.

APPENDIX 5.1. Signal intensity analysis of SYN1 on prophase I nuclei of wild-type, cisplatin-treated *Atspoll-1-4^{-/-}* and cisplatin free *Atspoll-1-4^{-/-}*.

	Col 0	<i>Atspoll-1-4^{-/-}</i> with cisplatin	<i>Atspoll-1-4^{-/-}</i> without cisplatin
1	79.106	38.457	28.251
2	111.44	51.38	19.292
3	89.241	44.537	3.656
4	93.176	42.411	22.953
5	73.012	60.64	14.62
6	42.873	60.533	0.856
7	80.394	60.636	28.282
8	46.075	42.925	10.516
9	44.864	53.865	17.735
10	58.082	50.349	11.618
11	29.171	42.955	26.971
12	72.667	38.936	25.128
13	52.933	68.012	25.957
14	42.713	36.057	10.749
15	42.714	68.636	24.088
16	48.126	59.565	8.075
17	59.884	48.199	5.075
18	40.172	61.178	42.779*
19	48.281	36.162	35.372*
20	56.289	44.328	50.257*
21	42.915	39.888	2.074
22	43.442	83.885	4.131
23	65.099	68.35	14.514
24	46.783	62.562	15.116
25	37.371	50.317	22.925
26	48.653	54.037	7.98
27	61.8	50.794	7.171
28	73.737	46.834	37.921
29	60.189	84.449	15.988
30	43.233	58.91	7.247
31	46.734	77.522	25.975
32	84.653	42.05	20.986
33	71.162	46.453	13.741
34	110.547	35.067	4.287
35	99.241	54.951	4.733
36	58.756	38.723	5.398
37	78.196	65.258	7.564
38	79.737	41.012	34.88
39	97.468	61.55	16.55
40	55.131	40.814	26.111
41	48.25	37.206	11.045
42	48.486	47.411	22.128
43	49.818	46.522	8.53
44	31.443	54.943	30.762
45	56.354	46.369	13.878
46	45.927	56.599	29.67
47	67.34	34.623	18.342
48	60.206	58.501	11.257
49	74.141	60.587	21.034
50	54.484	64.96	41.352*
SUM	3052.509	2620.908	915.52
Average	61.05018	52.41816	18.3104
STDEVP	19.887303	12.37164835	11.70871021
Standard error	2.81251633	1.749632068	1.655877558

Chapter 6

Conclusions

6.1 Introduction

SYN1 has been reported to be the *Arabidopsis* homologue of *REC8* (Bai et al., 1999; Bhatt et al., 1999). However, the function of *SYN1* in meiosis remains poorly understood. The aim of this research was to confirm whether *SYN1* has a role in sister chromatid cohesion and DNA DSB repair during early meiosis.

6.2. Is *SYN1* important in sister chromatid cohesion?

Previously, *SYN1* gene has been cloned and encodes a protein with similarity to *S. pombe* *RAD21/REC8* and *RAD21*-like proteins including frog *RAD21*, fission yeast *RAD21* and Human *RAD21* (Bai et al., 1999). This report revealed that *SYN1* is most similar (18% identity) to frog *RAD21* with great similarity at their N- and C-termini but little similarity at the middle region of the protein. According to the current BLAST database search, I have confirmed that *SYN1* is most similar (41% identity) to maize and rice *REC8* homologues, *AFD1* and *OsRAD21-4* (Figure 3.11). Our cytological analysis of *syn1* mutant showed that abnormal thin thread structure forming less condensed chromatin was observed during early prophase I (Figure 3.7A and B; Figure 3.9B), that has not been found and described in previous work (Bai et al., 1999; Bhatt et al., 1999). Chromosomes were also observed as tangled structures revealing unpaired homologous chromosomes (Figure 3.7C; D). If *SYN1* has a role in sister chromatid cohesion then I expect to see a less condensed chromatin structure. However, I discovered that centromeres of sister chromatids were associated during early prophase I but separated apart at metaphase I (Figure 3.9), indicating that a centromeric

cohesion is present in the *syn1* mutant during early prophase I. This finding was carried out with using centromeric FISH probes. Does SYN1 have a role in sister chromatid cohesion? To answer this question, I obtained the cytological evidence from *Atspo11-1-4^{-/-}xsyn1^{-/-}* showing that 10 univalents were found during diakinesis-like and metaphase I stages (Figure 5.2). This indicates that cohesion is still present between sister chromatids. However, cohesion is lost at sister centromeres during anaphase I. Therefore, sister chromatids are separated into opposite spindle poles. This observation suggests that SYN1 plays a crucial role at sister centromere cohesion during the first meiotic division. Currently, we do not know which proteins, in *Atspo11-1-4^{-/-}xsyn1^{-/-}*, maintain the sister chromatid cohesion during early prophase I. According to the yeast and mammalian reports, the mitotic kleisin subunit SCC1/RAD21 and meiotic kleisin subunit REC8 coexist at the sister chromatids in wild-type meiocytes (Klein et al., 1999; Prieto et al., 2004). I believe that this finding also applies to *Arabidopsis*. I propose that the cohesion of sister chromatids in *Atspo11-1-4^{-/-}xsyn1^{-/-}* is maintained by the mitotic kleisin subunit SYN2 and SYN4 during early prophase I. Therefore, 10 pairs of sister chromatids are detectable.

Does SYN1 affect other cohesin subunits? I have evidence to show that AtSCC3 signal was not detectable in the *syn1* meiocytes, indicating that loading of AtSCC3 on chromosomes is affected (Figure 4.17). Interestingly, abnormal fuzzy signal of AtSMC3 was observed in the *syn1* meiocytes (Figure 4.18). It is thought that AtSMC3 appears on chromosome before SYN1. However, the SMC3 could not form a stable cohesin complex when SYN1 was absent. As a consequence, fuzzy AtSMC3 signal was found during prophase I. These observations suggest that loading of cohesins, AtSCC3 and AtSMC3, on the chromosome is dependent on SYN1.

6.3 SYN1 is essential for meiotic recombination progression and SC polymerization/elongation.

Mutation of yeast REC8 revealed that axial elements are not formed, suggesting that cohesin is essential for the formation of SC (Klein et al., 1999). In mammals, it has been proposed that a platform for axial element assembly is provided by REC8 forming a so-called AE-like structure during meiotic S-phase (Eijpe et al., 2003). Interestingly, axis-associated protein ASY1, in the *syn1* mutant, appeared as aggregates in early meiosis, developing into abnormal linear signals in later stages. Furthermore, short SC protein, AtZYP1, colocalized with ASY1 (Figure 4.24), indicating that both axis formation and synapsis are compromised in the absence of SYN1. Previously, transmission electron microscopy (TEM) analysis revealed that short SC structure with distinct lateral elements is observed in the *syn1* mutant (Zhao et al., 2006). This report is entirely consistent with our finding. A similar phenotype is also found in the absence of AFD1, maize REC8 homologue (Golubovskaya et al., 2006). These observations suggest that SYN1 is not essential for formation of axial/lateral elements but is required for SC polymerization and elongation. A previous report suggests that ASY1 plays a role in coordinating the activity of meiotic recombination protein (Sanchez-Moran et al., 2007). Abnormal ASY1 in the *syn1* mutant might affect the distribution of recombination proteins. Our finding showed that both recombination proteins AtRAD51 and AtMLH1 appear as aggregates, which predominately co-localises with ASY1 (Figure 4.25; 4.26). This indicates that the processes of meiotic recombination including synapsis and DNA repair are affected in the absence of SYN1. This may be why short SC and chromosome fragmentation occur in the *syn1* mutant.

6.4 SYN1 plays an important role during DNA double strand break (DSB) repair

Although I propose that mitotic and meiotic kleisin cohesins coexist during early prophase I, the mitotic kleisin cohesin cannot function as SYN1 does, because severe chromosome fragmentation appears in the absence of SYN1. This fragmentation phenotype is also found in other REC8 mutants including maize *afd1*, *Sordaria sm-rec8*, mouse *rec8*, worm *rec8* and rice OsRAD21-4 depletion line (Yu and Dawe, 2000; Pasierbek et al., 2001; Xu et al., 2005; Zhang et al., 2006; Storlazzi et al., 2008). To determine the basis of chromosome fragmentation in the *syn1* mutant, I studied the double knockout mutant of *SYN1* and *AtSPO11-1* genes. Cytological analysis showed that background chromosome fragments were not seen at any stage of meiosis, indicating that chromosome fragmentation of *syn1* was rescued by the *Atspo11-1-4* mutant (Figure 5.2). In *C. elegans* and *S. macrospora* reports also showed that *spoil* mutation suppresses chromosome fragmentation of REC8 depletion line/*sm-rec8* mutant (Pasierbek et al., 2001; Storlazzi et al., 2008). This indicates that chromosome fragmentation in the *syn1* mutant is triggered by AtSPO11.

To further investigate the role of SYN1 in meiosis, I studied the phenotype of mutated *AtDMC1*, an *Arabidopsis* ortholog of yeast *DMC1*. DMC1 promotes interhomologue recombination, an essential process for the formation of the synaptonemal complex during meiosis I (Bishop et al., 1992; Couteau et al., 1999; Sanchez-Moran et al., 2007). Cytological analysis in *Atdmc1* mutant showed that chromosome fragmentation was not seen throughout the meiosis program (Figure 5.10). In contrast to *Atdmc1*^{-/-}, less condensed and tangled chromosome structure and fragments were found in the *syn1*^{-/-} x *Atdmc1*^{-/-} double mutant (Figure 5.11). This phenotype resembles to those seen in the *syn1*^{-/-} meiocytes, indicating that DSBs induced by AtSPO11-1 are restored in the absence of AtDMC1, but they are not fully

repaired when SYN1 was deleted in the *Atdmc1* mutant. This observation suggests that SYN1 plays an important role during DNA DSB repair.

I have shown that chromosome fragmentation in the *syn1* mutant is triggered by AtSPO11-1. It is important to investigate the distribution of SYN1 in the absence of AtSPO11-1. Immunolocalization result showed that signal of SYN1 was substantially reduced in *Atspo11-1-4^{-/-}* (Figure 5.5; 5.6). A similar reduction of REC8 is also observed in the yeast *spo11^{-/-}* meocytes (Beth Weiner, Personal communication). According to yeast studies, SPO11 associates at the REC8 binding sites around the time of meiotic S phase (Kugou et al., 2009). It is highly possible that the AtSPO11-1 associates to some of the SYN1 binding sites at the time of DNA replication. This association might be the reason that a large amount of SYN1 persists on chromosomes throughout meiosis I. Therefore, some SYN1 loading on the chromosomes might be regulated by AtSPO11-1.

To further investigate the loading of SYN1, *Atspo11-1-4^{-/-}* meocytes were treated with cisplatin, a platinum chemical complex which reacts with DNA to create a DSB. Immunolocalization studies showed that signal of SYN1 was increased on chromosomes of cisplatin-treated *Atspo11-1-4^{-/-}*, compared with untreated *Atspo11-1-4^{-/-}* (Figure 5.6). This indicates that loading of SYN1 can be restored in *Atspo11* mutant by artificially inducing DSB formation with cisplatin. This observation suggests that some SYN1 loading is dependent on DNA DSB induced by AtSPO11-1. Studies in yeast mitotic cells have shown that cohesin is recruited to DSB sites where it might facilitate DSB repair (Strom et al., 2004; Lowndes and Toh, 2005). I hypothesize that the meiotic kleisin subunit SYN1 loads on the chromosome at two different stages. (1) SYN1 gradually replaces mitotic kleisin cohesins and

then loads on sister chromatids during meiotic S-phase. Some mitotic kleisin subunit is still retained at the sister chromatids but it cannot function as SYN1 does. (2) During leptotene and zygotene stages, SYN1 is recruited to the DSB site forming patchy domains to stabilize the broken DNA. This stabilization allows the DNA repair proteins to load correctly on the DSB sites (Figure 6.1).

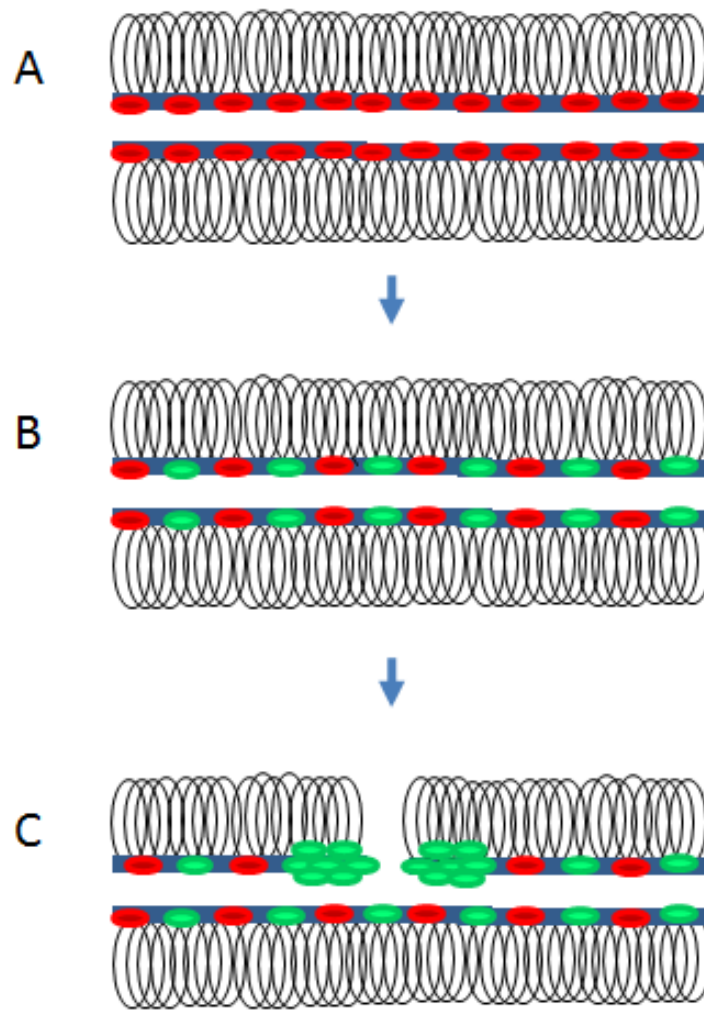


Figure 6.1. Loading of SYN1 in two different meiotic stages

- (A) During premeiotic S-phase, mitotic kleisin cohesins (●) appear on the sister chromatids.
- (B) Mitotic kleisin cohesins are gradually replaced by meiotic kleisin cohesin SYN1 (●) during S phase.
- (C) SYN1 is recruited to the DNA DSB site forming a domain to stabilize the DNA during leptotene and zygotene stages.

6.5 Future work (Further experiments to verify the role of SYN1)

A previous report suggested that SYN1 does not appear at centromere during early prophase I (Cai et al., 2003). However, immunostaining of SYN1 revealed that protein was detectable as a continuous signal along the chromosome during pachytene, suggesting that SYN1 could be present at centromeres. In the future, it is necessary to combine the immunostaining of SYN1 with FISH using centromeric probes to confirm the appearance of SYN1 in the centromeric region.

Cytological analysis of double knock-out, *syn1^{-/-} x Atdmc1^{-/-}* and *syn1^{-/-} x Atspo11-1-4^{-/-}* revealed that SYN1 plays a crucial role in DNA DSB repair during early prophase I. However, I have no evidence to suggest that SYN1 is directly involved with DNA repair proteins to restore the DNA broken region. In the future, biochemistry methods such as chromatin immunoprecipitation (ChIP) and yeast two hybrid (Y2H) can be used to study the relationship between SYN1 and DNA repair proteins during the formation of DSB. These experiments will provide new insights into the role of SYN1 during meiotic DNA DSB repair.

Does SYN1 have a role in mitosis? Our gene expression studies showed that *SYN1* gene transcript was detected in both flower buds and mature leaves. Previous reports (Bai et al., 1999; Bhatt et al., 1999) showed that *SYN1* is also expressed in seedlings of wild-type, suggesting that *SYN1* is expressed in mitotic and meiotic cells. Recent report showed that the meiotic cohesin REC8 is expressed in human tumour cells after gamma irradiation (Erenpreisa et al., 2009). Therefore, it is necessary to investigate the role of SYN1 in mitotic cells during DNA DSB. I do not support using seeds from heterozygous plants in these experiments because approximately 75% seeds contain wild-type *SYN1* gene. Therefore, the

result would be misleading. Cultured cells derived from wild-type and *synI* mutant will be examined in MS agar medium with different concentration of cisplatin to test their cisplatin sensitivity. This experiment will provide more convincing data.

Chapter 7

References

- Abe, K., Osakabe, K., Nakayama, S., Endo, M., Tagiri, A., Todoriki, S., Ichikawa, H., and Toki, S.** (2005). *Arabidopsis* RAD51C gene is important for homologous recombination in meiosis and mitosis. *Plant Physiol* **139**, 896-908.
- Akutsu, N., Iijima, K., Hinata, T., and Tauchi, H.** (2007). Characterization of the plant homolog of Nijmegen breakage syndrome 1: Involvement in DNA repair and recombination. *Biochem Biophys Res Commun* **353**, 394-398.
- Albala, J.S., Thelen, M.P., Prange, C., Fan, W., Christensen, M., Thompson, L.H., and Lennon, G.G.** (1997). Identification of a novel human RAD51 homolog, RAD51B. *Genomics* **46**, 476-479.
- Allers, T., and Lichten, M.** (2001). Differential timing and control of noncrossover and crossover recombination during meiosis. *Cell* **106**, 47-57.
- Anderson, L.K., Royer, S.M., Page, S.L., McKim, K.S., Lai, A., Lilly, M.A., and Hawley, R.S.** (2005). Juxtaposition of C(2)M and the transverse filament protein C(3)G within the central region of *Drosophila* synaptonemal complex. *Proc Natl Acad Sci U S A* **102**, 4482-4487.
- Argueso, J.L., Wanat, J., Gemici, Z., and Alani, E.** (2004). Competing crossover pathways act during meiosis in *Saccharomyces cerevisiae*. *Genetics* **168**, 1805-1816.
- Armstrong, S.J., and Jones, G.H.** (2003). Meiotic cytology and chromosome behaviour in wild-type *Arabidopsis thaliana*. *J Exp Bot* **54**, 1-10.
- Armstrong, S.J., Franklin F.C.H., and Jones G.H.** (2003). A meiotic time-course for *Arabidopsis thaliana*. *Sex Plant Reprod* **16**:141-149.
- Armstrong, S.J., Franklin, F.C., and Jones, G.H.** (2001). Nucleolus-associated telomere clustering and pairing precede meiotic chromosome synapsis in *Arabidopsis thaliana*. *J Cell Sci* **114**, 4207-4217.
- Armstrong, S.J., Sanchez-Moran, E., and Franklin, F.C.** (2009). Cytological analysis of *Arabidopsis thaliana* meiotic chromosomes. *Methods Mol Biol* **558**, 131-145.
- Armstrong, S.J., Caryl, A.P., Jones, G.H., and Franklin, F.C.** (2002). Asy1, a protein required for meiotic chromosome synapsis, localizes to axis-associated chromatin in *Arabidopsis* and *Brassica*. *J Cell Sci* **115**, 3645-3655.
- Bai, X., Peirson, B.N., Dong, F., Xue, C., and Makaroff, C.A.** (1999). Isolation and

characterization of SYN1, a RAD21-like gene essential for meiosis in *Arabidopsis*. *Plant Cell* **11**, 417-430.

- Berchowitz, L.E., Francis, K.E., Bey, A.L., and Copenhaver, G.P.** (2007). The role of AtMUS81 in interference-insensitive crossovers in *A. thaliana*. *PLoS Genet* **3**, e132.
- Bergerat, A., de Massy, B., Gadelle, D., Varoutas, P.C., Nicolas, A., and Forterre, P.** (1997). An atypical topoisomerase II from Archaea with implications for meiotic recombination. *Nature* **386**, 414-417.
- Bhatt, A.M., Lister, C., Page, T., Fransz, P., Findlay, K., Jones, G.H., Dickinson, H.G., and Dean, C.** (1999). The DIF1 gene of *Arabidopsis* is required for meiotic chromosome segregation and belongs to the REC8/RAD21 cohesin gene family. *Plant J* **19**, 463-472.
- Birkenbihl, R.P., and Subramani, S.** (1992). Cloning and characterization of rad21 an essential gene of *Schizosaccharomyces pombe* involved in DNA double-strand-break repair. *Nucleic Acids Res* **20**, 6605-6611.
- Birnboim, H.C., and Doly, J.** (1979). A rapid alkaline extraction procedure for screening recombinant plasmid DNA. *Nucleic Acids Res* **7**, 1513-1523.
- Bishop, D.K.** (1994). RecA homologs Dmc1 and Rad51 interact to form multiple nuclear complexes prior to meiotic chromosome synapsis. *Cell* **79**, 1081-1092.
- Bishop, D.K., and Zickler, D.** (2004). Early decision; meiotic crossover interference prior to stable strand exchange and synapsis. *Cell* **117**, 9-15.
- Bishop, D.K., Park, D., Xu, L., and Kleckner, N.** (1992). DMC1: a meiosis-specific yeast homolog of *E. coli* recA required for recombination, synaptonemal complex formation, and cell cycle progression. *Cell* **69**, 439-456.
- Bleuyard, J.Y., and White, C.I.** (2004). The *Arabidopsis* homologue of Xrcc3 plays an essential role in meiosis. *EMBO J* **23**, 439-449.
- Bleuyard, J.Y., Gallego, M.E., and White, C.I.** (2004a). The atspo11-1 mutation rescues atxrcc3 meiotic chromosome fragmentation. *Plant Mol Biol* **56**, 217-224.
- Bleuyard, J.Y., Gallego, M.E., and White, C.I.** (2004b). Meiotic defects in the *Arabidopsis* rad50 mutant point to conservation of the MRX complex function in early stages of meiotic recombination. *Chromosoma* **113**, 197-203.
- Bleuyard, J.Y., Gallego, M.E., Savigny, F., and White, C.I.** (2005). Differing requirements for the *Arabidopsis* Rad51 paralogs in meiosis and DNA repair. *Plant J* **41**, 533-545.
- Borner, G.V., Kleckner, N., and Hunter, N.** (2004). Crossover/noncrossover differentiation, synaptonemal complex formation, and regulatory surveillance at the leptotene/zygotene transition of meiosis. *Cell* **117**, 29-45.

- Bundock, P., and Hooykaas, P.** (2002). Severe developmental defects, hypersensitivity to DNA-damaging agents, and lengthened telomeres in *Arabidopsis* MRE11 mutants. *Plant Cell* **14**, 2451-2462.
- Buonomo, S.B., Clyne, R.K., Fuchs, J., Loidl, J., Uhlmann, F., and Nasmyth, K.** (2000). Disjunction of homologous chromosomes in meiosis I depends on proteolytic cleavage of the meiotic cohesin Rec8 by separin. *Cell* **103**, 387-398.
- Burgess, S.M.** (2002). Homologous chromosome associations and nuclear order in meiotic and mitotically dividing cells of budding yeast. *Adv Genet* **46**, 49-90.
- Cai, X., Dong, F., Edelmann, R.E., and Makaroff, C.A.** (2003). The *Arabidopsis* SYN1 cohesin protein is required for sister chromatid arm cohesion and homologous chromosome pairing. *J Cell Sci* **116**, 2999-3007.
- Caryl, A.P., Armstrong, S.J., Jones, G.H., and Franklin, F.C.** (2000). A homologue of the yeast HOP1 gene is inactivated in the *Arabidopsis* meiotic mutant *asy1*. *Chromosoma* **109**, 62-71.
- Cha, R.S., Weiner, B.M., Keeney, S., Dekker, J., and Kleckner, N.** (2000). Progression of meiotic DNA replication is modulated by interchromosomal interaction proteins, negatively by Spo11p and positively by Rec8p. *Genes Dev* **14**, 493-503.
- Chelysheva, L., Diallo, S., Vezon, D., Gendrot, G., Vrielynck, N., Belcram, K., Rocques, N., Marquez-Lema, A., Bhatt, A.M., Horlow, C., Mercier, R., Mezard, C., and Grelon, M.** (2005). AtREC8 and AtSCC3 are essential to the monopolar orientation of the kinetochores during meiosis. *J Cell Sci* **118**, 4621-4632.
- Chen, C., Zhang, W., Timofejeva, L., Gerardin, Y., and Ma, H.** (2005). The *Arabidopsis* ROCK-N-ROLLERS gene encodes a homolog of the yeast ATP-dependent DNA helicase MER3 and is required for normal meiotic crossover formation. *Plant J* **43**, 321-334.
- Ciosk, R., Zachariae, W., Michaelis, C., Shevchenko, A., Mann, M., and Nasmyth, K.** (1998). An ESP1/PDS1 complex regulates loss of sister chromatid cohesion at the metaphase to anaphase transition in yeast. *Cell* **93**, 1067-1076.
- Ciosk, R., Shirayama, M., Shevchenko, A., Tanaka, T., Toth, A., and Nasmyth, K.** (2000). Cohesin's binding to chromosomes depends on a separate complex consisting of Scc2 and Scc4 proteins. *Mol Cell* **5**, 243-254.
- Cnudde, F., and Gerats, T.** (2005). Meiosis: inducing variation by reduction. *Plant Biol (Stuttg)* **7**, 321-341.
- Cohen-Fix, O., Peters, J.M., Kirschner, M.W., and Koshland, D.** (1996). Anaphase initiation in *Saccharomyces cerevisiae* is controlled by the APC-dependent degradation of the anaphase inhibitor Pds1p. *Genes Dev* **10**, 3081-3093.

- Connelly, J.C., and Leach, D.R.** (2002). Tethering on the brink: the evolutionarily conserved Mre11-Rad50 complex. *Trends Biochem Sci* **27**, 410-418.
- Copenhaver, G.P., Housworth, E.A., and Stahl, F.W.** (2002). Crossover interference in *Arabidopsis*. *Genetics* **160**, 1631-1639.
- Couteau, F., Belzile, F., Horlow, C., Grandjean, O., Vezon, D., and Doutriaux, M.P.** (1999). Random chromosome segregation without meiotic arrest in both male and female meiocytes of a *dmc1* mutant of *Arabidopsis*. *Plant Cell* **11**, 1623-1634.
- da Costa-Nunes, J.A., Bhatt, A.M., O'Shea, S., West, C.E., Bray, C.M., Grossniklaus, U., and Dickinson, H.G.** (2006). Characterization of the three *Arabidopsis thaliana* RAD21 cohesins reveals differential responses to ionizing radiation. *J Exp Bot* **57**, 971-983.
- Daoudal-Cotterell, S., Gallego, M.E., and White, C.I.** (2002). The plant Rad50-Mre11 protein complex. *FEBS Lett* **516**, 164-166.
- Dawe, R.K., Sedat, J.W., Agard, D.A., and Cande, W.Z.** (1994). Meiotic chromosome pairing in maize is associated with a novel chromatin organization. *Cell* **76**, 901-912.
- de los Santos, T., Hunter, N., Lee, C., Larkin, B., Loidl, J., and Hollingsworth, N.M.** (2003). The Mus81/Mms4 endonuclease acts independently of double-Holliday junction resolution to promote a distinct subset of crossovers during meiosis in budding yeast. *Genetics* **164**, 81-94.
- De Silva, I.U., McHugh, P.J., Clingen, P.H., and Hartley, J.A.** (2002). Defects in interstrand cross-link uncoupling do not account for the extreme sensitivity of ERCC1 and XPF cells to cisplatin. *Nucleic Acids Res* **30**, 3848-3856.
- Dernburg, A.F., McDonald, K., Moulder, G., Barstead, R., Dresser, M., and Villeneuve, A.M.** (1998). Meiotic recombination in *C. elegans* initiates by a conserved mechanism and is dispensable for homologous chromosome synapsis. *Cell* **94**, 387-398.
- Dong, F., Cai, X., and Makaroff, C.A.** (2001). Cloning and characterization of two *Arabidopsis* genes that belong to the RAD21/REC8 family of chromosome cohesin proteins. *Gene* **271**, 99-108.
- Dosanjh, M.K., Collins, D.W., Fan, W., Lennon, G.G., Albala, J.S., Shen, Z., and Schild, D.** (1998). Isolation and characterization of RAD51C, a new human member of the RAD51 family of related genes. *Nucleic Acids Res* **26**, 1179-1184.
- Doutriaux, M.P., Couteau, F., Bergounioux, C., and White, C.** (1998). Isolation and characterisation of the RAD51 and DMC1 homologs from *Arabidopsis thaliana*. *Mol Gen Genet* **257**, 283-291.
- Eijpe, M., Heyting, C., Gross, B., and Jessberger, R.** (2000). Association of mammalian

SMC1 and SMC3 proteins with meiotic chromosomes and synaptonemal complexes. *J Cell Sci* **113** (Pt 4), 673-682.

- Eijpe, M., Offenbergh, H., Jessberger, R., Revenkova, E., and Heyting, C.** (2003). Meiotic cohesin REC8 marks the axial elements of rat synaptonemal complexes before cohesins SMC1beta and SMC3. *J Cell Biol* **160**, 657-670.
- Erenpreisa, J., Cragg, M.S., Salmina, K., Hausmann, M., and Scherthan, H.** (2009). The role of meiotic cohesin REC8 in chromosome segregation in gamma irradiation-induced endopolyploid tumour cells. *Exp Cell Res* **315**, 2593-2603.
- Franklin, F.C., Higgins, J.D., Sanchez-Moran, E., Armstrong, S.J., Osman, K.E., Jackson, N., and Jones, G.H.** (2006). Control of meiotic recombination in *Arabidopsis*: role of the MutL and MutS homologues. *Biochem Soc Trans* **34**, 542-544.
- Funabiki, H., Yamano, H., Kumada, K., Nagao, K., Hunt, T., and Yanagida, M.** (1996). Cut2 proteolysis required for sister-chromatid separation in fission yeast. *Nature* **381**, 438-441.
- Gallego, M.E., Jeanneau, M., Granier, F., Bouchez, D., Bechtold, N., and White, C.I.** (2001). Disruption of the *Arabidopsis* RAD50 gene leads to plant sterility and MMS sensitivity. *Plant J* **25**, 31-41.
- Gimenez-Abian, J.F., Sumara, I., Hirota, T., Hauf, S., Gerlich, D., de la Torre, C., Ellenberg, J., and Peters, J.M.** (2004). Regulation of sister chromatid cohesion between chromosome arms. *Curr Biol* **14**, 1187-1193.
- Golubovskaya, I.N., Harper, L.C., Pawlowski, W.P., Schichnes, D., and Cande, W.Z.** (2002). The pam1 gene is required for meiotic bouquet formation and efficient homologous synapsis in maize (*Zea mays* L.). *Genetics* **162**, 1979-1993.
- Golubovskaya, I.N., Hamant, O., Timofejeva, L., Wang, C.J., Braun, D., Meeley, R., and Cande, W.Z.** (2006). Alleles of *afd1* dissect REC8 functions during meiotic prophase I. *J Cell Sci* **119**, 3306-3315.
- Gorr, I.H., Boos, D., and Stemmann, O.** (2005). Mutual inhibition of separase and Cdk1 by two-step complex formation. *Mol Cell* **19**, 135-141.
- Grelon, M., Vezon, D., Gendrot, G., and Pelletier, G.** (2001). AtSPO11-1 is necessary for efficient meiotic recombination in plants. *EMBO J* **20**, 589-600.
- Gruber, S., Haering, C.H., and Nasmyth, K.** (2003). Chromosomal cohesin forms a ring. *Cell* **112**, 765-777.
- Gruber, S., Arumugam, P., Katou, Y., Kuglitsch, D., Helmhart, W., Shirahige, K., and Nasmyth, K.** (2006). Evidence that loading of cohesin onto chromosomes involves opening of its SMC hinge. *Cell* **127**, 523-537.

- Guacci, V., Hogan, E., and Koshland, D.** (1994). Chromosome condensation and sister chromatid pairing in budding yeast. *J Cell Biol* **125**, 517-530.
- Guacci, V., Koshland, D., and Strunnikov, A.** (1997). A direct link between sister chromatid cohesion and chromosome condensation revealed through the analysis of MCD1 in *S. cerevisiae*. *Cell* **91**, 47-57.
- Haering, C.H., and Nasmyth, K.** (2003). Building and breaking bridges between sister chromatids. *Bioessays* **25**, 1178-1191.
- Haering, C.H., Lowe, J., Hochwagen, A., and Nasmyth, K.** (2002). Molecular architecture of SMC proteins and the yeast cohesin complex. *Mol Cell* **9**, 773-788.
- Haering, C.H., Schoffnegger, D., Nishino, T., Helmhart, W., Nasmyth, K., and Lowe, J.** (2004). Structure and stability of cohesin's Smc1-kleisin interaction. *Mol Cell* **15**, 951-964.
- Hartung, F., and Puchta, H.** (2000). Molecular characterisation of two paralogous SPO11 homologues in *Arabidopsis thaliana*. *Nucleic Acids Res* **28**, 1548-1554.
- Hartung, F., and Puchta, H.** (2001). Molecular characterization of homologues of both subunits A (SPO11) and B of the archaeobacterial topoisomerase 6 in plants. *Gene* **271**, 81-86.
- Hartung, F., Angelis, K.J., Meister, A., Schubert, I., Melzer, M., and Puchta, H.** (2002). An archaeobacterial topoisomerase homolog not present in other eukaryotes is indispensable for cell proliferation of plants. *Curr Biol* **12**, 1787-1791.
- Hartung, F., Wurz-Wildersinn, R., Fuchs, J., Schubert, I., Suer, S., and Puchta, H.** (2007). The catalytically active tyrosine residues of both SPO11-1 and SPO11-2 are required for meiotic double-strand break induction in *Arabidopsis*. *Plant Cell* **19**, 3090-3099.
- Hauf, S., Waizenegger, I.C., and Peters, J.M.** (2001). Cohesin cleavage by separase required for anaphase and cytokinesis in human cells. *Science* **293**, 1320-1323.
- Hauf, S., Roitinger, E., Koch, B., Dittrich, C.M., Mechtler, K., and Peters, J.M.** (2005). Dissociation of cohesin from chromosome arms and loss of arm cohesion during early mitosis depends on phosphorylation of SA2. *PLoS Biol* **3**, e69.
- Heidinger-Pauli, J.M., Unal, E., Guacci, V., and Koshland, D.** (2008). The kleisin subunit of cohesin dictates damage-induced cohesion. *Mol Cell* **31**, 47-56.
- Heidmann, D., Horn, S., Heidmann, S., Schleiffer, A., Nasmyth, K., and Lehner, C.F.** (2004). The *Drosophila* meiotic kleisin C(2)M functions before the meiotic divisions. *Chromosoma* **113**, 177-187.

- Heo, S.J., Tatebayashi, K., Kato, J., and Ikeda, H.** (1998). The RHC21 gene of budding yeast, a homologue of the fission yeast rad21+ gene, is essential for chromosome segregation. *Mol Gen Genet* **257**, 149-156.
- Higgins, J.D., Armstrong, S.J., Franklin, F.C., and Jones, G.H.** (2004). The *Arabidopsis* MutS homolog AtMSH4 functions at an early step in recombination: evidence for two classes of recombination in *Arabidopsis*. *Genes Dev* **18**, 2557-2570.
- Higgins, J.D., Buckling, E.F., Franklin, F.C., and Jones, G.H.** (2008a). Expression and functional analysis of AtMUS81 in *Arabidopsis* meiosis reveals a role in the second pathway of crossing-over. *Plant J* **54**, 152-162.
- Higgins, J.D., Sanchez-Moran, E., Armstrong, S.J., Jones, G.H., and Franklin, F.C.** (2005). The *Arabidopsis* synaptonemal complex protein ZYP1 is required for chromosome synapsis and normal fidelity of crossing over. *Genes Dev* **19**, 2488-2500.
- Higgins, J.D., Vignard, J., Mercier, R., Pugh, A.G., Franklin, F.C., and Jones, G.H.** (2008b). AtMSH5 partners AtMSH4 in the class I meiotic crossover pathway in *Arabidopsis thaliana*, but is not required for synapsis. *Plant J* **55**, 28-39.
- Hopfner, K.P., Karcher, A., Shin, D.S., Craig, L., Arthur, L.M., Carney, J.P., and Tainer, J.A.** (2000). Structural biology of Rad50 ATPase: ATP-driven conformational control in DNA double-strand break repair and the ABC-ATPase superfamily. *Cell* **101**, 789-800.
- Hruz, T., Laule, O., Szabo, G., Wessendorp, F., Bleuler, S., Oertle, L., Widmayer, P., Gruissem, W., and Zimmermann, P.** (2008). Genevestigator v3: a reference expression database for the meta-analysis of transcriptomes. *Adv Bioinformatics* **2008**, 420747.
- Irniger, S., Piatti, S., Michaelis, C., and Nasmyth, K.** (1995). Genes involved in sister chromatid separation are needed for B-type cyclin proteolysis in budding yeast. *Cell* **81**, 269-278.
- Ishiguro, K., and Watanabe, Y.** (2007). Chromosome cohesion in mitosis and meiosis. *J Cell Sci* **120**, 367-369.
- Jackson, N., Sanchez-Moran, E., Buckling, E., Armstrong, S.J., Jones, G.H., and Franklin, F.C.** (2006). Reduced meiotic crossovers and delayed prophase I progression in AtMLH3-deficient *Arabidopsis*. *EMBO J* **25**, 1315-1323.
- Jean, M., Pelletier, J., Hilpert, M., Belzile, F., and Kunze, R.** (1999). Isolation and characterization of AtMLH1, a MutL homologue from *Arabidopsis thaliana*. *Mol Gen Genet* **262**, 633-642.
- Jiang, L., Xia, M., Strittmatter, L.I., and Makaroff, C.A.** (2007). The *Arabidopsis* cohesin protein SYN3 localizes to the nucleolus and is essential for gametogenesis. *Plant J* **50**, 1020-1034.

- Jones, S., and Sgouros, J.** (2001). The cohesin complex: sequence homologies, interaction networks and shared motifs. *Genome Biol* **2**, RESEARCH0009.
- Keeney, S.** (2001). Mechanism and control of meiotic recombination initiation. *Curr Top Dev Biol* **52**, 1-53.
- Keeney, S., Giroux, C.N., and Kleckner, N.** (1997). Meiosis-specific DNA double-strand breaks are catalyzed by Spo11, a member of a widely conserved protein family. *Cell* **88**, 375-384.
- Kim, J.S., Krasieva, T.B., LaMorte, V., Taylor, A.M., and Yokomori, K.** (2002). Specific recruitment of human cohesin to laser-induced DNA damage. *J Biol Chem* **277**, 45149-45153.
- Kitajima, T.S., Kawashima, S.A., and Watanabe, Y.** (2004). The conserved kinetochore protein shugoshin protects centromeric cohesion during meiosis. *Nature* **427**, 510-517.
- Kitajima, T.S., Yokobayashi, S., Yamamoto, M., and Watanabe, Y.** (2003). Distinct cohesin complexes organize meiotic chromosome domains. *Science* **300**, 1152-1155.
- Kitajima, T.S., Sakuno, T., Ishiguro, K., Iemura, S., Natsume, T., Kawashima, S.A., and Watanabe, Y.** (2006). Shugoshin collaborates with protein phosphatase 2A to protect cohesin. *Nature* **441**, 46-52.
- Klein, F., Mahr, P., Galova, M., Buonomo, S.B., Michaelis, C., Nairz, K., and Nasmyth, K.** (1999). A central role for cohesins in sister chromatid cohesion, formation of axial elements, and recombination during yeast meiosis. *Cell* **98**, 91-103.
- Krogh, B.O., and Symington, L.S.** (2004). Recombination proteins in yeast. *Annu Rev Genet* **38**, 233-271.
- Kudo, N.R., Wassmann, K., Anger, M., Schuh, M., Wirth, K.G., Xu, H., Helmhart, W., Kudo, H., McKay, M., Maro, B., Ellenberg, J., de Boer, P., and Nasmyth, K.** (2006). Resolution of chiasmata in oocytes requires separase-mediated proteolysis. *Cell* **126**, 135-146.
- Kugou, K., Fukuda, T., Yamada, S., Ito, M., Sasanuma, H., Mori, S., Katou, Y., Itoh, T., Matsumoto, K., Shibata, T., Shirahige, K., and Ohta, K.** (2009). Rec8 guides canonical Spo11 distribution along yeast meiotic chromosomes. *Mol Biol Cell* **20**, 3064-3076.
- Lam, W.S., Yang, X., and Makaroff, C.A.** (2005). Characterization of *Arabidopsis thaliana* SMC1 and SMC3: evidence that AtSMC3 may function beyond chromosome cohesion. *J Cell Sci* **118**, 3037-3048.
- Lee, J., Yokota, T., and Yamashita, M.** (2002). Analyses of mRNA expression patterns of cohesin subunits Rad21 and Rec8 in mice: germ cell-specific expression of rec8

mRNA in both male and female mice. *Zoolog Sci* **19**, 539-544.

- Lee, J., Okada, K., Ogushi, S., Miyano, T., Miyake, M., and Yamashita, M.** (2006). Loss of Rec8 from chromosome arm and centromere region is required for homologous chromosome separation and sister chromatid separation, respectively, in mammalian meiosis. *Cell Cycle* **5**, 1448-1455.
- Lee, J.Y., and Orr-Weaver, T.L.** (2001). The molecular basis of sister-chromatid cohesion. *Annu Rev Cell Dev Biol* **17**, 753-777.
- Li, W., Chen, C., Markmann-Mulisch, U., Timofejeva, L., Schmelzer, E., Ma, H., and Reiss, B.** (2004). The *Arabidopsis* AtRAD51 gene is dispensable for vegetative development but required for meiosis. *Proc Natl Acad Sci U S A* **101**, 10596-10601.
- Li, W., Yang, X., Lin, Z., Timofejeva, L., Xiao, R., Makaroff, C.A., and Ma, H.** (2005). The AtRAD51C gene is required for normal meiotic chromosome synapsis and double-stranded break repair in *Arabidopsis*. *Plant Physiol* **138**, 965-976.
- Lichten, M.** (2001). Meiotic recombination: breaking the genome to save it. *Curr Biol* **11**, R253-256.
- Liu Cm, C.M., McElver, J., Tzafir, I., Joosen, R., Wittich, P., Patton, D., Van Lammeren, A.A., and Meinke, D.** (2002). Condensin and cohesin knockouts in *Arabidopsis* exhibit a titan seed phenotype. *Plant J* **29**, 405-415.
- Liu, N., Schild, D., Thelen, M.P., and Thompson, L.H.** (2002). Involvement of Rad51C in two distinct protein complexes of Rad51 paralogs in human cells. *Nucleic Acids Res* **30**, 1009-1015.
- Liu, N., Lamerdin, J.E., Tebbs, R.S., Schild, D., Tucker, J.D., Shen, M.R., Brookman, K.W., Siciliano, M.J., Walter, C.A., Fan, W., Narayana, L.S., Zhou, Z.Q., Adamson, A.W., Sorensen, K.J., Chen, D.J., Jones, N.J., and Thompson, L.H.** (1998). XRCC2 and XRCC3, new human Rad51-family members, promote chromosome stability and protect against DNA cross-links and other damages. *Mol Cell* **1**, 783-793.
- Losada, A., Hirano, M., and Hirano, T.** (2002). Cohesin release is required for sister chromatid resolution, but not for condensin-mediated compaction, at the onset of mitosis. *Genes Dev* **16**, 3004-3016.
- Lowe, J., Cordell, S.C., and van den Ent, F.** (2001). Crystal structure of the SMC head domain: an ABC ATPase with 900 residues antiparallel coiled-coil inserted. *J Mol Biol* **306**, 25-35.
- Lowndes, N.F., and Toh, G.W.** (2005). DNA repair: the importance of phosphorylating histone H2AX. *Curr Biol* **15**, R99-R102.

- Macaisne, N., Novatchkova, M., Peirera, L., Vezon, D., Jolivet, S., Froger, N., Chelysheva, L., Grelon, M., and Mercier, R.** (2008). SHOC1, an XPF endonuclease-related protein, is essential for the formation of class I meiotic crossovers. *Curr Biol* **18**, 1432-1437.
- MacQueen, A.J., Colaiacovo, M.P., McDonald, K., and Villeneuve, A.M.** (2002). Synapsis-dependent and -independent mechanisms stabilize homolog pairing during meiotic prophase in *C. elegans*. *Genes Dev* **16**, 2428-2442.
- Manheim, E.A., and McKim, K.S.** (2003). The Synaptonemal complex component C(2)M regulates meiotic crossing over in *Drosophila*. *Curr Biol* **13**, 276-285.
- Masson, J.Y., and West, S.C.** (2001). The Rad51 and Dmc1 recombinases: a non-identical twin relationship. *Trends Biochem Sci* **26**, 131-136.
- Masson, J.Y., Stasiak, A.Z., Stasiak, A., Benson, F.E., and West, S.C.** (2001). Complex formation by the human RAD51C and XRCC3 recombination repair proteins. *Proc Natl Acad Sci U S A* **98**, 8440-8446.
- Mc Intyre, J., Muller, E.G., Weitzer, S., Snyderman, B.E., Davis, T.N., and Uhlmann, F.** (2007). In vivo analysis of cohesin architecture using FRET in the budding yeast *Saccharomyces cerevisiae*. *EMBO J* **26**, 3783-3793.
- McGuinness, B.E., Hirota, T., Kudo, N.R., Peters, J.M., and Nasmyth, K.** (2005). Shugoshin prevents dissociation of cohesin from centromeres during mitosis in vertebrate cells. *PLoS Biol* **3**, e86.
- McKim, K.S., Green-Marroquin, B.L., Sekelsky, J.J., Chin, G., Steinberg, C., Khodosh, R., and Hawley, R.S.** (1998). Meiotic synapsis in the absence of recombination. *Science* **279**, 876-878.
- Melby, T.E., Ciampaglio, C.N., Briscoe, G., and Erickson, H.P.** (1998). The symmetrical structure of structural maintenance of chromosomes (SMC) and MukB proteins: long, antiparallel coiled coils, folded at a flexible hinge. *J Cell Biol* **142**, 1595-1604.
- Mercier, R., Jolivet, S., Vezon, D., Huppe, E., Chelysheva, L., Giovanni, M., Nogue, F., Doutriaux, M.P., Horlow, C., Grelon, M., and Mezard, C.** (2005). Two meiotic crossover classes cohabit in *Arabidopsis*: one is dependent on MER3, whereas the other one is not. *Curr Biol* **15**, 692-701.
- Meuwissen, R.L., Offenber, H.H., Dietrich, A.J., Riesewijk, A., van Iersel, M., and Heyting, C.** (1992). A coiled-coil related protein specific for synapsed regions of meiotic prophase chromosomes. *EMBO J* **11**, 5091-5100.
- Michaelis, C., Ciosk, R., and Nasmyth, K.** (1997). Cohesins: chromosomal proteins that prevent premature separation of sister chromatids. *Cell* **91**, 35-45.
- Miller, K.A., Sawicka, D., Barsky, D., and Albala, J.S.** (2004). Domain mapping of the Rad51 paralog protein complexes. *Nucleic Acids Res* **32**, 169-178.

- Nasmyth, K.** (2001). Disseminating the genome: joining, resolving, and separating sister chromatids during mitosis and meiosis. *Annu Rev Genet* **35**, 673-745.
- Nasmyth, K.** (2002). Segregating sister genomes: the molecular biology of chromosome separation. *Science* **297**, 559-565.
- Nasmyth, K.** (2005). How might cohesin hold sister chromatids together? *Philos Trans R Soc Lond B Biol Sci* **360**, 483-496.
- Nasmyth, K., and Haering, C.H.** (2005). The structure and function of SMC and kleisin complexes. *Annu Rev Biochem* **74**, 595-648.
- Noble, D., Kenna, M.A., Dix, M., Skibbens, R.V., Unal, E., and Guacci, V.** (2006). Intersection between the regulators of sister chromatid cohesion establishment and maintenance in budding yeast indicates a multi-step mechanism. *Cell Cycle* **5**, 2528-2536.
- Olive, P.L., and Banath, J.P.** (2009). Kinetics of H2AX phosphorylation after exposure to cisplatin. *Cytometry B Clin Cytom* **76**, 79-90.
- Osakabe, K., Yoshioka, T., Ichikawa, H., and Toki, S.** (2002). Molecular cloning and characterization of RAD51-like genes from *Arabidopsis thaliana*. *Plant Mol Biol* **50**, 71-81.
- Osman, K., Sanchez-Moran, E., Mann, S.C., Jones, G.H., and Franklin, F.C.** (2009). Replication protein A (AtRPA1a) is required for class I crossover formation but is dispensable for meiotic DNA break repair. *EMBO J* **28**, 394-404.
- Page, S.L., and Hawley, R.S.** (2001). c(3)G encodes a Drosophila synaptonemal complex protein. *Genes Dev* **15**, 3130-3143.
- Panizza, S., Tanaka, T., Hochwagen, A., Eisenhaber, F., and Nasmyth, K.** (2000). Pds5 cooperates with cohesin in maintaining sister chromatid cohesion. *Curr Biol* **10**, 1557-1564.
- Parisi, S., McKay, M.J., Molnar, M., Thompson, M.A., van der Spek, P.J., van Drunen-Schoenmaker, E., Kanaar, R., Lehmann, E., Hoeijmakers, J.H., and Kohli, J.** (1999). Rec8p, a meiotic recombination and sister chromatid cohesion phosphoprotein of the Rad21p family conserved from fission yeast to humans. *Mol Cell Biol* **19**, 3515-3528.
- Pasierbek, P., Jantsch, M., Melcher, M., Schleiffer, A., Schweizer, D., and Loidl, J.** (2001). A *Caenorhabditis elegans* cohesion protein with functions in meiotic chromosome pairing and disjunction. *Genes Dev* **15**, 1349-1360.
- Pauli, A., Althoff, F., Oliveira, R.A., Heidmann, S., Schuldiner, O., Lehner, C.F., Dickson, B.J., and Nasmyth, K.** (2008). Cell-type-specific TEV protease cleavage reveals

cohesin functions in *Drosophila* neurons. *Dev Cell* **14**, 239-251.

- Pawlowski, W.P., and Cande, W.Z.** (2005). Coordinating the events of the meiotic prophase. *Trends Cell Biol* **15**, 674-681.
- Pelttari, J., Hoja, M.R., Yuan, L., Liu, J.G., Brundell, E., Moens, P., Santucci-Darmanin, S., Jessberger, R., Barbero, J.L., Heyting, C., and Hoog, C.** (2001). A meiotic chromosomal core consisting of cohesin complex proteins recruits DNA recombination proteins and promotes synapsis in the absence of an axial element in mammalian meiotic cells. *Mol Cell Biol* **21**, 5667-5677.
- Pezzi, N., Prieto, I., Kremer, L., Perez Jurado, L.A., Valero, C., Del Mazo, J., Martinez, A.C., and Barbero, J.L.** (2000). STAG3, a novel gene encoding a protein involved in meiotic chromosome pairing and location of STAG3-related genes flanking the Williams-Beuren syndrome deletion. *FASEB J* **14**, 581-592.
- Pittman, D.L., Weinberg, L.R., and Schimenti, J.C.** (1998). Identification, characterization, and genetic mapping of Rad51d, a new mouse and human RAD51/RecA-related gene. *Genomics* **49**, 103-111.
- Prieto, I., Suja, J.A., Pezzi, N., Kremer, L., Martinez, A.C., Rufas, J.S., and Barbero, J.L.** (2001). Mammalian STAG3 is a cohesin specific to sister chromatid arms in meiosis I. *Nat Cell Biol* **3**, 761-766.
- Prieto, I., Tease, C., Pezzi, N., Buesa, J.M., Ortega, S., Kremer, L., Martinez, A., Martinez, A.C., Hulten, M.A., and Barbero, J.L.** (2004). Cohesin component dynamics during meiotic prophase I in mammalian oocytes. *Chromosome Res* **12**, 197-213.
- Prieto, I., Pezzi, N., Buesa, J.M., Kremer, L., Barthelemy, I., Carreiro, C., Roncal, F., Martinez, A., Gomez, L., Fernandez, R., Martinez, A.C., and Barbero, J.L.** (2002). STAG2 and Rad21 mammalian mitotic cohesins are implicated in meiosis. *EMBO Rep* **3**, 543-550.
- Puizina, J., Siroky, J., Mokros, P., Schweizer, D., and Riha, K.** (2004). Mre11 deficiency in *Arabidopsis* is associated with chromosomal instability in somatic cells and Spo11-dependent genome fragmentation during meiosis. *Plant Cell* **16**, 1968-1978.
- Revenkova, E., Eijpe, M., Heyting, C., Gross, B., and Jessberger, R.** (2001). Novel meiosis-specific isoform of mammalian SMC1. *Mol Cell Biol* **21**, 6984-6998.
- Riedel, C.G., Katis, V.L., Katou, Y., Mori, S., Itoh, T., Helmhart, W., Galova, M., Petronczki, M., Gregan, J., Cetin, B., Mudrak, I., Ogris, E., Mechtler, K., Pelletier, L., Buchholz, F., Shirahige, K., and Nasmyth, K.** (2006). Protein phosphatase 2A protects centromeric sister chromatid cohesion during meiosis I. *Nature* **441**, 53-61.

- Robert, N.Y.** (2009). Investigating the control of homologous chromosome pairing and crossover formation in meiosis of *Arabidopsis thaliana*. A thesis submitted to The University of Birmingham (U.K.) for the degree of Doctor of Philosophy.
- Ross, K.J., Fransz, P., Armstrong, S.J., Vizir, I., Mulligan, B., Franklin, F.C., and Jones, G.H.** (1997). Cytological characterization of four meiotic mutants of *Arabidopsis* isolated from T-DNA-transformed lines. *Chromosome Res* **5**, 551-559.
- Sanchez-Moran, E., Santos, J.L., Jones, G.H., and Franklin, F.C.** (2007). ASY1 mediates AtDMC1-dependent interhomolog recombination during meiosis in *Arabidopsis*. *Genes Dev* **21**, 2220-2233.
- Sanchez Moran, E., Armstrong, S.J., Santos, J.L., Franklin, F.C., and Jones, G.H.** (2001). Chiasma formation in *Arabidopsis thaliana* accession Wassileskija and in two meiotic mutants. *Chromosome Res* **9**, 121-128.
- Scherthan, H., Weich, S., Schwegler, H., Heyting, C., Harle, M., and Cremer, T.** (1996). Centromere and telomere movements during early meiotic prophase of mouse and man are associated with the onset of chromosome pairing. *J Cell Biol* **134**, 1109-1125.
- Schild, D., Lio, Y.C., Collins, D.W., Tsomondo, T., and Chen, D.J.** (2000). Evidence for simultaneous protein interactions between human Rad51 paralogs. *J Biol Chem* **275**, 16443-16449.
- Schleiffer, A., Kaitna, S., Maurer-Stroh, S., Glotzer, M., Nasmyth, K., and Eisenhaber, F.** (2003). Kleisins: a superfamily of bacterial and eukaryotic SMC protein partners. *Mol Cell* **11**, 571-575.
- Schubert, V., Weissleder, A., Ali, H., Fuchs, J., Lermontova, I., Meister, A., and Schubert, I.** (2009). Cohesin gene defects may impair sister chromatid alignment and genome stability in *Arabidopsis thaliana*. *Chromosoma* **118**, 591-605.
- Shinohara, A., Ogawa, H., Matsuda, Y., Ushio, N., Ikeo, K., and Ogawa, T.** (1993). Cloning of human, mouse and fission yeast recombination genes homologous to RAD51 and recA. *Nat Genet* **4**, 239-243.
- Shonn, M.A., McCarroll, R., and Murray, A.W.** (2002). Spo13 protects meiotic cohesin at centromeres in meiosis I. *Genes Dev* **16**, 1659-1671.
- Skibbens, R.V., Corson, L.B., Koshland, D., and Hieter, P.** (1999). Ctf7p is essential for sister chromatid cohesion and links mitotic chromosome structure to the DNA replication machinery. *Genes Dev* **13**, 307-319.
- Smith, K.N., and Nicolas, A.** (1998). Recombination at work for meiosis. *Curr Opin Genet Dev* **8**, 200-211.
- Snowden, T., Acharya, S., Butz, C., Berardini, M., and Fishel, R.** (2004). hMSH4-hMSH5 recognizes Holliday Junctions and forms a meiosis-specific sliding clamp that

embraces homologous chromosomes. *Mol Cell* **15**, 437-451.

- Stacey, N.J., Kuromori, T., Azumi, Y., Roberts, G., Breuer, C., Wada, T., Maxwell, A., Roberts, K., and Sugimoto-Shirasu, K.** (2006). *Arabidopsis* SPO11-2 functions with SPO11-1 in meiotic recombination. *Plant J* **48**, 206-216.
- Storlazzi, A., Tesse, S., Ruprich-Robert, G., Gargano, S., Poggeler, S., Kleckner, N., and Zickler, D.** (2008). Coupling meiotic chromosome axis integrity to recombination. *Genes Dev* **22**, 796-809.
- Strom, L., Lindroos, H.B., Shirahige, K., and Sjogren, C.** (2004). Postreplicative recruitment of cohesin to double-strand breaks is required for DNA repair. *Mol Cell* **16**, 1003-1015.
- Sumara, I., Vorlaufer, E., Stukenberg, P.T., Kelm, O., Redemann, N., Nigg, E.A., and Peters, J.M.** (2002). The dissociation of cohesin from chromosomes in prophase is regulated by Polo-like kinase. *Mol Cell* **9**, 515-525.
- Sung, P., Krejci, L., Van Komen, S., and Sehorn, M.G.** (2003). Rad51 recombinase and recombination mediators. *J Biol Chem* **278**, 42729-42732.
- Sym, M., Engebrecht, J.A., and Roeder, G.S.** (1993). ZIP1 is a synaptonemal complex protein required for meiotic chromosome synapsis. *Cell* **72**, 365-378.
- Tebbs, R.S., Zhao, Y., Tucker, J.D., Scheerer, J.B., Siciliano, M.J., Hwang, M., Liu, N., Legerski, R.J., and Thompson, L.H.** (1995). Correction of chromosomal instability and sensitivity to diverse mutagens by a cloned cDNA of the XRCC3 DNA repair gene. *Proc Natl Acad Sci U S A* **92**, 6354-6358.
- Thompson, J.D., Higgins, D.G., and Gibson, T.J.** (1994). CLUSTAL W: improving the sensitivity of progressive multiple sequence alignment through sequence weighting, position-specific gap penalties and weight matrix choice. *Nucleic Acids Res* **22**, 4673-4680.
- Tomonaga, T., Nagao, K., Kawasaki, Y., Furuya, K., Murakami, A., Morishita, J., Yuasa, T., Sutani, T., Kearsy, S.E., Uhlmann, F., Nasmyth, K., and Yanagida, M.** (2000). Characterization of fission yeast cohesin: essential anaphase proteolysis of Rad21 phosphorylated in the S phase. *Genes Dev* **14**, 2757-2770.
- Toth, A., Ciosk, R., Uhlmann, F., Galova, M., Schleiffer, A., and Nasmyth, K.** (1999). Yeast cohesin complex requires a conserved protein, Eco1p(Ctf7), to establish cohesion between sister chromatids during DNA replication. *Genes Dev* **13**, 320-333.
- Trelles-Sticken, E., Loidl, J., and Scherthan, H.** (1999). Bouquet formation in budding yeast: initiation of recombination is not required for meiotic telomere clustering. *J Cell Sci* **112 (Pt 5)**, 651-658.

- Uhlmann, F.** (2003). Separase regulation during mitosis. *Biochem Soc Symp*, 243-251.
- Uhlmann, F., Lottspeich, F., and Nasmyth, K.** (1999). Sister-chromatid separation at anaphase onset is promoted by cleavage of the cohesin subunit Scc1. *Nature* **400**, 37-42.
- Uhlmann, F., Wernic, D., Poupard, M.A., Koonin, E.V., and Nasmyth, K.** (2000). Cleavage of cohesin by the CD clan protease separin triggers anaphase in yeast. *Cell* **103**, 375-386.
- Unal, E., Arbel-Eden, A., Sattler, U., Shroff, R., Lichten, M., Haber, J.E., and Koshland, D.** (2004). DNA damage response pathway uses histone modification to assemble a double-strand break-specific cohesin domain. *Mol Cell* **16**, 991-1002.
- Vazquez, J., Belmont, A.S., and Sedat, J.W.** (2002). The dynamics of homologous chromosome pairing during male *Drosophila* meiosis. *Curr Biol* **12**, 1473-1483.
- Wang, C.J., Carlton, P.M., Golubovskaya, I.N., and Cande, W.Z.** (2009). Interlock formation and coiling of meiotic chromosome axes during synapsis. *Genetics* **183**, 905-915.
- Wang, T.F., Kleckner, N., and Hunter, N.** (1999). Functional specificity of MutL homologs in yeast: evidence for three Mlh1-based heterocomplexes with distinct roles during meiosis in recombination and mismatch correction. *Proc Natl Acad Sci U S A* **96**, 13914-13919.
- Watanabe, Y.** (2005). Shugoshin: guardian spirit at the centromere. *Curr Opin Cell Biol* **17**, 590-595.
- Watanabe, Y., and Nurse, P.** (1999). Cohesin Rec8 is required for reductional chromosome segregation at meiosis. *Nature* **400**, 461-464.
- Watanabe, Y., and Kitajima, T.S.** (2005). Shugoshin protects cohesin complexes at centromeres. *Philos Trans R Soc Lond B Biol Sci* **360**, 515-521, discussion 521.
- Waterworth, W.M., Altun, C., Armstrong, S.J., Roberts, N., Dean, P.J., Young, K., Weil, C.F., Bray, C.M., and West, C.E.** (2007). NBS1 is involved in DNA repair and plays a synergistic role with ATM in mediating meiotic homologous recombination in plants. *Plant J* **52**, 41-52.
- Xu, H., Beasley, M.D., Warren, W.D., van der Horst, G.T., and McKay, M.J.** (2005). Absence of mouse REC8 cohesin promotes synapsis of sister chromatids in meiosis. *Dev Cell* **8**, 949-961.
- Xu, H., Beasley, M., Verschoor, S., Inselman, A., Handel, M.A., and McKay, M.J.** (2004). A new role for the mitotic RAD21/SCC1 cohesin in meiotic chromosome cohesion and segregation in the mouse. *EMBO Rep* **5**, 378-384.

- Yamamoto, A., Guacci, V., and Koshland, D.** (1996). Pds1p, an inhibitor of anaphase in budding yeast, plays a critical role in the APC and checkpoint pathway(s). *J Cell Biol* **133**, 99-110.
- Yanagida, M.** (2000). Cell cycle mechanisms of sister chromatid separation; roles of Cut1/separin and Cut2/securin. *Genes Cells* **5**, 1-8.
- Yu, H.G., and Dawe, R.K.** (2000). Functional redundancy in the maize meiotic kinetochore. *J Cell Biol* **151**, 131-142.
- Zhang, L., Tao, J., Wang, S., Chong, K., and Wang, T.** (2006). The rice OsRad21-4, an orthologue of yeast Rec8 protein, is required for efficient meiosis. *Plant Mol Biol* **60**, 533-554.
- Zhao, D., Yang, X., Quan, L., Timofejeva, L., Rigel, N.W., Ma, H., and Makaroff, C.A.** (2006). ASK1, a SKP1 homolog, is required for nuclear reorganization, presynaptic homolog juxtaposition and the proper distribution of cohesin during meiosis in *Arabidopsis*. *Plant Mol Biol* **62**, 99-110.
- Zickler, D., and Kleckner, N.** (1998). The leptotene-zygotene transition of meiosis. *Annu Rev Genet* **32**, 619-697.
- Zickler, D., and Kleckner, N.** (1999). Meiotic chromosomes: integrating structure and function. *Annu Rev Genet* **33**, 603-754.